C03017: Master of Engineering (Research)
CRICOS Code: 009468B
April 2026

Renewable Energy Zones Integration in Weak Transmission Networks

Sadnan Sakib

School of Electrical and Data Engineering
Faculty of Engineering & IT
University of Technology Sydney
NSW - 2007, Australia

Renewable Energy Zones Integration in Weak Transmission Networks

A thesis submitted in fulfillment of the requirements
for the degree of

Masters of Engineering (Research)

by

Sadnan Sakib

Email: sadnan.sakib@student.uts.edu.au

Principal Supervisor: Professor Dr. Jahangir Hossain
Email: jahangir.hossain@uts.edu.au

Co-supervisor: Associate Professor Dr. Li Li
Email: Li.Li@uts.edu.au

to

School of
Electrical and Data Engineering
Faculty of Engineering and Information Technology
University of Technology Sydney
NSW - 2007, Australia

April 2026

© 2025 by Sadnan Sakib
All Rights Reserved

CERTIFICATE OF ORIGINAL AUTHORSHIP

I, *Sadnan Sakib*, declare that this thesis, submitted in fulfilment of the requirements for the award of *Master of Engineering (Research)* in the *School of Electrical and Data Engineering*, *Faculty of Engineering and IT* at the University of Technology Sydney.

This thesis is wholly my own work unless otherwise referenced or acknowledged. In addition, I certify that all information sources and literature used are indicated in the thesis.

This document has not been submitted for qualifications at any other academic institution.

This research was supported by an Australian Government Research Training Program (RTP) Scholarship doi.org/10.82133/C42F-K220.

Production Note:

SIGNATURE: Signature removed prior to publication.

DATE: 23nd April, 2026

PLACE: Sydney, Australia

ABSTRACT

The rapid expansion of inverter-based renewable energy within Australia's Renewable Energy Zones (REZs) has intensified long-standing challenges in weak transmission networks, where low inertia, high impedance, and limited fault-clearing capability compromise voltage stability, frequency resilience, and overall system security. As synchronous machines are displaced by photovoltaic, wind, and storage technologies, conventional control and support mechanisms have become insufficient for maintaining reliable operation. Addressing these gaps requires system-level control strategies capable of enhancing stability under high renewable penetration.

The first major contribution of this thesis is the development of a cascaded control parameter optimisation framework that strengthens voltage stability and fault-ride-through (FRT) capability in weak-grid REZ environments. This contribution introduces a Dynamic Resilience Metric that quantitatively captures transient behaviour, fault-clearing margins, and post-fault recovery characteristics. Guided by this metric, an enhanced Particle Swarm Optimisation routine simultaneously tunes plant-level, network-level, and converter-level controllers, an approach that surpasses traditional single-layer optimisation. Extensive validation on a simplified Australian 14-Generator Test System demonstrates significant improvements in system stability, including reductions in voltage overshoot to 6-25% and extended permissible fault-clearing times of 255-270 ms. These results show that coordinated, multi-layer optimisation provides a scalable and systematic means of reinforcing weak renewable-dominated grids.

The second major contribution proposes a severity-aware coordinated control framework for Battery Energy Storage Systems (BESS), introducing a disturbance-driven mechanism that adaptively blends grid-following (GFL) and grid-forming (GFM) inverter modes. This strategy ensures efficient current-following during normal conditions while activating robust voltage-forming and frequency support during severe disturbances. Through parametric studies of GFM:GFL penetration ratios, the framework demonstrates monotonic improvements in frequency nadir, RoCoF suppression, and voltage recovery. A comparative evaluation of Droop and Virtual Synchronous Machine (VSM) techniques further clarifies their respective advantages, revealing Droop's superior transient performance and VSM's enhanced damping and black-start capability. This contribution establishes a practical, adaptive pathway for inverter coordination in renewable-rich weak networks.

Together, these contributions offer a unified and grid-aligned framework for enhancing the stability, resilience, and renewable hosting capacity of REZ-based weak

transmission systems, supporting Australia's transition toward a reliable and sustainable energy future.

Keywords: Battery Energy Storage Systems, dynamic resilience metric, frequency stability, grid-forming inverters, grid-following inverters, improved voltage stability, improved fault clearing time, modified particle swarm optimization, strengthening transmission networks, renewable integration, weak transmission networks.

Dedication

I would like to dedicate this thesis to my beloved parents, Professor Dr. K. B. M. Mahbubur Rahman and Assistant Professor Selina Yasmin, and to my elder brother Sabit Saleheen, whose unwavering patience, boundless love, and constant encouragement have supported me throughout this journey.

Acknowledgments

I would like to express my deepest gratitude to all those who have supported me throughout my Masters of Engineering (Research) journey.

First and foremost, I extend my sincere appreciation to my supervisor, Professor Dr Jahangir Hossain, for his invaluable guidance, expertise, and unwavering support. His insightful feedback, constructive criticism, and constant encouragement have been instrumental in shaping the direction and quality of this research.

I am also profoundly grateful to my co-supervisor, Associate Professor Dr Li Li, for her thoughtful guidance and continual support throughout this work.

My heartfelt thanks go to my research colleagues and peers for fostering an engaging and collaborative academic environment. Their intellectual discussions, feedback, and camaraderie have enriched my research experience and contributed significantly to my personal and professional growth.

I owe special gratitude to my family and friends for their unwavering love, patience, and motivation. Their belief in me has been a constant source of strength, enabling me to persevere through the challenges of this journey.

Finally, I sincerely acknowledge the collective support of everyone mentioned above. This thesis would not have been possible without their generosity, guidance, and encouragement. I remain truly grateful for their contributions.

Production Note:
Signature removed prior to publication.

Sadnan Sakib

School of Electrical and Data Engineering

Faculty of Engineering and Information Technology

University of Technology Sydney

NSW - 2007, Australia

Abbreviations

AC	Alternating Current
ACT	Alternating Capital Territory
AEMC	Australian Electricity Market Commission
AEMO	Australian Electricity Market Operator
AI	Artificial Intelligence
ANEM	Australian National Electricity Market
Model	
APC	Active Power Control
ARENA	Australian Renewable Energy Agency
BESS	Battery Energy Storage Systems
BIPV	Building-Integrated Photovoltaics
BMS	Battery Management System
CA	Compressed Air
Cap Bank	Capacitor Bank
CAS	Compressed Air Storage
CERs	Consumer Energy Resources
Chem	Chemical
CSC	Current Source Converter
CSI	Current Source Inverter
CSCR	Composite Short Circuit Ratio
DARC	Decoupled Active Reactive Control
DC	Direct Current
DPV	Distributed Photovoltaics
EA	Eigenvalue Analysis
EC	Electrochemical
Elec	Electrical
EMS	Energy Management Systems
EMSt	Energy Management Strategies
ESSs	Energy Storage Systems
EMTM	Electromagnetic Transient Modelling
EMT	Electromagnetic Transient
e.g.	For example
Exp.	Experimental
FACTS	Flexible AC Transmission Systems
FC	Fuel Cells
FCAS	Frequency Control Ancillary Services
FC	Fuzzy logic control
FPPT	Flexible Power Point Tracking
FFR	Fast Frequency Response
FRT	Fault-ride through
FNN	Fuzzy neural network
FNQ	Far North Queensland
GA	Genetic algorithms
GFM	Grid-Forming
GFL	Grid-Following
GFMI	Grid-Forming Inverters
GFLI	Grid-Following Inverters
GVSG	Generalized Virtual Synchronous Generator
HCCs	Hybrid Control Converters
HESS	Hybrid Energy Storage System
HiCCs	Hierarchical Control Coordinators
IBRs	Inverter-Based Resources
IEC	International Electrotechnical Commission
ISP	Integrated System Planning
LG	Line-to-Ground Fault
Li-ion	Lithium-ion
LLG	Line-to-Line-to-Ground Fault
LVRT	Low voltage ride through
MCFC	Molten carbonate fuel cells
Mech	Mechanical
MLD	Multi-Level Droop
MPC	Model predictive control
MPPT	Maximum power point tracking
MWh	Mega-Watt hour
NaS	Sodium sulphur
Ni-Cd	Nickel-Cadmium
Ni-MH	Nickel-Metal Hydride
NE	New England
NEM	National Electricity Market
NNC	Neural Network-Based Control
NSW	New South Wales
OSCR	Operating Short-Circuit Ratio
Pb-Acid	Lead,ÄìAcid
PCC	Point of Common Coupling
PHS	Pumped hydro storage
PI	Proportional-Integral
PLL	Phase-Locked Loop
PPC	Predictive power control
PSC	Power Synchronization Control
PSO	Particle swarm optimisation
PV	Photovoltaic
PWM	Pulse width modulation

QLD	Queensland
RE	Renewable Energy
Ref	Reference
RESs	Renewable Energy Sources
REZs	Renewable Energy Zones
RF	Redox flow
RFB	Redox flow batteries
RL	Reinforcement learning
RLS	Reinforcement learning scheme
RMS	Root Mean Square
RMSM	Root Mean Squared Modelling
RoCoF	Rate of Change of Frequency
RTDS	Real-Time Digital Simulator
RWFNN	Recurrent fuzzy neural network
SA	South Australia
SCs	Synchronous Condensers
SCADA	Supervisory Control and Data Acquisition
SCap	Supercapacitors
SCRs	Short-Circuit Ratios
SDGs	Sustainable Development Goals
SGs	Synchronous Generators
SMC	Sliding mode control
SMES	Superconducting magnetic energy storage
SMIB	Single Machine Infinite Bus
SoC	State of charge
SOFC	Solid oxide fuel cells
SOGI-PLL	Second order generalized integrator
SPWM	Sinusoidal PWMS
STATCOM	Static compensators
SSCI	Sub-synchronous Control Interaction
SVCs	Static VAR compensators
TC	Thermochemical
TCSS	Thermochemical storage system
TNSPs	Transmission Network Service Providers
TSOs	Transmission System Operators
UDE	Uncertainty and Disturbance Estimator
UNSDGs	United Nations Sustainable Development Goals
VIC	Victoria
VOC	Virtual Oscillator Control
VPPs	Virtual power plants
VRC	Voltage restoration control
VRE	Variable renewable energy
VRFB	Vanadium redox flow
VSC	Voltage Source Converter
VSG	Virtual Synchronous Generator
VSI	Voltage Source Inverter
VSM	Virtual Synchronous Machine
WA	Western Australia
WMZ	West Murray Zone
WSCR	Weighted Short Circuit Ratio
WT	Weighted Short Circuit Ratio
ZWG	Zonal weak grids

List of Publications

Related to the Topic:

1. **Sakib, S.**, Hossain, M. B., Zamee, M. A., Hossain, M. J., & Habib, M. A. (2025). Role of battery energy storage systems: A comprehensive review on renewable energy zones integration in weak transmission networks. Journal of Energy Storage, 128, 117223.

2. **Sakib, S.**, Zamee, M. A., Hossain, M. J., Hossain, M. B., & Habib, M. A. (2026). Strengthening Renewable-Rich Weak Grids Through Improved Voltage Stability and Fault-Ride Through Capability. IET Renewable Power Generation, 20(1), e70188.

3. **Sakib, S.**, Hossain, M. J., & Habib, M. A. (2026). Grid-Following and Grid-Forming Inverters: A Systematic Review of Their Cornerstone Role in Australia's Renewable Energy Zones Integration. Renewable and Sustainable Energy Reviews (First revision currently under review as of 23/04/2026).

4. **Sakib, S.** & Hossain, M. J. (2026). Severity-aware coordination of grid-forming and grid-following BESS for stability enhancement in weak transmission networks. Electric Power Systems Research, 254, 112658.

TABLE OF CONTENTS

List of Publications **xi**

List of Figures **xix**

List of Tables **xxiii**

1 Context for Grid Integration of Renewables **1**

1.1 Context and Motivation for REZs Integration 1
1.2 Background on Weak Transmission Networks and Renewable Integration 4
1.3 Problem Statement: Challenges of REZ Deployment in Weak Grids 7
1.4 Research Aim and Objectives for Strengthening REZ-Based Weak Networks 9
1.5 Research Questions Guiding REZ-Weak Grid Investigation 10
1.6 Overview of the methodological approach 11
1.7 Originality and Research Contributions 13
1.8 Significance of the Study 15
1.9 Scope and Limitations of REZ-Weak Grid Modelling 16
1.9.1 Scope and Limitations of the Thesis 18
1.10 Definition of Key Terms Related to REZ and Weak Transmission Networks 19
1.11 Structure of the Thesis 21

2 Comprehensive Literature Review on Renewable Grid Integration **25**

2.1 Introduction 26
2.2 Review Process 31
2.3 Renewable weak grid difficulties and threats 32
2.3.1 Frequency and voltage instability 33
2.3.2 Harmonic distortions and resonance 34
2.3.3 Propagation of voltage instability 35
2.3.4 Protection and control challenges 35

2.3.5 Reduced system strength 35
2.4 Addressing Weak Grid Threats: ESS as a Solution for Renewable Integration 36
2.4.1 Classification of ESSs and their application for REZs 36
2.4.2 Applications offered by ESSs in weak grids 37
2.5 Roles of ESSs in mitigating weak grid challenges 39
2.5.1 Limitations of non-battery storage technologies 39
2.5.2 Addressing Challenges through BESS for REZs integration in weak grids 40
2.6 Advancement of BESS technologies and their applications to weak power grids 42
2.6.1 Different types of BESS for weak power grid applications 42
2.6.2 BESS in zonal weak grids 45
2.7 Power management control strategies and algorithms used for BESS in weak grids 51
2.7.1 Overview of control strategies and energy management 52
2.7.2 Energy Management Systems 54
2.8 Applications of BESS in electrical weak grids 56
2.8.1 Enhancing Grid Stability 57
2.8.2 Role of BESS in providing reactive power support 58
2.9 Worldwide projects of BESS for real-world power grid applications 61
2.9.1 Supporting RE Integration 61
2.9.2 Mitigating intermittency and reducing curtailment 62
2.9.3 Facilitating Energy Arbitrage and Load Balancing 62
2.10 Discussion and Transition Pathways to Promote BESS 63
2.11 Findings and conclusions 65
2.12 Introduction 69
2.13 Review Methodology 75
2.14 Technical Background of Inverter Technologies 76
2.14.1 Grid-Following (GFL) Inverters 76
2.14.2 Grid-Forming (GFM) Inverters 79
2.14.3 GFL vs. GFM Comparison 81
2.15 Modeling Approaches in the Context of Australian REZs 82
2.15.1 General Modeling Approaches 82
2.15.2 Simulation Tools 86
2.15.3 Australia-Focused Modeling Studies 87

2.16 Control and Coordination Mechanisms of IBRs 90
2.16.1 Control Techniques for GFL Inverters 90
2.16.2 Control Strategies for GFM Inverters 94
2.16.3 GFM-GFL coordination 101
2.16.4 Impact on Grid Stability 104
2.17 Real-World Implementation in Australia 108
2.17.1 Overview of Implemented REZ Projects 108
2.17.2 Grid Performance Outcomes 109
2.17.3 Economic and Regulatory Implications 111
2.17.4 Challenges and Lessons Learned 112
2.18 Discussion and transition pathway to promote inverter technologies in REZs 113
2.19 Findings and conclusions 115
2.20 Chapter summary 119

3 Weak-Renewable-Grid Stability Enhancement 121
3.1 Introduction 122
3.1.1 Background 122
3.1.2 Motivation 122
3.1.3 Problem Statement 123
3.1.4 Novelty 124
3.1.5 Contributions 126
3.1.6 Organisation of the Chapter 127
3.2 Cascaded Control Framework for Renewable Energy Integration in Weak Transmission Networks 127
3.2.1 Multilevel Control Framework for Renewable Energy Integration in Weak Transmission Networks 127
3.3 Proposed Methodology 132
3.3.1 Power System Modeling & Initialization 132
3.3.2 Parameter Space Definition & PSO Initialization 133
3.3.3 Iterative Load Flow & Dynamic Simulation 133
3.3.4 Objective Function Evaluation 134
3.3.5 Optimization & Parameter Update 135
3.3.6 Final Controller Selection & Validation 136
3.4 Network and Cases Considered 138

3.4.1 Simplified 14-Generator Model of the South East Australian Power System . . . 138
3.4.2 Cases Considered . . . 138
3.5 Results and Discussion . . . 139
3.5.1 Case Study 1: Dynamic Voltage Stability and Fault-Clearing Time Analysis for PV and Wind Integration . . . 140
3.5.2 Case Study 2: Hybrid Renewable Energy Configurations . . . 148
3.6 Conclusion and future work . . . 155
3.7 Chapter summary . . . 156

4 Severity-Aware GFM-GFL BESS Coordination 157
4.1 Introduction . . . 157
4.2 Proposed Methodology . . . 162
4.2.1 Severity-Aware Coordination Framework . . . 162
4.2.2 Multi-Objective Optimization of GFM:GFL Penetration Ratios . . . 164
4.2.3 Comparative Evaluation of Droop and VSM Control . . . 166
4.3 Network and Cases Considered . . . 167
4.3.1 Network Considered . . . 168
4.3.2 Cases Considered . . . 168
4.4 Results and Discussion . . . 169
4.4.1 Severity-Aware GFM–GFL Coordination . . . 169
4.4.2 Optimisation of GFM:GFL Penetration Ratios . . . 171
4.5 Comparative Evaluation of Droop and VSM Control . . . 174
4.5.1 Black Start Capability . . . 176
4.6 Conclusion and Future Work . . . 177
4.7 Chapter summary . . . 178

5 Conclusion and Future Work 179
5.1 Overview . . . 179
5.2 Summary of Research Outcomes . . . 180
5.2.1 Insights from Literature Review Part 1 . . . 180
5.2.2 Insights from Literature Review Part 2 . . . 180
5.2.3 Key Findings from Chapter 3 . . . 181
5.2.4 Key Findings from Chapter 4 . . . 181
5.3 Research Contributions . . . 181
5.4 Limitations . . . 182

5.5 Future Research Directions 182
5.6 Final Remarks 183

Bibliography **185**

List of Figures

Figure **Page**

1.1 Overall methodological thesis framework 11

2.1 Electricity generation growth in Australia from RESs from 2019-2020 to 2022-2023 27
2.2 Flowchart of article selection method used in this work. 31
2.3 Sources of articles used in this journal 32
2.4 Percentage of articles published by publisher 32
2.5 Challenges and threats of RE integration in weak grids 33
2.6 Threats of RESs integration in weak grids: (a) Frequency Instability, (b) Voltage Instability, (c) Harmonic Distortion and (d) Resonance Effect. 34
2.7 ESSs classification applying for zonal weak grids 36
2.8 Key contributions of ESSs in overcoming grid challenges 37
2.9 Key Contribution of BESS in zonal weak grids 41
2.10 BESS schematic with hierarchical BMS for weak grids: battery pack integration, SOC/SOH monitoring, and stability optimization. 45
2.11 Islanded mode of zonal weak grids with RESs and BESSs 47
2.12 General configurations of grid-connected mode of zonal weak grids along with RESs and BESS 47
2.13 AC zonal weak grid architechture including BESSs and RESs 50
2.14 DC zonal weak grid architecture including BESS and RESs 51
2.15 Hybrid zonal weak grid architecture including BESSs and RESs 52
2.16 MPC block diagrams for BESS applications in weak grids; (a) MPC based on Predictive Current Control (PCC), (b) MPC based on Predictive Power Control (PPC) 52
2.17 BESS control using FLC; a) The parallel architecture of typical DC microgrid of the PV/Battery Hybrid Systems, b) Structure of the PV FLC and c) Control design and configuration of proposed BESS using FLC. 53

2.18 BESS control strategies for weak grids; (a) General flow chart of PSO, (b) General structure of GA, (c) Generalized RLS. 55
2.19 Active/reactive power control and voltage restoration control (VRC) of BESS . 59
2.20 Factors related to smooth transition pathways to promote BESS to support integration of REZs in weak grids 66
2.21 Overview of the second part of the literature review 69
2.22 Australia's RESs and target overview: (a) RE targets for states and territories, (b) RESs powering industries, homes, and businesses 70
2.23 Evolution of power systems towards inverter-dominated architectures 71
2.24 Classification of electrical energy generation systems by grid interface type . 72
2.25 Review methodology illustrating staged screening of inverter studies for REZs relevance. 75
2.26 Conceptual models of (a) GFL and (b) GFM converters 77
2.27 Classification of grid-connected converters based on GFL and GFM control structures for integration within REZs. 77
2.28 Control strategies supporting IBRs integration in REZs: (a) GFL inverter control architecture with BESS, (b) Enhanced GFL control for PV systems . 78
2.29 Control strategies supporting IBR integration in REZs: (a) GFM inverter architecture with droop-based voltage and frequency control for BESS, (b) VSM control framework enabling GFM capabilities for stable REZ operation. 80
2.30 Key attributes of GFM and GFL inverters linked with steady-state and dynamic modelling approaches for REZ applications. 84
2.31 Overview of simulation platforms used in reviewed REZ studies 87
2.32 Simplified SA Power System (Area 5) 89
2.33 Block diagrams of GFLI control methods relevant to REZs: (a) PQ control, (b) droop-based current control and (c) VSG-inspired current control. 94
2.34 Frequency (a) and voltage (b) droop control for GFMI in REZs. 95
2.35 VSG control strategies for REZs: (a) Active power control, (b) Frequency droop emulation, and (c) Voltage control. 97
2.36 PSC block diagrams for angle (a) and voltage (b) control in REZ-integrated inverter systems. 98
2.37 Synchronverter-based GFM control architecture for stable inverter integration in REZs. 99
2.38 (a) Matching control and (b) VOC-based control for inverter synchronization in REZs. 103

2.39 Structural overview of a hybrid inverter control framework integrating GFM and GFL functionalities for REZ applications. 105
2.40 Strategic drivers, current practices, and key challenges guiding the transition to coordinated GFM-GFL inverter deployment in REZs with weak grids. . . . 116

3.1 Overall methodology for this research 126
3.2 Block diagrams of the hierarchical control structure: (a) Cascaded framework, (b) Plant-Level Control, (c) Electrical Control, (d) Generator/Converter-Level Control 128
3.3 Flowchart of proposed methodology 136
3.4 Simplified Australian Power System. 139
3.5 Voltage performance comparison under different conditions in PV scenario . . 143
3.6 Voltage performance comparison under different conditions in wind scenario. 144
3.7 Convergence comparison of generalized and Modified PSO using $\mathscr{R}^{\Delta V\downarrow}_{t_{\text{clear}}\uparrow}$. . . . 147
3.8 Performance comparison under different conditions in hybrid scenario. 150
3.9 Voltage and DC-link responses under unsymmetrical fault conditions. (a) AC bus voltage profiles; (b) corresponding DC-link voltage variations. 152
3.10 Voltage and harmonic performance comparison under different conditions in Case Study 2, Scenario 2. (a) Voltage profile before optimization; (b) Voltage profile after optimization; (c) Voltage profile at Bus 507 (before vs. after); (d) Harmonic spectrum comparison. 154

4.1 Overall proposed methodology framework 161
4.2 Sensitivity of S to variations in the weighting coefficients α, β, and γ 163
4.3 Simplified Australian power system test network (Area 5). 168
4.4 Dynamic response at Bus 509 across four cases: (a) frequency, (b) active power, (c) voltage, and (d) reactive power 170
4.5 Comparative performance across four control schemes: (a) RoCoF and frequency nadir, and (b) voltage dip and overshoot. 171
4.6 Frequency (a) and voltage (b) responses at Bus 502 under varying GFM/GFL penetration levels 173
4.7 Variation of (a) frequency and voltage indicators, and (b) objective function (J) and ITAE across different GFM penetration levels. 173
4.8 Frequency (a) and voltage (b) responses of droop and VSM controls at 50% and 75% GFM penetration levels. 175
4.9 Variation of (a) droop coefficients and (b) inertia constants. 175

4.10 Black start restoration at Bus 509 using GFM-BESS showing voltage and frequency performance with (a) droop control and (b) VSM control. 176

List of Tables

Table		Page
2.1	Recent review articles on RE integration and BESS in weak grids.	30
2.2	Comparison of Various Energy Storage Systems (ESSs)	38
2.3	Summary of Major BESS Technologies	43
2.4	Key information of different BESS	44
2.5	Role of BESS and Integration of REZs in Islanded Zonal Weak Grids and Grid Connected Weak Grids	48
2.6	Key differences between islanded zonal weak grids and grid-connected zonal weak grids (with AC, DC, and Hybrid Configurations)	49
2.7	Control Strategies and their Characteristics for BESS in Weak Grids	56
2.8	EMSt in BESS	57
2.9	Comparison of Reactive Power Support Technologies for Voltage Stability	58
2.10	Key advantages of BESS compared to other technologies	58
2.11	Applications of BESS in Reactive Power Support for Voltage Stability and Grid Reliability in Weak Grid Scenario	60
2.12	BESS Case Studies with Battery Types	64
2.13	Comparative analysis of recent inverter-focused reviews and their coverage of REZ-specific research attributes	73
2.14	Advanced Operational Comparison Between GFL and GFM Inverters	82
2.15	Comparative Summary of GFL and GFM Inverters in Weak and Low-SCR Grids	83
2.16	Advanced Feature Matrix of Inverter Technologies for REZ Deployment	83
2.17	Modelling Tools and Parameters Used in studies relevant to Australian REZs	85
2.18	Summary of GFMI Control Objectives and Roles in Weak Grids Relevant to Australian REZs	91
2.19	Stability Metrics and Control Approaches in Reviewed Inverter Studies	92
2.20	REZ-oriented comparison of inverter control strategies	102

2.21 Control Approaches and Coordination Strategies in GFL and GFM Systems . 104
2.22 Comparison of Stability Contributions from GFL and GFM Inverters 106
2.23 Control Requirements for REZs Integration 107
2.24 Key Australian REZ projects using GFM inverters to support renewable integration and grid stability. 108
2.25 Performance Metrics Observed in REZ Deployments with IBRs 110

3.1 Comparison of this work with existing studies on voltage stability enhancement, FRT improvement, and renewable-rich weak-grid control. 125
3.2 Key Parameters and Their Roles in the Cascaded Control Framework 132
3.3 Control Variables and Parameter Bounds 134
3.4 Controller parameters values used for PV and Wind for before optimization cases. 140
3.5 Hybrid renewable energy configuration scenarios with power allocations. . . . 140
3.6 Voltage stability metrics using before optimized PV values 141
3.7 Voltage stability metrics using after optimized PV values 142
3.8 Voltage stability metrics using before optimized wind values 145
3.9 Voltage stability metrics using after optimized wind values 145
3.10 Parameter settings for optimization algorithms. 146
3.11 Control Variables and Optimized Parameters 148
3.12 Breakdown of Fault Clearing Times by Voltage Levels 149
3.13 Voltage stability metrics using before optimized values in hybrid scenario . . 153
3.14 Voltage stability metrics using after optimized values in hybrid scenario . . . 153

4.1 Comparison of studies on GFM-GFL coordination and weak-grid, renewable-dominated system performance. 160
4.2 Allocation of GFM and GFL Power Across Scenarios 165
4.3 Voltage and frequency performance across four cases. 169
4.4 Frequency stability metrics under different GFM:GFL ratios. 172
4.5 Voltage stability metrics under different GFM:GFL ratios. 172
4.6 Comparison of droop and VSM control at 50% and 75% GFM share. 174
4.7 Black start restoration sequence enabled by GFM-BESS. 177

CHAPTER 1

CONTEXT FOR GRID INTEGRATION OF RENEWABLES

Chapter Composition

This chapter establishes the motivation for studying renewable integration in Australia's Renewable Energy Zones (REZs) and outlines the technical challenges posed by weak transmission networks dominated by inverter-based resources. It explains how low system strength, reduced inertia, poor voltage stiffness, and inadequate fault performance undermine stable REZ operation, and highlights the limitations of existing fragmented control approaches. The chapter formulates the problem statement, defines the research aim, and introduces two core objectives focused on cascaded controller optimisation and severity-aware coordinated GFM-GFL BESS control. It then presents the research questions, summarises the methodological framework combining weak-grid modelling, optimisation, and inverter coordination, and outlines the originality and contribution of the proposed Dynamic Resilience Metric ($\mathscr{R}^{\Delta V\downarrow}_{t_{\text{clear}}\uparrow}$) and adaptive BESS strategy. The significance, scope, limitations, key term definitions, and the overall thesis structure are provided to guide the remainder of the work.

1.1 Context and Motivation for REZs Integration

The global transition toward low-carbon and sustainable energy systems has accelerated the deployment of large-scale renewable energy sources (RESs), driven

by the need to combat climate change, address long-term energy security risks, and reduce the environmental pollution associated with fossil-fuel-based generation [1], [2]. Australia is undergoing one of the most ambitious renewable energy transformations worldwide, with national and state-level policies targeting 80-100% renewable penetration by 2030-2040 [3]. Over the past decade, declining costs of wind and solar technologies, increasing public support for decarbonization, and innovations in consumer energy resources (CERs) have collectively reshaped the structure and operational dynamics of the electricity grid [3]. Major infrastructure strategies have complemented this shift, the most prominent being the establishment of Renewable Energy Zones (REZs), geographically defined areas with high renewable potential and coordinated transmission upgrades designed to enable efficient, large-scale integration and export of renewable generation.

REZs provide a strategic framework for clustering renewable assets, reducing connection bottlenecks, and optimizing network investment. Their relevance has intensified as renewable output in Australia increased from approximately 59,930 GWh (2019-2020) to more than 93,112 GWh in 2022-2023 [4]. Beyond national trends, local initiatives, including electrified transport, distributed rooftop PV adoption, and university-led net-zero innovation, continue to reinforce Australia's renewable trajectory [5, 6]. However, much of this renewable development is concentrated in regional and remote areas where existing transmission infrastructure is weak, characterized by low short-circuit ratios (SCRs), high reactance lines, and insufficient reactive power reserves. These factors collectively define what is known as weak transmission networks, a critical barrier to reliable REZ operation [7, 8].

The shift from synchronous generators (SGs) to inverter-based resources (IBRs), including PV, wind, and battery systems, has fundamentally altered grid behavior in these regions [9]. Unlike SGs, which naturally provide mechanical inertia, damping, short-circuit current, and voltage support, IBRs lack these inherent stabilizing characteristics [10]. As a result, REZ-dominated networks commonly experience reduced inertia, elevated rates of change of frequency (RoCoF), depressed frequency nadirs, and diminished fault-ride-through (FRT) capability during contingencies [11]. Reports from AEMO consistently highlight that weak-grid REZ locations face severe voltage stability reductions and transient instability risks, especially under high renewable penetration, where faults or disturbances propagate more rapidly due to low system strength [12]. These issues are further exacerbated by the intermittent and non-dispatchable nature of solar and wind resources, which introduce unpredictable power fluctuations and

complicate real-time operational balancing [9].

In addition to frequency and voltage stability concerns, weak grids face substantial power-quality challenges, including voltage sags and surges, harmonic distortions, inter-harmonics, and flicker phenomena originating from fast-switching power electronic converters [13]. Mitigating these issues requires advanced compensation technologies such as active power filters, Static VAR Compensators (SVCs), and real-time harmonic monitoring systems [14, 15]. However, such solutions add financial and operational complexity and fail to address the core structural weakness of REZ networks.

In this context, Battery Energy Storage Systems (BESS) have emerged as critical assets due to their rapid response times, high controllability, dispatchability, and suitability for providing synthetic inertia, voltage support, and frequency regulation [9]. BESS can convert variable renewable energy into dispatchable power, enhancing grid flexibility and making it indispensable for maintaining stable grid operations [16]. Nevertheless, the effectiveness of BESS depends heavily on the control strategy implemented at the inverter interface. Two primary modes exist: Grid-Following (GFL) and Grid-Forming (GFM) control. GFL inverters synchronize to the grid via phase-locked loops and inject current based on external references, making them prone to instability in low-SCR environments and incapable of supporting black-start operations [17, 18]. GFM inverters, by contrast, regulate voltage and frequency autonomously, emulate SG behavior, and provide synthetic inertia and FRT capability, making them well-suited for REZ-specific weak-grid conditions [18, 19].

While numerous studies have explored GFL and GFM control strategies independently, research remains fragmented, with limited emphasis on weak-grid behavior, multi-inverter interactions, and real-world REZ deployment constraints. Existing literature often investigates isolated aspects of frequency and voltage control, converter topologies, or device-level enhancements without offering a holistic understanding of system-level dynamics in REZ environments. Research gaps are particularly evident in three domains: (i) lack of coordinated operation between GFM and GFL inverters within BESS architectures, (ii) insufficient examination of how varying GFM:GFL penetration ratios influence frequency nadir, RoCoF, voltage resilience, and FRT performance, and (iii) absence of integrated modelling frameworks that validate control strategies under realistic, weak-grid REZ test conditions.

Technical gaps also persist in renewable-rich weak networks where traditional hardware-based protection schemes, optimization-driven reactive power controllers, and low-voltage ride-through (LVRT) enhancements often improve performance only at

local or device-specific levels. These approaches typically fail to scale across heterogeneous renewable portfolios and do not provide unified solutions for system-wide dynamic coordination. Moreover, many academic studies rely on simplified or strong-grid models, underestimating the difficulties inherent to REZ-specific weak-grid operation.

Together, these environmental, economic, operational, and technical factors clearly demonstrate the urgent need for innovative, system-level solutions that enable stable and reliable renewable integration in weak transmission networks. Addressing REZ stability challenges is fundamental not only for meeting Australia's national decarbonization objectives but also for ensuring affordable, clean, and resilient energy systems aligned with Sustainable Development Goals (SDG) 7 and 13. This thesis is motivated by these pressing needs and seeks to develop advanced control and optimization frameworks capable of strengthening REZ-based weak grids, improving FRT performance, enhancing voltage and frequency stability, and supporting the continued expansion of renewable energy across Australia.

1.2 Background on Weak Transmission Networks and Renewable Integration

The rapid expansion of renewable energy infrastructure has fundamentally transformed the technical landscape of modern power systems, particularly in countries undergoing accelerated decarbonization, such as Australia [20]. As wind, solar photovoltaics (PV), and battery storage continue to replace fossil-fuel-based synchronous generators (SGs), the physical characteristics of the electricity grid are evolving more rapidly than the underlying transmission infrastructure can adapt [21]. This transition has intensified the presence and impact of weak transmission networks in grid regions defined by low short-circuit strength, high impedance, and limited reactive power reserves. Understanding the behaviour of these weak networks and their interaction with inverter-based renewable sources is essential for ensuring reliable Renewable Energy Zone (REZ) operation [22].

Weak grids typically emerge in remote or sparsely populated areas, where long transmission corridors connect geographically dispersed renewable generation centres to major load centres [23]. These regions often have low fault current levels and poor voltage stiffness due to insufficient synchronous inertia and minimal grid reinforcement [24]. In traditional power systems, SGs inherently provide mechanical inertia, voltage regulation, short-circuit current, and frequency damping, thereby enabling stable operation during disturbances [25]. Conversely, inverter-based resources (IBRs) lack these natural stabi-

lizing characteristics [26]. Their control and synchronization are implemented through algorithms rather than physical dynamics, leaving them more sensitive to rapid system changes and fault-induced voltage depressions [27].

As renewable penetration increases within REZs, the operational challenges become more pronounced. Low system strength reduces the electrical stiffness of the grid, causing voltage and frequency deviations to propagate more rapidly [18]. Under high renewable penetration conditions, weak grids experience excessive rates of change of frequency (RoCoF), depressed frequency nadirs, and diminished fault-ride-through (FRT) capability, each of which threatens the secure operation of inverter-dominated systems [18, 28]. Moreover, the fluctuating output of wind and solar resources introduces uncertainty and variability, further complicating system balancing, fault recovery, and reserve scheduling [29]. These challenges create a strong dependency on advanced control strategies and complementary technologies to maintain acceptable voltage and frequency profiles.

In addition to stability challenges, weak grids are highly susceptible to power quality disturbances [30]. The increasing reliance on power-electronic converters leads to voltage sags, surges, harmonic distortions, inter-harmonics, and flicker effects that compromise both customer-side equipment and system-level reliability [31]. Advanced compensation devices such as Static VAR Compensators (SVCs), Static Synchronous Compensators (STATCOMs), and active power filters are commonly deployed to mitigate these issues [32]. However, these technologies alone do not fully address the structural weaknesses of REZ-based transmission networks nor the increasing operational complexities introduced by high levels of IBR penetration.

Compounding these challenges is the non-dispatchable nature of renewable resources. Solar and wind generation depend on environmental conditions and therefore cannot maintain a constant output [33]. This intermittency reduces the predictability of supply, stressing system reserves and leading to over-generation or under-generation events. As a result, power systems operating within weak REZs require additional flexibility sources, capable of absorbing surplus energy and injecting or regulating power during deficits.

Battery Energy Storage Systems (BESS) have gained prominence as a critical technology for addressing these challenges [34, 35]. BESS can convert variable renewable resources into dispatchable energy, respond rapidly to disturbances, and provide synthetic inertia, voltage support, and frequency regulation [36]. Yet, the degree to which BESS can stabilise weak grids depends heavily on its inverter control strategy. Traditional GFL inverters synchronize to the grid through a phase-locked loop and inject

current based on external voltage references [37]. While effective in strong grids, GFL inverters can destabilise weak grids due to their dependence on a reliable voltage waveform. In contrast, GFM inverters generate voltage and frequency autonomously, emulating synchronous generator behaviour and providing vital services such as inertia emulation, black-start capability, and enhanced FRT performance [17].

The growing recognition of the importance of GFM inverters has revitalised research efforts on modelling methodologies, stability metrics, and coordination strategies for mixed GFM-GFL deployments [38]. However, existing academic literature remains fragmented, with many studies analysing frequency regulation, voltage control, or converter topology in isolation. The lack of integrated frameworks for weak-grid modelling has limited the understanding of multi-inverter dynamics, hosting capacity constraints, and interaction phenomena such as control-loop oscillations in REZ conditions. Likewise, despite the deployment of GFM technology in several Australian REZ projects, including Dalrymple ESCRI, New England, and Central-West Orana, practical insights regarding controller performance, fault recovery, and interoperability with GFL devices remain underrepresented in scholarly discourse.

Furthermore, traditional approaches to enhancing weak-grid stability, such as improved LVRT schemes, localized reactive power compensation, hardware-assisted protection circuits, and optimisation-based converter tuning, have demonstrated benefit at the device or subsystem level but fall short of providing coordinated, system-wide robustness [39]. Weak grids demand advanced solutions capable of addressing multi-layer control dynamics across renewable plants, BESS units, and transmission networks. Consequently, the industry and research community are increasingly shifting toward holistic stability frameworks, combining optimal controller tuning, coordinated GFM-GFL operation, and realistic weak-grid testing environments.

In summary, integrating renewable energy into weak transmission networks poses a complex interplay of stability, power quality, dispatchability, and control challenges. These challenges are intensified in REZs, where renewable concentration is high and system strength is inherently low. Understanding the technical characteristics of weak grids and the limitations of IBR-dominated systems provides essential background for the research undertaken in this thesis. It also highlights the urgent need for innovative approaches such as cascaded controller optimisation, dynamic resilience metrics, and coordinated GFM-GFL BESS strategies to ensure secure, reliable, and scalable renewable operation within Australia's future energy landscape.

1.3 Problem Statement: Challenges of REZ Deployment in Weak Grids

Despite Australia's ambitious renewable energy targets and the strategic development of REZs, the integration of large-scale renewable generation into weak transmission networks remains one of the most significant technical challenges facing modern power systems [13, 18]. Weak grids defined by low short-circuit strength, high impedance, limited synchronous inertia, and insufficient reactive power reserves exhibit inherently fragile dynamic behaviour. When exposed to the rapid influx of inverter-based RESs, these networks experience severe degradation in voltage and frequency stability, compromising both system reliability and regulatory compliance [40].

The displacement of synchronous generators (SGs) with inverter-based resources (IBRs) exacerbates these problems [41]. Unlike SGs, which provide mechanical inertia, strong fault current support, and inherent voltage regulation, IBRs rely entirely on control algorithms for synchronization and stability support [42]. As renewable penetration increases, weak-grid REZs face elevated rates of change of frequency (RoCoF), depressed frequency nadirs, degraded FRT capability, and heightened susceptibility to fault-induced voltage instability [43]. These conditions threaten secure system operation, particularly during disturbances when multiple IBRs may disconnect simultaneously, increasing the risk of cascading failures.

Compounding these issues is the non-dispatchable and variable nature of renewable energy, which introduces unpredictable fluctuations in power output [42]. Weak networks lack sufficient flexibility and system strength to absorb these fluctuations without significant control intervention [44]. Furthermore, power quality challenges, including harmonic distortion, interharmonics, flicker, and rapid voltage deviations, become more prominent in inverter-dominated environments, where the dynamic behaviour of power electronic converters drives additional stress on transmission equipment and sensitive loads [41].

Although BESS have emerged as an essential asset for supporting renewable integration in weak grids, their effectiveness depends critically on the inverter control mode employed [35]. Conventional GFL inverters are inadequate in low-SCR environments because they depend on externally provided voltage references that deteriorate under weak-grid conditions [34]. GFM inverters can overcome many of these limitations by emulating synchronous generator characteristics, but deploying them at scale introduces new challenges, including stability interactions, controller tuning complexities, and un-

certainties in multi-inverter coordination [37]. The absence of unified frameworks that integrate GFM and GFL behaviour within BESS architectures further restricts their stabilizing potential.

Current research and industry practices often address only isolated aspects of the problem such as improving low-voltage ride-through (LVRT) performance, tuning converter protection systems, or implementing localized reactive power compensation. These approaches are insufficient for REZ environments, where system-wide interactions between plant-level controls, network characteristics, and inverter dynamics require coordinated, multi-layered solutions. Moreover, most existing studies rely on simplified grid conditions or strong-grid assumptions, leading to limited insight into the true operational challenges of REZs.

As a result, a critical gap exists in developing holistic, scalable, and adaptive control and optimisation strategies tailored to the complexity of REZ-based weak transmission networks. Specifically, there is a lack of:

- Unified optimisation frameworks that tune plant-level, network-level, and converter-level controllers under weak-grid conditions.
- Quantitative resilience metrics capable of assessing both transient and long-term stability for renewable-rich networks.
- Coordinated BESS control strategies that blend GFM and GFL modes based on system severity.
- Parametric understanding of how varying GFM:GFL contributions influence frequency response, voltage resilience, and FRT performance.
- Realistic weak-grid simulation environments that reflect REZ-specific constraints and multi-inverter interactions.

These unresolved challenges collectively hinder Australia's ability to integrate renewable energy at the scale envisioned for REZs. Addressing them is essential for achieving a stable, reliable, and future-ready power system capable of delivering on national decarbonization commitments. This thesis is therefore motivated by the urgent need to develop advanced, system-level solutions that strengthen weak-grid resilience, enhance renewable hosting capacity, and support the secure expansion of REZ-based renewable generation.

1.4 Research Aim and Objectives for Strengthening REZ-Based Weak Networks

The integration of large-scale renewable energy into Australia's Renewable Energy Zones (REZs) introduces complex stability challenges arising from low system strength, high inverter penetration, and reduced inertia across weak transmission corridors. As established in the preceding sections,Äîand reinforced by the literature review presented in Chapter 2, two technological domains emerge as central enablers for addressing these challenges:

1. **Battery Energy Storage Systems (BESS)** as dispatchable, fast-acting stabilising assets; and

2. **Grid-Forming (GFM) and Grid-Following (GFL) inverters** as foundational control mechanisms for renewable-dominated grids.

Weak-grid conditions exacerbate voltage instability, frequency deviations, fault vulnerability, and adverse multi-inverter interactions. These issues require system-level strategies that move beyond traditional device-centric improvements. The first part of Chapter 2 literature review highlights the increasing importance of BESS in maintaining grid resilience under high renewable penetration, while the second part underscores the critical need for coordinated GFM-GFL inverter behaviour tailored to REZ operating environments. Together, these insights establish a clear need for optimisation frameworks and adaptive control mechanisms purpose-built for weak-grid REZs.

In response to the technical, operational, and stability challenges identified throughout the preceding sections, this thesis advances a focused research agenda that aligns emerging inverter technologies with the stability requirements of weak-grid Renewable Energy Zones. Grounded in the research gaps identified in earlier studies and supported by the comprehensive literature review in Chapter 2, the following research aim and objectives have been formulated to guide the development of structured, impactful, and scalable solutions for REZ integration:

Research Aim: To develop advanced optimisation and control frameworks that enhance voltage stability, frequency resilience, and fault performance in weak transmission networks characteristic of Australia's REZs. The aim is achieved through two complementary objectives addressing key REZ integration challenges.

Objective 1: Cascaded Control Optimisation. To develop a multi-layer controller optimisation framework that tunes plant, electrical, and generator-level controllers to enhance voltage stability and FRT performance.

This objective introduces two major contributions:

- Enhanced PSO-based multi-layer controller coordination.
- Dynamic Resilience Metric (DRM) combining voltage deviation, fault duration, and post-fault recovery.

Objective 2: Severity-Aware GFM-GFL BESS Coordination. To develop a severity-aware coordinated control mechanism that adaptively blends GFM and GFL operation to improve frequency and voltage resilience in weak-grid REZs.

This objective introduces three major contributions:

- Disturbance severity index-driven inverter mode switching.
- Analysis of GFM:GFL ratios on RoCoF, nadir, and voltage recovery.
- Comparative assessment of Droop vs. VSM based GFM control.

To support these objectives and frame the analytical scope, the next section presents the research questions that guide the investigation of REZ-based weak grid challenges.

1.5 Research Questions Guiding REZ-Weak Grid Investigation

The research aim and objectives outlined in Section 1.4 reflect two fundamental challenges associated with integrating large-scale renewable energy into weak transmission networks:

- enhancing system-wide voltage stability and fault-ride-through performance through coordinated controller optimisation, and
- improving frequency resilience and dynamic support through adaptive GFM-GFL BESS control.

To address these challenges systematically, the thesis is guided by the following two research questions:

1. **Research Question 1 (Corresponding to Objective 1)**: How can a cascaded control parameter optimisation framework be designed and implemented to improve voltage stability and fault-ride-through performance in renewable-rich weak transmission networks characteristic of REZ environments?

2. **Research Question 2 (Corresponding to Objective 2)**: How can a severity-aware coordinated GFM-GFL BESS control strategy be formulated to enhance frequency stability, voltage resilience, and overall system robustness under weak-grid conditions in Renewable Energy Zones?

These two research questions collectively support the central aim of the thesis by targeting both system-level controller optimization and inverter-level coordination, two key pathways for strengthening the operational stability of weak-grid REZs. The next section provides an overview of the methodological approach developed to address these questions.

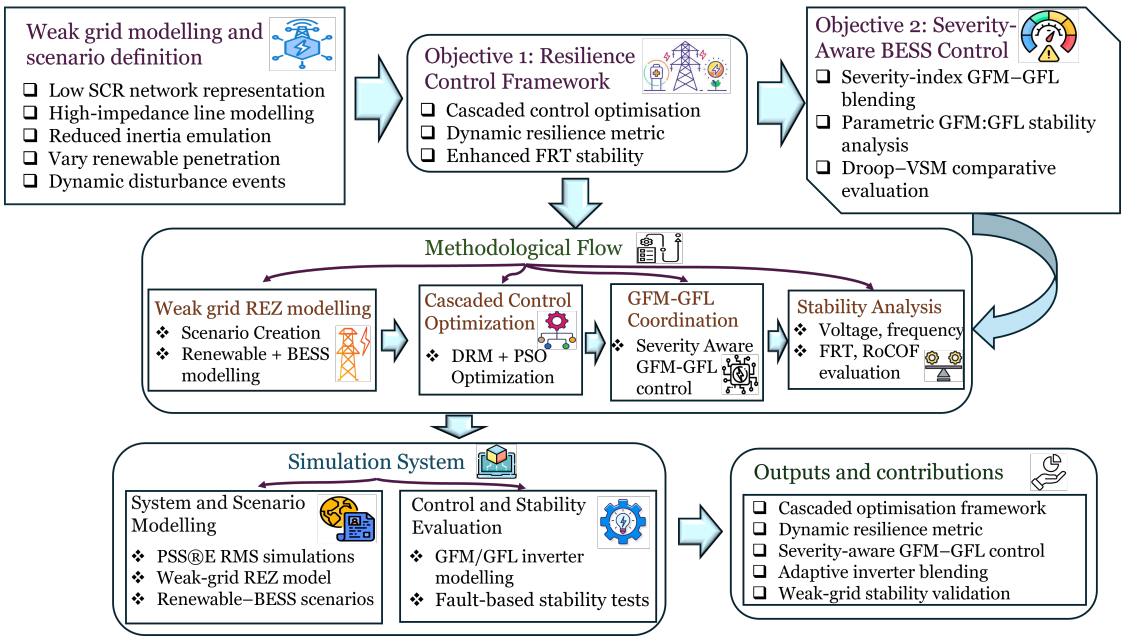


Figure 1.1: Overall methodological thesis framework

1.6 Overview of the methodological approach

The methodological approach adopted in this thesis is structured to address the two research questions outlined in Section 1.5 directly and to provide a coherent pathway for enhancing the stability of weak transmission networks characteristic of Australia's REZs.

The approach integrates system-level modelling, dynamic simulation, optimisation, and inverter control design, ensuring that both voltage stability and frequency resilience are systematically evaluated and improved. Broadly, the methodology is organized into two complementary research streams aligned with the two thesis objectives. An overall illustration of the integrated methodological flow, combining weak-grid modelling, controller development, simulation procedures, and resulting contributions, is presented in Fig. 1.1.

The first stream focuses on system-wide cascaded control parameter optimisation. This begins with the construction and adaptation of a weak-grid benchmark model representative of REZ operating conditions, incorporating renewable technologies such as photovoltaic (PV) systems, wind farms, and BESS. A hierarchical multi-layer control structure, spanning plant-level, electrical network-level, and converter-level controllers, is then established. An enhanced PSO algorithm is employed to tune these controllers in a coordinated manner. Central to this stream is a newly developed DRM that captures time-weighted voltage deviations, fault-clearing performance, and post-fault recovery characteristics, serving as the optimisation criterion under varying renewable penetration conditions. A full methodological exposition for Objective 1 is presented in Chapter 3.

The second methodological stream centres on severity-aware coordinated GFM-GFL BESS control. This begins with the development of detailed models for GFL and GFM inverter operation under weak-grid constraints. A severity index is formulated to quantify disturbance intensity and enable dynamic blending of GFL and GFM modes. Parametric analyses are carried out to evaluate the influence of varying GFM:GFL penetration ratios on key stability metrics such as frequency nadir, RoCoF suppression, and voltage recovery. Additionally, comparative assessments of prominent GFM strategies, particularly Droop and VSM control, are performed at representative penetration levels to determine their suitability for REZ conditions. A full methodological exposition for Objective 2 is presented in Chapter 4.

Both research streams rely on extensive time-domain dynamic simulations conducted on a modified Australian 14-generator test system (Area 5) configured to reflect REZ-specific weak-grid characteristics. Throughout the analysis, compliance with Australian grid codes, FRT standards, and operational constraints is ensured.

In summary, the methodology combines weak-grid modelling, hierarchical optimisation, severity-aware inverter coordination, and comparative control assessment into a unified analytical framework. This enables a comprehensive investigation of how advanced control and optimisation mechanisms can support the secure, scalable, and

resilient integration of renewable energy within Australia's emerging REZs. Building on this methodological foundation, the next subsection outlines the originality and key research contributions of the thesis.

1.7 Originality and Research Contributions

The research presented in this thesis offers several original contributions that advance the state of knowledge on renewable integration in weak transmission networks, particularly within the operational context of Australia's emerging REZs. While existing literature has extensively examined isolated aspects of renewable integration, such as device-level LVRT, inverter protection schemes, reactive power compensation, or standalone GFM control, few studies address the system-wide, multi-layered, and coordinated challenges intrinsic to REZ environments. Supported by insights from the two comprehensive review studies, this thesis introduces novel concepts, methodologies, and coordinated control strategies that fill critical gaps in the academic literature and industry practice.

The originality of this thesis stems from three overarching aspects. First, it provides a unified system-level optimisation framework that jointly considers plant-level, network-level, and converter-level control parameters, overcoming the fragmented treatment of stability mechanisms found in prior studies. Second, it introduces a new resilience-oriented performance metric that captures both transient and long-term recovery characteristics, addressing shortcomings of traditional stability indices that evaluate disturbances in isolation. Third, it develops an adaptive BESS-based GFM-GFL coordination strategy capable of dynamically adjusting inverter behaviour according to a disturbance severity approach that has received minimal attention in existing weak-grid and REZ research.

Drawing on the deep technical insights explained in chapters 3 and 4, the primary research contributions of this thesis are summarised as follows:

- Contribution 1: A Novel Cascaded Control Parameter Optimisation Framework for Weak-Grid Renewable Networks

  This thesis presents a multi-layer cascaded optimisation framework that simultaneously tunes plant, network, and converter-level control parameters using an enhanced PSO algorithm, addressing a key gap in weak-grid studies where tuning is typically performed in isolation. A central innovation is the Dynamic Resilience

Metric ($\mathscr{R}^{\Delta V\downarrow}_{t_{\text{clear}}\uparrow}$), which unifies time-weighted voltage deviation, fault-clearing duration, and post-fault recovery smoothness into a single resilience-oriented indicator. By integrating coordinated optimisation with this comprehensive metric, the proposed framework significantly enhances voltage stability and FRT performance in REZ-based weak networks, surpassing the limitations of earlier modelling and control approaches as discussed in Chapter 2, Part 1.

- Contribution 2: A Severity-Aware Coordinated GFM-GFL BESS Control Strategy for Frequency and Voltage Stability Enhancement

  The thesis develops a severity-aware BESS control framework that adaptively blends GFL and GFM modes according to the real-time intensity of system disturbances. A novel severity index governs this transition, enabling efficient GFL operation during mild disturbances and robust GFM support during severe faults. This contribution fills a critical research gap identified in Chapter 2, Part 2, where coordination between GFM-GFL inverters, particularly within BESS architectures, remains largely unexplored. The framework is further supported by a parametric analysis of GFM:GFL penetration ratios, revealing how different inverter mixes influence RoCoF suppression, frequency nadir, FRT capability, and voltage resilience. Additionally, the thesis provides a comparative evaluation of Droop vs VSM control at representative GFM shares, offering clear insights into their relative suitability for weak transmission conditions commonly found in REZs.

- Contribution 3: A Unified Stability Enhancement Pathway for REZs

  By integrating the outcomes of the cascaded optimisation framework (Contribution 1) and the severity-aware GFM-GFL coordination strategy (Contribution 2), this thesis establishes a unified, scalable, and REZ-specific pathway for improving stability in renewable-rich weak transmission networks. The combined contributions offer a holistic solution that addresses voltage stability, frequency resilience, transient recovery, inverter coordination, and grid-code compliance, thereby supporting secure and reliable operation of REZs.

In summary, this thesis provides original, system-level contributions that bridge key research gaps and advance the practical feasibility of high-renewable penetration in weak-grid REZs. The combined methodological and control solutions developed in this work offer a robust foundation for future research and deployment of stable, scalable,

and resilient RESs in Australia and beyond. The next section discusses the significance of these findings within broader academic and industry contexts.

1.8 Significance of the Study

Australia's transition to high renewable penetration places increasing pressure on weak transmission networks, particularly within REZs where system strength is low and inverter-based resources dominate. Ensuring stable and reliable operation in these environments is essential for meeting national decarbonisation goals, maintaining energy security, and enabling large-scale renewable integration. This thesis contributes to this transition by developing advanced control and optimisation frameworks tailored to the operational characteristics of REZ-based weak grids.

The significance of the study arises from three key contributions. First, it addresses fundamental technical challenges, including voltage instability, FRT capability, and frequency vulnerability, exacerbated by the decline of synchronous generation. The proposed cascaded control optimisation framework offers a coordinated and scalable solution to these issues, improving dynamic stability without relying on costly network reinforcements.

Second, the thesis advances coordinated inverter control, an emerging requirement for renewable-dominated grids. While GFM and GFL inverters have been individually explored, their coordinated behaviour within BESS architectures remains underexamined. The severity-aware GFM-GFL control strategy introduced here provides an adaptive mechanism that enhances both steady-state efficiency and fault resilience, supporting compliance with evolving grid codes and strengthening system frequency performance.

Third, the research is directly relevant to Australia's REZ implementation efforts. Using a modified Australian weak-grid benchmark, the study quantifies how inverter penetration ratios and control strategies affect critical stability metrics, offering practical insights for planners, operators, and policymakers. These findings align with AEMO's Integrated System Plan and broader sustainability objectives under SDGs 7 and 13.

More broadly, the methodologies developed, including the $\mathscr{R}^{\Delta V\downarrow}_{t_{\text{clear}}\uparrow}$, cascaded optimisation structure, and severity-aware inverter coordination, provide system-level tools applicable to weak grids worldwide, particularly in regions with high renewable potential but limited system strength.

In summary, this study delivers technically innovative and practically relevant solutions that strengthen the stability, scalability, and resilience of renewable-rich weak

networks. The next section outlines the scope and limitations of the REZ-weak grid modelling framework employed in this thesis.

1.9 Scope and Limitations of REZ-Weak Grid Modelling

The scope of this thesis is deliberately focused on the stability challenges of integrating large-scale renewable energy into weak transmission networks, particularly within Australia's emerging REZs. Given the complexity of modern power systems and the wide range of technological, economic, and policy factors influencing renewable integration, the study concentrates specifically on the dynamic stability, control, and optimisation aspects most critical to weak-grid performance. The goal is not to provide a full-scale planning or market assessment of REZs, but rather to deliver technically robust solutions that enhance system stability under high inverter-based renewable penetration.

The research scope includes the following key elements:

- Weak-grid modelling and dynamic behaviour assessment, focusing on REZ-relevant conditions such as reduced system strength, high impedance, low short-circuit ratios (SCRs), and limited synchronous inertia.
- Hierarchical control parameter optimisation across plant-level, electrical network-level, and converter-level controllers using an enhanced Particle Swarm Optimisation (PSO) framework (Objective 1).
- Inverter control strategies for Battery Energy Storage Systems (BESS), with emphasis on severity-aware coordination between Grid-Following (GFL) and Grid-Forming (GFM) modes (Objective 2).
- Comparative evaluation of advanced GFM strategies, particularly Droop and Virtual Synchronous Machine (VSM) control, under representative weak-grid conditions.
- Use of a modified Australian 14-generator test system, adapted to replicate REZ-specific constraints such as high renewable penetration and weak-grid operating characteristics.
- Dynamic simulation studies, conducted using industry-standard power system analysis tools compliant with Australian grid code and FRT requirements.

While the thesis develops comprehensive and technically advanced frameworks, several limitations should be acknowledged to contextualise the findings and guide future research:

- Model complexity and representativeness: The test system used is a modified benchmark model rather than a full-scale, geographically detailed REZ network. Although designed to capture the essential dynamics of weak-grid behaviour, it does not account for all real-world complexities such as distributed energy resources (DER), detailed protection schemes, or phase-domain electromagnetic transients.

- Focus on control and optimisation, not market or economic analysis: The study does not examine cost-benefit analysis, market constraints, or planning investment strategies for REZ deployment. Its emphasis remains on improving technical stability metrics rather than evaluating commercial viability or policy mechanisms.

- Inverter technology scope: The thesis focuses specifically on GFM and GFL control modes for BESS. Other converter types, hybrid storage technologies, and advanced FACTS devices (e.g., STATCOMs, SVCs) are referenced but not modelled in detail.

- Limited consideration of communication delays and cyber-physical interactions: Although inverter coordination is studied, communication constraints, cyber-security risks, and wide-area control delays are outside the scope.

- Renewable resource variability: Intermittency is captured implicitly through dynamic disturbances rather than through long-term stochastic renewable forecasting or probabilistic resource modelling.

Despite these limitations, the research provides a robust and scalable foundation for future studies. The optimisation frameworks, adaptive control mechanisms, and resilience metrics developed herein can be readily extended to more detailed network models, multi-inverter configurations, and industry datasets. As such, the scope and limitations of this thesis reflect a balance between depth and practicality, enabling rigorous exploration of critical weak-grid challenges while maintaining relevance to real-world REZ deployment. In addition to the above technical scope, it is important to clarify the methodological boundaries within which this research has been conducted. These aspects are outlined in the following subsection.

1.9.1 Scope and Limitations of the Thesis

This thesis is conducted within a simulation-based framework, with the following methodological scope and limitations:

- **Simulation-level analysis:** All analyses are performed using industry-standard power system tools within a controlled computational environment, without physical system implementation.
- **RMS-based dynamic modelling:** The study employs RMS (phasor-domain) simulations, which are well-suited for analysing large-scale system behaviour, control interactions, and stability performance under network-level disturbances.
- **Exclusion of EMT modelling:** While RMS modelling provides computational efficiency and is widely adopted for system-level studies, it does not capture fast electromagnetic transients and converter switching dynamics with the same fidelity as Electromagnetic Transient (EMT) simulations. Therefore, detailed EMT-based validation of inverter-level dynamics is beyond the scope of this work.
- **No hardware or real-time validation:** The research does not include hardware-based or real-time validation methods such as Hardware-in-the-Loop (HIL) or Real-Time Digital Simulator (RTDS) implementations.
- **Benchmark test system validation:** The proposed control strategies and optimisation frameworks are validated through extensive simulation studies using a modified benchmark weak-grid test system, specifically the Simplified Australian 14-generator system adapted to reflect REZ-relevant operating conditions.
- **Justification of scope:** These methodological boundaries are intentionally defined to ensure a focused and in-depth investigation of weak-grid stability challenges and control optimisation, while maintaining computational tractability and reproducibility.
- **Future research directions:** Future work may extend this research by incorporating EMT-based modelling, real-time simulation platforms, and experimental validation to further enhance practical applicability.

The next subsection introduces key terms and definitions relevant to REZs and weak transmission networks to support clarity throughout the thesis.

1.10 Definition of Key Terms Related to REZ and Weak Transmission Networks

This section provides definitions of key technical terms used throughout the thesis. These definitions establish clarity and consistency in the context of renewable integration, weak-grid stability, and inverter-based control systems.

- Renewable Energy Zone (REZ): A geographically defined area with high-quality renewable resources (such as wind and solar) that is supported by coordinated transmission planning and investment. REZs enable large-scale renewable generation to be efficiently connected and exported to load centres. They are central to Australia's renewable expansion strategy and often coincide with weak-grid regions due to remote geographic locations.

- Weak Transmission Network (Weak Grid): A power system region characterised by low short-circuit strength, high network impedance, limited synchronous inertia, and reduced voltage stiffness. Weak grids exhibit heightened sensitivity to disturbances, such as faults or sudden changes in power injection, and are more susceptible to instability when dominated by inverter-based resources.

- Short-Circuit Ratio (SCR): A numerical indicator of system strength defined as the ratio of the short-circuit current available at the point of interconnection to the rated current of the connected generator or inverter. Low SCR values indicate weak-grid conditions where voltage regulation and inverter stability are more challenging.

- Inverter-Based Resources (IBRs): Renewable or energy storage technologies, such as photovoltaic (PV) systems, wind turbines, and Battery Energy Storage Systems (BESS), that interface with the grid through power electronic converters. Unlike synchronous generators, IBRs do not inherently provide inertia or fault current, making their behaviour heavily dependent on control algorithms.

- Grid-Following (GFL) Inverter: An inverter control mode that synchronises with the grid using a phase-locked loop (PLL) and injects controlled current based on externally provided voltage and frequency references. GFL inverters perform well in strong grids but struggle under weak-grid conditions due to their dependence on accurate voltage waveforms.

- Grid-Forming (GFM) Inverter: An inverter control mode that establishes voltage and frequency autonomously, emulating synchronous generator behaviour. GFM inverters provide virtual inertia, frequency support, and improved fault-ride-through (FRT) capability, making them essential for weak-grid and islanded operation.

- Battery Energy Storage System (BESS): An energy storage technology, typically lithium-ion based, that provides rapid charge and discharge capability. BESS units support voltage and frequency stability, offer synthetic inertia, absorb renewable variability, and enhance system resilience in weak-grid environments.

- Fault-Ride-Through (FRT): The ability of a generating unit or inverter to remain connected and support the grid during and after a fault. FRT requirements ensure that renewables contribute to system recovery rather than disconnecting during disturbances. In weak grids, maintaining adequate FRT performance is essential for preventing cascading outages.

- Rate of Change of Frequency (RoCoF): The speed at which system frequency changes following a disturbance, typically measured in hertz per second (Hz/s). High RoCoF values indicate low system inertia and can trigger protection schemes, making RoCoF suppression crucial in renewable-dominated grids.

- Dynamic Stability: The capability of the power system to maintain synchronism and recover acceptable operating conditions following short-term disturbances such as faults, switching events, or rapid changes in renewable output. It includes aspects of voltage stability, frequency stability, and transient recovery.

- Dynamic Resilience Metric ($\mathscr{R}_{t_{\text{clear}}\uparrow}^{\Delta V\downarrow}$): The DRM is introduced in this thesis as a comprehensive performance indicator to quantify a power system's ability to withstand and recover from disturbances under weak-grid conditions. In simple terms, it evaluates how severely the system is affected during a fault and how effectively it returns to stable operation.

  Technically, the DRM combines time-weighted voltage deviations, fault-clearing duration, and post-fault recovery characteristics into a unified quantitative metric. This enables simultaneous consideration of both disturbance severity and recovery performance. The DRM is used as the primary objective function in the optimisation framework (Objective 1), guiding the tuning of control parameters to enhance overall system resilience.

- Severity Index ($S(t)$): The Severity Index is defined as a real-time quantitative measure of disturbance intensity, representing how critical a system event is at any given instant. It provides an intuitive indication of whether the system is experiencing a mild or severe disturbance.

  In this thesis, the Severity Index is computed based on key system indicators such as frequency deviation, rate of change of frequency (RoCoF), and voltage deviation, normalised with respect to grid-code limits. This index governs the adaptive coordination between Grid-Following (GFL) and Grid-Forming (GFM) modes in the proposed BESS control framework. Specifically, lower severity values favour GFL-dominant operation for fast current-limited response, while higher severity values trigger increased GFM contribution to provide voltage support and inertia-like behaviour.

- Particle Swarm Optimisation (PSO): A population-based metaheuristic optimisation algorithm inspired by swarm intelligence. In this thesis, an enhanced PSO variant is employed to coordinate control parameter tuning across multiple hierarchical control layers in weak-grid renewable systems.

These key terms provide the technical foundation for the methodologies, analyses, and discussions presented in subsequent chapters. Their definitions reflect the specific operational and modelling requirements associated with REZs and weak transmission networks. The next subsection outlines the overall structure of the thesis and how each chapter contributes to the research aims.

1.11 Structure of the Thesis

This thesis is organised into five chapters, each building upon the previous to develop a comprehensive understanding of renewable integration challenges in weak transmission networks and to present the proposed optimisation and control frameworks tailored to REZs. The structure is designed to ensure a logical progression from background context to methodological development, technical implementation, and final evaluation.

- Chapter 1 - Introduction: This opening chapter outlines the broader context and motivation for studying renewable integration within weak-grid REZ environments. It presents the problem statement, research aim, objectives, research questions,

methodological overview, originality, and scope. Key terms relevant to weak-grid stability and inverter-based control are also defined.

- Chapter 2 - Literature Review: This chapter synthesises existing research on two major themes:
  - Battery Energy Storage Systems (BESS) for REZ and weak-grid integration, including challenges in system strength, power quality, volatility management, and energy storage deployment.
  - GFM and GFL inverter control strategies, focusing on modelling frameworks, stability considerations, and Australian REZ deployment insights. The review establishes key limitations in prior work and identifies the research gaps that motivate the contributions of this thesis.
- Chapter 3 - Cascaded Control Parameter Optimisation Framework: This chapter presents the complete methodology, modelling approach, and simulation analysis for Objective 1, which focuses on improving voltage stability and FRT capability in weak transmission networks. It introduces the modified Australian 14-generator test system (Area 5), describes the multi-layer cascaded optimisation structure, formulates the $\mathscr{R}^{\Delta V\downarrow}_{t_{\text{clear}}\uparrow}$, and evaluates system performance under varying levels of renewable penetration. Extensive simulation results demonstrate the effectiveness of the proposed optimisation framework.
- Chapter 4 - Severity-Aware Coordinated GFM-GFL BESS Control Framework: This chapter delivers the full technical development and analysis for Objective 2, which aims to enhance frequency resilience and voltage support through coordinated BESS inverter control. It details the formulation of the severity index, development of adaptive GFM-GFL control logic, modelling of inverter strategies (including Droop and VSM), and parametric studies of GFM:GFL penetration ratios. Dynamic simulation results highlight improvements in RoCoF suppression, frequency nadir, voltage recovery, and overall resilience in REZ-specific weak-grid conditions.
- Chapter 5 - Conclusions and Future Work: The final chapter summarises the key findings of the research, emphasising contributions made to weak-grid stability enhancement and REZ integration. It reflects on the effectiveness of the cascaded optimisation and severity-aware control frameworks and outlines opportunities for future work, such as full-scale REZ modelling, hybrid storage coordination, cyber-physical considerations, and advanced grid-forming strategies.

In summary, the thesis is structured to provide a coherent and detailed progression from foundational concepts to advanced methodological development and system-level validation. This structure enables a comprehensive exploration of how optimisation techniques and coordinated inverter control can strengthen the operational resilience of REZs in weak transmission networks.

CHAPTER 2

Comprehensive Literature Review on Renewable Grid Integration

Chapter Composition

This chapter presents a **two-part literature review** that establishes the technical foundations and research gaps associated with stability enhancement in Renewable Energy Zones (REZs). The **first part** reviews the role of BESS in weak transmission networks, examining system strength limitations, voltage instability mechanisms, FRT challenges, and existing approaches to controller tuning and coordination. The **second part** focuses on inverter-based control strategies, analysing GFL and GFM behaviour, advanced GFM techniques such as droop and VSM control, and the interaction challenges that arise in multi-inverter weak-grid environments. Collectively, the review highlights significant gaps in unified control optimisation, coordinated GFM-GFL operation, and REZ-specific weak-grid modelling, thereby providing a clear foundation for the methodological developments presented in Chapters 3 and 4.

** 1st Part Literature Review **

The first part of this literature review examines the role of BESS in supporting renewable energy integration within weak transmission networks characteristic of REZs. It explores how BESS enhance system stability through voltage support, frequency regulation, syn-

thetic inertia provision, and improved fault-ride-through performance. By reviewing control strategies, EMS architectures, and practical deployment experiences, this section establishes the foundational understanding of how BESS address the operational challenges of weak grids and enables reliable large-scale renewable integration.

2.1 Introduction

The global shift towards sustainable energy systems has intensified the focus on renewable energy sources (RESs) as a solution to the environmental and economic challenges posed by fossil fuels. In Australia, fossil fuels have historically dominated electricity generation, accounting for over 86% of the total energy supply [45]. However, this dependency has resulted in significant environmental degradation, including high per capita greenhouse gas emissions, rising sea levels, and severe weather events [4]. Public health has also been impacted, with an increase in respiratory and cardiovascular diseases linked to air pollution caused by sulphur dioxide and nitrogen oxides. The urgent need for clean energy alternatives has become particularly evident in regions like Far North Queensland (FNQ), where reliance on diesel generators is both economically unsustainable and environmentally harmful [46]. Additionally, Australia's reliance on imported liquid fuels highlights the vulnerability of fossil fuel systems to global market fluctuations, further emphasizing the need for a transition to sustainable energy solutions. Aging fossil fuel infrastructure exacerbates these issues. Many coal-fired power plants are nearing the end of their operational lifespans, presenting both an opportunity and a challenge for Australia's energy transition [47]. The continued reliance on fossil fuels delays the adoption of renewable systems, perpetuating environmental harm and economic instability.

To address these pressing challenges, the Australian Government has accelerated the adoption of RE through the establishment REZs [45]. To promote REZs integration, Figure 2.1 demonstrates the remarkable growth in renewable electricity generation between 2019-2020 and 2022-2023, with total output increasing from 59,930.3 GWh to 93,112.3 GWh [4]. This statistic reflects a strong commitment to global climate agreements, such as the Paris Agreement, and highlights the critical role of wind and solar energy in the nation's energy mix [46]. At the same time, the increasing frequency of extreme weather events, such as bushfires and floods, underscores the urgency for robust climate action [47]. These efforts are further supported by localized initiatives, including the Australian Capital Territory's (ACT) adoption of electric vehicles and renewable-powered public

transport, which provide scalable examples of decarbonization [48]. Additionally, universities and private institutions are championing net-zero innovations, fostering systemic change [49]. However, the transition remains challenging due to persistent barriers such as policy fragmentation and social inequities. Despite these obstacles, market-driven solutions and inclusive governance frameworks provide a promising pathway to align environmental sustainability with economic growth [50].

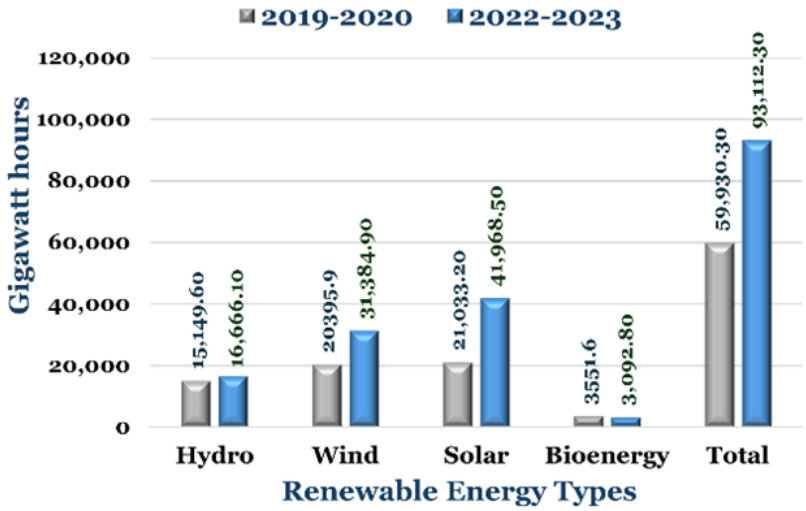


Figure 2.1: Electricity generation growth in Australia from RESs from 2019-2020 to 2022-2023

Strengthening these efforts, RE technologies have proven their ability to provide diverse and scalable solutions to the limitations of fossil fuels. For instance, tools like spatial decision-support systems enable efficient planning and deployment of wind, solar, and geothermal resources, optimizing energy output and minimizing environmental impact [51]. In urban areas, hybrid renewable systems that integrate solar, wind, and biomass enhance reliability and reduce lifecycle costs [52]. Furthermore, innovations like building-integrated photovoltaics (BIPV) and smart grids improve energy efficiency and facilitate seamless integration into existing infrastructure [53]. Remote regions also stand to benefit significantly, with studies indicating over 90% emissions reductions when transitioning from diesel generators to renewables [54]. In addition to addressing environmental concerns, RE fosters economic growth and social equity through mechanisms such as public-private partnerships and feed-in tariffs [55]. While these advancements are promising, challenges in integrating renewables into existing infrastructure remain substantial, particularly in balancing energy supply and demand [56].

Among the most pressing challenges, ensuring grid stability remains a significant obstacle, as inverter-based renewable systems lack the inherent inertia provided by traditional synchronous generators (SGs). This increases the risk of frequency deviations during disturbances and complicates operations, particularly in regions with high renewable penetration [57]. Voltage stability issues add another layer of complexity, necessitating solutions such as virtual inertia emulation, grid-forming inverters (GFI), and Flexible AC Transmission Systems (FACTS) to maintain reliable grid operations [57], [58]. These technologies are critical for ensuring that RE can be seamlessly integrated into weak grids. The classification of a power grid as 'weak' or 'strong' is primarily determined by technical factors such as short-circuit strength, system impedance, and inertia [59, 60]. Strong grids possess high fault current capacity, low impedance, and abundant synchronous generation, providing robust voltage and frequency stability during disturbances [61]. In contrast, weak grids are characterized by lower short-circuit strength, higher impedance, and reduced inertia, making them more vulnerable to instabilities and posing greater challenges for the integration of renewable energy systems, particularly inverter-based resources [59, 60]. Features such as long transmission distances, high concentrations of renewable energy, and diminished fault ride-through capabilities further exacerbate weak grid conditions [61]. In this study, the term "weak grid" specifically refers to power networks exhibiting these characteristics, where renewable energy integration has a pronounced impact on system stability.

In addition to grid stability, the variability of RE introduces significant power quality challenges, such as voltage sags, surges, and harmonic distortions caused by nonlinear inverter behavior [62]. Advanced mitigation technologies, including active power filters and Static VAR Compensators (SVCs), play a vital role in addressing these issues and ensuring consistent grid performance [30]. Furthermore, high-order non-linearity issues, including inter-harmonics and flicker, arise from the dynamic nature of RES and power converters. Addressing these requires the implementation of real-time monitoring systems and harmonic compensators to maintain stability [31], [63].

Another critical challenge is the non-dispatchable nature of RESs, such as solar and wind, which are dependent on weather conditions and cannot provide consistent energy output. BESSs offer a transformative solution by converting non-dispatchable resources into dispatchable ones, thereby enhancing grid flexibility and reliability [9]. Furthermore, hybrid energy storage systems (HESSs) that incorporate advanced technologies like hydrogen storage provide additional benefits, ensuring a steady energy supply and cost efficiency while addressing the intermittency of renewables [64].

Significant research and development efforts are being undertaken by academic institutions, industry leaders, and government agencies worldwide to integrate large-scale BESSs into power systems, particularly those characterized by high RE penetration and weak grid conditions, to maintain a reliable, uninterrupted power supply. Table 2.1 presents a selection of recent review articles on ESSs, with a particular focus on integrating REZs into weak grids using BESS. This comparative analysis highlights the growing significance of this research area while underscoring the unique contributions of this study. By comparing existing literature with the insights synthesized in this section, the table establishes the foundation upon which the subsequent research builds and highlights the importance of conducting this comprehensive literature review.

This study provides a comprehensive review of RES integration into weak grids, emphasizing the role of Battery Energy Storage Systems (BESSs) in addressing key challenges. The primary contributions arising from this literature review are as follows:

- **Critical Analysis:** Identifies challenges in renewable energy integration within weak grids, including grid stability, power quality, and non-dispatchable generation.
- **Evaluation of ESSs:** Reviews various Energy Storage Systems (ESSs), particularly non-BESS technologies, discussing their classifications, fundamentals, advantages, limitations, applications, and operational complexities.
- **BESS Technologies:** Examines different BESS types, their foundations, applications, and advantages over non-BESS solutions, highlighting their effectiveness in mitigating renewable intermittency and enhancing grid reliability in weak zonal grids.
- **BESS Deployment Strategies:** Explores BESS architectures (AC, DC, and hybrid) in islanded and grid-connected weak grids, covering advanced control strategies, energy management techniques, and real-world case studies.
- **Pathway for Large-Scale Adoption:** Beyond summarizing BESS benefits, this review proposes a strategic transition plan to accelerate large-scale BESS adoption in renewable-rich weak grids. This supports a sustainable, clean energy future aligned with the United Nations Sustainable Development Goals (UNSDGs) 7 and 13.

In summary, analyzing the obstacles to RE integration in weak grids, reviewing various ESSs (with a focus on non-battery solutions), examining BESS technologies in weak

grid contexts, deploying appropriate BESS zonal weak grid architectures and control and energy management strategies (EMSt), and advocating for BESS in renewable-rich weak grids are the primary contributions of this study.

Table 2.1: Recent review articles on RE integration and BESS in weak grids.

Ref	RE challenges in weak grids	ESS applications	Limitations of Non-battery ESS	Classification of BESS	Role of BESS in zonal weak grids	Control Strategies in BESS for weak grids	EMS involved in BESS for weak grids	Transition pathway to promote BESS for REZs integration in weak grids
[65]	✗	✓	✓	✗	✗	✗	✗	✗
[62]	✗	✓	✓	✗	✗	✗	✗	✗
[30]	✗	✗	✗	✗	✗	✗	✗	✗
[66]	✓	✗	✗	✗	✗	✗	✗	✗
[67]	✗	✗	✗	✗	✗	✗	✗	✗
[34]	✗	✗	✗	✗	✗	✗	✗	✗
[68]	✗	✓	✓	✓	✗	✗	✗	✗
[69]	✗	✗	✗	✗	✗	✗	✗	✗
[70]	✗	✗	✗	✗	✗	✗	✗	✗
[71]	✗	✗	✗	✗	✗	✗	✗	✗
[35]	✗	✗	✗	✗	✗	✗	✗	✗
[36]	✗	✗	✗	✗	✗	✗	✗	✗
[72]	✗	✗	✗	✗	✗	✗	✗	✗
[73]	✗	✗	✗	✗	✗	✗	✗	✗
This research	✓	✓	✓	✓	✓	✓	✓	✓

The first part of the review is organized into ten sections, each addressing critical aspects of RE integration and energy storage solutions in weak grids. The remainder of this review is organized as follows: Section 2.2 discusses the review process used in this study. Section 2.3 examines the challenges of integrating RE into weak grids, focusing on threats to grid stability and reliability. Section 2.4 explores ESSs as a potential solution to these challenges, providing an overview of their capabilities and limitations. Section 2.5 addresses the challenges associated with ESS technologies in weak grids and introduces BESS as a promising alternative to overcome these limitations. Section 2.6 highlights advancements in BESS technologies and their applications in power grids, emphasizing their role in improving grid performance and RE utilization. Section 2.7 discusses power management control strategies and algorithms essential for optimizing BESS performance in diverse weak grid scenarios. Sections 2.8 and 2.9 focus on the practical applications of BESS in electrical grids, demonstrating their effectiveness in mitigating RE integration challenges. Section 2.10 proposes transition pathways for large-scale BESS integration and outlines directions for future research in this field.

Finally, Section 2.11 concludes this review by summarizing key findings and underscoring the importance of continued innovation in developing sustainable energy systems.

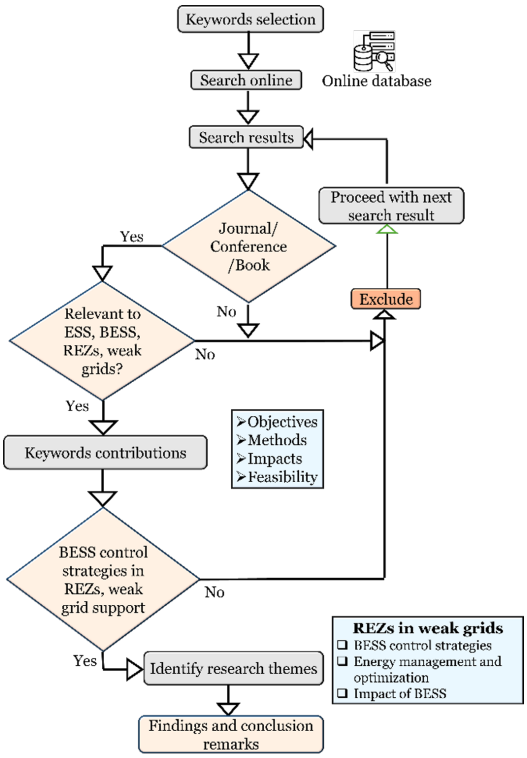


Figure 2.2: Flowchart of article selection method used in this work.

2.2 Review Process

The literature search and selection process for this review followed a systematic approach to ensure a comprehensive and structured analysis of recent advancements in BESSs for REZs and weak transmission networks. The review primarily considered recently published and highly relevant studies, with sources obtained from academic databases. The search was conducted using relevant keywords related to BESS applications in weak grids, REZs, control strategies, grid stability, and EMS. The retrieved publications were filtered and categorized based on their relevance to keywords, such as "ESS", "BESS control strategies", "energy management", and "weak grids". The publication is sorted from the search list depending on the approach, such as BESS control strategies and energy management based on REZs integration in a weak grid scenario. The article search and selection process is displayed in figure 2.2. The information was collected from scholarly resources such as journals, conferences, books and websites. Figure 2.3 shows

the percentages of information sources. Similarly, Figure 2.4 illustrates the percentage distribution of the articles across various publishers.

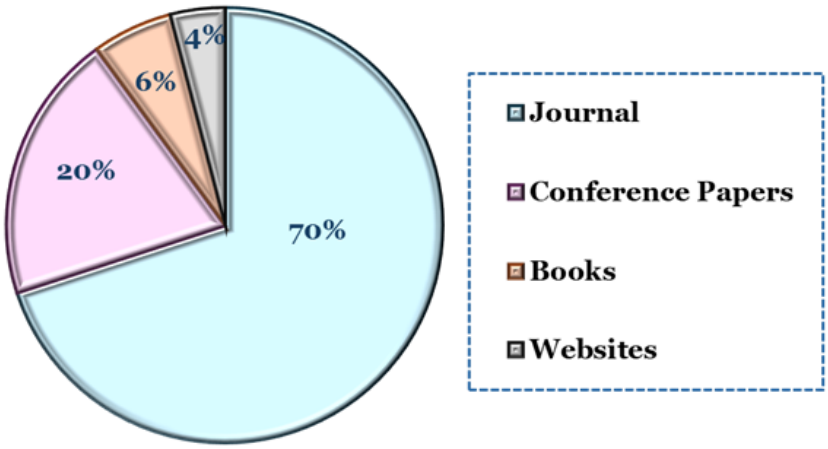


Figure 2.3: Sources of articles used in this journal

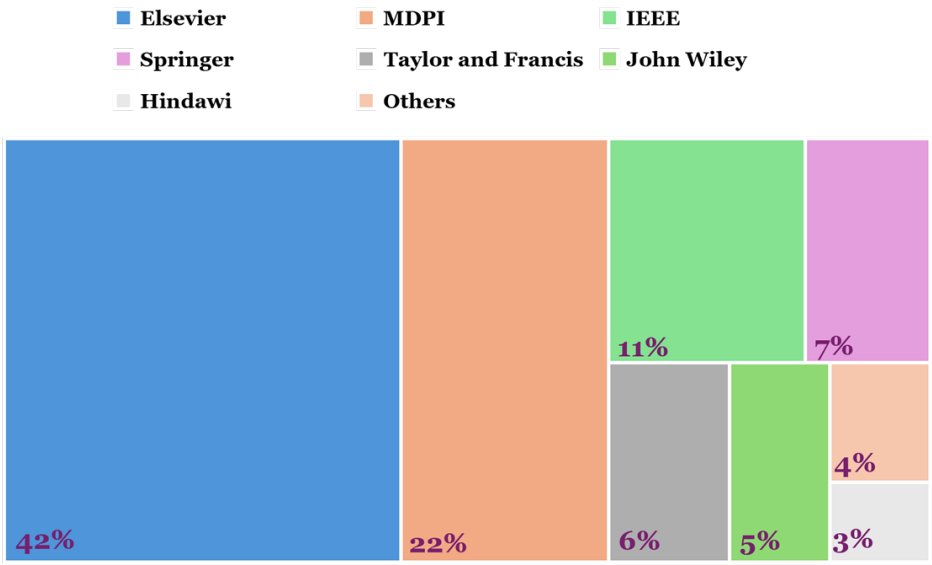


Figure 2.4: Percentage of articles published by publisher

2.3 Renewable weak grid difficulties and threats

The integration of RESs into weak grids presents a complex landscape of technical, operational, and structural challenges. Weak grids, defined by their low system strength, high impedance, and limited short-circuit capacity, are inherently less robust and more

vulnerable to disturbances than their stronger counterparts. These vulnerabilities are magnified as the penetration of RESs increases, driven by the global transition toward sustainable energy [40]. While RE systems offer significant environmental benefits, their intermittent and weather-dependent nature introduces volatility that weak grids struggle to accommodate [74]. This imbalance sets the stage for a cascade of challenges, ranging from frequency and voltage instability to harmonic distortions and protection system inadequacies, threatening the stability, power quality, and reliability of the entire grid [40, 74, 75]. Figure 2.5 illustrates the key challenges and their overall impact on grid performance, which are examined in detail in the following subsection.

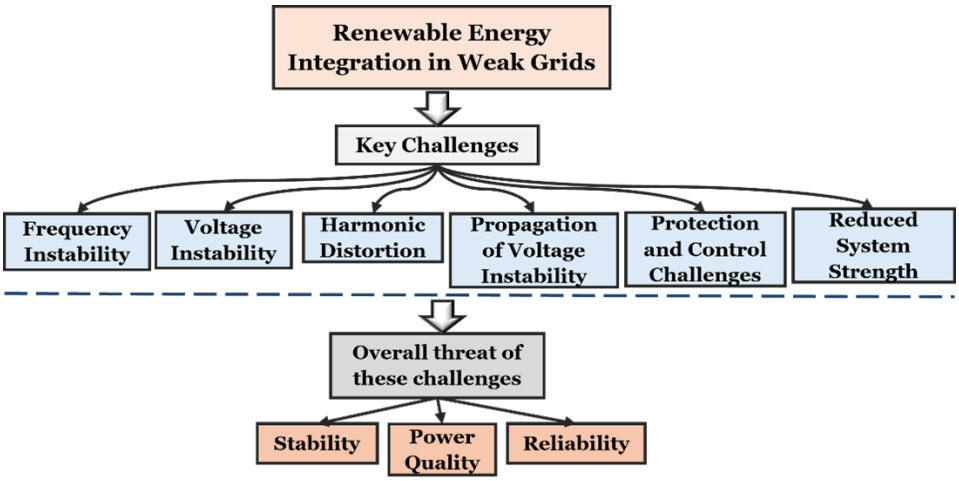


Figure 2.5: Challenges and threats of RE integration in weak grids

2.3.1 Frequency and voltage instability

Frequency and voltage instability are among the most critical challenges in weak grids. The inherent intermittency of RESs, caused by fluctuations in solar irradiance and wind speed, leads to imbalances between supply and demand (Figure 2.6a and Figure 2.6b). Weak grids, with limited inertia, are less equipped to handle these variations [74, 76]. As the displacement of conventional SGs reduces the rotational inertia traditionally used to stabilize grid frequency, weak grids become prone to faster and more severe frequency deviations during disturbances [40, 77]. Voltage instability is equally problematic. Weak grids are highly sensitive to active and reactive power fluctuations, meaning sudden changes in RESs output can result in rapid voltage dips or surges [59, 60]. This poses risks to grid-connected equipment and overall reliability. Advanced control strategies and reactive power support mechanisms are necessary to maintain voltage stability;

otherwise, weak grids face an elevated risk of cascading failures, particularly under high-RES penetration [59, 76, 77].

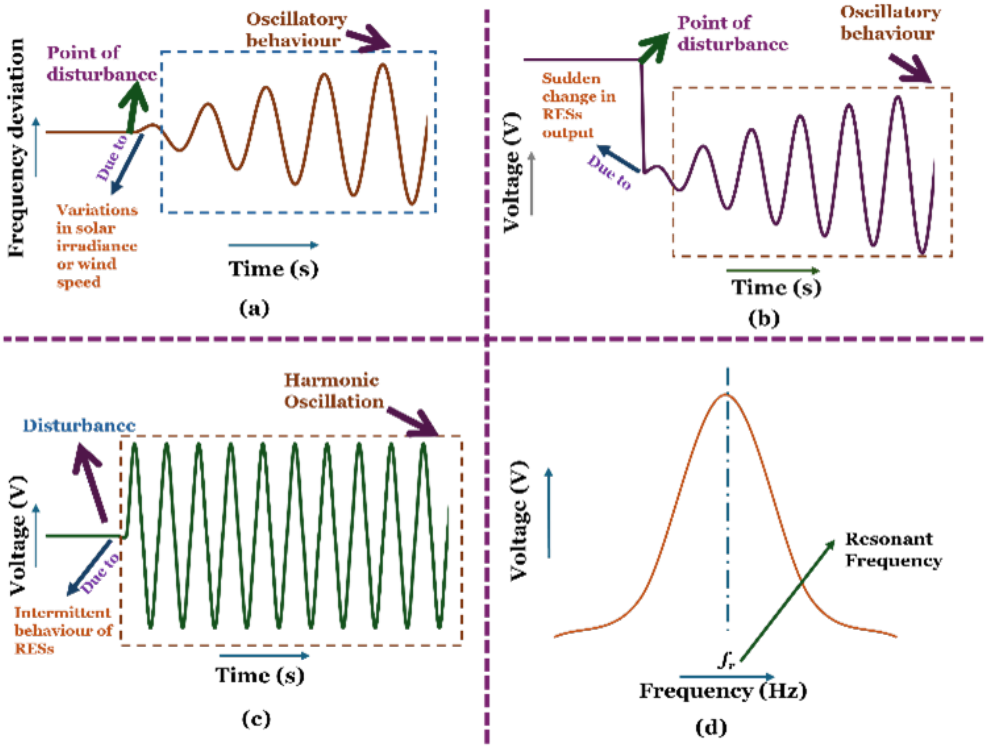


Figure 2.6: Threats of RESs integration in weak grids: (a) Frequency Instability, (b) Voltage Instability, (c) Harmonic Distortion and (d) Resonance Effect.

2.3.2 Harmonic distortions and resonance

Harmonic distortions, caused by power electronic converters in RESs, represent a significant threat to power quality in weak grids. These distortions, characterized by the presence of higher-order frequency components, degrade the quality of the voltage waveform, leading to overheating, increased losses, and equipment malfunctions [76, 77]. Weak grids, with their limited short-circuit capacity, are less able to suppress these distortions, making them more susceptible to harmonic resonance (Figure 2.6 c and d). Resonance amplifies specific frequencies, exacerbating system instability and reducing the lifespan of grid infrastructure. Advanced filters and control mechanisms are crucial to mitigating these issues [59, 74, 75].

2.3.3 Propagation of voltage instability

The propagation of voltage instability is another critical concern. Due to the high impedance of weak grids, localized disturbances are amplified and can cascade across the network [60, 78]. The replacement of SGs with inverter-based RESs further reduces reactive power reserves, intensifying the grid's vulnerability. Without enhanced reactive power compensation and fault ride-through capabilities, weak grids often experience widespread disruptions during fault conditions [40, 59, 60] as shown in Figure 2.6.

2.3.4 Protection and control challenges

Weak grids also face limitations in protection and control systems. Reduced fault current levels hinder the performance of traditional overcurrent-based protection mechanisms, delaying fault detection and isolation [60, 77]. This increases the risk of equipment damage and prolonged outages. Additionally, weak grids demand faster and more adaptive control mechanisms to respond to disturbances. However, the high impedance and reduced system strength often limit the effectiveness of conventional protection strategies. Adaptive protection schemes and dynamic grid management approaches are essential to overcome these limitations [40, 59].

2.3.5 Reduced system strength

System strength, a critical measure of a grid's ability to maintain stable voltage and frequency, is inherently low in weak grids (Figure 2.6 a and b). High-RES penetration further diminishes system strength by displacing SGs, reducing the grid's fault current capability [39], [41]. This increases susceptibility to transient oscillations, voltage instability, and reliability issues. Deploying system-strengthening measures, such as synchronous condensers (SCs) and advanced inverters, is crucial to mitigate these impacts and ensure stable grid operations [59, 76].

The next section explores how these challenges can be effectively mitigated, focusing on ESSs as a potential solution for enhancing grid stability and facilitating renewable integration.

2.4 Addressing Weak Grid Threats: ESS as a Solution for Renewable Integration

The integration of RE into weak grids poses challenges, including frequency and voltage instability, harmonic distortion, and reduced system strength, necessitating effective solutions to maintain stability, power quality, and reliability. ESSs offer a promising approach to address these issues and support the seamless integration of RESs. This section begins with a classification of ESS technologies, highlighting their diversity and flexibility. It then examines their role in enhancing grid stability, managing intermittency, and providing reactive power support. A detailed analysis of key ESS technologies is presented, covering their operating principles, advantages, limitations, and applications, followed by a comparative evaluation of their suitability under different grid conditions. Together, these discussions provide a foundation for mitigating weak-grid challenges and supporting the transition toward resilient and sustainable energy systems.

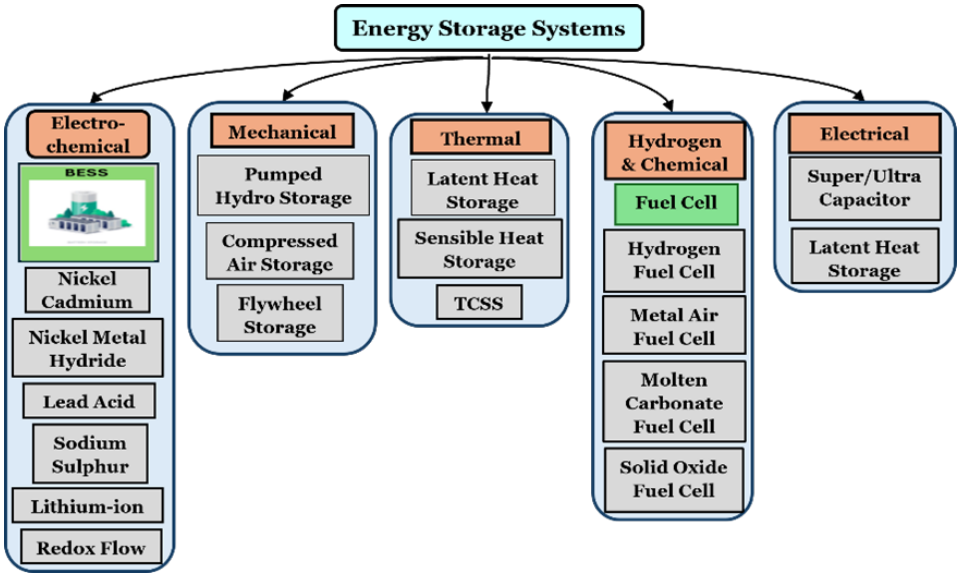


Figure 2.7: ESSs classification applying for zonal weak grids

2.4.1 Classification of ESSs and their application for REZs

The classification of ESSs is fundamental to addressing the challenges of RE integration into weak grids. ESS technologies are categorized into five principal types: Electrochemical (EC), Mechanical (Mech), Thermal (TCSS), Hydrogen and Chemical (Chem), and Electrical (Elec), each with unique characteristics suited to specific grid applications. These technologies play a pivotal role in enhancing grid stability, managing intermittency,

and supporting RE integration. Figure 2.7 and Table 2.2 provide a detailed breakdown of ESS types, highlighting their principles, applications, benefits, and limitations, and establishing the foundation for exploring their strategic implementation to address weak-grid challenges.

2.4.2 Applications offered by ESSs in weak grids

Building on the classification of ESSs in Section 2.4.1, this section examines how these technologies provide practical solutions to weak-grid challenges, as illustrated in Fig. 2.8. ESSs enable rapid frequency and voltage stabilisation (e.g., Li-ion batteries and flywheels), compensating for reduced inertia in inverter-dominated systems that have replaced traditional SGs [79].

Flow batteries and supercapacitors (SCaps) offer reactive power support in high inverter-penetration grids, while advanced technologies such as Superconducting Magnetic Energy Storage (SMES) mitigate power quality issues, including harmonics and voltage sags [80], [81]. To address intermittency, hybrid configurations (e.g., PHS with Li-ion batteries) smooth supply-demand imbalances, reduce reliance on fossil-fuel reserves, and enhance availability during peak periods [81]. ESSs also minimise RE curtailment by storing excess generation for later use.

Beyond stability, ESSs improve system resilience through black-start capability and support microgrid development, particularly in remote areas [71]. Although associated with high initial costs, their long-term benefits, including reduced dependence on peaking plants, lower maintenance, and revenue from ancillary services, enhance economic viability [82]. Moreover, enabling higher renewable penetration significantly reduces greenhouse gas emissions, reinforcing the transition toward sustainable and carbon-neutral energy systems [47], [50], [71].

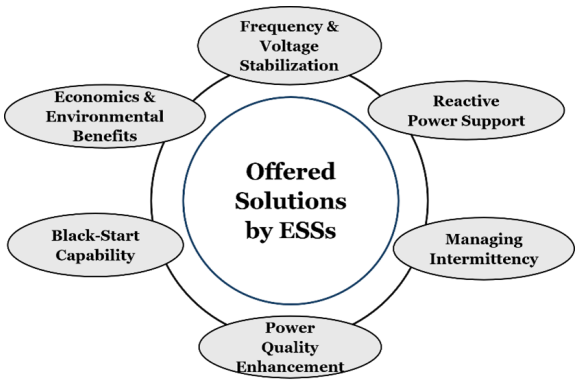


Figure 2.8: Key contributions of ESSs in overcoming grid challenges

Table 2.2: Comparison of Various Energy Storage Systems (ESSs)

Ref	ESSs	Key Attributes	Foundations	Applications	Advantages	Disadvantages
[66], [78], [80]	EC	**Capacity:** 0.25–300 MWh **Efficiency:** 65–92% **Lifetime:** 5–20 years	Chemical reactions using Cd, Li-ion, and RF electrolytes	Peak shaving, Frequency regulation, Isolated grid operations	High energy density (Li-ion), Long lifespan (VRF), Scalability	Toxic material disposal (NiCd), High operating temperature (NaS)
[83], [84], [85]	Mech	**Capacity:** Up to 3 GW **Efficiency:** 70–95% **Lifetime:** Up to 50 years **Response Time:** 1–2 min	Gravitational energy, Pressurized air, Rotational kinetic energy storage	Energy arbitration, Load leveling, Spinning reserve, Voltage support	Long lifespan, High efficiency, Scalability	High installation cost, Greenhouse gas emissions (CA), Limited operational periods (flywheel)
[66], [86], [87], [88]	TCSS	**Efficiency:** 50–100% **Storage Medium:** Versatile (sensible, latent, thermochemical)	Phase change materials, Thermal storage in solids/liquids, Chemical heat reactions	Solar thermal, Co-generation	Long storage durations, Compatibility with RESs	Lower energy density (sensible heat), Complex material handling (TC)
[16], [89], [90]	Chem	**Operating Temp:** 600–1100°C **Efficiency:** Up to 65% Flexible fuel compatibility	EC hydrogen conversion, Reactions with oxygen, Molten carbonate or Solid oxide electrolytes	Hydrogen utilization, Co-generation, High-temperature operations	High energy efficiency, Diverse fuel sources, Co-generation capabilities	High operating temperature, Expensive raw materials
[16], [90], [91]	Elec	**Power Range:** 10 kW to 10 MW **Efficiency:** 90–95% **Response Time:** ms	Electrostatic and phase-change energy storage	Voltage quality, Frequency support, Peak shaving	Rapid response, High reliability, Low energy losses	High capital cost, Magnetic field management

2.5 Roles of ESSs in mitigating weak grid challenges

Building on the solutions discussed in Section 2.4, ESSs play a crucial role in addressing weak grid challenges, but non-battery systems like mechanical, thermal, chemical, and electrical storage often face limitations such as slower response times, lower efficiency, and reduced flexibility. In contrast, BESSs provide superior efficiency, adaptability, and rapid response capabilities, making them particularly effective in stabilizing weak grids, managing power fluctuations, and integrating RESs. This section highlights the limitations of non-battery storage technologies and positions BESSs as a more practical and versatile solution for modern grid needs, paving the way for enhanced grid stability and reliable RE integration.

2.5.1 Limitations of non-battery storage technologies

ESSs such as mechanical, thermal, chemical, and electrical storage systems are essential for addressing grid vulnerabilities and managing RE intermittencies. However, these technologies exhibit significant limitations that constrain their practical deployment. Mech ESSs, including PHS and CAS, are restricted by geographic and structural dependencies. PHS requires large-scale water reservoirs and significant elevation differences, making it unsuitable for flat or water-scarce regions. Despite their high efficiency (70-85%) and long lifetimes, the upfront installation costs are substantial [71]. CAS, on the other hand, necessitates underground formations for compressed air, adding to its environmental and capital complexities. Flywheel storage, while capable of delivering rapid response times, suffers from limited energy storage capacity, short operational lifespans, and high mechanical wear [92], [93]. A detailed comparison of the key attributes, applications, advantages, and disadvantages of these ESS technologies is summarized in Table 2.2. Thermal ESSs face challenges tied to their energy density and operational costs. Sensible heat storage systems, which store energy in solids or liquids, exhibit low energy density, making large-scale applications impractical [94], [95], [96]. Latent heat and thermochemical storage systems (TCSS), though promising in terms of efficiency (up to 100%), involve high material costs and complex operational processes, particularly in managing advanced phase change materials and chemical reactions [70]. The need for specialized infrastructure further increases deployment expenses, limiting their feasibility for weak-grid integration [95].

Chem ESSs, including hydrogen FCs, molten carbonate fuel cells (MCFC), and solid oxide fuel cells (SOFC), demonstrate high energy efficiency and compatibility with RESs.

However, their reliance on high operating temperatures (600-1100°C) and expensive raw materials significantly hampers their economic viability [67], [70], [93]. Additionally, the conversion processes for chemical storage often involve complex electrochemical reactions that demand precise control systems, increasing maintenance costs and operational complexity [79], [82].

Elec ESSs, such as SCap and SMES, offer high efficiencies (90-95%) and rapid response times, making them suitable for power quality applications like frequency regulation and voltage stabilization [70], [93]. However, these systems are limited by their low energy density, which restricts their use for long-duration energy storage. Moreover, SMES requires extremely low temperatures for superconductivity, leading to high capital and operational costs associated with cryogenic systems. SCap, while efficient, have limited storage durations and faces scalability issues for large-scale grid applications [95], [97].

To address these limitations, BESSs emerge as a superior solution due to their flexibility, scalability, and cost-effectiveness. As discussed in the next subsection, BESSs offer the capability to stabilize grid operations, manage renewable intermittencies, and enhance power quality.

2.5.2 Addressing Challenges through BESS for REZs integration in weak grids

BESS have emerged as the most advanced and practical solution to overcome the limitations of non-BESSs, ensuring grid stability and the seamless integration of RESs. Unlike mech and thermal systems that face geographic, structural, or operational constraints, BESS offers unmatched flexibility, scalability, and efficiency [36], [72]. Figure 2.9 highlights the key contributions of BESS in zonal weak grids, showcasing its role in enhancing grid stability, operational reliability, and RE utilization.

BESSs play a pivotal role in stabilizing grid frequency and voltage, responding almost instantaneously to fluctuations caused by RE intermittency. Technologies such as Li-ion batteries excel in delivering fast response times and ensuring grid inertia, where SGs are limited. Additionally, BESS contributes to power quality improvement by addressing voltage sags, harmonic distortions, and grid anomalies, which are increasingly critical in renewable-rich power systems [73], [98].

One of the most significant contributions of BESS is its capability to manage renewable intermittency effectively. By storing surplus energy during periods of low demand

and discharging it during peak loads, BESS minimizes RE curtailment while enhancing system reliability. This functionality is particularly beneficial for maintaining energy balance in weak or isolated grids, where other storage technologies face limitations [99].

Furthermore, BESS provides resilience through black-start capabilities, allowing grids to recover independently from outages without relying on conventional fossil-fuel generators. Technologies such as Li-ion and NaS batteries are particularly suited for this function due to their rapid response times and scalability [35], [72]. Black-start capability ensures operational continuity and reinforces grid reliability during unforeseen disruptions.

Despite the higher upfront costs associated with BESS, the technology offers long-term economic and environmental benefits. Continuous advancements in battery chemistries, including VRF and next-generation sodium-based batteries, are improving efficiency, reducing costs, and extending operational lifespans [35], [92]. These advancements position BESS as a cornerstone for modern energy storage, enabling greater RE penetration while reducing greenhouse gas emissions [66].

The critical role of ESSs in mitigating grid challenges has been demonstrated, with Battery Energy Storage Systems (BESSs) emerging as a superior and adaptable solution [67], [70], [92]. Unlike non-battery ESS technologies, which face significant limitations in practical implementation, BESS provides robust solutions to address frequency and voltage instability, power quality issues, renewable intermittency, and grid resilience [36]. By leveraging advanced chemistries and configurations, BESS offers unmatched efficiency, flexibility, and scalability, making it the cornerstone of modern energy storage strategies.

As we transition to Section 2.6, the focus shifts toward the advancements in BESS technologies and their wide-ranging applications to weak power grids.

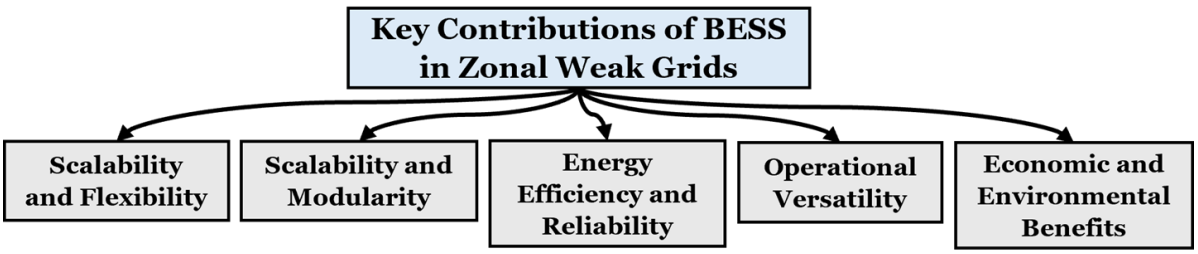


Figure 2.9: Key Contribution of BESS in zonal weak grids

2.6 Advancement of BESS technologies and their applications to weak power grids

Building on the discussion in Section 2.4 about the limitations of non-BESSs, BESS stands out as a powerful solution for modern power grids. This section focuses on the progress in BESS technologies, their important role in improving weak grid stability and supporting RE integration, and the strategies used to manage and control their operations. By examining the basics, comparing their performance, and exploring innovative control methods, this section highlights why BESS is crucial for solving grid challenges and advancing toward a more sustainable energy future.

2.6.1 Different types of BESS for weak power grid applications

BESS play a vital role in modern power grids by storing and converting chemical energy into electrical energy, thereby supporting RE integration and addressing grid stability challenges. Key BESS technologies include Li-ion batteries, known for their high energy density and reliability; Pb-acid batteries, which are cost-effective and have a long operational history; NaS batteries, well-suited for large-scale applications despite high-temperature requirements; RFB, offering scalability and extended discharge durations; and Ni-based batteries, recognized for their durability but limited by toxicity or cost. As summarized in Table 2.3, each technology varies in foundational principles, advantages, and typical applications, providing a spectrum of solutions to meet diverse energy storage needs.

2.6.1.1 Comparative study among different BESS technologies

BESS are critical enablers of modern power systems, addressing the challenges posed by the integration of variable renewable energy (VRE) sources such as solar and wind. These systems ensure flexibility, stability, and reliability in the power grid, where the intermittency of RE poses significant challenges to traditional grid operations. As the penetration of RE continues to grow, selecting the right BESS technology for specific applications has become vital. This section provides an in-depth comparative analysis of key BESS technologies, focusing on their efficiency, lifecycle, cost, and application performance.

BESS encompasses a range of technologies, each with distinct attributes that make them suitable for diverse grid applications. Li-ion batteries, known for fast response and

Table 2.3: Summary of Major BESS Technologies

References	**Name of BESS**	**Foundation**	**Advantages**	**Applications**
[79], [100], [101]	Li-ion	Movement of Li-ions between the anode and cathode during charge/discharge	- High energy density - Lightweight - Fast response time - Reliability - Long cycle life	- Grid-scale energy storage - Electric vehicles - Consumer electronics
[34], [79], [82]	Pb-Acid	Chemical reaction between lead dioxide (cathode), lead (anode), and sulfuric acid electrolyte	- Low cost - Ease of deployment - Proven performance	- Backup power - Off-grid microgrids
[34], [35], [36]	NaS	High-temperature operation (300°C) using molten sodium and sulfur electrodes	-High energy efficiency (75-85%) - Extended operational life - Effective for large-scale storage	- Load leveling - RE integration - Grid-scale deployments
[79], [97]	RFB, e.g. VRFB	Energy stored in liquid electrolytes with redox reactions occurring in separate tanks	- Scalability - Long operational lifespan - Flexible discharge durations	- Long-duration energy storage - Large-scale grid applications
[67], [97], [102]	Ni-Cd, NiMH	EC reactions involving nickel and cadmium or nickel-metal hydride	- Ni-Cd: Durable, efficient in extreme temperatures - NiMH: Higher energy density	- Backup power - Industrial applications (Ni-Cd) - Consumer electronics (NiMH)

efficiency (90-95%), dominate the market and are widely used in utility-scale storage, RE integration, and electric vehicles [103]. Pb-acid batteries, as one of the most established technologies, offer low cost and simplicity, making them ideal for backup power and off-grid systems, despite their lower energy density. NaS batteries, operating at high temperatures (300°C) with an efficiency of 85-90%, are well-suited for grid-scale applications like load leveling and RE integration but require robust thermal management systems [36]. RFB provide unparalleled scalability and extended lifespans, 20 years,

excelling in long-duration energy storage and grid stabilization, although their lower energy density and high upfront costs limit smaller applications [35]. Ni-based batteries, including Ni-Cd and Ni-MH, are valued for their durability in extreme conditions, catering to niche industrial and specialized markets. As the global energy landscape continues to transition toward RE, BESS technologies will play an increasingly vital role in maintaining grid stability and efficiency [67], [81], [97]. The comparative analysis, summarized in Table 2.4, highlights the unique strengths of each technology, providing valuable guidance for stakeholders in selecting the most appropriate solution for specific energy storage needs. Future advancements in cost reduction, lifecycle management, and efficiency are expected to further enhance the capabilities and adoption of these technologies. While this comparative study highlights the relative merits of different BESS technologies, their effective deployment in weak grids critically depends on sophisticated BMSs to ensure stable and reliable operation [35]. The following section explores the pivotal role of BMSs in facilitating BESS integration within weak grid environments.

Table 2.4: Key information of different BESS

Technology	**Battery cell energy density (Wh/kg)**	**Battery cell power density (W/kg)**	**Capacity (MWh)**	**Lifespan (Years)**	**Cost ($/kWh)**	**Efficiency (%)**	**Most Suitable Grid Applications**
Li-ion [85]	70-250	1000	0.25-25	10-15	300-1500	90-95	High-demand scenarios requiring rapid response
Pb-Acid [79]	50	500	0.25-50	5-15	200-400	70-85	Cost-sensitive projects, backup power systems
NaS [97]	150	100	≤ 300	10-15	300-500	85-90	Large-scale RE integration
RFB [104]	25	100	≤ 250	15-20	150-1000	65-85	Long-duration applications requiring high scalability and safety
NiCd [85]	-	-	-	Around 10	800-1500	70-90	Harsh environments with extreme temperatures
NiMH [104]	-	-	-	Around 5	600-1200	65-85	Specialized use cases with limited space or specific temperature demands

2.6.1.2 Role of BMSs in BESS operation for weak grids

The efficient and safe operation of BESS heavily depends on robust Battery Management Systems (BMS). A BMS continuously monitors voltage, current, and temperature while estimating critical states like State of Charge (SOC) and State of Health (SOH) [35]. These capabilities are critical for preventing thermal runaway, overcharging, or deep discharging issues that accelerate degradation in large-scale BESS deployments integrated into weak grids [35, 105]. As shown in Figure 2.10, each battery pack employs a dedicated

BMS for cell balancing, thermal management, and fault protection. Multiple packs are coordinated via Supervisory System Control (SSC), which optimizes power flow to meet grid demands. Predictive, model-based BMS frameworks further enhance performance by minimizing degradation and enabling adaptive charge/discharge strategies under variable loads [35]. For lithium-ion and flow batteries, BMS functionalities extend to internal state inference and electrolyte flow control, respectively [103]. In renewable-rich weak grids, intelligent BMS integration is vital to stabilize voltage/frequency fluctuations and maximize BESS longevity while delivering services like peak shaving and frequency regulation [35, 103, 105].

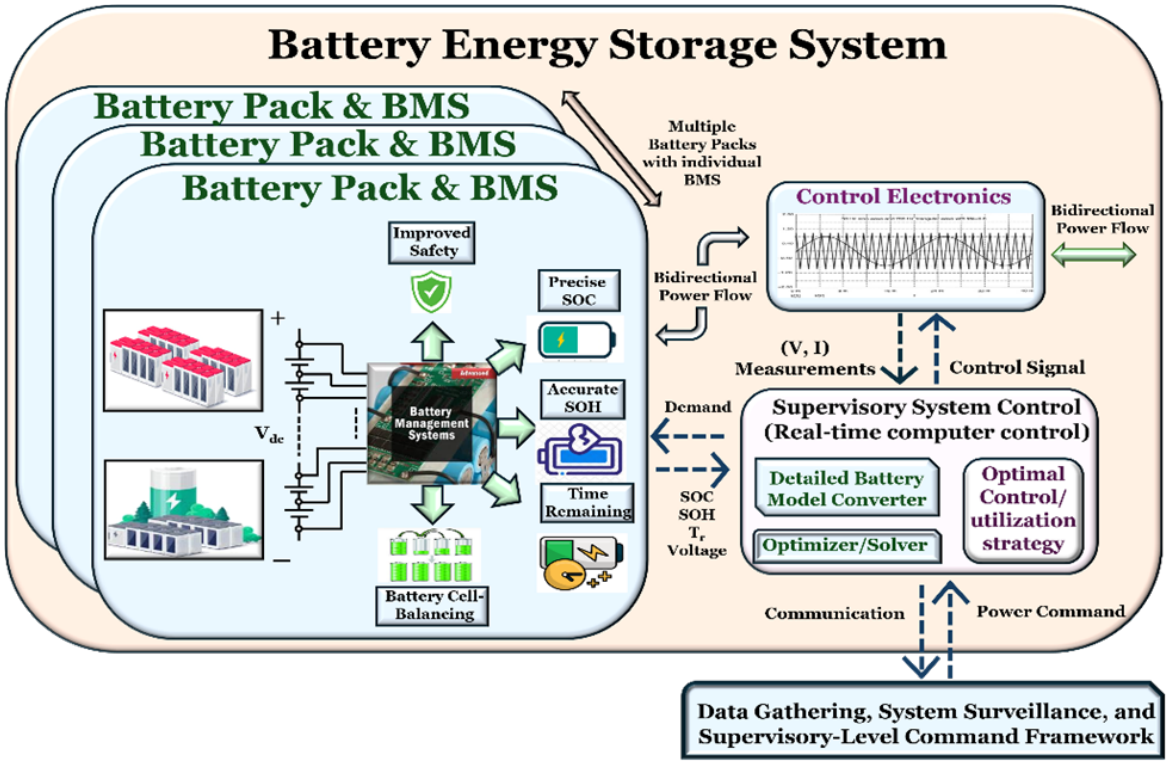


Figure 2.10: BESS schematic with hierarchical BMS for weak grids: battery pack integration, SOC/SOH monitoring, and stability optimization.

2.6.2 BESS in zonal weak grids

This subsection discusses BESS in its role in zonal weak grid systems. Weak grid environments, characterized by high impedance and limited fault capacity, pose significant challenges for RE integration and grid stability. BESS emerges as a pivotal solution to manage power quality, mitigate instabilities, and optimize energy usage in such systems.

The following subsections explore BESSs in various zonal weak grid configurations and their associated control and EMSt.

2.6.2.1 Zonal weak grid configurations

A zonal weak grid refers to a geographically defined section of a power system characterized by low system strength, typically associated with low SCR, high impedance, and a high penetration of inverter-based renewable energy sources. Unlike microgrids, which operate at a localized scale, zonal weak grids represent larger network regions (e.g., REZs) where system-wide stability challenges arise due to reduced synchronous generation. Zonal weak grids can be classified into islanded weak grids and grid-connected weak grids, each presenting unique operational challenges and opportunities [106], [107], [108], [60]. By applying the advanced control and EMSt developed for microgrids, BESS plays a critical role in stabilizing voltage and frequency, mitigating RE variability, and ensuring efficient energy utilization within zonal weak grids [32]. The seamless application of these strategies across both microgrids and zonal weak grids highlights the indispensable role of BESS in bridging localized and regional energy systems, creating a cohesive approach to RE integration and grid modernization [60].

2.6.2.2 Islanded zonal weak grid

Islanded zonal weak grids operate independently of a larger grid, relying entirely on localized energy generation, often from RESs [108]. In REZs, these grids are crucial for harnessing and distributing renewable power effectively without direct support from a strong grid. Within islanded weak grids, BESS plays a critical role in stabilizing voltage and frequency, mitigating fluctuations from VRSs, and maintaining the power supply-demand balance [107], [60]. Figure 2.11 shows the Islanded mode of zonal weak grids with RESs and BESS along with static switch for transition purposes.

2.6.2.3 Grid-connected zonal weak grid

Grid-connected zonal weak grids operate in synchronization with the central grid, enabling enhanced grid stability and efficient integration of REZs [60]. These grids are pivotal for leveraging localized RE while maintaining reliability through the support of the main grid [109], [61]. BESS play a central role in managing power quality, optimizing energy flow, and ensuring seamless coordination between local RESs and the central

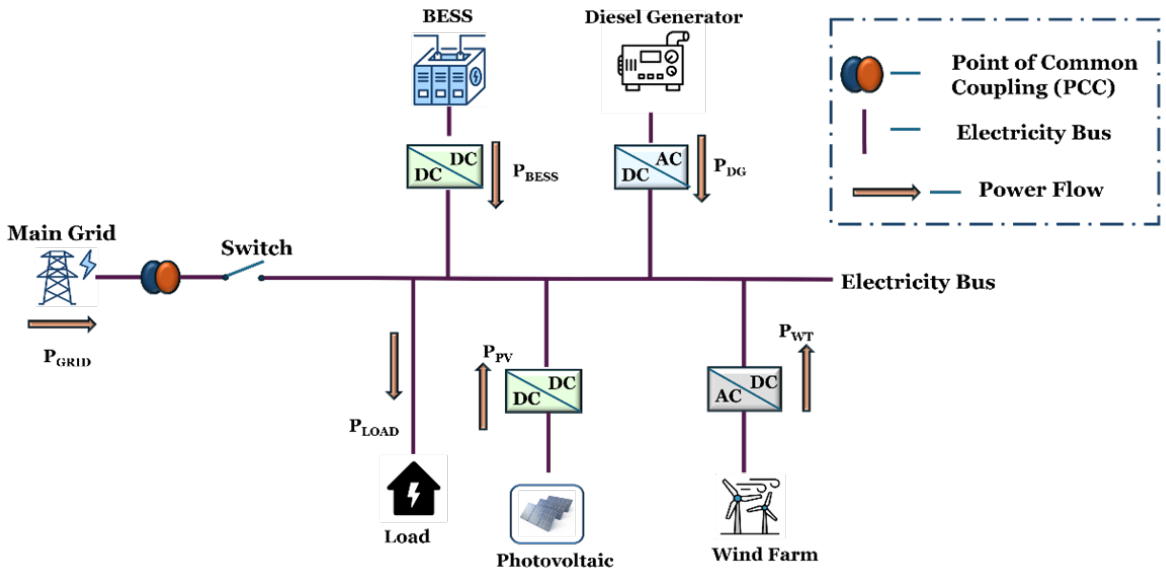


Figure 2.11: Islanded mode of zonal weak grids with RESs and BESSs

grid [36], [110]. Figure 2.12 highlights the general configuration of grid connected mode of zonal weak grids along with RESs and BESS [106].

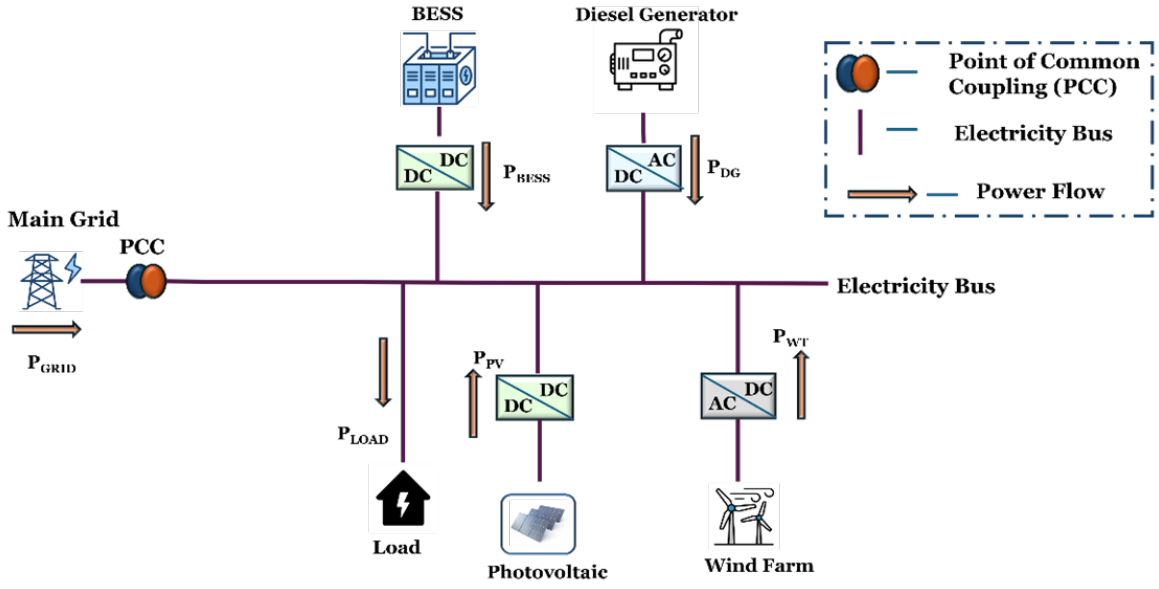


Figure 2.12: General configurations of grid-connected mode of zonal weak grids along with RESs and BESS

Table 2.5 further highlights the key role of BESS while integrating the REZs in islanded zonal weak grids along with grid connected zonal weak grids, discussing its key roles, opportunities involved, challenges associated with it and future potential of

BESSs. Each configuration offers unique advantages and challenges in integrating RE, as detailed below.

Table 2.5: Role of BESS and Integration of REZs in Islanded Zonal Weak Grids and Grid Connected Weak Grids

Aspect	**Details (Islanded Zonal Weak Grids)**	**Details (Grid Connected Weak Grids)**
Key Role of BESS	Stores excess RE during high-generation periods.	Manages power quality by providing voltage regulation and frequency stabilization.
	Discharges energy during low-generation periods to ensure a consistent power supply.	Stores excess RE and discharges it during low-generation periods.
	Mitigates intermittency and reduces RE curtailment.	Reduces RE curtailment and mitigates intermittency.
	Provides ancillary services like voltage regulation, frequency stabilization, and black start capabilities.	Supports peak shaving and energy arbitrage for economic benefits.
	Enables energy arbitrage and peak shaving to enhance economic outcomes.	Improves grid reliability by acting as a buffer between REZs and the central grid.
	Improves overall grid reliability and energy utilization.	-
Opportunities	Enhanced grid reliability through seamless integration of RESs.	Enhances grid resilience by integrating RE effectively.
	Improved power quality by mitigating fluctuations and instabilities in isolated systems.	Improves power quality and minimizes disturbances in grid operations.
	Increased penetration of RESs, making islanded grids more sustainable.	Increases the penetration of renewables in centralized systems.
	Economic benefits from operational cost reductions and optimized energy usage.	Reduces operational costs through optimized energy usage.
Challenges	Limited fault current capacity in weak grids, which complicates stability.	Requires robust converters and advanced control systems for seamless operation.
	High sensitivity to disturbances, requiring advanced control and management systems.	High sensitivity to disturbances, requiring real-time adjustments.
	Complex control requirements for managing diverse RE inputs.	Complex coordination with the central grid and distributed resources.
	Need for precise forecasting and real-time adjustments to accommodate variability and intermittency.	Integration challenges due to diverse RESs and configurations.
	Integration challenges due to the remote locations of REZs.	-
Future Potential of BESS	Evolution of BESS technologies to provide more robust and scalable solutions.	Advances in hybrid control systems to optimize operations across AC and DC subsystems.
	Development of predictive models for real-time optimization.	Development of predictive models for real-time coordination with the central grid.
	Increased deployment in REZs to unlock their full potential.	Increased deployment in grid-connected REZs to maximize resource utilization.

Further, Table 2.6 further highlights some of the key differences between islanded zonal weak grids and grid-connected zonal weak grids.

Table 2.6: Key differences between islanded zonal weak grids and grid-connected zonal weak grids (with AC, DC, and Hybrid Configurations)

Aspect	**Islanded Zonal Weak Grids**	**Grid-Connected Zonal Weak Grids**
Definition	Operates independently of a larger grid, relying entirely on localized generation.	Operates in synchronization with the main grid while integrating local generation.
Primary Power Sources	RESs, such as solar PV and wind, with no external grid support.	Combination of RESs and centralized grid power.
Applications	Ideal for remote and isolated REZs.	Suitable for urban and semi-urban areas with centralized grid connectivity.
Key Grid Types	**AC Weak Grid:** Requires BESS for frequency stabilization and reactive power support.	**AC Weak Grid:** Relies on BESS for peak shaving, voltage regulation, and grid ancillary services.
	DC Weak Grid: Simplifies power flow and reduces energy losses with direct renewable-BESS connections.	**DC Weak Grid:** Improves energy transfer efficiency and supports solar-dominated systems with BESS.
	Hybrid Weak Grid: Integrates AC and DC systems for diverse energy sources, with BESS ensuring stability.	**Hybrid Weak Grid:** Balances mixed energy flows with advanced BESS coordination across AC and DC subsystems.
Economic Potential	Reduces reliance on fossil fuels, operational cost optimization through storage.	Reduces demand charges, supports RE markets, and enhances grid stability.

2.6.2.4 AC zonal weak grid

AC zonal weak grids are prevalent in traditional power systems and are widely used to interface with RESs such as wind turbines and solar inverters as shown in Figure 2.13 [69]. Operating with AC, these grids ensure compatibility with conventional power systems and RESs. AC weak grids can function in both islanded and grid-connected modes, making them versatile for various applications [106], [108]. In these grids, BESS plays a crucial role in ensuring stability and reliability [36]. BESS supports voltage regulation by providing reactive power to stabilize voltage levels, enhances frequency stabilization by managing deviations caused by renewable intermittency and load fluctuations, and facilitates peak shaving by discharging energy during high-demand periods to reduce grid stress [36], [111]. Advanced control strategies like droop control and H-infinity robust control are commonly employed to ensure stability and dynamic performance. AC weak grids are particularly effective in wind-dominated REZs, where BESS mitigates variability and supports ancillary grid operations seamlessly in both islanded and grid-connected configurations [104].

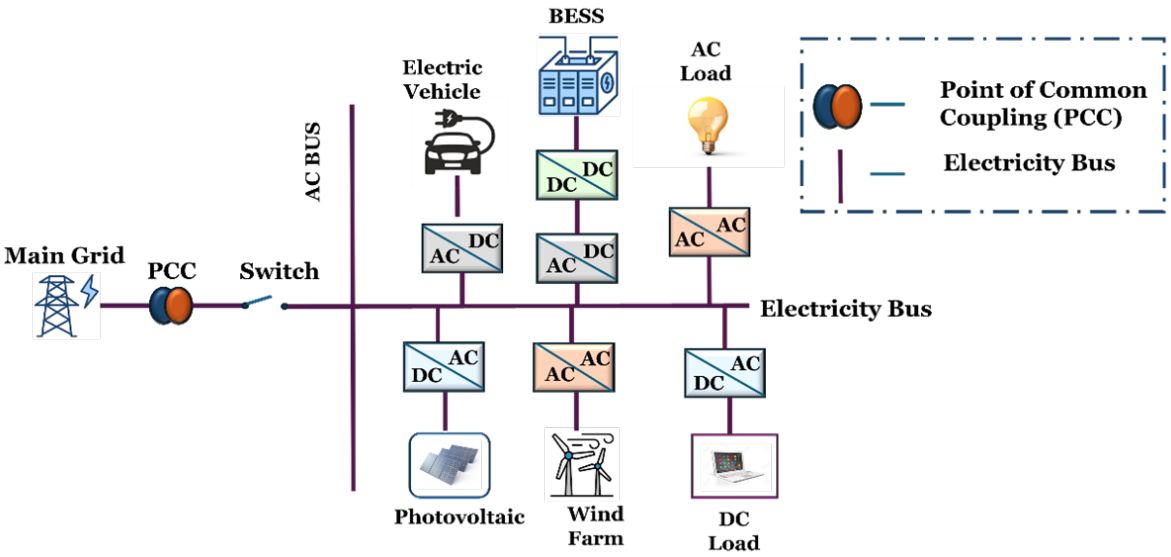


Figure 2.13: AC zonal weak grid architechture including BESSs and RESs

2.6.2.5 DC zonal weak grid

DC zonal weak grids are gaining prominence due to their high compatibility with modern RE technologies such as solar PV systems and electric vehicle charging stations [109]. Figure 2.14 shows the typical DC zonal weak grid architecture with the inclusion of RESs and BESS [106]. Operating with DC, these grids simplify energy management by eliminating the need for complex AC-DC conversions and significantly reducing energy losses [112]. BESS in DC weak grids ensure efficient energy transfer by minimizing losses during the connection of RESs and loads, mitigates power fluctuations to maintain a consistent energy flow and stabilizes voltage levels across the grid. Advanced control strategies, such as DC-DC converters and EMSs, are employed to optimize the grid's performance. DC weak grids are particularly well-suited for solar-dominated REZs, where BESS stores surplus energy during high-generation periods and ensures stability during low-generation periods, addressing variability and maximizing the utilization of RESs [113].

2.6.2.6 Hybrid zonal weak grid

Hybrid zonal weak grids integrate both AC and DC systems, combining the advantages of each configuration to support diverse energy sources and loads [60], [61]. Figure 2.15 further highlights the hybrid zonal weak grids with the integration of BESS and RESs [106]. These grids offer flexibility and efficiency, making them particularly effective in

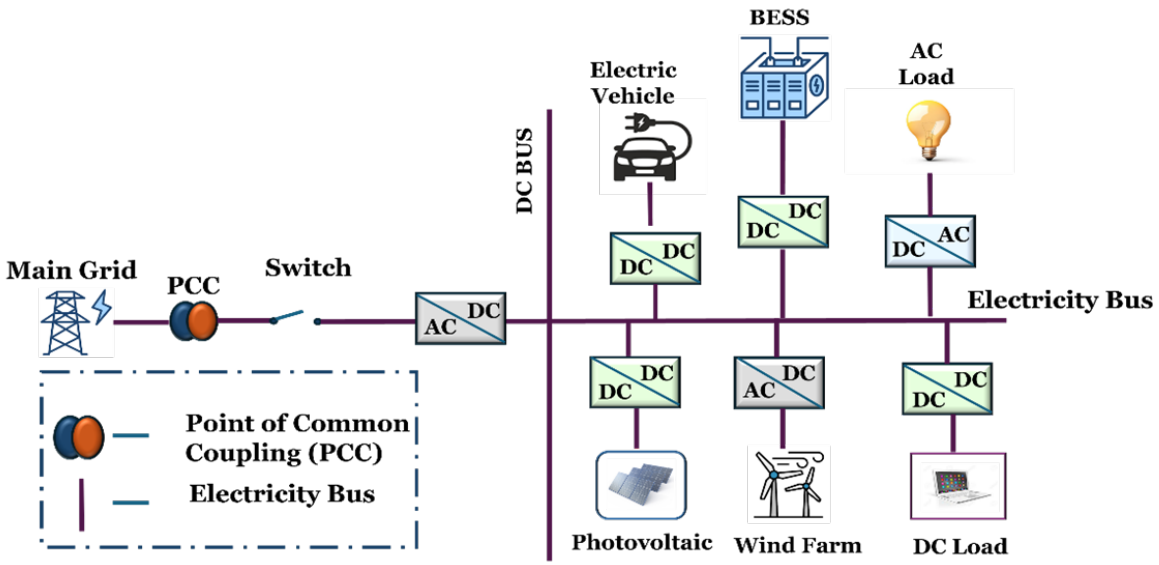


Figure 2.14: DC zonal weak grid architecture including BESS and RESs

REZs with mixed-generation resources. In hybrid weak grids, BESS serves as a central component, acting as a buffer to balance supply and demand while facilitating power flow management across AC and DC subsystems [112], [114]. BESS also mitigates power quality issues, such as voltage and frequency instability in AC systems and voltage drops in DC systems, ensuring stable operation. Hybrid grids excel in RE integration, enabling optimal utilization of mixed RESs like wind (AC) and solar PV (DC). To ensure stability and efficiency in these complex systems, hybrid controllers such as Model Predictive Control (MPC), Particle Swarm Optimization (PSO), and Fuzzy Logic Control (FLC) are deployed [115], [112], [114]. These grids are particularly valuable in mixed-generation REZs, where dynamic coordination and optimized performance are essential for reliable and sustainable energy delivery [108], [115], [113].

Having explored the advancements of BESS technologies and their applications in weak power grids, the next section now examines power management control strategies and algorithms essential for optimizing BESS performance in these grids.

2.7 Power management control strategies and algorithms used for BESS in weak grids

As the role of BESSs in modern power grids continues to expand, the need for sophisticated control strategies and energy management algorithms has become increasingly

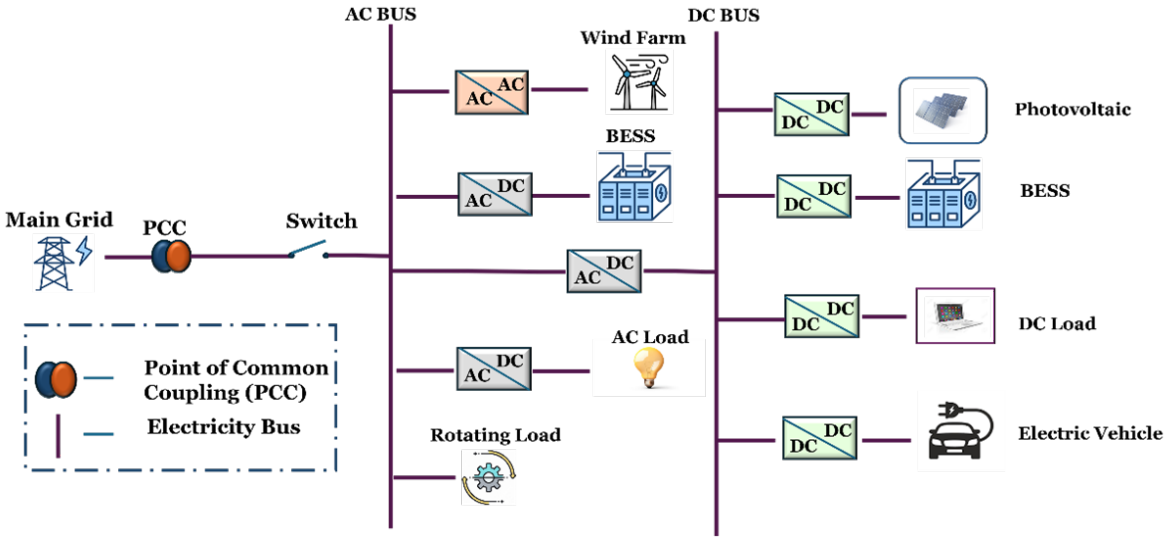


Figure 2.15: Hybrid zonal weak grid architecture including BESSs and RESs

apparent. These mechanisms ensure that BESS operates optimally to provide critical services such as frequency regulation, RE integration, and peak load shaving. This section explores the recent advancements in BESS in weak grid operation regarding control strategies and EMSt.

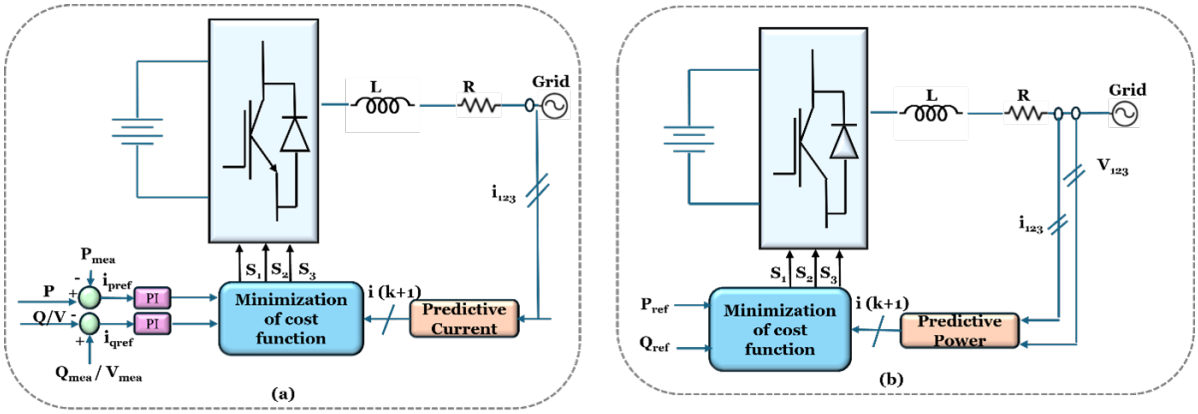
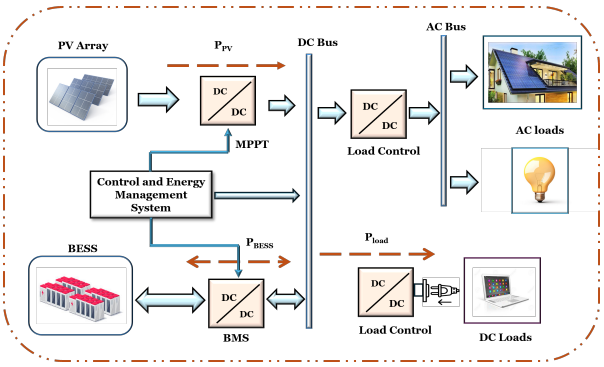


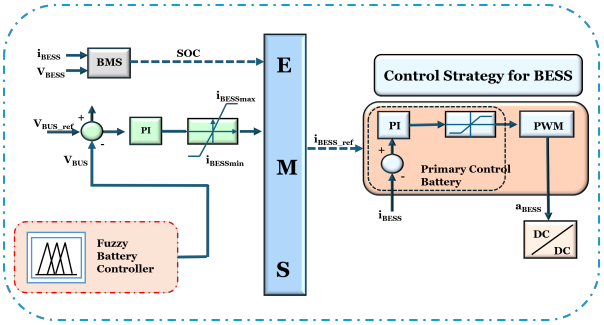
Figure 2.16: MPC block diagrams for BESS applications in weak grids; (a) MPC based on Predictive Current Control (PCC), (b) MPC based on Predictive Power Control (PPC)

2.7.1 Overview of control strategies and energy management

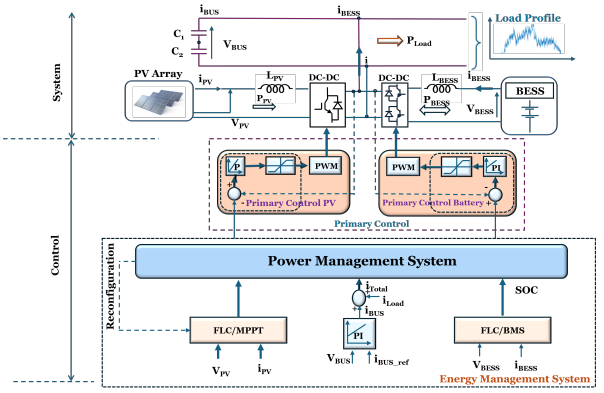
BESSs are pivotal in modern power systems, requiring robust control strategies and EMS to maximize efficiency, enhance grid stability, and optimize energy usage. Advanced controllers are designed to address diverse operational goals, such as managing RE intermittency, balancing supply and demand, and improving economic outcomes.



((a))



((b))



((c))

Figure 2.17: BESS control using FLC; a) The parallel architecture of typical DC microgrid of the PV/Battery Hybrid Systems, b) Structure of the PV FLC and c) Control design and configuration of proposed BESS using FLC.

2.7.1.1 Control Strategies

Control strategies for BESSs are integral to ensuring efficient operation, grid stability, and seamless integration of RESs. Among these, Proportional-Integral (PI) controllers are widely used for their simplicity and reliability in steady-state conditions, while MPC

excels in dynamic grid environments by predicting future states and optimizing real-time operations [104], [112], [116]. Figure 2.16 highlights the MPC block diagrams for BESS application in weak grids. FLC is effective for managing non-linear and uncertain systems, making it ideal for renewable integration [114], [117], whereas SMC provides high robustness in dynamic conditions but may suffer from inefficiencies due to chattering [118]. Figure 2.17 illustrates BESS control using fuzzy FLC. Advanced methods like H-infinity robust control ensure stability under extreme uncertainties [119], and Neural Network-Based Control (NNC) leverages data-driven techniques to adapt and optimize operations dynamically [105]. Figure 2.18 further shows some control strategies algorithms used to optimize BESS for weak grids especially while integrating it in REZs. RL introduces self-learning capabilities for unpredictable environments (2.18c), while PSO and Genetic Algorithms (GA) (2.18a, 2.18b) focus on optimizing BESS sizing, placement, and scheduling for long-term efficiency [120], [121]. Decentralized approaches such as Droop Control balance power among distributed resources [122], and Adaptive Control dynamically adjusts parameters to respond to varying grid conditions [120]. Finally, Decoupled Active-Reactive Control (DARC) ensures stability and efficiency in hybrid systems by managing active and reactive power separately [104], [123], [124]. These diverse strategies collectively address the challenges posed by renewable intermittency, variability, and operational optimization. These strategies' details, applications, advantages, challenges, and suitability for various RESs are summarized in Table 2.7.

2.7.2 Energy Management Systems

EMSs in BESS build upon the robust control strategies discussed in the previous subsection to optimize their operational efficiency, enhance grid stability, and support economic and technical objectives. While control strategies such as PI controllers, MPC, and FLC govern the real-time behaviour of BESS, EMSt operate at a broader level to ensure long-term system performance and reliability. These strategies include cost optimization, which leverages electricity price fluctuations to maximize economic returns, and load shifting and peak shaving, which alleviate grid stress and reduce peak demand by strategically managing energy storage and release [103], [32], [125]. Effective State of Charge (SoC) management complements these efforts by maintaining safe operating limits for the battery, thereby extending its lifespan and reliability [128]. RE integration, a key focus of BESS, is facilitated by storing excess energy during high-generation periods and discharging during deficits, thereby mitigating intermittency and reducing curtailment [129]. Strategies such as energy arbitrage, frequency and voltage regulation, and black

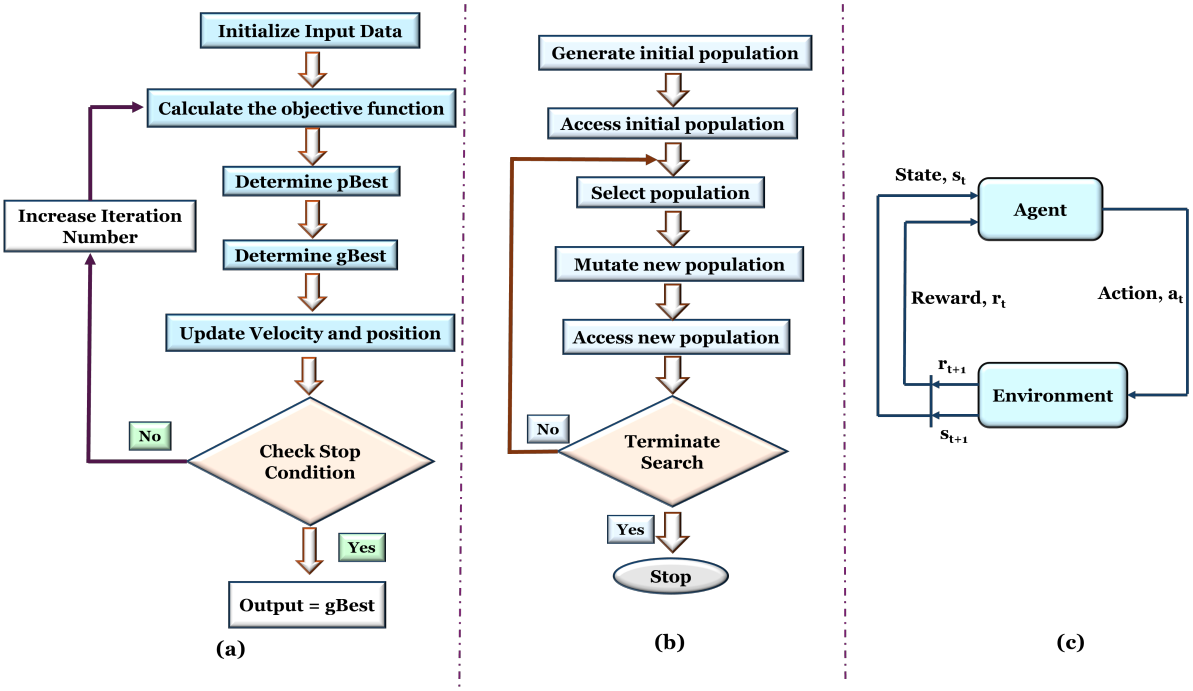


Figure 2.18: BESS control strategies for weak grids; (a) General flow chart of PSO, (b) General structure of GA, (c) Generalized RLS.

start capabilities further enhance the grid's operational stability and resilience [130]. Emerging techniques, such as decentralized energy trading and Demand-Side Management (DSM), promote flexibility and encourage renewable adoption [131]. Table 2.8 provides a detailed overview of these EMSt, highlighting their descriptions, applications, advantages, and challenges, thereby illustrating the critical role of BESS in modern energy systems and their seamless integration into dynamic energy environments.

While conventional control strategies such as PI and droop control offer simplicity and ease of implementation for BESS deployment in weak grids, their rigidity limits their effectiveness in dynamic, renewable-rich environments. In contrast, advanced methods, including MPC, FLC, and RL, demonstrate greater adaptability to grid instability, stochastic generation patterns, and load fluctuations. Among these, hybrid approaches that combine predictive optimization (e.g., MPC and PSO) with real-time adaptability (e.g., FLC or RL) stand out as the most suitable. These integrated strategies enhance system stability and operational efficiency, making them well-aligned with the evolution of intelligent energy systems. Ultimately, the convergence of adaptive control techniques with EMS frameworks is critical to maximizing the role of BESS in strengthening grid resilience and supporting large-scale decarbonization.

After a detailed exploration of power management control strategies and algorithms

Table 2.7: Control Strategies and their Characteristics for BESS in Weak Grids

Control Strategy	Description	Applications	Advantages	Challenges	Suitable RES	Ref
PI	Basic control for maintaining steady-state voltage and power stability.	Steady-state charging/discharging operations.	Simplicity, reliability, and ease of implementation.	Limited effectiveness in dynamic environments.	Solar PV, Wind	[36], [104]
MPC	Predicts future system behavior for real-time optimization.	RE smoothing, load balancing, state-of-charge regulation.	Handles multiple variables, system robustness.	Computationally intensive; highly sensitive to model accuracy.	Solar PV, Wind	[36], [104], [40], [124]
FLC	Rule-based learning system for managing uncertainty and non-linearity.	Frequency regulation, voltage stabilization, power injection.	High adaptability, no need for precise mathematical models.	Limited performance in highly complex networks.	Wind	[117], [121], [125]
SMC	Non-linear sliding mode control using high-frequency switching.	Fast response frequency and voltage regulation.	Robust under variable conditions and disturbances.	Can cause oscillations due to "chattering."	Wind, Hybrid Systems	[104], [114], [123], [126]
H-infinity Robust Control	Ensures stability under uncertainty and disturbances.	Grids with variable renewable penetration.	Reliable in extreme situations, robust under uncertainty.	Requires sophisticated control models and computational power.	Solar PV, Wind	[104], [119]
NNC	Data-driven control using artificial intelligence for real-time optimization.	Renewable generation, grid balancing, and real-time control.	Learns complex patterns, dynamically adapts to changing scenarios.	Requires data training and computational resources.	Solar PV, Wind	[36], [104], [127]
RL	Self-learning approach using trial-and-error methods.	Adaptive to uncertain scenarios without pre-programming.	Adapts to unpredictable grid conditions.	Requires long training times, large datasets.	Wind	[36],[114], [127]
PSO	Optimized BESS placement and scheduling.	Effective for solving large-scale optimization problems.	Optimizes resource allocation efficiently.	Sensitive to system parameter changes.	Solar PV, Wind	[35], [114], [110], [121]
GA	Evolutionary algorithm for optimal sizing and scheduling of BESS.	Effective for complex optimization scenarios.	Optimizes long-term cost and system reliability.	Computationally intensive.	Solar PV, Wind	[36],[104]
Droop Control	Real-time adjustment of parameters based on system changes.	Microgrids and distributed energy systems.	Plug-and-play functionality, decentralized operation.	Limited scalability for high-renewable systems.	Solar PV, Hybrid Systems	[104], [105]
Adaptive Control	Continuous adjustment of parameters based on system changes.	Environments with high load and generation variability.	Maintains stability and performance under changing conditions.	Complex system design and implementation.	Solar PV, Wind	[104], [120]

for BESS in weak grids, the next section provides an in-depth discussion on the application of BESS in electrical grids.

2.8 Applications of BESS in electrical weak grids

The increasing integration of RE into electrical grids has necessitated the development of robust technologies to address challenges such as intermittency, curtailment, and grid stability. BESSs have emerged as a key solution due to their ability to provide dynamic support across various operational scenarios. This section reviews the role of BESSs in enhancing grid stability and supporting RE integration, synthesizing findings from existing literature and highlighting practical applications.

Table 2.8: EMSt in BESS

Ref	EMSt	Description	Applications	Advantages	Challenges
[103], [131]	Cost Optimization	Maximizing economic returns by charging during low-price periods	Energy arbitrage, reducing operational costs	Maximizes economic benefits, dynamic pricing	Requires accurate forecasting
[125], [127]	Load Shifting	Shifting energy usage from peak to off-peak periods to balance supply	Balancing RE generation, reducing demand	Reduces RE curtailment	Requires load forecasts and battery capacity management
[32], [131]	Peak Shaving	Reducing peak power demand by discharging stored energy	Industrial peak reduction, improving grid reliability	Reduces demand charges, enhances grid stability	Limited by storage size
[128], [131]	SoC Management	Ensuring battery operates with safe charge and discharge limits	Prevents overheating, enhances reliability	Extends battery life	Requires real-time monitoring
[129], [131]	RE Integration	Mitigating power fluctuations by providing stored energy	Reducing RE curtailment, ensuring grid stability	Maximizes RE utilization	Requires sophisticated control systems
[130], [131]	Energy Arbitrage	Buying electricity at low prices	Enhancing profitability in electricity markets	Increases revenue	Highly dependent on market conditions
[104], [132]	Frequency Regulation	Maintaining grid stability by managing charging cycles	Grid stabilization, sensitive frequency response	Provides fast response times	Requires real-time monitoring
[121], [133]	Voltage Regulation	Supporting voltage stability	Improving voltage support in weak grids	Maintains voltage	Requires real-time data analysis
[131], [134]	Black Start Capability	Providing power in post-outage scenarios	Restoring grid loads	Improves system restart reliability	Requires significant inverter capacity
[36], [135]	Energy Trading	Enabling BESS participation in energy markets	Supporting RE integration	Increases revenue	Requires blockchain or secure transaction platforms

2.8.1 Enhancing Grid Stability

The stability of modern power grids is increasingly challenged by fluctuating generation from RESs, growing loads, and aging infrastructure. Various reactive power support technologies have been developed and deployed to address these challenges, ensuring voltage stability, power quality, and operational reliability. Among these, BESS have

gained significant attention as a flexible and efficient solution for reactive power support. However, understanding how BESS stands out requires an overview of the available technologies and their comparative performance. The following section is going to discuss the overview and the comparison of the reactive power support technologies, followed by the role of BESS on providing reactive power support.

Table 2.9: Comparison of Reactive Power Support Technologies for Voltage Stability

Technology	**Response Time**	**Dynamic Adjustment**	**Cost**	**Scalability**	**Inertia**	**Advantages**	**Disadvantages**
SC [90]	Moderate (Seconds)	Limited	High	Moderate	Yes	Provides inertia for grid stability; suitable for high-disturbance scenarios.	Large physical footprint and high maintenance requirements.
SVC [107]	Fast (Milliseconds)	Moderate	Moderate	Moderate	No	Compact design and effective for steady-state voltage regulation.	Limited ability to handle rapidly changing grid conditions.
STATCOM [60]	Very Fast (Milliseconds)	High	High	High	No	Faster response than SVC; ideal for renewable integration and fault ride-through.	Higher capital and operational cost compared to SVC.
Cap Bank [115]	Slow (Fixed Output)	None	Very Low	High	No	Low-cost solution; simple and easy to deploy.	No dynamic adjustment capability; unsuitable for grids with high renewable penetration.

Table 2.10: Key advantages of BESS compared to other technologies

Feature	**BESS**	**Closest Alternative**
Response Time	Milliseconds	STATCOM (Milliseconds to Seconds)
Dynamic Adjustment	Very High	STATCOM (High)
Scalability	Very High	Synchronous Condensers (Moderate)
Integration with Renewables	Seamless	STATCOM (Limited to Reactive Power Only)
Dual Active/Reactive Capability	Yes	None

2.8.2 Role of BESS in providing reactive power support

Reactive power support is essential for maintaining voltage levels in power grids, enabling the efficient operation of electrical equipment and ensuring reliable power delivery.

Multiple technologies are available to provide reactive power support, each with its strengths, limitations, and suitability for specific grid conditions. These technologies include BESSs, SCs, static var compensators (SVC), static synchronous compensators (STATCOM), capacitor banks (Cap Bank) and FACTS. Each of these technologies has its response times, dynamic adjustments, cost measurements, scalability, inertia contribution and applications. Table 2.9 summarizes all the required information in detail for these technologies, including its advantages and disadvantages.

While the technologies shown in Table 2.9 has served reactive power needs in traditional and evolving grids, the increasing penetration of RE necessitates a more versatile and responsive solution. BESS have emerged as a fruitful technology, combining the fast response and dynamic capabilities of STATCOM with the flexibility of scalable deployments. Table 2.10 further highlights the key advantages of BESS compared to other technologies. BESS provides not only reactive power support but also active power compensation, making it uniquely positioned to address the challenges of RE integration, load balancing, and transient stability [104, 121, 136, 137]. Unlike traditional reactive power devices, BESS can dynamically adapt to varying grid conditions while offering additional services like frequency regulation and energy arbitrage [138–140]. These capabilities position BESS as the most advanced and comprehensive solution for modern grid stability needs.

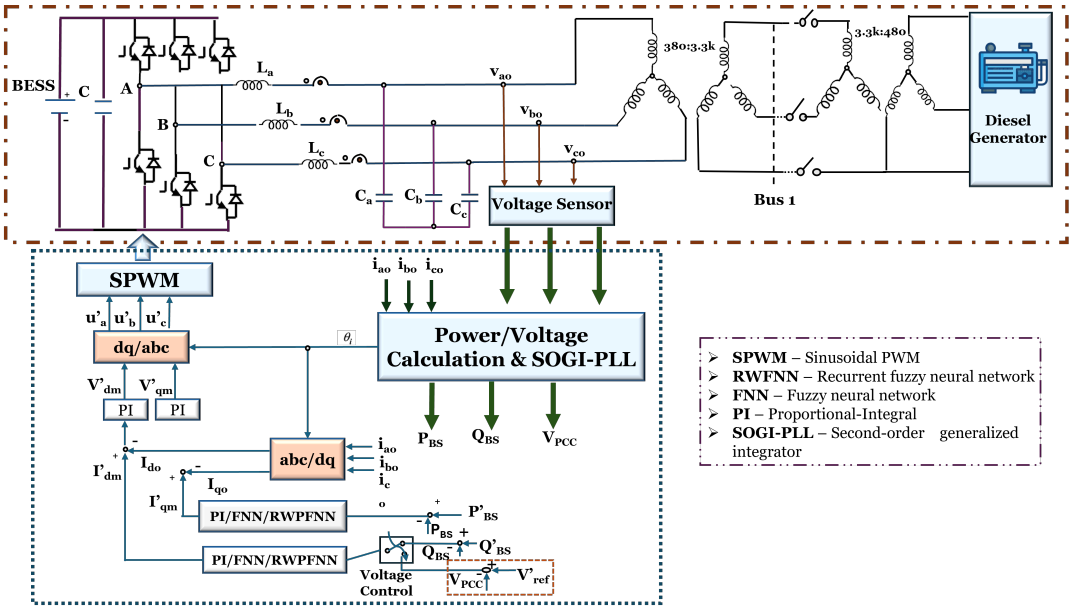


Figure 2.19: Active/reactive power control and voltage restoration control (VRC) of BESS

Reactive power plays a critical role in maintaining voltage stability within power

grids, as discussed in the previous section. Unlike active power, which performs the real work of powering loads, reactive power ensures the proper operation of electrical equipment by maintaining voltage levels. With the increasing penetration of RESs, which inherently lack reactive power generation capabilities, maintaining grid voltage has become a significant challenge. BESS have emerged as a viable solution to provide reactive power support due to their fast response times and ability to handle both active and reactive power independently. Figure 2.19 shows the active/reactive power control and voltage restoration control of BESS for weak grids used in [141].

The ability of BESSs to control reactive power stems from its bidirectional power flow capabilities. Through advanced inverter technologies, BESSs can dynamically adjust the reactive power it delivers or absorbs, stabilizing voltage levels in real time. This capability of BESS makes it suitable to use in weak grids for several applications and scenarios, as highlighted in detail in Table 2.11.

Table 2.11: Applications of BESS in Reactive Power Support for Voltage Stability and Grid Reliability in Weak Grid Scenario

Application	**Description**	**Control Strategies**	**References**
Weak Transmission Networks	High renewable penetration leads to voltage instability. BESS compensates by injecting or absorbing reactive power in real-time. Supports voltage profiles by reducing dependency on conventional generation.	Voltage Source Converters (VSC), Dynamic Voltage Regulation, Reactive Power Optimization Algorithms.	[104, 121, 123, 126]
Disturbance Recovery	BESS stabilizes voltage by dynamically adjusting reactive power during disturbances. Rapid response during fault recovery minimizes cascading grid failures.	Droop Control, Feedback-Based Control, Real-Time Monitoring and Control Systems	[123, 126]
Power Quality Improvement	BESS mitigates voltage sags and surges, enhancing reliability and reducing power quality issues. Ensures uninterrupted power supply to sensitive loads.	Independent control of active and reactive power (VSC), PI Control	[104, 126]
Grid Frequency Stabilization	BESS aids in maintaining grid frequency through reactive power compensation during frequency deviations. Prevents overloading of transmission lines by balancing power flow	Frequency-Watt Droop Control, Hybrid Control Algorithms, Reactive power-voltage (Q-V) control	[104, 121]
Integration with RE	Reduces curtailment and stabilizes voltage during periods of high renewable generation variability.	Machine learning-based predictive control	[104, 121, 123]
Voltage Collapse Prevention	Prevents voltage collapse in weak grid areas during peak loads or high renewable penetration. Enables grid operators to maintain grid voltage within operational limits.	Predictive Load Sharing, Dynamic Voltage Setpoints	[121, 123]
Microgrid Applications	BESS ensures voltage stability in islanded microgrids or during grid disconnections. Balances power between distributed energy resources and real-time demand.	SOC-Based Reactive Power Control, Hierarchical Control Strategies	[36, 123]
Emergency Grid Support	Provides reactive power to stabilize the grid during emergencies, such as extreme weather conditions or black-start scenarios.	Fast Response Droop Control, Voltage Support Algorithms	[121, 123, 126]

2.9 Worldwide projects of BESS for real-world power grid applications

Based on the discussion of reactive power support technologies and the pivotal role of BESSs in providing reactive power support, real-world applications further illustrate the versatility and effectiveness of BESS in addressing grid stability challenges. BESS have become indispensable for modern power grids, as evidenced by numerous global case studies showcasing their role in enhancing grid stability and supporting RE integration. For example, the Qinghai Luneng Gelmud multi-energy complementary project (China) and the Henan grid-side distributed BESS project (China), both operational since December 2018, use Li-ion batteries with capacities of 50 MW/100 MWh and 100.8 MW/125.8 MWh, respectively, to smoothen output fluctuations, provide peak regulation, and ensure frequency stability [68]. Similarly, the SDG&E Escondido BESS project (USA), operational since 2017, employs a 30 MW/120 MWh Li-ion battery for electricity market participation, while the Virginia Beech Ridge BESS project (USA), with a 31.5 MW/12.06 MWh Li-ion battery, has been facilitating frequency regulation since 2015 [68]. Additionally, projects like the Zhangbei wind-photovoltaic-storage-transmission demonstration project (China) demonstrate the integration of multiple battery types, including Li-ion, RF, and Pb-acid batteries, to provide comprehensive voltage regulation [104]. Recent projects, such as the West Murray Zone GFM BESS Project (Australia) (2023) and the Distributed PV-BESS Curtailment Project (South Australia) (2023), highlight the use of advanced GFI and distributed BESS configurations for mitigating sub-synchronous oscillations and reducing energy curtailment, respectively [142], [143]. Moreover, some of the upcoming projects like Waratah Super Battery, Liddell BESS and Orana BESS (Australia, NSW) are targeting to ensure grid reliability and stability along with smooth transition for RE integration. A detailed overview of these projects, including their configurations, battery types, and primary functions, is presented in Table 2.12, illustrating the diverse and impactful applications of BESS in real-world operations.

2.9.1 Supporting RE Integration

Building upon the role of BESS in providing reactive power support and enhancing grid stability, another crucial application lies in facilitating the seamless integration of RESs into power grids. The intermittent nature of solar and wind energy, coupled with periods of excess generation, poses significant challenges such as grid instability, energy

curtailment, and load mismatches. BESS have proven to be highly effective in addressing these challenges by mitigating intermittency, reducing curtailment, facilitating energy arbitrage, and supporting load balancing. The following subsection will discuss how BESS help to mitigate intermittency and reduce curtailment along with how BESS facilitate energy arbitrage and load balancing using some of the projects discussed in Table 2.12 as reference.

2.9.2 Mitigating intermittency and reducing curtailment

RESs often produce excess power during periods of low demand, leading to curtailment and wasted energy. BESS helps alleviate this by storing surplus energy during high-generation periods and releasing it during low-generation times, ensuring better utilization of RE. For instance:

- The Distributed PV-BESS Curtailment Project (South Australia) integrates distributed PV systems with 13.5 kWh Li-ion batteries to reduce overvoltage and curtailment in low-voltage networks [142].
- The Zhangbei wind-photovoltaic-storage-transmission demonstration project(China) leverages a combination of Li-ion, RF, and Pb-acid batteries to smoothen RE output, enhancing grid stability and RE utilization [104].
- The Aomori Rokkasho-Futamata wind farm (Japan) employs a 34 MW/245 MWh NaS battery to address LVRT issues and provide reactive power compensation [104].

2.9.3 Facilitating Energy Arbitrage and Load Balancing

Energy arbitrage, where energy is stored during periods of low electricity prices and discharged during high-price periods, is another critical application of BESS. This not only provides economic benefits but also ensures real-time load balancing, minimizing stress on grid infrastructure. Examples include:

- The South Australia Virtual Power Plant (VPP), where residential Li-ion battery systems are integrated into a VPP to enable DSMs, fast frequency response, and system stress reduction [142].
- The Henan grid-side distributed BESS project (China) utilizes a 100.8 MW/125.8 MWh Li-ion battery system for peak shaving and load leveling, ensuring energy supply aligns with demand patterns [104].

- The Waratah Super Battery(NSW, Australia), scheduled for 2025, will provide 700 MW/1400 MWh capacity to enhance grid reliability following coal plant retirements and to support RE integration [144].

Following a detailed examination of BESS applications in weak electrical grids, the next section shifts focus to the discussion and transition pathway for promoting BESS adoption.

2.10 Discussion and Transition Pathways to Promote BESS

The global imperative to reduce carbon emissions and ensure affordable, clean energy (as articulated in the UNSDGs 7 and 13) has elevated the role of BESSs in modern power grids. In contrast to other energy storage options, such as mechanical, thermal, or chemical storage that often contend with slower response times or lower round-trip efficiencies, BESS deliver rapid power injection or absorption, high energy density, and excellent scalability [131], [145]. Consequently, BESS have emerged as vital technologies for enhancing the reliability, stability, and economic performance of weak or remote grids as they integrate higher shares of renewables [36], [10]. Figure 2.20 discusses the factors related to smooth transition pathways to promote BESS to support integration of REZs in weak grids.

Within these weak grids, the variability and non-dispatchable nature of RESs (e.g., solar and wind) can exacerbate issues such as frequency instability, voltage fluctuations, and reduced system inertia. By actively smoothing power outputs, providing ancillary services like frequency regulation and reactive power support, and alleviating curtailment risks during off-peak generation times, BESS address these concerns effectively [36], [73]. Moreover, they enable peak shaving and load shifting to better align energy supply with demand, reducing reliance on emission-intensive peaking plants and thereby supporting SDG 13 (Climate Action) [35], [111].

From a policy and market design perspective, promoting BESS involves establishing robust frameworks and incentives that appropriately recognize and reward the services they provide such as voltage regulation, spinning reserve, black-start capability, or deferred transmission investments. Collaboration among policymakers, grid operators, private sector stakeholders, and local communities is essential to creating transparent market rules, tariff structures, and compensation schemes [111], [146].

Table 2.12: BESS Case Studies with Battery Types

Project Name (Case Studies)	**Date of Operation**	**Configuration**	**Main Function**
Qinghai Luneng Gelmud multi-energy complementary national project (China)	Dec. 2018	Li-ion battery: 50 MW/10 MWh	1) Instruction tracking, 2) Smoothen output fluctuations, 3) Frequency & voltage regulation
Henan grid-side distributed BESS project (China)	Dec. 2018	Li-ion battery: 100.8 MW/125.8 MWh	1) Peak regulation, 2) Frequency and voltage regulation, 3) Emergency response
Jiangsu Zhenjiang grid-side distributed BESS project (China)	Jul. 2018	Li-ion battery: 101 MW/202 MWh	1) Peak regulation, 2) Frequency and voltage regulation, 3) Emergency response.
SDG& E Escondido BESS project (USA)	Feb. 2017	Li-ion battery: 30 MW/120 MWh	Participate in electricity market transactions
Golmud New era energy 50-MWp photovoltaic power station (China)	Jul. 2016	Li-ion battery: 15 MW/18 MWh	1) Instruction tracking; 2) reduction of the abandonment of PV power generation; and 3) Smoothen output fluctuations
Virginia Beech Brdge BESS project (USA)	May 2015	Li-ion battery: 31.5 MW/12.06 MWh	1) Participate in the frequency regulation market
West Sendai substation frequency regulation BESS (Japan)	Feb. 2015	Li-ion battery: 40 MW/20 MWh	1) Frequency regulation
Primus, California Irrigation community project (USA)	Oct. 2012	RFB: 25 MW/100 MWh	1) Smoothen output fluctuations, 2) Stability support, 3) Improve power quality
Zhangbei wind-photovoltaic-storage-transmission demonstration Project (China)	Dec. 2011	Li-ion battery: 14 MW/63 MWh; RFB: 2 MW/20 MWh; Pb-acid: 2 MW/2 MWh; NaS battery: 3 MW/34 MWh	1) Instruction tracking, 2) Smoothen output fluctuations, 3) Frequency and voltage regulation
Aomori, Rokkasho-Futamata wind farm (Japan)	Aug. 2008	NaS battery: 34 MW/245 MWh	1) Smoothen output fluctuations, 2) Improve reliability, 3) Load-following, 4) Reactive power support
West Murray Zone GFM BESS Project (Australia)	2023	GF BESS: 200 MW capacity, Battery type: Not specified	1) Enables sub-synchronous oscillations mitigation, 2) Supports grid stability in weak grids
Optimal Sizing BESS for IEEE 39-bus system	2022	Multiple BESS placements across key load points, Battery type: Not specified	1) Improve frequency stability using optimal BESS sizing; and 2) Placement under uncertainty
Distributed PV-BESS Curtailment (South Australia)	2023	Distributed PV (5 kW) coupled with BESS (13.5 kWh) in LV networks; Battery type: Li-ion	1)Analyze and reduce energy curtailment in distributed PV-BESS systems due to overvoltage
South Australia VPP Project	2020	Residential BESS fleet integrated into VPPs Battery type: Not specified	1) Facilitate demand-side response; 2) provide fast frequency response; reduce system stress
Waratah Super Battery (NSW, Australia)	Targeted for 2025	RLi-ion battery: 700 MW/1400MWh	1) Provide grid reliability after coal plant retirements, 2) Support system security and capacity
Liddell BESS (NSW, Australia)	2023-2024 (planned)	Li-ion up to 500 MW	1) Grid reliability as Liddell coal station retires, 2) Frequency control (FCAS) and rapid response, 3) Smoothing renewables (wind/solar) output
Orana BESS (NSW, Australia)	-	Likely to be Li ion; Exact size not specified	1) Grid stability & supporting new renewables in the Orana region, 2) Peak shaving / load shifting, 3) Frequency & voltage control

Additionally, investment in digital infrastructure enhances forecasting, optimal dis-

patch, and performance analytics for BESS, leveraging machine learning and artificial intelligence to support dynamic, data-driven decision making. Such digitization also opens pathways for novel business models like VPPs and aggregated energy trading, further aligning with SDG 7 (Affordable and Clean Energy) [45], [55],[145].

Technological innovation remains a cornerstone of this transition pathway. Advancements in battery chemistry, improvements in life-cycle performance, the optimization of recycling processes, and the exploration of next-generation options such as solid-state batteries are critical for alleviating concerns over cost, sustainability, and raw material availability [36], [121], [124]. These efforts pave the way for more robust, longer-lasting battery solutions with smaller environmental footprints, thereby enabling wider adoption of BESS consistent with the vision of sustainable development.

In remote or islanded grids, the transformative impact of BESS is especially pronounced. By substantially reducing diesel fuel consumption, enhancing local grid reliability, and integrating higher levels of renewables, BESS strengthen energy access, improves air quality, and lowers operating costs. Overcoming upfront capital barriers can be justified by the long-term benefits of emission reduction, economic savings, and higher-quality power outcomes that advance both SDG 7 and SDG 13 [48],[50], [145].

In summary, the transition pathway to promote BESS spans regulatory reforms, technological breakthroughs, market-based incentives, and digitization strategies, all of which jointly support the global drive for affordable, clean, and resilient energy systems. By aligning these elements, stakeholders accelerate the deployment of BESS, paving the way for a future in which higher levels of renewable penetration are seamlessly integrated into weak grids. This evolution not only advances the objectives of SDG 7 (Affordable and Clean Energy) and SDG 13 (Climate Action) but also contributes to the broader sustainability agenda, fostering inclusive, robust, and carbon-neutral energy infrastructures worldwide.

2.11 Findings and conclusions

This review presents a comprehensive analysis of the role of Battery Energy Storage Systems (BESSs) in enhancing renewable energy (RE) utilization within weak grids, driven by the environmental and economic drawbacks of non-renewable sources that have prompted the Australian government to develop Renewable Energy Zones (REZs). It begins by examining the challenges of integrating renewables into weak grids, identifying Energy Storage Systems (ESSs) as a potential solution while acknowledging the

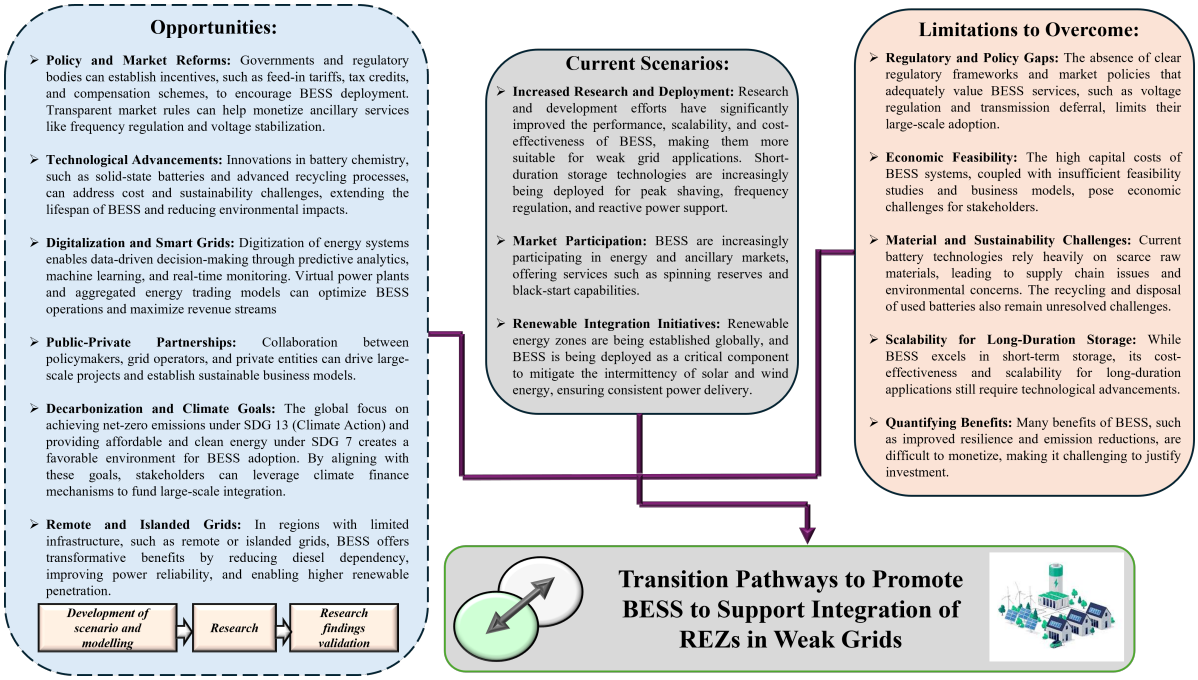


Figure 2.20: Factors related to smooth transition pathways to promote BESS to support integration of REZs in weak grids

limitations of non-BESS technologies.

Focusing on BESSs as a promising alternative, the review compares different battery types and explores their deployment in both islanded and grid-connected weak grids. It also analyzes real-world BESS implementations, emphasizing their impact on grid stability, power flow management, and energy optimization. Additionally, the study investigates advanced control strategies, operational algorithms, and energy management techniques tailored to weak grid environments.

Finally, this review proposes a strategic transition pathway to accelerate large-scale BESS integration, fostering a more sustainable, climate-friendly, and cost-effective energy system. It concludes by outlining key directions for future research in this rapidly evolving field. The major findings and conclusions of this study are as follows:

- **Challenges in REZs Integration:** Weak grids, defined by high impedance, limited fault current capacity and short circuit ratio, and vulnerability to disturbances, present significant obstacles to renewable energy (RE) integration. Key challenges include grid stability issues, such as inertia deficits, voltage fluctuations, and frequency instability, along with power quality concerns like sags, surges, and harmonics. Additionally, the non-dispatchable nature of renewables further compli-

cates reliable operation. Addressing these barriers requires innovative solutions to ensure the seamless and stable integration of RE into weak grids.

- **Limitations of Non-BESSs:** Non-BESS energy storage technologies, including mechanical, thermal, and chemical storage systems, face several limitations such as geographic constraints, high installation costs, and complex operational requirements. Mechanical storage methods like pumped hydro storage (PHS) and compressed air storage (CAS) are restricted by environmental and site-specific factors. Chemical storage solutions, such as hydrogen fuel cells (FCs), encounter challenges related to cost and efficiency. While thermal energy storage (TCSS) shows potential, it is limited by low energy density and significant infrastructure demands, making large-scale implementation challenging.

- **BESS as a Promising Solution:** BESS emerges as a flexible, scalable, and cost-effective technology to address the limitations of non-BESS. Li-ion batteries, in particular, offer high energy density, rapid response times, and scalability, making them ideal for weak grid environments. Other battery technologies, such as VRFB and NaS batteries, also demonstrate potential in specific applications. The review highlights the versatility of BESS in mitigating renewable intermittency, stabilizing voltage and frequency, and improving overall grid reliability.

- **Projects on BESS Integration:** Real-world case studies are analyzed to illustrate the practical deployment of BESS in Renewable Energy Zones (REZs) and weak grids. These projects demonstrate how BESS enhances grid stability in high-renewable penetration areas, manages load fluctuations, and reduces renewable energy curtailment. The findings highlight key benefits such as improved power quality, enhanced energy reliability, and economic feasibility, offering valuable insights for policymakers and industry stakeholders.

- **Control Strategies and EMSs:** Effective BESS operation relies on advanced control algorithms, including Model Predictive Control (MPC), Fuzzy Logic Control (FLC), and Neural Network Control (NNC), which enable real-time optimization of power flow, energy storage, and grid stability. Additionally, energy management techniques such as load shifting, state-of-charge (SoC) optimization, and peak shaving play a crucial role in maximizing both the economic and technical benefits of BESS deployment.

- **Future Directions and Transition Pathways:** To enable large-scale BESS adoption, innovative policy frameworks, advanced grid infrastructure, and continued research are essential. Future studies should explore Hybrid Energy Storage Systems (HESSs), novel control algorithms, and lifecycle optimization to further enhance BESS viability in weak grids and REZs. Additionally, the development of adaptive energy systems and robust market regulations is crucial for achieving a sustainable, climate-friendly energy transition.

  In conclusion, this comprehensive review establishes BESS as a key technology for improving renewable energy utilization and addressing the challenges of weak grid environments. Real-world deployments, such as the 700 MW / 1400 MWh Waratah Super Battery and the 34 MW/245 MWh NaS battery project in Japan, demonstrate the effectiveness of BESS in enhancing stability and reducing curtailment in weak grids. Large-scale battery systems in South Australia-such as the Hornsdale Power Reserve-enhance grid stability by delivering rapid frequency regulation, supporting greater integration of wind and solar energy, and reducing dependence on fossil fuels. With efficiencies reaching up to 95% and millisecond-level response times, BESS technologies, particularly Li-ion systems, are well-suited for supporting voltage and frequency stability. By providing insights into BESS applications, control strategies, EMS frameworks, and real-world case studies, this review offers a roadmap for advancing BESS deployment in REZs. These findings contribute to the broader goal of achieving clean, affordable, and sustainable energy systems, aligning with the vision of a zero-carbon future.

In conclusion, this chapter establishes BESS as a pivotal technology for enhancing RE utilization and addressing the complexities of weak grid environments. By offering practical insights into their applications, control strategies, EMSts, and real-world case studies, this review provides a roadmap for advancing BESS deployment in REZs. These findings contribute to the broader goal of achieving affordable, clean, and sustainable energy systems, aligning with the vision of a zero-carbon future. Building on this foundation, the next section presents the second part of the literature review, offering a systematic examination of GFLIs and GFMIs and their cornerstone role in enabling stable REZ integration within Australia's evolving power system.

2nd Part Literature Review

The second part of this literature review examines the cornerstone role of GFL and GFM inverters in enabling stable and scalable REZ integration within the Australian context. As illustrated in Figure 2.21, this section explores inverter control principles, coordinated GFM-GFL operation, and their contribution to enhancing grid stability, flexibility, and renewable hosting capacity. It further highlights key REZ integration challenges, benchmark simulation constraints, and emerging control strategies that collectively form a resilient inverter deployment roadmap for Australia's future weak-grid environments.

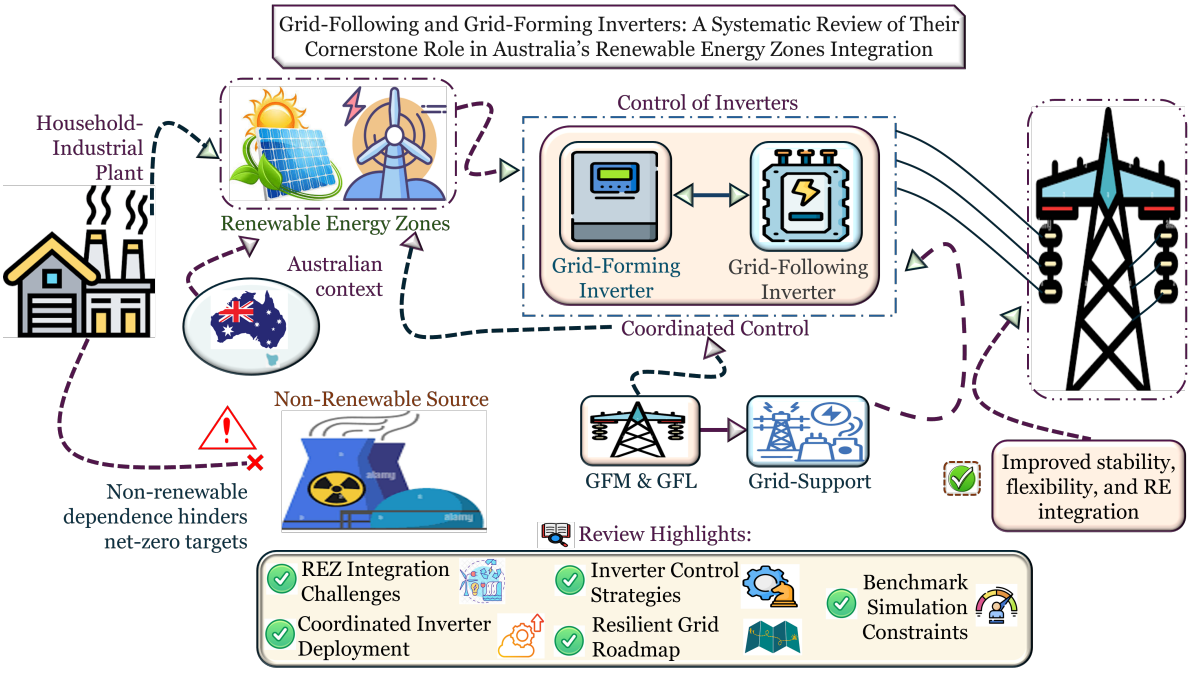


Figure 2.21: Overview of the second part of the literature review

2.12 Introduction

The increasing urgency to mitigate climate change and ensure long-term energy security has positioned renewable energy sources (RESs) at the core of global power system transitions. In Australia, this transformation is particularly pronounced. The nation is undergoing one of the most ambitious renewable energy (RE) transitions in the world, driven by national decarbonization policies, technological innovation, and declining costs of wind and solar power [1–3]. According to the Australian Energy Market Operator

(AEMO), the country is on track to source over 80% of its electricity from renewable sources by 2030 [1, 3]. Reinforcing this national ambition, most Australian states and territories have established aggressive renewable energy (RE) targets, many aiming 100% or higher by 2030 or 2040. Figure 2.22a) visualizes these targets across jurisdictions, highlighting variations in ambition and policy timelines [2]. Beyond targets, this transition is reshaping both the operational dynamics and infrastructure of the electricity grid.

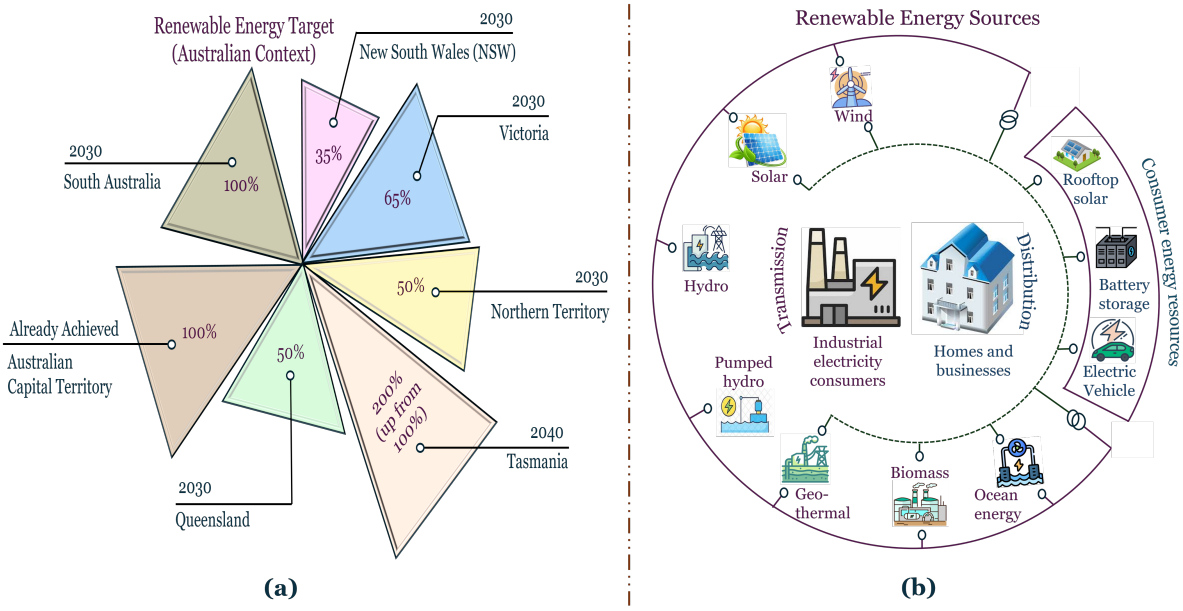


Figure 2.22: Australia's RESs and target overview: (a) RE targets for states and territories, (b) RESs powering industries, homes, and businesses

As illustrated in Figure 2.22b), Australia's RE system integrates both large-scale grid-connected RESs (such as solar, wind, hydro, biomass, ocean, geothermal, and pumped hydro) and distributed consumer energy sources (CERs) like rooftop solar, battery storage, and electricity vehicles [3]. These resources support the growing demand from homes, businesses and industries enabled by advanced transmission and distribution networks [147, 148]. A significant share of this development is concentrated within Renewable Energy Zones (REZs), geographically identified areas with optimal renewable potential, co-located with necessary grid infrastructure upgrades to enable efficient large-scale integration and export [149, 150]. Public support remains robust, with surveys by the Australian Renewable Energy Agency (ARENA) indicating that 85% of Australians favour the renewable energy transition [2, 151]. Together, these trends underscore a holistic transformation spanning policy, infrastructure, and societal alignment toward a

low-carbon energy future [3, 152]. This transformation is increasingly embodied in the development of REZs.

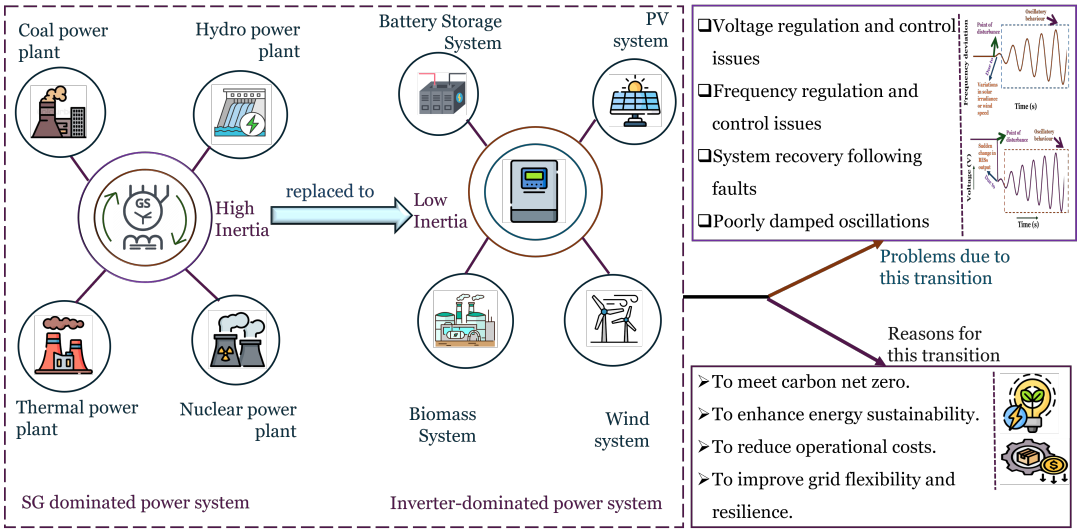


Figure 2.23: Evolution of power systems towards inverter-dominated architectures

While REZs offer a strategic framework for clustering renewable generation assets and streamlining their grid connection, they simultaneously introduce complex operational and stability challenges [152, 153]. As illustrated in Figure 2.23, the traditional power system, dominated by large-scale synchronous generators (SGs) such as coal, thermal, hydro, and nuclear plants, naturally provides high system inertia, robust voltage regulation, and strong short-circuit support [154]. These characteristics are crucial for maintaining stable frequency and voltage dynamics during disturbances [155, 156]. However, the modern evolution toward REZs has shifted system architecture toward an inverter-dominated power system, where energy is primarily supplied by inverter-based resources (IBRs) such as PV, wind, battery storage, and biomass systems [1, 157–159]. As shown in the right section of Figure 2.23, this transition leads to a significant reduction in system inertia, impairing the grid's ability to resist rapid frequency deviations [160]. Furthermore, because IBRs do not inherently contribute to short-circuit current or voltage regulation like SGs, REZs commonly experience low short-circuit ratios (SCRs), increased rate of change of frequency (RoCoF), and diminished frequency nadirs following contingencies [160, 161]. These challenges are even more pronounced in weak or remote transmission zones, where physical constraints on network reinforcement amplify the vulnerability of the system [152, 162]. The right portion of the Figure 2.23 highlights these dynamic stability issues with schematic illustrations of RoCoF and

frequency nadir deterioration under high IBR penetration, emphasizing the urgent need for GFM capabilities and advanced control strategies in REZs [18, 19].

Despite the increasing deployment of GFM and GFL inverter technologies, the academic literature remains fragmented in its analysis of their operational characteristics, particularly under the complex and variable conditions associated with REZs [150, 163, 164]. As depicted in Figure 2.24, power generation technologies may be broadly categorized by their grid-interface mechanisms, including SGs, induction machines, and converter-based non-SGs [148, 165]. Within converter-based systems, current-source converters (CSCs) generally operate in GFL mode, whereas voltage-source converters (VSCs) are capable of enabling true GFM behaviour. These converter technologies form the primary interface between RESs, such as photovoltaic (PV) arrays, battery energy storage systems (BESS), and wind turbines, and the electrical grid [153, 166–168].

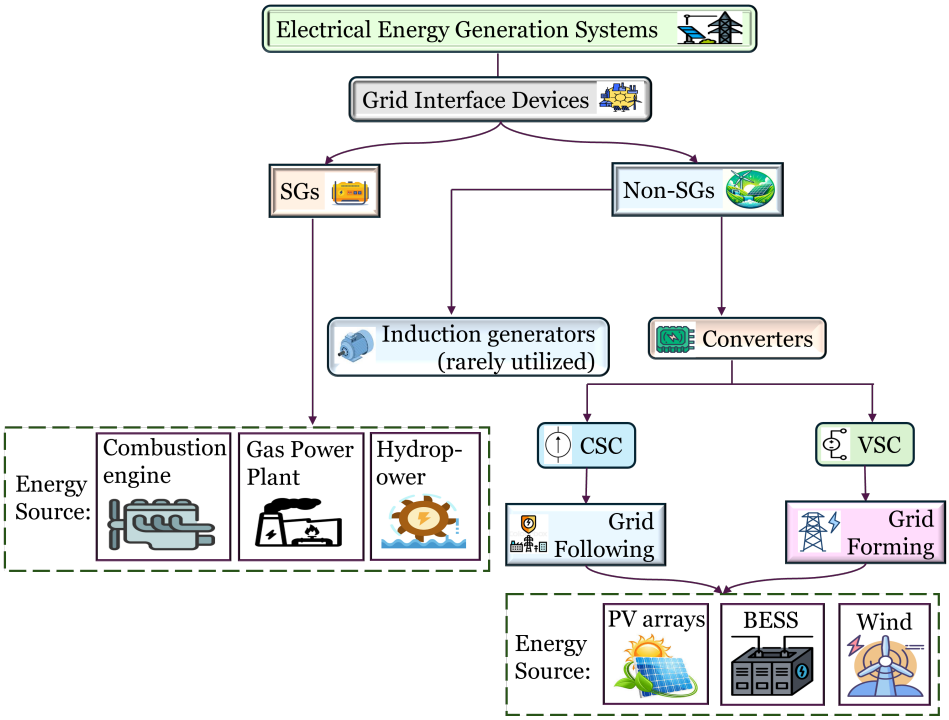


Figure 2.24: Classification of electrical energy generation systems by grid interface type

A critical limitation in the existing body of review literature is its narrow thematic scope. Prior studies have largely concentrated on isolated aspects, such as frequency regulation, voltage control, or specific converter topologies, without presenting an integrated perspective that encompasses modelling approaches, control strategies, simulation environments, and practical deployment considerations. This reductionist approach is insufficient, particularly in the context of REZs where weak-grid conditions, limited

hosting capacity, and low short-circuit ratios exacerbate the behavioural divergences between GFL and GFM inverters. Consequently, significant insights into system-wide performance and control coordination are often excluded from conventional academic discourse.

Furthermore, a disconnect persists between theoretical advancements and practical implementation outcomes. Empirical evidence from notable Australian REZ projects, such as Riverina, Central-West Orana, New England, Liddell, Dalrymple ESCRI, Hunter Central Coast, and South-West Queensland, demonstrates both the potential and the technical challenges of scaling GFM inverter deployment in real-world settings [20, 169, 170]. However, the operational lessons derived from these deployments are seldom reflected in the academic literature, despite recent updates to Australian grid codes that necessitate inverter-based systems to replicate critical grid-support functions historically provided by SGs.

Table 2.13: Comparative analysis of recent inverter-focused reviews and their coverage of REZ-specific research attributes

Ref.	Publication Year	Control Structures		Research Attributes									RWP & TP
		GFM	GFL	R1	R2	R3	R4	R5	R6	R7	R8	R9	
[1]	2025	✓	✓	✗	✗	✗	✗	✗	✗	✗	✓	✗	✗
[18]	2025	✓	✓	✗	✗	✗	✗	✗	✗	✗	✓	✗	✗
[147]	2024	✓	✓	✓	✓	✓	✓	✗	✗	✗	✓	✓	✗
[148]	2024	✓	✓	✓	✓	✗	✓	✓	✓	✓	✓	✓	✗
[157]	2024	✓	✓	✓	✓	✗	✓	✗	✗	✗	✗	✗	✗
[160]	2024	✗	✓	✓	✓	✗	✓	✗	✗	✗	✓	✗	✗
[161]	2024	✓	✓	✓	✓	✓	✓	✗	✗	✗	✓	✓	✗
[29]	2023	✓	✓	✗	✗	✗	✗	✗	✗	✗	✓	✗	✗
[162]	2023	✓	✓	✓	✓	✗	✓	✗	✗	✗	✗	✓	✗
[163]	2023	✓	✗	✗	✗	✗	✗	✗	✗	✗	✓	✗	✗
[21]	2022	✓	✗	✗	✗	✗	✗	✗	✗	✗	✓	✗	✗
[164]	2022	✗	✗	✗	✗	✗	✗	✗	✗	✓	✗	✗	✗
[165]	2022	✓	✗	✓	✓	✓	✓	✗	✗	✗	✓	✗	✗
[166]	2021	✓	✓	✗	✗	✗	✗	✗	✗	✓	✗	✗	✗
[167]	2021	✓	✓	✗	✓	✗	✓	✗	✗	✗	✓	✓	✗
[168]	2021	✓	✓	✗	✗	✗	✓	✗	✗	✗	✗	✗	✗
This study	N/A	✓	✓	✓	✓	✓	✓	✓	✓	✓	✓	✓	✓

R: Research Attributes; R1: Mathematical Control Model; R2: Control Architecture; R3: REZ-Specific GFM-GFL Limits; R4: Modelling Framework; R5: Simulation Environment; R6: Benchmark Test Network; R7: Frequency-Stability Metrics; R8: Voltage-Support Capability; R9: GFL‚ÄìGFM Coordination; RWP: Real-World Project; TP: Transition Pathways

To address these deficiencies, Table 2.13 offers a comparative synthesis of existing review studies, examining key dimensions such as inverter typologies, control architectures, modelling frameworks, simulation tools, benchmark networks, performance metrics, REZ-specific constraints, and coordination strategies. This comprehensive evaluation underscores both the timeliness and the distinct contribution of the present study, which aims to provide a unified, context-sensitive framework for understanding GFM inverter deployment in REZ environments.

Building on the identified gaps, this comprehensive study offers a systematic and integrated sreview of GFL and GFM inverter technologies in the context of Australia's REZs. It synthesizes findings from peer-reviewed literature and technical reports spanning control strategies, modelling approaches, regulatory standards, and field implementations. The key contributions of this literature review are summarized as follows:

- **Technical Foundation of Inverter Technologies:** Presents a detailed technical foundation of GFM and GFL inverters, including their mathematical control models, design architectures, and limitations in REZ conditions such as low SCR, fast RoCoF, and multi-inverter interactions.

- **Modelling and Simulation Frameworks:** Categorizes the modeling approaches, simulation environments, and benchmark test systems used in evaluating inverter behaviour under weak-grid scenarios.

- **Control Coordination and Stability Metrics:** Reviews and compares control coordination strategies in mixed GFL-GFM environments and evaluates their influence on dynamic stability metrics.

- **Insights from Australian REZ Deployments:** Compiles lessons from recent and ongoing REZ deployments across Australia, synthesizing insights from engineering practice, regulatory interventions, and economic assessments.

- **Transition Pathways to Inverter Technologies Adoption:** Proposes a strategic transition discussion to accelerate adoption of these technologies in the REZ context, supporting a sustainable, clean energy future aligned with the United Nations Sustainable Development Goals (UNSDGs) 7 and 13.

The remainder of the study is organized as follows. Section 2.13 describes the review methodology, including the search strategy, inclusion criteria, and data extraction process.

Section 2.14 outlines the technical fundamentals of inverter technologies. Section 2.15 examines modelling approaches and benchmark test systems. Section 2.16 reviews control strategies and coordination architectures. Section 2.17 explores real-world implementations within Australian REZs. Section 2.18 proposes strategic transition pathways and highlights future research directions. Finally, Section 2.19 concludes with key findings and emphasizes the need for continued innovation in sustainable energy systems.

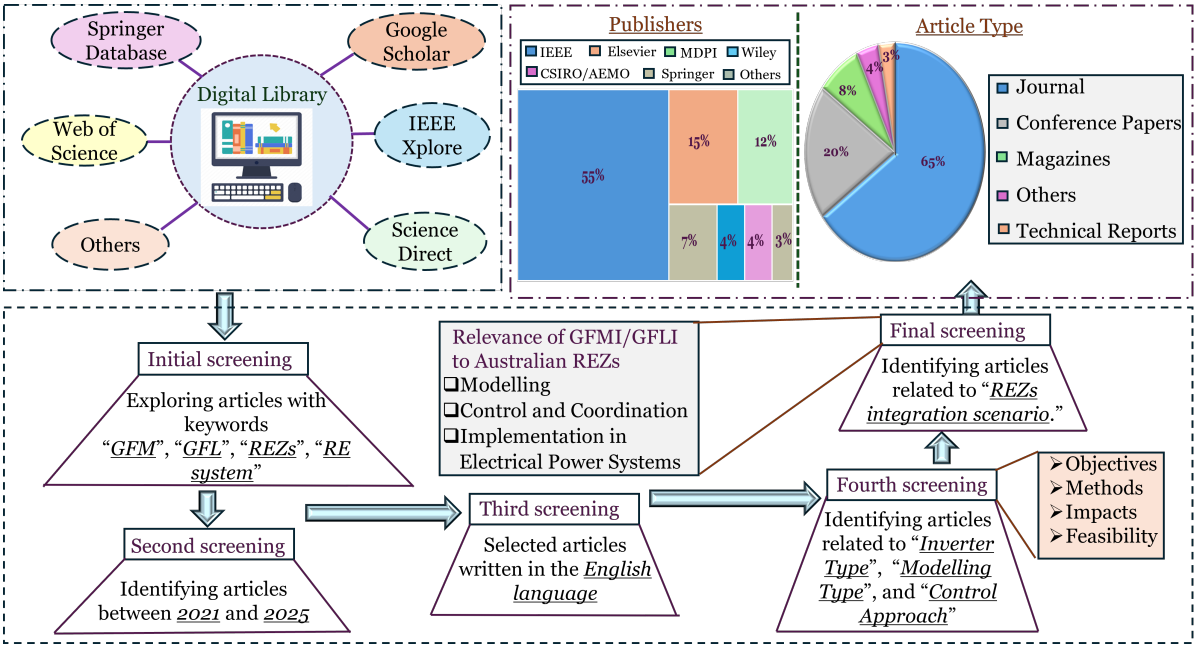


Figure 2.25: Review methodology illustrating staged screening of inverter studies for REZs relevance.

2.13 Review Methodology

The literature review followed a systematic methodology to evaluate the role of GFL and GFM inverters in Australia's REZs. As shown in Figure 2.25, the process included four phases: identification via multi-source digital search, application of inclusion/exclusion criteria, a five-stage screening protocol, and final data extraction. Studies were sourced from IEEE Xplore, ScienceDirect, Springer, Web of Science, Google Scholar, and others using keywords like "GFMIs", "GFLIs", and "inverter control in weak grids". Most studies were retrieved from IEEE and Elsevier, reflecting their dominance in this field.

Inclusion criteria required peer-reviewed status, relevance to inverter control in weak grids or REZs, and a focus on modelling or implementation. The screening stages involved keyword filtering, year and language limits (2021-2025, English), content relevance, and

final alignment with REZ scenarios. Selected studies were then categorized by control strategy, modelling framework, test system, and metrics such as RoCoF and voltage support. The publisher distribution in Figure 2.25 highlights IEEE and Elsevier as leading contributors to this research area.

2.14 Technical Background of Inverter Technologies

GFL and GFM inverters are examined in this section to their working principles, mathematical control models, and system architectures. Their performance under weak-grid conditions is assessed by highlighting key control strategies, including FRT and black-start capabilities. A comparative analysis of their operational features is presented, followed by a critical evaluation of their overall suitability for deployment in REZs.

2.14.1 Grid-Following (GFL) Inverters

2.14.1.1 Working Principles

GFL inverters are extensively used in PV and BESS applications due to their maturity, cost-effectiveness, and standardized control frameworks [19, 147, 169]. These inverters synchronize with the grid using a PLL, which tracks the grid voltage phase and frequency, enabling the inverter to inject current in phase with the grid. Operating as controlled current sources, GFL inverters depend entirely on the external grid for voltage and frequency references, limiting their ability to support system stability, particularly in weak or islanded networks [18, 171, 172]. As shown in Figure 2.26(a), the inverter's output is dictated by the grid, highlighting its passive response during dynamic events. Figure 2.27 further classifies GFL inverters into grid-feeding and grid-supporting types. Grid-feeding inverters inject predefined active and reactive power based on setpoints, while grid-supporting inverters incorporate advanced current control strategies, such as droop control and VSG emulation, to offer limited dynamic grid interaction, though still reliant on PLL-based synchronization [161]. The following section outlines the mathematical model and control loops of GFLIs.

2.14.1.2 Mathematical Model and Control Loops of GFLIs

Building on GFL inverter principles, their control architecture typically follows a cascaded structure comprising a PLL, outer power control loop, and inner current regulation loop within the synchronous dq reference frame [148, 149, 173]. The PLL tracks the

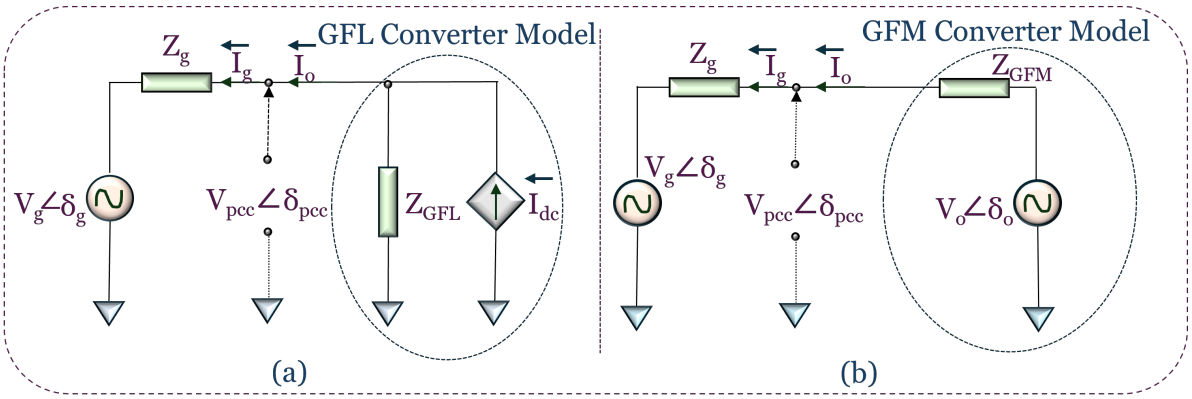


Figure 2.26: Conceptual models of (a) GFL and (b) GFM converters

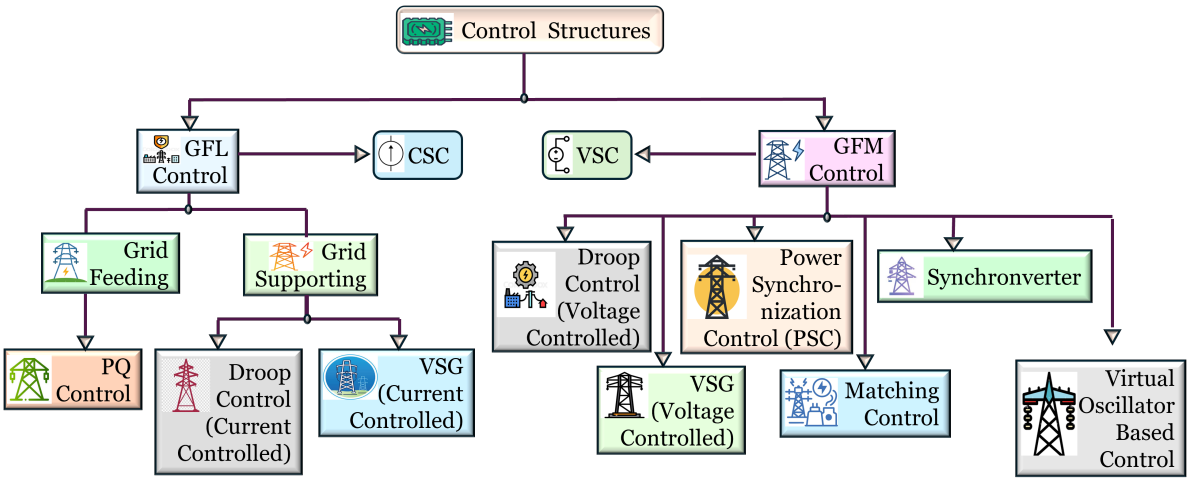


Figure 2.27: Classification of grid-connected converters based on GFL and GFM control structures for integration within REZs.

grid voltage phase θ to enable transformation into the dq domain. Based on frequency and voltage deviations, the outer loop generates power references adjusted using droop characteristics:

$$P_i = P_{\text{ref}} + m_p(\omega_{\text{meas}} - \omega_{\text{ref}}), \quad Q_i = Q_{\text{ref}} + m_q(V_{\text{grid}} - V_{\text{ref}}) \tag{2.1}$$

These are converted into current commands $i_{d\text{ref}}$ and $i_{q\text{ref}}$, which are tracked by PI-based inner current controllers. Figure 2.28(a) illustrates this structure for BESS applications. To improve performance under disturbances, enhanced versions (Figure 2.28b) incorporate adaptive droop and low-voltage ride-through (LVRT) features, enabling limited support under abnormal conditions in weak grids, as further discussed in the next section on operational limitations.

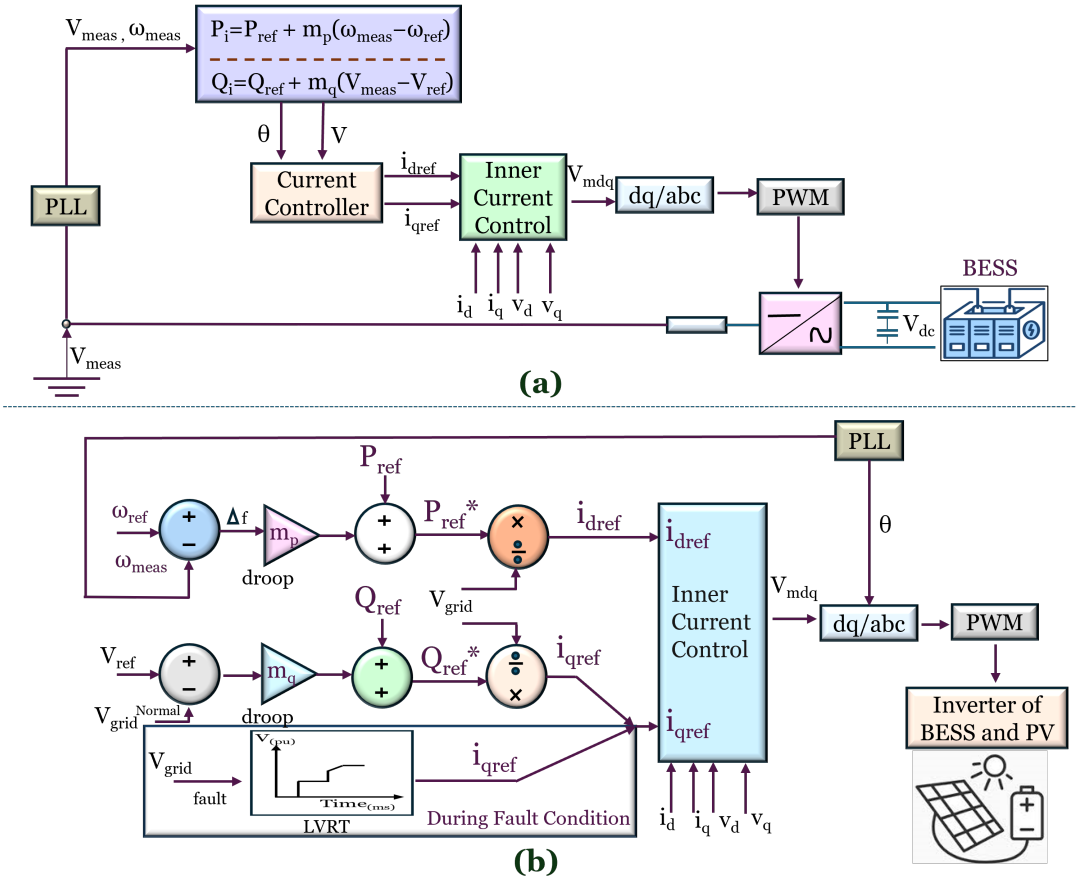


Figure 2.28: Control strategies supporting IBRs integration in REZs: (a) GFL inverter control architecture with BESS, (b) Enhanced GFL control for PV systems

2.14.1.3 Limitations in Weak Grids

Despite their effectiveness in strong grids, GFL inverters face major challenges in weak-grid environments with low SCR, where their dependence on external voltage and frequency references limits voltage support and FRT capability [14, 19, 174]. The PLL, central to GFL operation, becomes unstable during large disturbances, especially in high inverter-penetration scenarios with reduced system strength [157, 175]. These issues are critical in REZs, where synchronous generation is minimal, and IBRs must maintain grid stability [7, 21, 176]. Even with enhancements like droop and LVRT, GFL architectures often fall short under such conditions. To address this, the focus is shifting toward GFM inverters, which can independently regulate voltage and frequency [148, 161, 177]. The following section examines their control strategies and role in overcoming GFL limitations in weak grids.

2.14.2 Grid-Forming (GFM) Inverters

2.14.2.1 Definitions and Operating Modes

GFM inverters mark a significant shift from GFL approaches by operating as voltage sources capable of independently setting and regulating grid voltage and frequency [178–180]. Unlike GFL inverters, GFM units do not rely on external references, making them more suitable for weak-grid and islanded environments. As shown in Figure 2.26(b), a GFM inverter outputs a controlled voltage waveform $V_o\angle\delta_o$ and defines system conditions to which other devices synchronize, with internal impedance Z_{GFM} enabling droop-based control. GFM inverters operate in standalone, grid-connected, or hybrid modes, allowing them to either fully establish or share grid parameters [147, 181]. Their use is especially valuable in REZs, where high inverter penetration and low inertia challenge system stability. Recent studies highlight their importance for black-start, inertial response, and FRT services in future low-inertia power systems [168, 182, 183], with the following section detailing their control strategies and mathematical models.

2.14.2.2 Droop Control, Virtual Synchronous Generator (VSG), and Virtual Oscillator Control (VOC)

To ensure stable and decentralized operation in REZs, GFM inverters emulate synchronous machine dynamics through advanced control strategies such as droop control, VSG, and VOC [148, 161]. These approaches enable autonomous voltage and frequency regulation, critical for weak and low-inertia grids [1, 33]. Figure 2.27 illustrates the classification of GFM and GFL control structures.

Droop control adjusts frequency and voltage based on power deviations, supporting decentralized coordination without communication:

$$\theta^* = \int \omega dt, \quad P_m = P_{\text{ref}} + K_p(\omega - \omega_{\text{ref}}), \quad \frac{d\omega}{dt} = \frac{1}{2H}(P_m - P_{\text{meas}} - D\Delta\omega) \tag{2.2}$$

$$V^* = V_{\text{ref}} + K_q(Q_{\text{meas}} - Q_{\text{ref}}) \tag{2.3}$$

This structure, shown in Figure 2.29(a), is widely used in grid-forming BESS.

VSG control enhances dynamic stability by embedding virtual inertia and damping into the swing equation:

$$P_m = P_{\text{ref}} + K_p(\omega_{\text{ref}} - \omega), \quad \frac{d\omega}{dt} = \frac{1}{2H}(P_m - P), \quad \theta^* = \int \omega dt \tag{2.4}$$

$$V_q = V_{\text{ref}} + K_q(Q_{\text{ref}} - Q_{\text{meas}}) \tag{2.5}$$

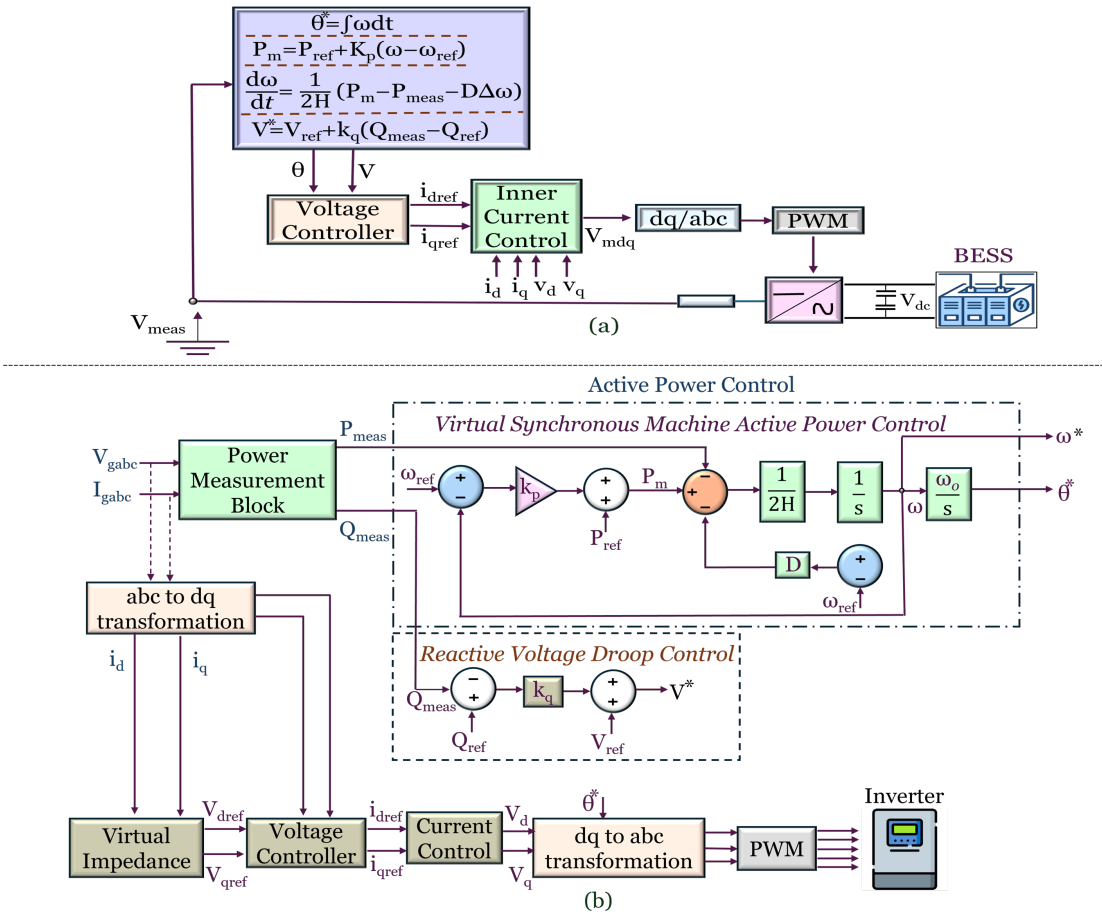


Figure 2.29: Control strategies supporting IBR integration in REZs: (a) GFM inverter architecture with droop-based voltage and frequency control for BESS, (b) VSM control framework enabling GFM capabilities for stable REZ operation.

Figure 2.29(b) illustrates its implementation for smooth grid synchronization.

VOC, unlike droop and VSG, eliminates the need for PLLs by using nonlinear oscillators for voltage generation. A typical VOC uses the Van der Pol oscillator:

$$\frac{d^2x}{dt^2} - \mu(1-x^2)\frac{dx}{dt} + \omega_0^2 x = 0 \tag{2.6}$$

where x represents the voltage waveform and ω_0 the nominal frequency. VOC enables fast, decentralized synchronization, especially in microgrids, as shown in Figure 2.27.

Together, these control methods offer scalable, resilient solutions for integrating inverter-based resources in REZs. The following subsection explores their black-start and FRT capabilities, essential for grid recovery during contingencies.

2.14.2.3 Black-Start and Fault-Ride Through Capability

Building on the capabilities of droop, VSG, and VOC architectures, GFM inverters offer essential services beyond standard voltage and frequency regulation, most notably, black-start and FRT [148, 177]. Unlike GFL inverters, GFM units can independently establish voltage and frequency, enabling black-start operation without synchronous machine support, crucial for restoring de-energized networks in remote or islanded REZs [178, 181]. GFM inverters also outperform GFL systems in FRT, remaining connected and regulating grid parameters during faults thanks to their virtual inertia and damping [184, 185]. Studies confirm their effectiveness in limiting fault currents and maintaining stability during severe disturbances, validating their role as core assets in inverter-dominated grids [38, 163, 165]. The next subsection provides a comparative analysis of GFL and GFM inverters, highlighting their relative advantages, limitations, and suitability across different REZ operating conditions.

2.14.3 GFL vs. GFM Comparison

2.14.3.1 Operational Differences

A concise comparison of GFL and GFM inverters is presented in Table 2.14, highlighting their core operational distinctions. GFL inverters rely on external voltage references and operate effectively only in strong grids, offering limited support during faults or instability [161, 186]. In contrast, GFM inverters establish voltage and frequency autonomously, thereby contributing to system inertia and enabling critical services such as black start and FRT [148, 187]. These differences underscore the superior suitability of GFM inverters for weak-grid and REZ environments.

2.14.3.2 Suitability for REZs Integration

GFM inverters offer superior suitability for REZ integration due to their inherent capability to operate under low system strength and weak grid conditions [6, 18, 174]. As summarized in Table 2.15 and Table 2.16, they provide essential grid services such as FFR, voltage regulation, black-start capability, and synthetic inertia, features critical for stabilizing low-inertia REZ environments [5, 157, 188]. Additionally, simulation-based evidence confirms their effectiveness in enhancing system strength and maintaining dynamic stability under high renewable penetration and weak grid scenarios [167, 185, 189]. The following section explores modeling approaches adopted in the context of

Australian REZs, focusing on how these control-oriented capabilities are evaluated in simulation environments.

2.15 Modeling Approaches in the Context of Australian REZs

This section examines the general modelling approaches and simulation tools used to study inverter-based systems, with a specific focus on modelling practices relevant to the Australian REZ context.

2.15.1 General Modeling Approaches

2.15.1.1 Steady-State vs. Dynamic Modelling

Modelling inverter-dominated Australian REZs requires a comprehensive approach that captures both long-term system adequacy and short-term operational stability. As illustrated in Figure 2.30, steady-state methods are commonly applied for tasks such as economic dispatch, power flow feasibility, and system adequacy assessment, where IBRs are treated as static power injections [8, 190]. However, such methods often fail to reflect fast dynamics arising in low-inertia networks or during disturbances [191].

Table 2.14: Advanced Operational Comparison Between GFL and GFM Inverters

Aspect	**GFL Inverter**	**GFM Inverter**
Control Type	CSI; injects controlled current based on external voltage	VSI; sets voltage waveform and regulates frequency internally
Reference Signal	Depends on PLL to track grid voltage and frequency	Generates its own voltage and frequency reference (no PLL required)
Grid Synchronization	Follows an existing grid	Establishes grid conditions; other devices synchronize to it
Dynamic Stability Role	Passive element; relies on grid strength for stability	Actively enhances grid stability through synthetic inertia and damping
Inertia Contribution	Does not contribute to system inertia	Emulates inertia using control algorithms (e.g., VSG, droop)
FRT	Typically disconnects or destabilizes under faults	Maintains voltage and frequency during disturbances
Black-Start Capability	Cannot initiate system restoration	Can energize and restore a de-energized grid without external support
Operational Suitability	Requires high SCR; unstable in weak grids	Operates reliably in low-SCR or islanded systems
Grid Support Services	Limited to steady-state power injection; needs strong grid	Provides voltage/frequency regulation, inertial response, and fault support
Application in REZs	Unsuitable without strong synchronous support	Essential for stability in inverter-dominated REZs

Table 2.15: Comparative Summary of GFL and GFM Inverters in Weak and Low-SCR Grids

Control Attribute	**GFL Inverter**	**GFM Inverter**	**Ref(s)**
Synchronization	PLL-based; requires external voltage reference	Self-synchronizing; sets its own voltage and frequency	[149, 190]
Stability Role	Passive; relies on grid for frequency and voltage stability	Active; contributes directly to frequency and voltage regulation	[19, 147]
Grid Dependency	Operates only in strong (stiff) grids	Operates in both strong and weak (low-SCR) grids	[174, 179]
Inertia Contribution	None; increases ROCOF and system sensitivity	Provides synthetic inertia via droop or VSG control	[5, 178, 192]
Frequency Support	Limited; frequency response degrades with PV/RES share	Stable response through embedded inertia and droop control	[5, 178, 192]
Voltage Stability	Maintains voltage only above SCR ≥ 3; fails in weak grids	Maintains voltage even at low SCR; supports dynamic voltage control	[174, 179]
Fault Ride-Through (FRT)	Likely to disconnect or destabilize under fault	Remains stable and connected; enhances post-fault recovery	[148, 193]
Protection Compatibility	Susceptible to relay mis-operation in low-inertia grids	Enhances relay operation due to stable voltage and current response	[19, 174]
Cascading Failure Mitigation	High risk due to low inertia and voltage instability	Helps prevent cascading events via fast stabilization response	[19, 147]
Suitability for REZs	Limited; needs synchronous support	Highly suitable; ensures autonomous and resilient operation	[6, 157, 181]

Table 2.16: Advanced Feature Matrix of Inverter Technologies for REZ Deployment

Ref(s)	**Feature**	**GFL**	**GFM**	**Relevance to REZs**
[19, 21, 147, 148, 182]	Black-Start Capability	✗	✓	Allows autonomous restoration of de-energized zones without synchronous machine support
[19, 148]	Power Control (P/Q)	✓	✓	Enables active/reactive power injection, critical for voltage stability in weak grids
[8, 147, 148, 194]	Fast Frequency Response (FFR)	✗	✓	Mitigates ROCOF in low-inertia networks, supporting system stability in REZs
[6, 148, 181]	System Strength Contribution	✗	✓	Enhances grid stiffness and improves short-circuit ratio in weak or remote REZs
[1, 148, 157, 178]	Grid Code Compliance (AEMO/NEM)	Partial	Targeted	Meets evolving regulatory requirements for inverter-based generation in REZs

Dynamic modeling becomes critical for analyzing the behavior of GFM inverters, particularly for evaluating frequency stability, RoCoF compliance, and FRT capability [195, 196]. Studies have shown the limitations of static models under weak grid conditions [41, 197] and the operational complexities introduced by high IBR penetration [198]. National modeling efforts further emphasize the need for dynamic simulations that incorporate voltage and frequency support functions to ensure secure REZ operation [199, 200]. As GFM and GFL technologies advance, integrated modeling frameworks

must evolve to reflect key control capabilities such as fast frequency response, damping support, black start, and harmonic absorption [201, 202]. The next subsection further explores the comparative roles of electromagnetic transient (EMT) and root mean square (RMS) modeling in representing such dynamic behaviors with appropriate temporal and control resolution.

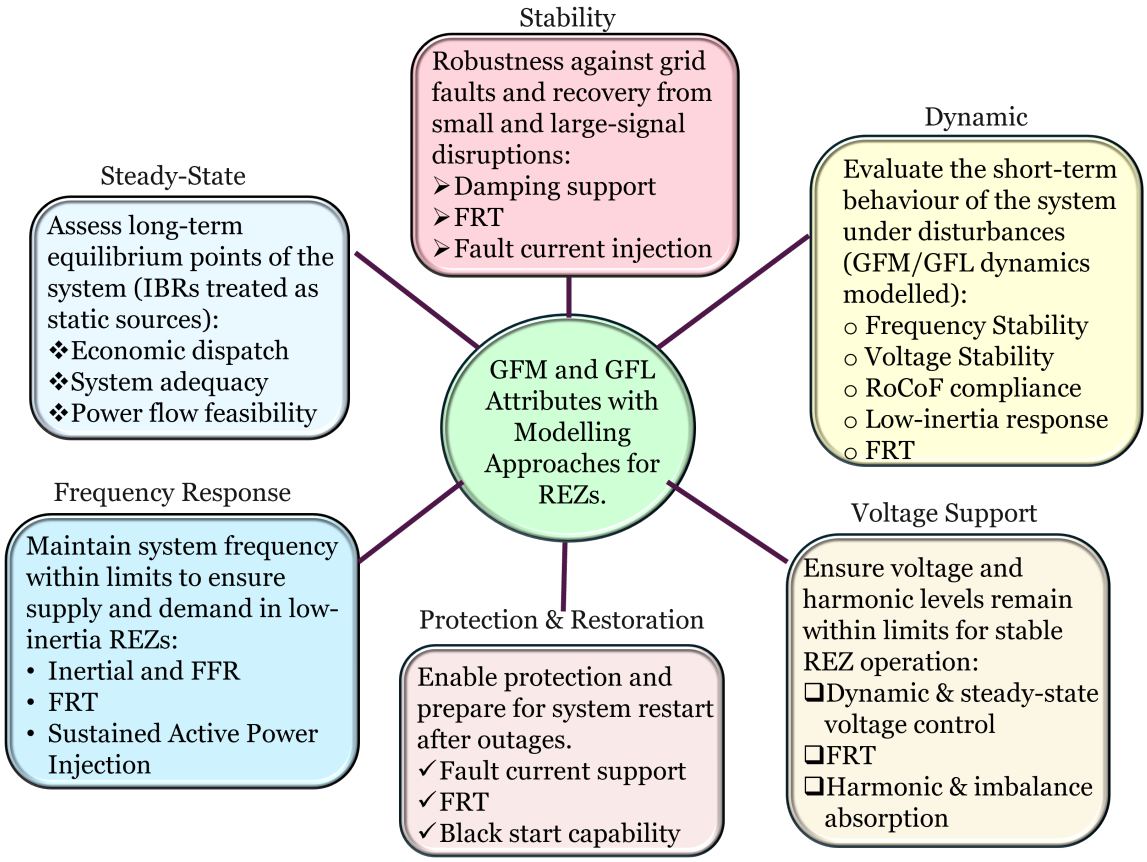


Figure 2.30: Key attributes of GFM and GFL inverters linked with steady-state and dynamic modelling approaches for REZ applications.

Table 2.17: Modelling Tools and Parameters Used in studies relevant to Australian REZs

Ref.	Simulation Tool	Model Type	Test System	Key Application	Validation	Relevance to Australian REZs
[203]	PSCAD	EMT	Modified 9-bus power system	Black-start with GFM-IBR interaction	Simulation	Models post-blackout conditions in weak grids; addresses stability and restoration in REZs
[204]	PSCAD/EMTDC	EMT	Kilmarnock South BESS	Grid-forming BESS for short-circuit & inertia	Simulation	Replicable in low-inertia, weak REZs (SA, NE)
[205]	MATLAB/Simulink	RMS	2-area, 2-machine system	Power-sharing in multi-GFM systems	Simulation	Supports coordinated GFM tuning in REZs; aligns with AEMO's system strength
[195]	PSCAD	EMT + EA	IEEE-9 + QLD grid	Battery ramp-rate limit on VSM stability	Simulation	Queensland REZ context; informs safe VSM in weak grids
[206]	PSCAD/EMTDC	EMT	WMZ, NEM	GFMI for damping SSCI	Simulation	WMZ REZ context; informs GFMI tuning and strategies in weak NEM zones
[207]	MATLAB/Simulink + Monte Carlo	RMS + ES	IEEE-30/57/118	Inverter placement for synchronization	Simulation	Guidance for inverter placement in weak-grid REZs (SA, NE)
[208]	MATLAB/Simulink	EMT	Low-voltage microgrid: 3 residential load groups	Multi-master black-start sequence	Simulation	Supports autonomous black-start in weak REZ feeders; ideal for inverter-heavy, communication-constrained REZs in Australia
[197]	PSCAD/EMTDC	EMT	100 MW wind farm	GFM inverter control to support weak grid integration	Simulation	Directly applicable to Australian REZs with low SCR; supports inverter-only integration for replacing SCs in wind-based REZs
[209]	HOMER + DIgSILENT PowerFactory	RMS + EMT	Melville Island microgrid	Dynamic dispatch strategy optimization for remote islanded REZ	Simulation	Directly applicable to remote REZs in Australia needing off-grid resilience
[210]	PSS®E	EMT	2030 QLD grid	FFR vs simulated inertia from BESS	Simulation	Informs AEMO and REZ planners on optimal BESS allocation and GFM roles in low-inertia scenarios
[211]	MATLAB/PLECS + Imperix HIL	EMT	Single-machine + Multi-inverter grid	GVSG under RoCoF compliance	Simulation + HIL	Applicable to weak-grid REZs in the NEM; improves inverter-based plant resilience and stability
[212]	PSCAD/EMTDC	EMT	Dalrymple, Melbourne	GFMI behavior in grid-connected and islanded microgrids under high RES	Field + simulation	Demonstrates microgrid stability, FCAS readiness, and ancillary services critical for REZs in weak-grid scenarios
[213]	MATLAB/PLECS + MOSEK	EMT	Single-machine GFM inverter with SCR = 10.6 and 1.9	H_∞ controller for GFM damping	HIL	Enables stable GFM control in low-inertia REZs using systematic H_∞ tuning
[198]	PSS®E+ PSCAD+RTDS	EMT + RMS	Tasmanian power grid	Operational paradigms at 90% IBR	RTDS	Demonstrates field-proven inertia/strength strategies; critical reference case for REZ-scale 100% IBR transitions
[186]	MATLAB/Simulink	EMT	Single-phase GFL	Feedback linearization PLL	HIL	Applicable for REZs with weak grid strength; supports robust PLL design and multi-inverter coordination
[214]	PSCAD/EMTDC	EMT	8 MW GFM offshore wind turbine	Transformer energization with virtual resistance	Simulation	Supports blackstart/restoration in inverter-dominated REZs; avoids diesel/resistor-based energization in weak grids
[215]	MATLAB/Simulink	RMS + Exp.	QLD-NSW interconnection	BESS droop control for PFC	Simulation	Targets frequency stability challenges in high-RE zones of the NEM; applicable to REZs using decentralized BESS
[216]	MATLAB/Simulink	EMT + Lab	MV distribution feeder (VIC)	FPPT inverter with frequency support	Simlulation + exp.	Addresses frequency stability in REZs with high DPV; supports field integration planning strength

2.15.1.2 EMT vs. RMS Modeling

EMT and RMS modelling frameworks offer complementary capabilities in simulating REZ systems. RMS-based simulations are commonly employed for large-scale, steady-state or quasi-dynamic analyses due to their lower computational demands [164, 215]. However, this abstraction limits their effectiveness in capturing the fast dynamics characteristic of inverter-dominated REZs, particularly under low SCR conditions or when modelling advanced GFM inverter controls [217, 218]. In such scenarios, EMT-based approaches are more suitable, as they enable sub-cycle resolution of system behaviour and detailed representation of control interactions [197, 203, 206]. For example, several studies have demonstrated the role of EMT modeling in analyzing the transient stability of GFM inverters in weak grids [195, 211, 212], where accurate depiction of current control loops and impedance dynamics is critical.

Additionally, EMT simulations have facilitated black-start investigations [208] and FRT assessments [214], where RMS techniques fall short due to their limited temporal resolution. To balance scalability with dynamic accuracy, hybrid co-simulation approaches that combine EMT and RMS modelling are increasingly adopted. Research efforts [198, 209] have leveraged such techniques to evaluate the operational performance of IBRs under both interconnected and islanded conditions [219–221]. These hybrid frameworks enable broader scenario analysis while preserving the fidelity needed for validating protection schemes and advanced control responses. Ultimately, the choice of modeling framework is closely aligned with the specific analytical needs of REZ studies, especially in environments characterized by high inverter penetration and system strength challenges. Table 2.17 summarizes the modelling tools, system configurations, validation approaches, and REZ-specific applications adopted across a range of Australian simulation-based studies.

The following subsection outlines the simulation tools used in Australian REZ-focused studies and how their capabilities align with key modelling approaches.

2.15.2 Simulation Tools

A diverse range of simulation platforms has been employed across recent studies to evaluate the integration and stability of RE in weak grids, particularly relevant to REZs. Among them, PSCAD/EMTDC is the most widely adopted tool for EMT studies, favored for its ability to capture fast dynamics of IBRs, black-start behavior, and grid-forming controls in low-inertia systems [195, 197, 203, 204, 206, 212, 214]. MATLAB/Simulink

has been frequently used either independently or in conjunction with advanced solvers such as MOSEK, Monte Carlo techniques, and HIL platforms to simulate RMS dynamics, design optimal inverter control schemes, and implement robust tuning strategies such as H_∞ damping controllers [186, 205, 207, 208, 213, 215]. System-level tools like PSS®E, DIgSILENT PowerFactory, and HOMER have been applied for dynamic dispatch optimization, frequency stability analysis, and hybrid microgrid planning in both interconnected and islanded REZ contexts [198, 209, 210, 216].

The selection of simulation tools is closely aligned with the study's application focus. EMT platforms are predominant in high-fidelity inverter and transient stability studies, while RMS and optimisation-based tools enable broader system-level and energy management analyses. Figure 2.31 illustrates the range of simulation environments employed across REZ studies, highlighting the diversity in tool selection based on modeling objectives. Table 2.17 presents a detailed comparison of simulation tools, model types, validation methods, and key applications across these studies. The next subsection will explore how these modelling approaches have been contextualized within Australian REZ development and planning efforts.

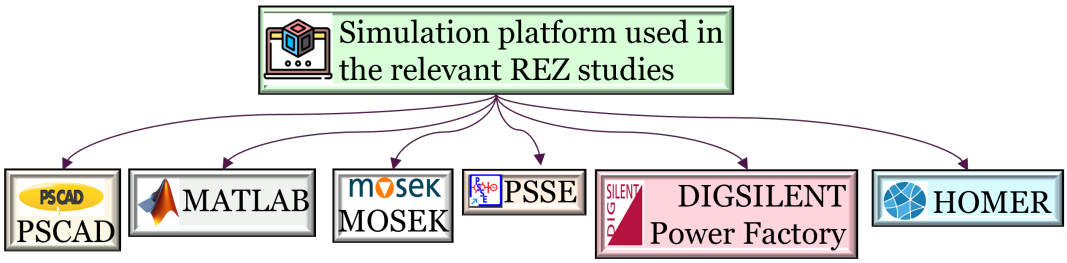


Figure 2.31: Overview of simulation platforms used in reviewed REZ studies

2.15.3 Australia-Focused Modeling Studies

2.15.3.1 Test System Structures

The selection of test systems across REZ-focused modeling studies is highly dependent on the simulation objective and the desired level of system granularity. Several studies utilize standardized benchmark networks such as the IEEE 9-bus, 14-bus, 30-bus, and 118-bus systems to evaluate the dynamic behavior of IBRs under varying control strategies and fault scenarios [195, 203, 207]. These systems serve as a controlled environment to test advanced concepts such as VSM tuning, inverter synchronization, and black-start coordination. For instance, the IEEE 9-bus system was extended with

Queensland-specific parameters to study VSM ramp-rate constraints in weak grids [195], while larger testbeds like the IEEE 118-bus network were used for probabilistic inverter placement optimization under uncertain operating conditions [207]. Figure 2.32 illustrates an example of a modified benchmark network adapted for REZ studies, showing how classical test systems can be tailored to reflect region-specific inverter integration challenges [222].

In contrast, other studies employ realistic or modified representations of Australian power systems, such as the 2030 Queensland grid [210], the Dalrymple and Melbourne microgrids [212], and the WMZ of the NEM [206]. These models incorporate region-specific characteristics, including low system strength, high inverter penetration, and BESS deployments, making them highly relevant for REZ planning. Additionally, isolated microgrids and low-voltage feeders, such as Melville Island and a VIC MV distribution network, have been modelled to support dynamic dispatch and frequency stability analysis in remote or off-grid REZ contexts [209, 216]. Table 2.17 illustrates the breadth of test systems, ranging from generic to geographically specific models, underpinning the versatility of REZ studies. The next subsection will examine how these test systems have been utilized for grid strength evaluation, a critical metric for REZ operability and inverter control design.

2.15.3.2 Grid Strength Evaluation

The ability of GFMI to operate reliably in weak or low-inertia power systems is a central focus in recent literature, particularly in the context of REZs across Australia and comparable systems globally. A review of selected studies (see Table 2.18) reveals that most modeling efforts concentrate on low-strength or weak grids, where synchronous machine support is minimal and the presence of IBRs dominates. For example, studies such as [194, 195, 197, 203, 204, 206] simulate GFMI behavior in islanded microgrids or regional grids with low SCR, highlighting dynamic issues like black-start stability, ramp-rate limitations, and fault current injection. Particularly, the work by [206] on a weak NEM zone with SCR = 3 and [197] with SCR = 1.5 for wind integration emphasizes the significance of tuning droop and voltage control mechanisms to ensure stability under stressed grid conditions.

Furthermore, some research aims to compare GFMI responses across different SCR regimes, providing valuable benchmarks for inverter design. For instance, [213] conducts a detailed comparative evaluation between strong (SCR = 10.6) and weak (SCR = 1.9) grids, using an H_∞-based decentralized control strategy to maintain compliance with

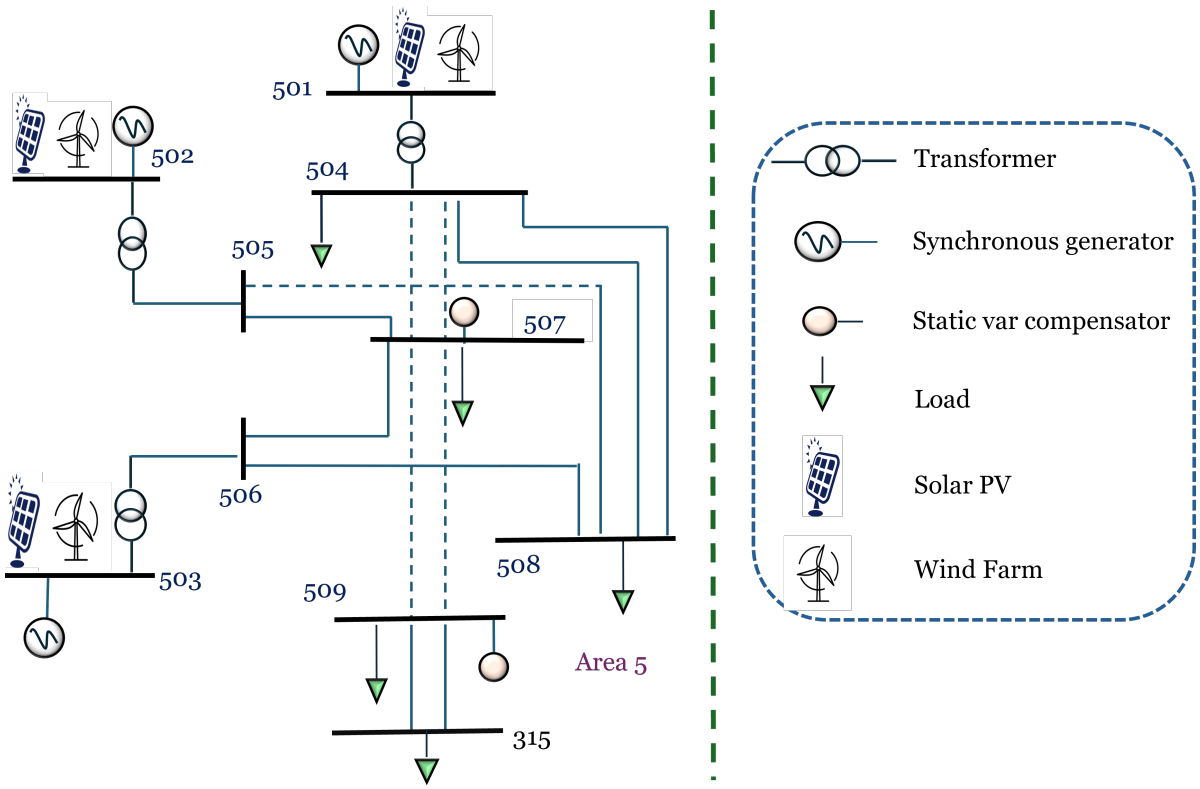


Figure 2.32: Simplified SA Power System (Area 5)

inertia and damping requirements. Although not all studies explicitly report SCR values, they often infer grid weakness through system topology, such as islanded or low-inertia conditions [195, 209, 210]. The diversity in grid strength assumptions across studies in Table 2.18 underscores the urgent need for context-aware control strategies tailored to specific REZ characteristics. This also reflects a broader trend toward validating GFMI performance under realistic weak-grid scenarios, especially relevant for Australian REZ deployments where high inverter penetration coincides with declining synchronous inertia. The implications of these grid strength classifications on system resilience and control effectiveness are further explored in the next subsection, which examines the specific stability metrics evaluated across the reviewed studies.

2.15.3.3 Stability Metrics Evaluation

Table 2.19 provides a detailed comparison of stability metrics evaluated across a range of GFM, GFL, and hybrid inverter control studies under diverse disturbance scenarios. The most widely assessed metric is the RoCoF, which serves as a key indicator of inertial response, particularly in low-inertia grids. Numerous studies incorporating GFM

inverters, such as those employing droop-based control [203], adaptive PI regulation [194], or VSM frameworks [195], demonstrate explicit evaluation of RoCoF, frequency nadir, and voltage recovery following system faults or black-start events. In addition to RoCoF, metrics like overshoot, settling time, and set-point tracking accuracy have also been employed to evaluate dynamic performance under load or power-reference disturbances [211, 213]. Furthermore, small-signal eigenvalue analysis was conducted in select works [195] to examine stability margins under varying system conditions.

The table also highlights more complex stability evaluations in hybrid or GFL-based inverter configurations. For instance, [209] investigates coordinated droop and governor control in a mixed GFM-GFL environment, measuring system-level frequency and voltage responses under generator loss. Similarly, [198] and [216] focus on GFL inverters operating under wide-area frequency deviations and low fault-level conditions, analyzing FRT performance and frequency recovery times. Some studies emphasize EMT-level stability [206], synthetic inertia contributions [204], and damping of sub-synchronous control interactions (SSCI) [206], reflecting the increasing complexity of stability concerns in inverter-dominated networks. These varied metrics not only inform control design but also establish the foundation for coordinated multi-inverter operation, which is the subject of the next section on control and coordination mechanisms.

2.16 Control and Coordination Mechanisms of IBRs

This section covers control strategies for GFL and GFM inverters and their coordination, focusing on their impact on grid stability in REZs.

2.16.1 Control Techniques for GFL Inverters

2.16.1.1 PQ control

PQ control is a fundamental strategy widely adopted in GFLIs deployed within REZs [149, 161, 223]. As illustrated in Figure 2.33(a), the controller regulates the active and reactive power outputs by minimizing the error between the measured and reference values of P and Q through PI regulators [161]. These regulators generate reference current components ($i_{g,d}^{\text{ref}}, i_{g,q}^{\text{ref}}$) for the inner current control loop. The control objective can be expressed as:

$$i_{g,d}^{\text{ref}} = \left[k_p + \frac{k_i}{s}\right](P^{\text{ref}} - P), \quad i_{g,q}^{\text{ref}} = \left[k_p + \frac{k_i}{s}\right](Q^{\text{ref}} - Q) \tag{2.7}$$

While this method is computationally simple and effective under stiff grid conditions, it lacks dynamic grid support and is therefore less suitable for weak grid scenarios typical in REZs [147, 224, 225].

Table 2.18: Summary of GFMI Control Objectives and Roles in Weak Grids Relevant to Australian REZs

Ref.	**Modeling Objective**	**Inverter Role**	**Grid Strength**	**SCR (if stated)**	**GFM Control Type**
[203]	Investigate dynamic stability issues during black-start in SG+IBR hybrid systems	GFM	Weak (Islanded)	Not stated	MLD, VSG-based control
[194]	Enhance microgrid protection by increasing GFMI SC capability	GFM	Low-strength	Not stated	Decentralized vector control with adaptive PI
[204]	Validate large-scale GFMI BESS for fault current and inertia in weak grids	GFM	Low-strength (Scottish grid)	Not stated	Decentralized swing-equation with inertia emulation
[195]	Analyze VSM instability caused by battery ramp-rate limits during frequency events	GFM	Weak grid (QLD system with high IBR share)	Not stated	Decentralized droop-based VSM with AC/DC voltage loops (primary + secondary)
[206]	Assess GFMI effectiveness in improving system strength and damping in weak NEM zones	GFM	Weak (WMZ with high IBR share)	SCR = 3 (for SMIB tests)	Decentralized droop and VSM with local voltage control (primary + secondary)
[197]	Simulate GFM inverter performance for integrating a 100 MW wind farm in weak grids	GFM	Weak	SCR = 1.5	Decentralized droop control (P-f and Q-V with implicit secondary PI)
[209]	Optimize dispatch and stability of an islanded hybrid microgrid with PV, wind, diesel, and BESS	BESS(GFM); PV/Wind (GFL)	Implicitly weak (low-inertia off-grid system)	Not stated	Droop/governor for diesel and VSCs; coordinated via dispatch strategies
[210]	Compare FFR (GFL) and simulated inertia (GFM) from BESS for frequency support in low-inertia grids	GFL; GFM BESSs	Low-inertia grid (QLD 2030 scenario)	Not stated	VSM
[213]	Design H_∞-based GFM control for damping and inertia compliance under load/faults	GFM	Both strong (SCR=10.6) and weak (SCR=1.9)	SCR = 10.6, 1.9	Fully decentralized APC with droop, damping, inertia loops.
[218]	Define service needs (inertia, voltage, black-start) for high-IBR grid stability	GFM(VSG-style); GFL (PLL-VSC)	Varied (low to high)	Not stated	Decentralized; primary, secondary, tertiary layers specified

Table 2.19: Stability Metrics and Control Approaches in Reviewed Inverter Studies

Ref.	Inverter Type	Control Hierarchy	Stability Metrics Evaluated	Disturbance
[203]	GFM	Droop (f,V), voltage restoration	RoCoF, freq. oscillation, voltage overshoot	Black-start, fault
[194]	GFM	Adaptive PI current control; decentralized voltage loop	Current stability under inductor saturation	LG, LLG, 3-phase faults
[204]	GFM	Fast inner current loop, outer droop loop with swing equation	Fault current, synthetic inertia, RoCoF response	Three-phase fault
[205]	GFM	Local VSG + droop + optional inner loops	Frequency deviation, RoCoF, active power sharing ratios	Balanced load disturbance in two-area system
[195]	GFM	Droop-based VSM control with AC/DC voltage regulation loops	Frequency nadir, settling frequency, small-signal eigenvalues, DC/AC voltage behavior	Generator trip
[206]	GFM	Inverter-level droop/VSM loops + plant-level voltage control	SSCI damping, voltage support, EMT stability, post-fault recovery	Balanced and unbalanced faults
[197]	GFM	Local droop control + implicit secondary PI regulators	Voltage/frequency stability, active/reactive power damping, POC voltage under SCR variation	Symmetrical and asymmetrical faults
[209]	GFM + GFL	Droop/governor for diesel, VSC inner loops for BESS, GFL for renewables	Frequency/voltage response, reliability indices	3-phase short-circuit faults, frequency deviation under generator loss
[211]	GFM	Local inverter control with droop, virtual inertia, and lead-lag damping	Frequency nadir, RoCoF, settling time, set-point tracking accuracy	Load disturbance, mode transitions
[213]	GFM	Local droop, damping, and inertia via second-order discrete-time controller	Overshoot, settling time, RoCoF compliance	Power-reference step changes
[198]	GFL	Market-based dispatch + FCSPS + local controls	RoCoF, frequency nadir, voltage stability, FRT performance	Deep two-phase fault, wide-area frequency deviation, dynamic IBR constraint under low fault level
[216]	GFL	Local frequency measurement + droop-based FPPT control	RoCoF, frequency nadir, recovery time to nominal	Frequency disturbance (under/over-frequency), high-PV, low-inertia scenarios

2.16.1.2 Droop-based current control

Droop-based current control introduces virtual droop behavior to enhance GFLI participation in frequency and voltage regulation, offering an intermediate solution suitable for moderately weak grids within REZs [148, 161, 177]. As shown in Figure 2.33(b), frequency and voltage magnitude deviations are translated into power references using droop coefficients $K_{\omega P}^{\text{droop}}$ and K_{vQ}^{droop}. These power references are then processed through PI regulators to generate inverter current commands.

The droop mechanism is governed by:

$$\begin{aligned} P^{\text{ref}} &= P_0 + K_{\omega P}^{\text{droop}}(\omega - \omega^*) \\ Q^{\text{ref}} &= Q_0 + K_{vQ}^{\text{droop}}(\|v_{\text{pcc,dq}}\| - v^*) \\ i_{g,d}^{\text{ref}} &= \left[k_p + \frac{k_i}{s}\right](P^{\text{ref}} - P) \\ i_{g,q}^{\text{ref}} &= \left[k_p + \frac{k_i}{s}\right](Q^{\text{ref}} - Q) \end{aligned} \tag{2.8}$$

This approach provides limited yet valuable dynamic support to the grid, making it more suitable than basic PQ control in REZs with evolving network strength.

2.16.1.3 VSG-Inspired Current Control

VSG-inspired current control is particularly well-suited for REZs operating under weak grid conditions, where inverter-based resources must emulate SG behavior [161]. As shown in Figure 2.33(c), this approach incorporates synthetic inertia and damping through a modified swing equation framework. The active power control loop derives its reference from both inertial and damping responses to frequency deviations:

$$\begin{aligned} \Delta\omega &= \omega^* - \omega \\ \Delta P_i &= \omega^* J s(\Delta\omega), \quad \Delta P_d = \omega^* D_p(\Delta\omega) \\ P^{\text{ref}} &= P_0 + \Delta P_t + \Delta P_d \\ i_{g,d}^{\text{ref}} &= \left[k_p + \frac{k_i}{s}\right](P^{\text{ref}} - P) \\ Q^{\text{ref}} &= Q_0 + K_{vQ}^{\text{droop}}(v^* - \|v_{\text{pcc,dq}}\|) \\ i_{g,q}^{\text{ref}} &= \left[k_p + \frac{k_i}{s}\right](Q^{\text{ref}} - Q) \end{aligned} \tag{2.9}$$

Here, J denotes the virtual inertia, D_p the damping coefficient, and ω^* the nominal grid frequency. Reactive power is managed via a droop-based controller, while PI regulators govern the inner current loops. This strategy allows GFL inverters to contribute synthetic inertia and damping, improving frequency stability and enhancing REZ performance under high renewable penetration.

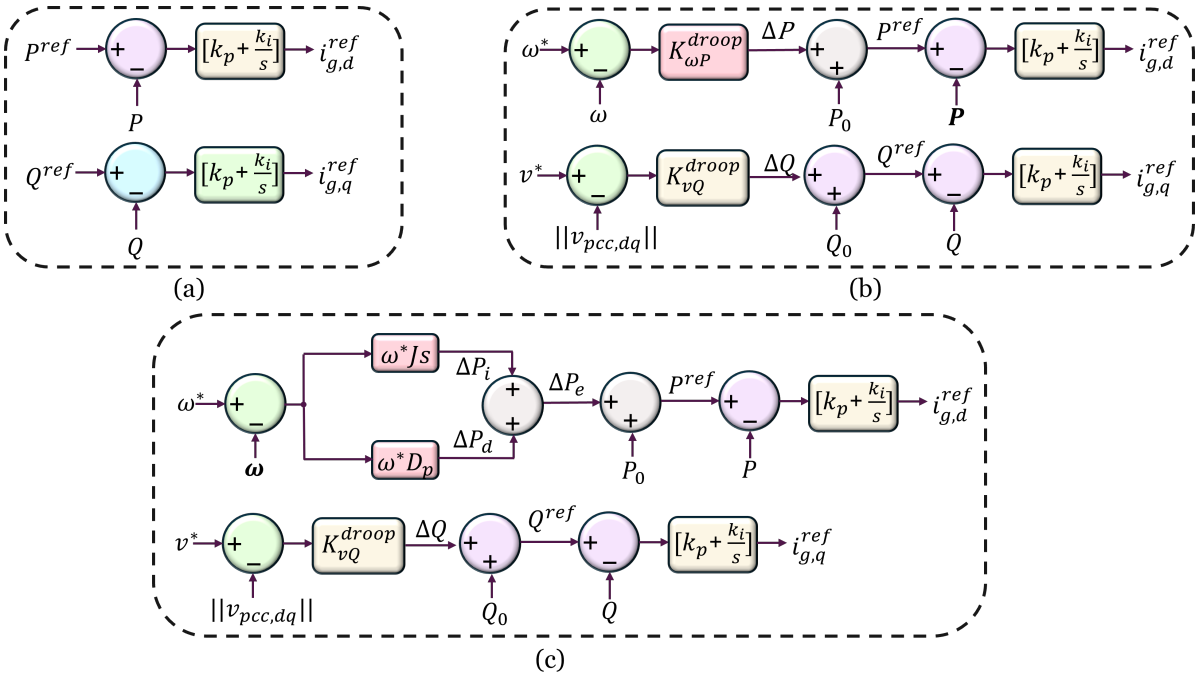


Figure 2.33: Block diagrams of GFLI control methods relevant to REZs: (a) PQ control, (b) droop-based current control and (c) VSG-inspired current control.

2.16.2 Control Strategies for GFM Inverters

2.16.2.1 Droop-Control Mechanisms

In REZs, where grid strength is often low and synchronous inertia is limited, droop-based control strategies for GFMI provide essential support for frequency and voltage stability [148, 161]. As illustrated in Figure 2.34, the frequency droop control (Figure 2.34a) emulates inertial response by adjusting the inverter's output frequency based on active power deviations, governed by the proportional droop coefficient $K_{P\omega}^{\text{droop}}$. This ensures system-wide frequency coordination among distributed energy resources without direct communication. Similarly, the voltage droop control (Figure 2.34b) modulates the inverter's voltage magnitude in proportion to reactive power deviations using the coefficient K_{Qv}^{droop}, thereby contributing to voltage regulation and reactive power sharing across the REZ. Together, these decentralized, measurement-driven control loops allow inverter-based resources to mimic synchronous generator behavior, enabling stable power exchange in weak-grid conditions. The fundamental control laws for frequency and voltage droop are expressed as:

$$
\begin{aligned}
\Delta\omega &= K_{P\omega}^{\text{droop}}(P^{\text{ref}} - P),\\
\omega &= \omega^* + \Delta\omega,\\
\theta^{\text{ref}} &= \int \omega\, dt,\\
\Delta v_{\text{pcc},d} &= K_{Qv}^{\text{droop}}(Q^{\text{ref}} - Q),\\
v_{\text{pcc},d}^{\text{ref}} &= v^* + \Delta v_{\text{pcc},d}
\end{aligned}
\tag{2.10}
$$

where ω^* and V^* represent the nominal frequency and voltage, and P^*, Q^* are the set-points for active and reactive power, respectively.

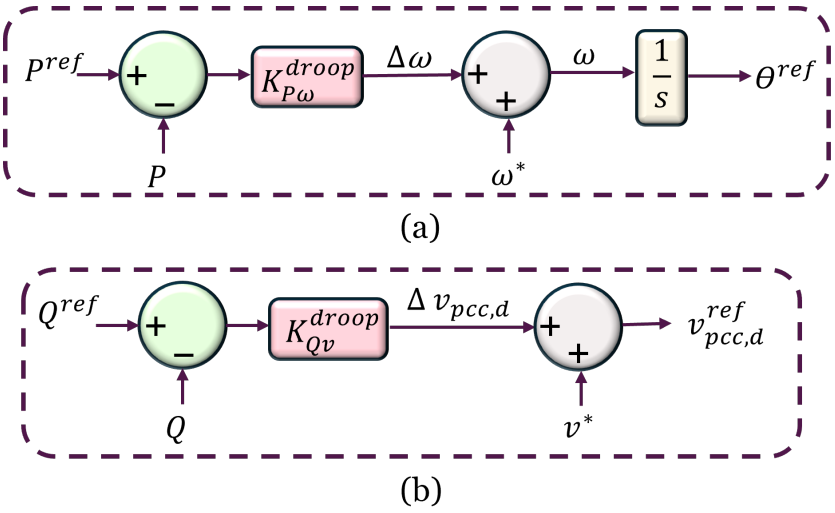


Figure 2.34: Frequency (a) and voltage (b) droop control for GFMI in REZs.

2.16.2.2 Virtual Synchronous Generator (VSG) Control

VSG control has emerged as a promising strategy for stabilizing frequency and voltage in REZs [148, 161]. VSG-based inverters emulate the inertial and damping behavior of synchronous machines, allowing IBRs to actively support grid dynamics. As shown in Figure 2.35, a demonstrates the basic APC of VSG is demonstrated, where the swing equation is digitally replicated to mimic synchronous machine response. The active power error is processed through virtual inertia J and damping coefficient D_p, enabling frequency adaptation in real time which can be expressed as:

$$
\begin{aligned}
J\frac{d\omega}{dt} + D_p(\omega - \omega^*) &= \frac{1}{\omega^*}(P^{\text{ref}} - P)\\
\theta^{\text{ref}} &= \int \omega\, dt
\end{aligned}
\tag{2.11}
$$

To enhance frequency regulation in REZs, the VSG framework is extended with droop characteristics, as depicted in Figure 2.35b. This implementation integrates droop-based correction K_{ω}^{vsg} with the swing dynamics, enabling decentralized load sharing and frequency synchronization without communication. The droop mechanism adjusts frequency based on power imbalances while maintaining the virtual inertia profile, ensuring robust performance under disturbances and variable renewable generation. This coordinated emulation improves the system's ability to withstand fluctuations, which is crucial in REZs where traditional synchronous machines are absent. The equation related to this control can be written as:

$$\begin{aligned} J\frac{d\omega}{dt} + D_p(\omega - \omega^*) &= \frac{1}{\omega^*}(P^{\text{ref}} - P) + K_{\omega}^{\text{vsg}}(\omega^* - \omega) \\ \theta^{\text{ref}} &= \int \omega \, dt \end{aligned} \tag{2.12}$$

In addition to frequency control, voltage stability is maintained using a closed-loop voltage regulator, illustrated in Figure 2.35c. The reactive power error is processed through a proportional-integral controller scaled by a voltage inertia constant M_f, resulting in dynamic voltage regulation at the point of common coupling [148]. This tri-layered control structure allows VSGs to provide synthetic inertial response, droop-based coordination, and voltage support simultaneously, making them particularly suitable for weak-grid applications in REZs. The governing VSG frequency control dynamics are given by:

$$\begin{aligned} e_v(t) &= v^* - \left\| v_{\text{pcc},dq}(t) \right\| \\ i_0(t) &= \frac{1}{M_f}\left[k_p \, e_v(t) + k_i \int_0^t e_v(\tau) \, \mathrm{d}\tau \right] \\ \mathbf{v}_{\text{pcc},abc}^{\text{ref}}(t) &= 2\omega M_f \, i_0(t) \begin{bmatrix} \sin\big(\Theta(t)\big) \\ \sin\big(\Theta(t) - \frac{2\pi}{3}\big) \\ \sin\big(\Theta(t) - \frac{4\pi}{3}\big) \end{bmatrix} \end{aligned} \tag{2.13}$$

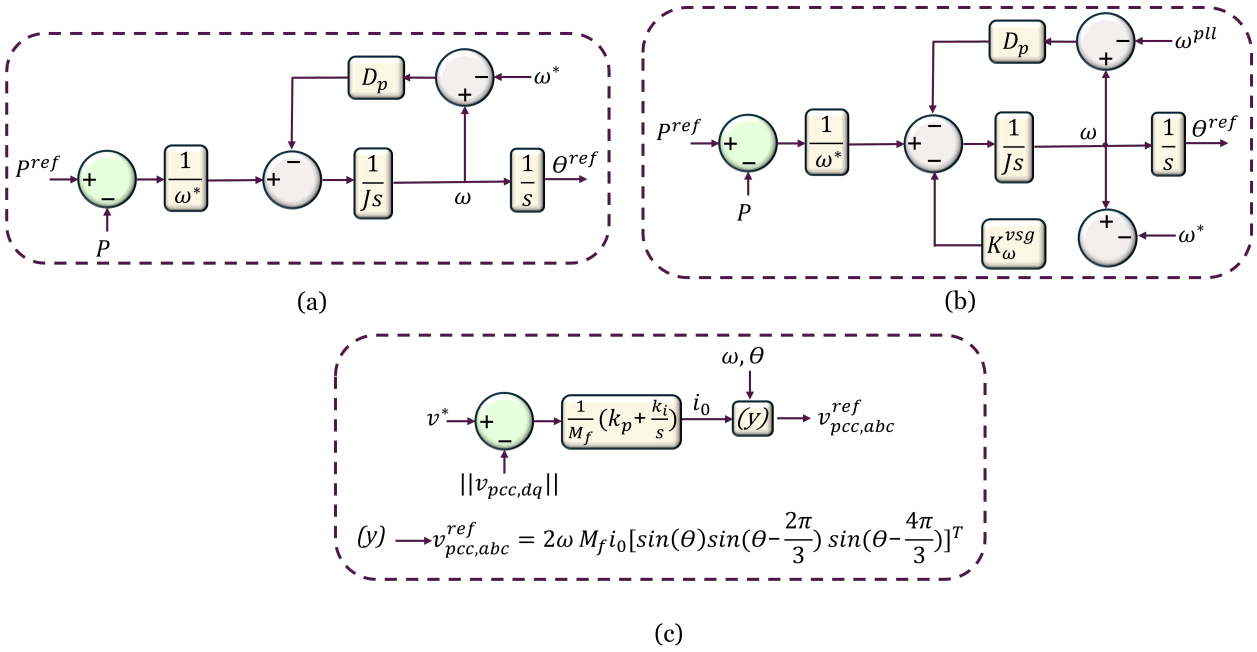


Figure 2.35: VSG control strategies for REZs: (a) Active power control, (b) Frequency droop emulation, and (c) Voltage control.

2.16.2.3 Power Synchronization Control (PSC)

PSC is a GFM control strategy designed to enable the stable integration of IBRs in weak grids such as those commonly found in REZs [148, 161, 226]. Unlike PLL-based controllers, which rely heavily on grid strength, PSC emulates SG behaviour by aligning the inverter's internal angle with the power angle of the grid. This approach improves stability under low SCR conditions and enhances dynamic response during disturbances. As illustrated in Figure 2.36, the active power control loop 2.36(a) utilizes a synchronizing mechanism where the phase angle is regulated via an integrator with gain $K_{P\theta}^{PSC}$, while the reactive power control loop 2.36 (b) employs a direct voltage feedback with gain K_{Qv}^{PSC}. The resulting control dynamics are governed by:

$$\begin{aligned} \theta^{ref}(t) &= \theta^*(t) + K_{P\theta}^{PSC} \int \left(P^{ref}(t) - P(t)\right) dt \\ v_{pcc,d}^{ref} &= v^* + K_{Qv}^{PSC} \cdot \left(Q^{ref} - Q\right) \end{aligned} \tag{2.14}$$

These equations collectively ensure both angle synchronization and voltage support, making PSC a robust candidate for inverter-dominated REZ applications.

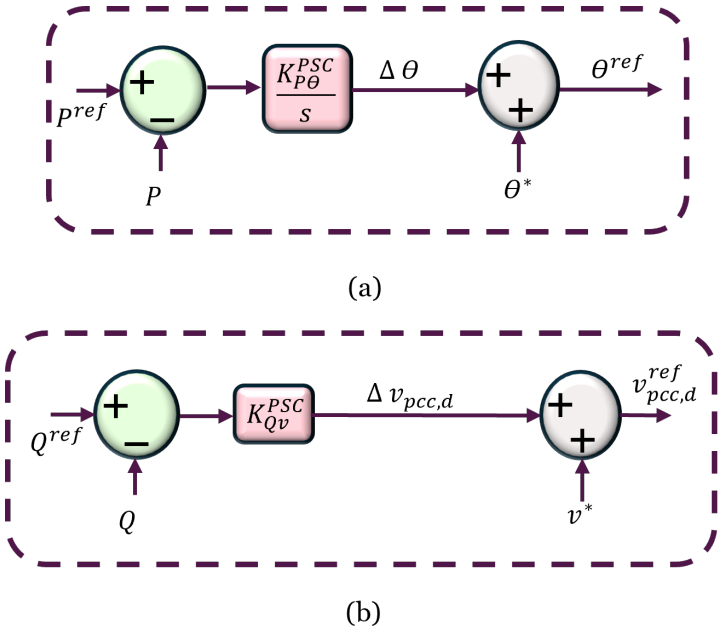


Figure 2.36: PSC block diagrams for angle (a) and voltage (b) control in REZ-integrated inverter systems.

2.16.2.4 Synchronverter Control

Synchronverter control is another GFM technique that virtually replicates the physical dynamics of synchronous machines, thereby enabling IBRs to contribute to the power system's inertia and damping [161, 226]. This emulation is particularly valuable in REZs, where conventional SG is limited and system strength is low. As depicted in Figure 2.37, the control structure integrates a virtual swing equation, damping terms D_p and D_q, and electromagnetic torque generation through current-voltage interactions. The inverter terminal voltage reference is computed using the internal angle θ^{ref}, excitation current i_f, and modulation factor M_f, leading to:

$$v_{pcc,abc}^{ref} = \omega M_f i_f \begin{bmatrix} \sin(\theta^{ref}) \\ \sin\left(\theta^{ref} - \frac{2\pi}{3}\right) \\ \sin\left(\theta^{ref} + \frac{2\pi}{3}\right) \end{bmatrix} \tag{2.15}$$

The corresponding electrical output power and reactive power are derived as:

$$
\begin{aligned}
P_e &= M_f i_f \omega^* \begin{bmatrix} i_{o,a}\sin(\theta^{ref}) \\ i_{o,b}\sin\left(\theta^{ref} - \frac{2\pi}{3}\right) \\ i_{o,c}\sin\left(\theta^{ref} + \frac{2\pi}{3}\right) \end{bmatrix} \\
Q &= -\theta^{ref} M_f i_f \begin{bmatrix} i_{o,a}\cos(\theta^{ref}) \\ i_{o,b}\cos\left(\theta^{ref} - \frac{2\pi}{3}\right) \\ i_{o,c}\cos\left(\theta^{ref} + \frac{2\pi}{3}\right) \end{bmatrix}
\end{aligned}
\tag{2.16}
$$

These equations ensure the inverter behaves in synchrony with the grid while offering dynamic voltage and frequency regulation capabilities crucial for REZ stability.

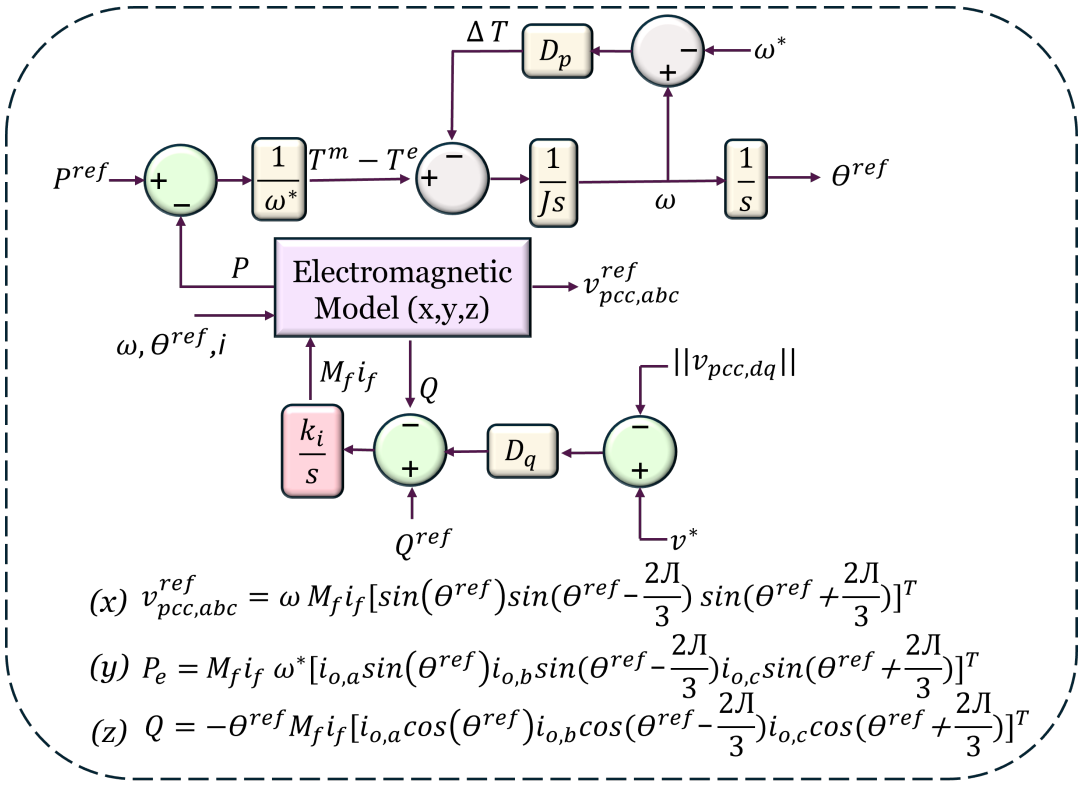


Figure 2.37: Synchronverter-based GFM control architecture for stable inverter integration in REZs.

2.16.2.5 Matching and Virtual Oscillator Based Control

Matching control is a GFM control strategy designed to replicate the voltage-current dynamics of synchronous machines by aligning the inverter's internal dynamics with

that of the grid [148, 161, 180]. It ensures that the inverter naturally synchronizes with the grid while contributing to voltage support and frequency stability, key requirements in weak-grid environments such as REZs. As illustrated in Figure 2.38a, the control framework leverages the DC-link voltage v_{dc} to generate a virtual frequency signal ω via a proportional gain k_Θ, followed by angle integration to obtain Θ^{ref}. The outer voltage loop regulates the magnitude μ through a PI controller, which modulates the reference output voltage vector as:

$$v_{pcc,a,b}^{ref} = \mu \begin{bmatrix} -\sin(\Theta^{ref}) \\ \cos(\Theta^{ref}) \end{bmatrix} \tag{2.17}$$

Here (2.38a), μ is governed by:

$$\mu = \left(k_p + \frac{k_i}{s}\right)\left(v_{pcc}^{*} - \left\|v_{pcc,dq}\right\|\right) \tag{2.18}$$

By tightly coupling voltage generation with the inverter's internal state, matching control enables fast and robust voltage regulation under fluctuating grid conditions, promoting reliable inverter-grid interactions in REZ applications [226].

VOC is a time-domain, nonlinear control strategy that enables GFM to synchronize through self-organized dynamics rather than relying on PLL or GFL feedback [161]. Inspired by nonlinear oscillator theory, VOC operates by emulating a damped LC oscillator whose voltage and current dynamics drive synchronization with the grid. As shown in Figure 2.38b, the VOC structure consists of a virtual inductor L_{vo}, capacitor C_{vo}, and a nonlinear damping function $f(v_{vo}, i_{L,vo})$ that introduces limit-cycle behavior. The oscillator's internal dynamics are described by:

$$L_{vo}\frac{di_{L,vo}}{dt} = v_{vo}, \quad C_{vo}\frac{dv_{vo}}{dt} = i_{in} - f(v_{vo}, i_{L,vo}) \tag{2.19}$$

The nonlinear function $f(v_{vo}, i_{L,vo})$ is often chosen to match Van der Pol or Duffing oscillator characteristics, enabling robust phase and frequency locking under varying load or grid conditions. The output current is regulated via a gain k_i, ensuring appropriate power injection as:

$$i_0 = k_i \cdot i_{in} \tag{2.20}$$

By coordinating inverter behavior through physical oscillator emulation, VOC facilitates decentralized synchronization, making it highly suitable for weakly interconnected

or inverter-dominated REZs [161, 227]. The following section presents strategic control solutions tailored to the operational needs of inverter-dominated REZs.

2.16.2.6 Strategic Control Solutions for Inverter-Dominated REZs

Table 2.20 presents a targeted comparison of inverter control strategies for REZs, focusing on their adaptability to weak grids, low inertia, and limited communication. Droop-based methods are simple and decentralized but lack inertia support, making them less effective in dynamic REZ conditions [161, 228, 229]. VSG and Synchronverter controls offer synthetic inertia and improved damping but can suffer under measurement delays and fault stress [227–229]. PSC and Matching Control enhance synchronization in low-SCR networks without relying on PLLs, but may lack dynamic flexibility [148, 161]. Emerging strategies, such as VOC, offer decentralised and fast synchronisation suitable for microgrids, although large-scale validation is still in its early stages [226, 227, 230]. Overall, each method offers trade-offs, and their deployment must align with the specific needs of REZ configurations. These considerations set the stage for the following discussion on GFM-GFL coordination, addressing interoperability challenges and communication-based control.

2.16.3 GFM-GFL coordination

2.16.3.1 Interoperability Issues

In renewable-rich power systems, effective coordination between GFM and GFL inverters is critical to maintaining system stability, particularly under weak grid conditions. As shown in Table 2.21, the coexistence of PLL-based GFL inverters and droop- or VSG-controlled GFM units can lead to issues such as sub-synchronous oscillations, harmonics, and control-loop interference [5, 6, 147, 179, 231]. Researchers in [149] address this challenge by proposing an Online Short-Circuit Ratio (OSCR) estimator that enables adaptive switching between GFL and GFM modes, improving small-signal stability in systems with high inverter penetration. In another approach, [223] demonstrates the benefit of unified hybrid control strategies that combine GFM and GFL branches to ensure smoother mode transitions.

Table 2.20: REZ-oriented comparison of inverter control strategies

Method	Topology	REZ-Relevant Features	REZ-Specific Advantages	REZ-Specific Limitations
(a) Droop Control	Common features	Fully decentralized; requires only local measurements.	Easy to deploy across REZs with limited comms or SCADA.	No inertia or damping; not suitable for high renewable variability.
	(a1) Single-loop	Basic frequency and voltage droop; minimal control complexity.	Fast implementation in low-complexity REZ nodes.	Inaccurate reactive power sharing in weakly meshed REZs.
	(a2)Multi-loop	Includes inner voltage and current control loops.	Better control for long REZ feeders with high impedance.	More sensitive to tuning; less robust under intermittency.
	(a3)UDE-based	Handles uncertainty and model mismatch.	Stable reactive power sharing under grid disturbances.	Limited to reactive power; lacks active power control needed in REZs.
	(a4) Adaptive	Adjusts droop coefficients and virtual impedance in real time.	Maintains stable operation in REZs with high wind/-solar variability.	Computational complexity may challenge real-time use in edge devices.
(b) VSG Control	Common features	Emulates SG swing equation; provides virtual inertia and damping.	Improves small-signal frequency stability in low-inertia REZs; supplies fast inertial support without extra hardware.	Active-power oscillations can appear in very weak grids; effective inertia drops if measurement delays grow.
	(b1) VSG (no PLL)	Pure voltage-source mode, avoiding PLL sensitivity.	Lower overshoot and better damping useful for REZ feeders with rapid power ramps.	Slower frequency transients may hinder FFR compliance in high-renewable events.
	(b2) VSG with frequency-droop (uses PLL)	Adds droop to track system frequency via PLL; mixes inertia with primary control.	Faster dynamic response than basic VSG helps stabilize REZ nodes with severe PV variability.	PLL-cascaded structure can lose voltage support during faults; less effective in very weak REZs where PLLs struggle.
(c) PSC	Common features	Uses angle-power balance directly; no reliance on frequency derivative; PLL optional.	More resilient than GFL in low-SCR REZs; suitable for weak-grid synchronization.	No inertia or damping support,Äîlimiting dynamic stability during REZ-wide disturbances.
	(c1) PSC with PLL	Switches to backup PLL during faults.	Enhances voltage support during faults in weak REZ feeders.	Suffers from frequency swings during faults; sensitive to power mismatch.
	(c2) Robust PSC	Includes robust tuning for DC link and power control gains.	Helps maintain stability margin in REZs using DC-coupled assets (e.g., BESS, PV).	Not compatible with (b1) type controllers; limited scalability for multi-inverter REZs.
(d) Synchro-verter	Common features	Emulates SG; provides synthetic inertia and damping.	Enhances frequency stability and inertial response in low-inertia REZs.	Can cause oscillatory power and excessive current injection during REZ faults.
	(d1) Fast current loop	Includes delay compensation, frequency droop, and virtual capacitors.	More robust to sensor/processing delays in weak and imbalanced REZ networks.	No major fault limitation; risk of overcurrent in low-SCR REZs.
	(d2) Virtual impedance-based	Controls output current via virtual inductors (5th-order model).	Reduces fault current and stabilizes transient events, useful for fault-prone REZ lines.	Complex to tune and implement across diverse REZ assets.
	(d3) With FRT capability	Integrates FRT strategies: average and enhanced power control.	Helps mitigate oscillations and ensures current-limited response during faults,Äîcritical for REZ protection compliance.	May require fast coordination with external grid-side protections.
(e) Matching Control	Common features	Establishes a direct analogy with SGs without needing inner voltage/current loops.	High robustness under DC current constraints; beneficial for converter-heavy REZs.	All control depends on a single gain,Äîlimits flexibility in diverse REZ operating conditions.
(f) VOC	Common features	Time-domain nonlinear control based on oscillator dynamics; does not rely on PLL or voltage loops.	Easy to implement in decentralized REZs; fast synchronization and power sharing in low-inertia microgrids.	Still under research; lacks validation in large-scale or fault-prone REZ environments.
	(f1) Classical VOC	No P/Q sensing; current-controlled; simple setup	Suits inverter-heavy REZs with limited sensing	No voltage control; limited dispatchability

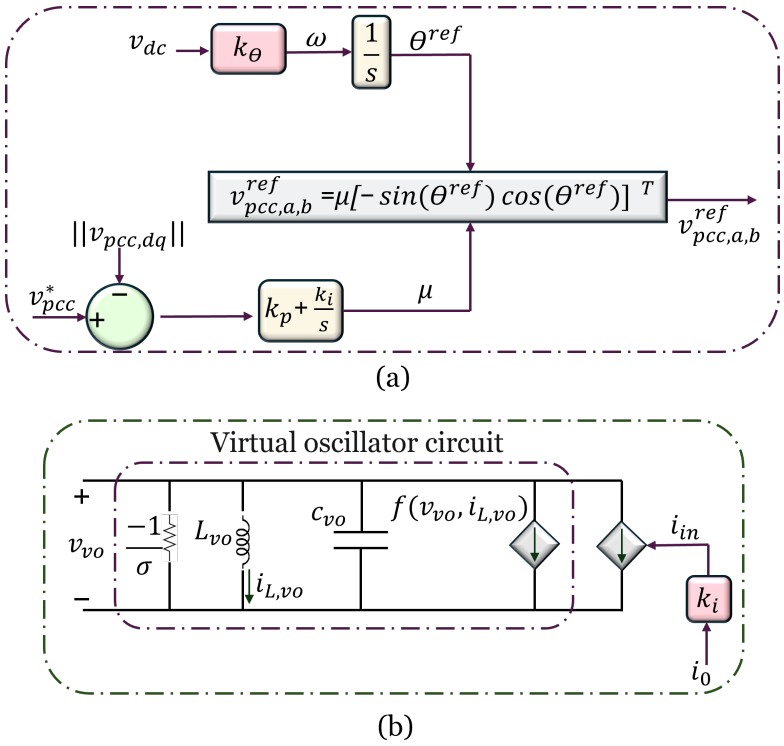


Figure 2.38: (a) Matching control and (b) VOC-based control for inverter synchronization in REZs.

Studies such as [224] further reveal that uncoordinated GFL operation can weaken grid strength, especially without the support of GFM anchors or fast-responding BESS with prioritized reactive power control. As indicated by [232], such coordination is particularly relevant for REZs, where varying SCR demand requires flexible and interoperable control frameworks.

2.16.3.2 Communication and Decentralized Control

In contrast to the centralized scheduling frameworks traditionally employed by GFL systems, GFM inverters facilitate decentralized operation by inherently supporting autonomous synchronization and voltage regulation without continuous communication [3, 150, 233]. Nonetheless, hybrid configurations involving both GFM and GFL units, such as those described in Table 2.21 necessitate partial coordination to maintain system-wide stability, particularly under varying strength conditions. To address this, advanced coordination schemes have emerged, including grid-forming setpoint broadcasting [232], hierarchical voltage control [157], and agent-based dispatch mechanisms leveraging local droop or VSG tuning [27]. The 2024 Integrated System Plan (ISP) by

AEMO [3] underscores the importance of establishing communication-assisted GFM zones within REZs, enabled by dynamic system strength assessments and hybrid control paths. Complementary studies [223, 232] further indicate that integrating predictive control with event-triggered communication can achieve scalable inverter coordination with minimal latency and reduced bandwidth overhead, supporting both reliability and cost-effective deployment in future REZ architectures. These advancements directly inform the following discussion on their impact on overall grid stability.

Table 2.21: Control Approaches and Coordination Strategies in GFL and GFM Systems

Control Domain	**Method**	**Key Features**	**Ref**
GFL, GFM, Hybrid	PLL with dq PI, PSC, Unified PLL + Droop, Reactive-Power-Prioritized VSC	Tracks voltage phase;enhances stability under low SCR; supports adaptive switching (GFL ↔ GFM); ensures black-start and LVRT; prioritizes reactive support in weak grids	[147, 149, 223, 224]
GFL, GFM, Hybrid	PLL with dq PI, Power Synchronization Control, VSG-based Droop Control, Unified PLL + p-ω Droop, Virtual Inertia with FFR	Enhances voltage phase tracking, stability under low SCR, and adaptive switching; emulates inertia (VSG); supports LVRT, black-start, ancillary services, and FFR for nadir improvement.	[6, 148, 179, 234]
GFMI Control; IBR System Integration	Real-world GFM pilots with phasor validation; multi-operator IBR integration study; RMS comparison of droop, VSG, and synchronverter in weak grids; frequency-shaping control for low-inertia systems.	Demonstrates GFM roles in strength, RoCoF arrest, and SynCon replacement; highlights IBR risks across 5 grids; quantifies nadir and voltage recovery of GFMI strategies; introduces nadir-free frequency-shaping control; includes real, simulated, and hybrid validations for REZ design.	[26, 193, 235, 236]
Hybrid GFM, GFL Control	Adaptive mode-switching based on Operating Short Circuit Ratio (OSCR); Unified hybrid control fusing GFM and GFL branches; p-ω droop with PLL-based synchronization	Enables seamless GFM-GFL transition; improves frequency stability, black-start, and LVRT; uses decentralized EMT and small-signal validation; suited for REZs with varying SCR and inertia.	[149, 223, 232]
Hybrid Control (GFM/GFL) and Integrated REZ Planning	Hybrid Control Converter with parallel GFM-GFL paths; Multi-stage REZ planning via AEMO's ISP; Scenario-based dispatch and co-optimization with network constraints	Supports seamless transition and inertia via hybrid VSC; REZ planning considers resource, network, and Indigenous factors; ISP uses half-hourly dispatch, Monte Carlo outages, and long-term outlook; 35-43 REZs mapped for actionable deployment.	[3, 150, 232]

2.16.4 Impact on Grid Stability

2.16.4.1 Frequency Nadir and RoCoF

The deployment of GFM inverters significantly enhances frequency stability in low-inertia networks by reducing the RoCoF and improving frequency nadir through virtual

inertia and FFR mechanisms. As summarized in Table 2.22, GFM inverters provide instantaneous frequency support via VSG and droop-based control strategies, enabling RoCoF reduction by up to 50% and achieving sub-second FFR [148, 157, 166, 224, 234, 235].

In contrast, GFL inverters exhibit delayed and limited frequency response due to their dependence on PLL and current injection, making them vulnerable during frequency excursions and high RoCoF events. Real-world evidence from [237] in the 100% renewable Kauai system demonstrates GFM efficacy in maintaining RoCoF within ¬ ± 1 Hz/s. Additionally,[166] reveals that GFM-based BESS configurations require 25% less energy capacity than their GFL counterparts to ensure compliance with frequency stability standards. Analytical insights from [234] further quantify the influence of inertia and damping parameters on dynamic frequency behavior, providing a practical basis for GFM tuning in REZs.

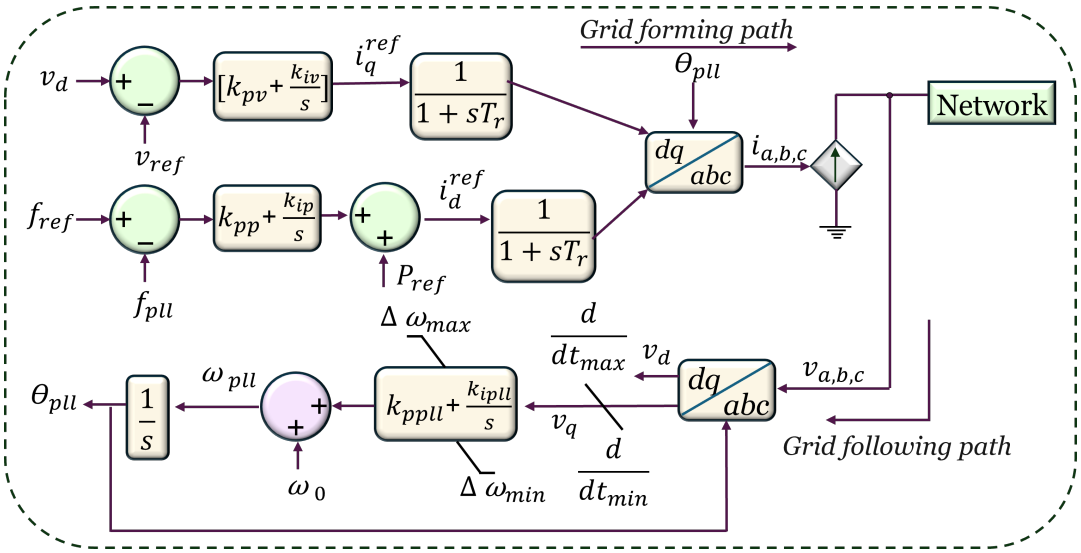


Figure 2.39: Structural overview of a hybrid inverter control framework integrating GFM and GFL functionalities for REZ applications.

2.16.4.2 Inertia and Voltage Support

GFM inverters significantly enhance system resilience by providing synthetic inertia and robust voltage support, especially under weak grid conditions common in REZs. As shown in Table 2.22, GFM technologies such as droop control, VSG, and synchronverter frameworks offer FFR, reduced RoCoF, and stable voltage recovery, even during severe disturbances [148, 157, 193, 235]. These capabilities enable functions like black-start and sustained operation under low SCR, outperforming conventional GFL inverters that often

fail to maintain synchronization below SCR of 3 [166, 234]. Real-world implementations, such as the Kiamal solar farm retrofit with a synchronous condenser [238], exemplify how system strength and inertia can be bolstered through hybridization. Additionally, studies show that a 100 MVA GFM-VSC can resynchronize nearly three times faster post-fault than an equivalent synchronous machine, improving voltage recovery and minimizing downtime [239]. Hybrid GFL-GFM schemes further improve system adaptability by switching between control modes based on grid strength or power conditions, thereby combining the robustness of GFM with the flexibility of GFL [149, 223, 232]. Figure 2.39 shows the structural overview of a hybrid inverter control scenario integrating GFM and GFL functionalities for REZ applications in [240] The Illawarra urban REZ project [241] underscores the growing need for such coordinated control strategies to meet grid-wide voltage and inertia objectives in urban-integrated REZs.

Table 2.22: Comparison of Stability Contributions from GFL and GFM Inverters

Inverter Type	**Frequency Support Capability**	**Voltage Support / FRT Capability**	**Ref.**
GFL	Limited via current control; RoCoF ~0.5 Hz/s; slower recovery (1.2 s)	Susceptible to SCR instability; loses PLL lock at SCR<3; weak FRT	[148, 166, 224]
GFM	Virtual inertia reduces RoCoF by ~50%; FFR (~0.5 s)	Provides robust FRT, voltage reference holding, black-start; stable at SCR<3	[148, 166, 224]
GFL	PLL-based current injection; limited frequency response; susceptible to RoCoF excursions and delayed FFR response (e.g., 100 ms delay for VI)	Susceptible to SCR instability, relies on grid strength; weak voltage recovery; unable to maintain voltage reference during faults	[157, 234, 235]
GFM	Virtual inertia provision with droop/VSG/VSM; instantaneous frequency forming; reduces RoCoF and improves nadir; primary FFR response improves dynamic resilience	Provides robust voltage forming; enables black-start, LVRT/HVRT, fast FRT; sustains voltage at PCC during sag or fault	[157, 234, 235]
GFM	Droop enables fast active power support; VSG and synchronverter emulate inertia and damping; frequency-shaping eliminates nadir with tunable RoCoF; filtered droop achieves SC-like inertial response.	VSG and synchronverter improve voltage recovery and reactive power control; filtered droop ensures voltage stiffness and fast FRT with tunable current limits.	[193, 236, 239]
Hybrid GFL-GFM	Adaptive/unified schemes switch between droop/VSG and PLL based on SCR or power; enhance RoCoF, emulate inertia, track power; include frequency shaping and synthetic inertia.	Support LVRT, voltage regulation, and fast FRT; enable black-start and voltage stiffness in weak or islanded grids; ensure reactive power accuracy and seamless mode transitions.	[149, 223, 232]

Table 2.23: Control Requirements for REZs Integration

REZ Control Objective	**Required Inverter Capability**	**Challenges**	**Ref.**
Frequency Stability and Inertia Support under High Renewable Penetration	GFM with virtual inertia, droop/VSM control, and FFR coordination (GFM and enhanced GFL); integrated with system-wide inertia estimation	RoCoF containment, low inertia margins, synchronization with GFLs, weak grid stabilization, lack of standardized performance metrics	[234, 235, 237]
Stability Under Weak Grid and SSCI Conditions	Adaptive switching between GFL/GFM, droop/VSM-based GFM, reactive-priority GFL, and PLL/VSC tuning in BESS	SSCI suppression, dynamic voltage instability, mode-switching under low SCR, RoCoF containment, DC-link and PLL instability under fast transients	[149, 224, 231]
Unified GFM-GFL Control and REZ Operational Planning	HCCs with parallel GFM/GFL branches, GFMI emulation strategies, inverter performance benchmarks in REZs	Lack of unified control to deliver both precise power tracking and grid support; absence of quantifiable metrics for inverter performance in REZs; planning uncertainty in inverter-based REZ deployment	[3, 27, 232]
Frequency Shaping, System Strength, and Coordinated Inverter Stability in Low-Inertia REZs	GFM inverters with frequency-shaping control, synchronous condensers for short-circuit strength, and dual-loop VOC for multi-inverter stability	Eliminating nadir and RoCoF in low-inertia grids, mitigating oscillations in inverter-dominated microgrids, ensuring voltage/frequency stability in weak networks, and tuning nonlinear controls under parasitic conditions	[236, 238, 242]

2.16.4.3 Control Strategies and Operational Needs for REZ Integration

The successful integration of REZs into weak transmission networks demands advanced inverter control strategies tailored to diverse stability challenges. As summarized in Table 2.23, GFM inverters equipped with virtual inertia, droop or VSM control, and FFR are essential for maintaining frequency stability and mitigating the impacts of reduced inertia and high RoCoF events in REZs [234, 235, 237]. In weak grids prone to SSCI, adaptive control schemes, capable of switching between GFL and GFM modes, reactive-priority GFL operation, and coordinated PLL tuning in BESS are required to manage transient instabilities and mode-switching under low SCR conditions [149, 224, 231]. To address the dual need for precise power tracking and grid support, hybrid control configurations such as HiCCs with parallel GFM/GFL branches and GFMI emulation are gaining traction, despite the current absence of standardized performance metrics in REZ environments [3, 27, 232]. Furthermore, system-wide stability in low-inertia REZs necessitates coordinated frequency shaping through nonlinear GFM schemes, synchronous condensers for short-circuit strength, and voltage oscillation damping using VOC [236, 238, 242]. Collectively, these control strategies emphasize the need for dynamic, context-specific inverter functionalities and robust operational planning to ensure reliable REZ deployment. This necessity is further discussed in the next section.

Table 2.24: Key Australian REZ projects using GFM inverters to support renewable integration and grid stability.

Project Name /REZs	**Location**	**Year**	**Inverter Type**	**Main function/ Key Attributes**	**Rated Power & Energy Capacity**
Hornsdale Power Reserve	SA	2017-2020	GFM (BESS)	Large scale battery providing FFR	150MW/194MWh
Dalrymple ESCRI	SA	2018-2019	GFM (BESS)	GFM battery enabling islanded operation support.	30MW/8MWh
Wallgrove BESS	NSW	2020-2024	GFM (BESS)	Synthetic inertia and FFR	50MW/75MWh
Wandoan South	QLD	2022	GFM (BESS)	Provides grid stability, frequency regulation, and supports RE integration	100MW/150MWh
Broken Hill	NSW	2025	GFM (BESS)	GFM backup and firming support	50MW/50MWh
Liddell Project	NSW	2026	GFM (BESS)	GFM storage for grid stability.	500MW/1000MWh
Palmerston	Tasmania	–	GFM (BESS)	System strength and inertia support.	100MW/200MWh
Torrens Island	SA	2023	GFM (BESS)	Grid stability, fast-start backup generation	250MW/250MWh
Central-West Orana	NSW	2021	—	Integrate large-scale renewables into grid	6000MW/7700MWh
New England	NSW	2021	GFM (BESS)	Enable large-scale RE integration.	8000MW/30000MWh
Hunter-Central Coast	NSW	2023	—–	Facilitate renewable energy integration and grid modernization.	1000MW/–
South West	NSW	2021	GFM (BESS)	Enable large-scale RE integration and support weak-grid regions with firming/storage capacity	2500MW/—
Illawara	NSW	2023	—	Facilitate the development of RE projects	17000MW/—

2.17 Real-World Implementation in Australia

2.17.1 Overview of Implemented REZ Projects

Australia has emerged as a global test-bed for high-renewable, inverter-rich power systems, with several REZs now featuring GFM-BESS. As summarised in Table 2.24,

these projects span all mainland NEM regions and already account for over 11 GW of committed or operating capacity, with power ratings from the 30 MW Dalrymple North ESCRI system in SA to the 8 GW New England REZ in New NSW. Early deployments such as the Hornsdale Power Reserve (150 MW/194 MWh) and Wallgrove BESS (50 MW/75 MWh) have proven that GFM inverters can deliver FFR, synthetic inertia, and voltage support in weak grids, thereby providing a technical foundation for larger REZ roll-outs [161, 187]. Concurrently, the AEMO's *Renewable Integration Study* and *Engineering Framework* have set detailed performance envelopes for IBRs, enabling tariff, connection, and market reforms that accelerate the uptake of GFM technology [20].

A second wave of projects, including Wandoan South in Queensland (100 MW/150 MWh), Broken Hill in far-west NSW (50 MW/50 MWh), and the 500 MW/1 GWh Liddell BESS repurposing a retiring coal site, illustrates the transition from demonstration to system-critical applications. These installations are designed not only to supply firming and contingency services but also to unlock gigawatt-scale renewable hosting capacity in their respective REZs. For instance, Central-West Orana (6 GW/7.7 GWh) and Illawarra (17 GW) adopt a "hybrid" pipeline model in which dedicated system-strength batteries operate alongside wind and solar plants to maintain a secure operating envelope under low-inertia conditions [170, 243]. Collectively, the projects in Table 2.24 demonstrate that GFM-equipped BESS can meet or exceed SGs performance standards, particularly for RoCoF containment and islanded grid operation, thereby providing a replicable blueprint for future high-penetration grids worldwide [23]. The effectiveness of these deployments is further evidenced by recent grid performance outcomes, which are explored in detail in the next section.

2.17.2 Grid Performance Outcomes

2.17.2.1 Voltage Stability and Black Start

Voltage stability remains a key challenge in REZs with high IBR penetration, particularly under low SCR conditions. Observations from projects such as Hornsdale and Dalrymple confirm that GFM inverters, with inherent voltage-forming capability, enable rapid voltage recovery, typically within 0.48 to 2 seconds, through dynamic reactive support and voltage stiffness [179, 181, 193]. Additionally, Table 2.25 highlights that GFM inverters, particularly when integrated with BESS, can autonomously perform black-start sequences, a feature demonstrated in pilot projects such as RINGO [160, 161, 181]. These capabilities, also validated by AEMO, support islanding and reconnection

operations, thereby improving grid restoration and overall resilience.

2.17.2.2 Frequency Regulation and Fast Response

As detailed in Table 2.25, GFM inverters demonstrate superior performance in frequency regulation by delivering fast inertial responses via virtual inertia mechanisms. Observed rates of change of frequency (RoCoF) in REZ deployments typically range between 0.38-0.44 Hz/s, with frequency nadirs recorded between 49.57-49.62 Hz [226, 244]. GFM inverters, through advanced controls such as droop response and virtual synchronous machine emulation, significantly lower RoCoF and improve frequency nadir stability within the first few seconds of a disturbance.

Table 2.25: Performance Metrics Observed in REZ Deployments with IBRs

Metric	**Typical Value (Observed)**	**GFM Benefit**	**Comparison with GFL**	**Refs.**
Frequency Response Time	RoCoF (0.38-0.44 Hz/s), nadir (49.57-49.62 Hz)	GFM provides fast inertial response via virtual inertia (3s), better nadir, lower RoCoF, faster return to steady state	GFL uses PLL and droop only, no inertia; results in higher RoCoF and deeper nadir, slower return	[226, 244]
Voltage Recovery Time	~0.48 s [179]; ~1-2 s [193]	Fast voltage restoration via reactive support and voltage stiffness, effective in weak grids	GFLs lack voltage-forming ability; delayed or poor recovery under low-SCR	[179, 193]
Black-start Sequence	Qualitative (based on pilot deployments like RINGO)	GFM inverters (especially BESS-based) enable autonomous black-start without SG dependency; supports resilient restoration in weak/remote grids	GFL inverters rely on external voltage reference, incapable of initiating black-start autonomously	[161, 181]
RoCoF Control Margin	<1 Hz/s during black-start; frequency nadir improved by 20-30%	GFM (droop/PSC/VOC) provides virtual inertia, reduces RoCoF, and enhances dynamic stability in weak grids	GFL shows higher RoCoF and slower damping due to reliance on external voltage reference	[177, 245]

In contrast, GFL inverters lack inherent inertial capabilities due to their dependence on PLLs and droop control alone, resulting in higher RoCoF values and deeper frequency nadirs. The improved dynamic response of GFM systems not only facilitates faster return to steady-state conditions but also enhances resilience in weak grid environments with low system inertia [177, 245], setting the stage for the next section on economic and regulatory implications of their large-scale deployment.

2.17.3 Economic and Regulatory Implications

2.17.3.1 Cost–Benefit Trade-offs of GFM Integration

The integration of GFM inverters into REZs presents a strategic tradeoff between higher initial investment and long-term system-wide benefits. Although GFM technologies entail elevated capital costs and more complex commissioning compared to traditional GFL inverters, emerging evidence from Australian REZ deployments indicates that these costs are offset by a range of economic and operational advantages. Studies have shown that GFM-enabled systems can replace or reduce the reliance on synchronous condensers, avoid renewable energy curtailment, and improve network resilience under low inertia conditions [29, 246, 247]. Quantitative analyses from demonstration projects in SA and NSW have highlighted that the inclusion of GFM inverters, particularly when coupled with BESS, enhances frequency and voltage stability, thereby deferring network upgrades and reducing the risk of load shedding [248, 249]. These findings underscore that while upfront expenses are higher, the overall life cycle benefits including increased hosting capacity, reduced FCAS procurement, and improved compliance with system strength frameworks, justify GFM deployment in weak grid REZ contexts. The following subsection explores how market incentives and policy support can further accelerate this transition.

2.17.3.2 Market Incentives and Policy Support

The increasing penetration of IBRs has necessitated a regulatory shift towards market frameworks that actively incentivize advanced inverter functionalities, particularly GFM capabilities. In response, the AEMO has introduced a suite of technical and economic instruments, including the "Minimum Inertia Requirements" and the development of FFR markets, to monetize critical services such as frequency containment and virtual inertia provision [162, 250]. These mechanisms aim to create new revenue streams for IBRs capable of delivering essential system services traditionally offered by synchronous machines.

In parallel, state-level investment schemes and infrastructure roadmaps have increasingly aligned with the ISP, ensuring a supportive policy environment that reduces investor uncertainty and encourages the deployment of GFM-enabled assets [143, 251]. Furthermore, industry case studies, such as those conducted in the West Murray Zone, demonstrate that policy support, combined with appropriate technical standards, can unlock both stability benefits and increased renewable hosting capacity [252]. This in-

tegrated approach to market design and policy coordination is especially critical for REZs, where economic viability and system reliability must be balanced to enable a secure transition to high-renewable, low-inertia grid conditions. The next subsection examines the remaining challenges and lessons learned, focusing on integration barriers, engineering constraints, and operational gaps.

2.17.4 Challenges and Lessons Learned

2.17.4.1 Integration Barriers

Despite significant progress in inverter technology and control frameworks, the integration of IBRs into weak and high-renewable grids continues to face persistent challenges. One of the foremost issues is the absence of robust, standardized testing protocols that reflect the unique operational conditions of Australian networks, particularly in low-voltage and distribution-level settings with high penetration of rooftop PV and residential battery systems [253]. This gap leads to variability in inverter responses across different manufacturers and limits the predictability of system-wide behavior. Compounding this issue is the lack of real-time visibility into inverter capabilities, such as FFR, inertia emulation, and FRT performance hindering the ability of system operators to coordinate and dispatch resources effectively during dynamic events [254].

Furthermore, grid planners often struggle to validate the performance of GFM inverters in non-ideal network conditions, such as those characterized by low SCR, high harmonic distortion, and limited system damping. These validation difficulties are especially pronounced when multiple vendors with varying control implementations are integrated into a single REZ, leading to interoperability concerns and increased risk of instability during faults or switching events [33]. The complexity of managing mixed GFM and GFL units without a unified control hierarchy adds another layer of difficulty, particularly when relying on decentralized droop-based responses in the absence of a system-wide frequency or inertia estimation framework. Addressing these barriers requires coordinated standards development, improved data sharing mechanisms, and enhanced simulation and testing methodologies that can reflect real-world operating challenges in REZ deployments.

2.17.4.2 Engineering and Operational Gaps

Despite promising demonstrations of GFM converters, several engineering limitations hinder their seamless integration into high-IBR power systems. Contemporary planning

frameworks still rely heavily on conventional system strength indicators, such as SCR and its variants, which fall short of capturing the fast dynamics introduced by GFM units, particularly in weak-grid environments like REZs[183]. This mismatch often results in poorly defined fault level envelopes, ambiguous protection settings, and inadequate specifications for inertia support. Additionally, the lack of streamlined coordination among Transmission Network Service Providers (TNSPs), inverter manufacturers, and system operators such as AEMO contributes to prolonged commissioning timelines. As reported across various pilot projects, repeated iterations of EMT and RMS validation cycles are common, reflecting the fragmented nature of model development and tuning procedures [187].

Operational challenges further compound these engineering issues. Existing dispatch frameworks and ancillary service markets are designed around SG behaviors and have not yet evolved to accommodate the autonomous functionalities of GFM-based inverters, such as synthetic inertia, voltage source operation, fast frequency response, and islanding support [255]. As a result, many of the advanced capabilities of GFM systems remain underutilized in day-to-day grid operations. Addressing these challenges calls for the development of integrated system-strength assessment tools, standardised performance validation protocols, and market reforms that recognize and reward GFM-specific services. Without such systemic updates, the transformative potential of GFM technologies will remain constrained, particularly in future grids dominated by IBRs. This underscores the need for a strategic transition pathway, which is discussed in the following subsection with a focus on promoting inverter technologies in REZs.

2.18 Discussion and transition pathway to promote inverter technologies in REZs

The rapid evolution of Australia's REZs, driven by the nation's decarbonization commitments under SDG 7 (Affordable and Clean Energy) and SDG 13 (Climate Action), necessitates a strategic transition in inverter technologies. As traditional SGs are phased out, IBRs, particularly GFMI and GFLI are becoming foundational to the stability and reliability of future power systems. Compared to legacy mechanical-based systems, advanced inverters provide precise and rapid response capabilities, superior frequency regulation, and enhanced voltage support [161, 180, 230]. Their deployment is especially critical in weak grid conditions, where low inertia, high variability of renewables, and spatial isolation increase the likelihood of instability and blackouts [148, 256]. Figure

2.40 illustrates the key enablers, current developments, and existing challenges associated with the transition pathway for promoting inverter technologies in the integration of REZs within low-inertia grids.

The operational complementarity between GFM and GFL inverters defines a promising transition pathway. GFM inverters emulate the dynamic behavior of SGs by establishing voltage and frequency references, enabling autonomous operation even under islanded or weak grid conditions. Conversely, GFL inverters rely on external grid signals to synchronize and inject power, making them ideal for high-efficiency energy conversion when grid strength is sufficient [161, 177, 245]. Coordinated deployment allows GFM inverters to stabilize the grid and provide GFM services, while GFL units maximize generation output. Hybrid topologies combining both modes, especially in large-scale solar and wind farms, can deliver system-level benefits by balancing dynamic stability and operational efficiency [5, 171].

From a systems integration standpoint, inverter coordination enables enhanced provision of ancillary services, including synthetic inertia, FFR, black-start capability, and reactive power support. This is particularly relevant in REZs where the asynchronous nature of renewables can otherwise reduce system strength. Strategic placement of GFM inverters at critical nodes-such as weak grid endpoints or near major renewable clusters can improve local voltage profiles and reduce reliance on synchronous condensers or diesel generators [227, 228]. Meanwhile, advanced control schemes such as droop control, VSM, and VOC are allowing GFM inverters to mimic the inertia and damping behavior of conventional machines, enhancing transient stability in REZs.

However, significant regulatory and operational barriers persist. The absence of clear performance standards for GFM behaviour, unresolved interoperability issues between GFM and GFL units, and inadequate market signals for grid services limit the scalability of inverter-based architectures [148, 177, 180]. Furthermore, current network planning tools and protection systems are primarily designed for synchronous-dominated grids and may not fully capture the dynamic interactions of multiple IBRs. To overcome these barriers, grid codes must evolve to specify response times, FRT characteristics, and harmonization protocols for mixed inverter environments. Simultaneously, simulation tools and real-time monitoring systems should be upgraded to model GFM/GFL dynamics with greater fidelity.

Technological innovation will continue to underpin the successful deployment of coordinated inverter systems. Advances in power electronics, wide-bandgap semiconductor materials, control algorithms, and digital twin-based validation platforms can enable

superior accuracy, faster control loops, and more robust performance under system stress conditions [190, 203]. Moreover, the digitization of power systems through high-speed telemetry, machine learning-based state estimation, and dynamic hosting capacity assessments can inform optimal inverter siting and real-time dispatch strategies. Emerging concepts such as autonomous inverter clusters and GFM microgrids further demonstrate the potential of inverter-based systems to serve as foundational building blocks in REZs.

In summary, promoting inverter technologies in Australia's REZs requires a holistic transition pathway that integrates policy support, advanced controls, digital infrastructure, and market reform. Coordinated deployment of GFM and GFL inverters offers a technically robust and economically viable path to achieving high renewable penetrations without compromising system security. By aligning this transition with national grid modernization goals and international climate commitments, stakeholders can accelerate the development of resilient, inverter-based REZs. This evolution not only addresses the operational challenges of weak grids but also supports the broader vision of a carbon-neutral, renewables-driven energy future. The final section presents the key findings and conclusions drawn from this review.

2.19 Findings and conclusions

This study presents a systematic review of the cornerstone role played by IBRs in the integration of Australia's REZs. Driven by the environmental and economic limitations of conventional fossil-fuel generation, the Australian government has prioritized REZ development as a pathway toward a cleaner, more sustainable grid. The review begins by exploring the concept of REZs and the associated grid integration challenges, particularly within low-inertia, weak networks. It also traces the evolution of modern power systems toward inverter-dominated architectures, identifying the growing inadequacies of SG-based systems under high renewable penetration.

Focusing on inverter technologies, specifically GFM and GFL inverters, the review provides a technical overview of their operation, supported by mathematical control models and hierarchical control structures. It further analyzes REZ-specific constraints, simulation environments used in modelling, benchmark test networks, and the performance metrics commonly employed for validation. Real-world implementations of GFM-GFL coordination are also reviewed to provide insight into practical deployment challenges and system-level outcomes. Additionally, the study investigates advanced control strategies such as droop control, VSM, and VOC, presenting a detailed feature

matrix aligned with Australia's REZ requirements.

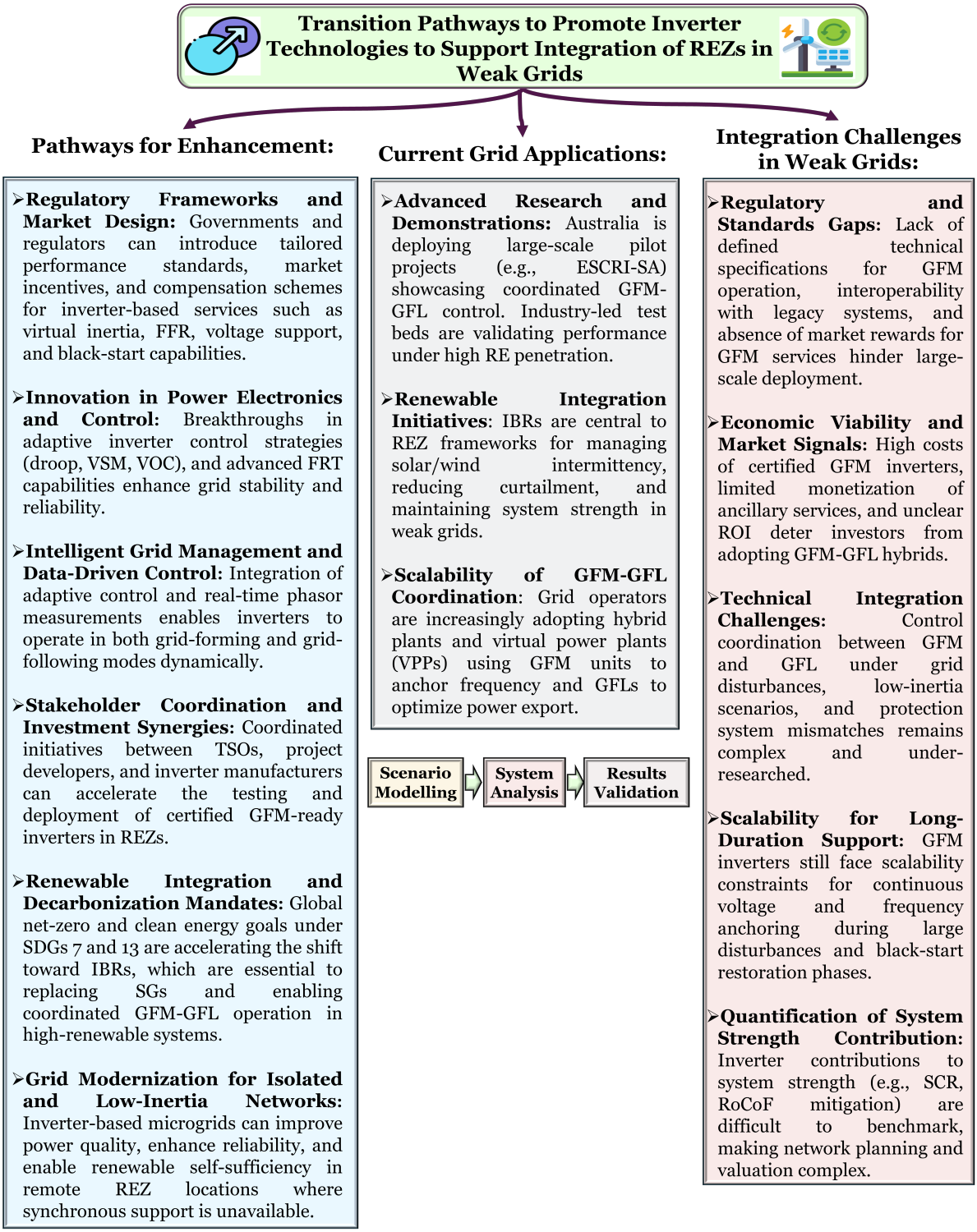


Figure 2.40: Strategic drivers, current practices, and key challenges guiding the transition to coordinated GFM-GFL inverter deployment in REZs with weak grids.

Building on these findings, the review proposes a strategic transition pathway to accelerate the adoption of inverter technologies in REZs. This includes regulatory support, technical innovation, and coordinated deployment to achieve a more reliable, climate-friendly, and economically viable power system. The review concludes by identifying key directions for future research that can support the continued evolution of inverter-dominated grids and ensure successful large-scale renewable integration across Australia.

The major findings and conclusions of this study are as follows:

- **Challenges in REZs integration:** REZs face critical challenges, including reduced system inertia, low SCR, weakened voltage regulation, and increased RoCoF due to high reliance on IBRs. These issues are especially severe in weak and remote grids, where network strength is limited. Addressing these concerns requires the development of advanced GFM-GFL control strategies, which should be a key focus of future research and real-world deployment efforts.

- **Limitations of SG dominated power system:** Conventional SG-based systems provide essential inertia and voltage support but rely heavily on fossil fuels, contributing to greenhouse gas emissions and environmental degradation. Their centralized structure and limited flexibility also restrict the integration of variable renewable sources. Future work should prioritize transitioning to cleaner, inverter-based alternatives that support sustainable development goals while ensuring reliable and resilient grid operations in renewable-rich networks.

- **Inverter technologies as a promising solution:** Inverter-based resources offer enhanced controllability, modularity, and compatibility with renewable generation, making them ideal for modern power systems. Coordinated operation between GFM and GFL inverters enables the establishment of voltage and frequency references while ensuring responsive power injection and system support. To fully realize their potential, future work must focus on developing standardized coordination strategies, improving interoperability, and validating large-scale deployment through real-world pilot projects and advanced simulation frameworks.

- **Gaps in Modelling and Simulation Tools:** Existing RMS and EMT platforms inadequately capture the complex dynamics of both GFM and GFL inverters in low-inertia, fault-prone grids. Challenges include limited resolution in control behavior, poor harmonic representation, and lack of validated models for droop, VSG, VOC,

and PLL-based GFL control. Proprietary vendor models hinder transparency and benchmarking. Future work should focus on open-access, high-fidelity libraries to support standardized assessments under weak grid conditions.

- **Need for Large-Scale Field Validation and Standards:** Despite successful project-level demonstrations (e.g., Hornsdale, Dalrymple), Australia lacks a unified national framework for testing GFM and GFL inverters. The absence of standard protocols for black-start, synthetic inertia, and FFR compliance increases deployment uncertainty. Inconsistent commissioning practices across operators further elevate costs. Future work must prioritize developing standardized validation procedures and adopting national guidelines aligned with IEEE 2800 and Europe's RfG to ensure interoperability and scalability.

- **Deployment of inverter technologies in Australia's REZs:** IBRs, particularly GFM and advanced GFL inverters, are increasingly deployed in Australia's REZs to address challenges posed by declining SGs. Projects like Dalrymple and Hornsdale have demonstrated their potential for system strength, frequency control, and black-start capabilities. Future work should focus on expanding these deployments through standardized technical requirements, coordinated planning, and real-time validation to ensure reliable, scalable integration across all REZ developments.

- **Australian projects on GFM (BESS):** A growing number of REZ developments across Australia, such as Hornsdale, Dalrymple, and Central-West Orana, have deployed GFM inverters with BESS to deliver fast frequency response, system strength, and black-start capabilities. These projects range from pilot-scale (30MW/8MWh) to grid-scale (17000MW), enabling renewable integration and grid resilience. Future work must focus on coordinated control strategies and performance benchmarking to standardize GFM deployment across diverse grid conditions.

- **Control strategies:** Grid-connected converters in REZs are classified into GFL and GFM control structures. GFL systems rely on grid conditions and include PQ, droop (current-controlled), and VSG (current-controlled) modes. In contrast, GFM systems offer grid-supportive capabilities via droop (voltage-controlled), PSC, VSG (voltage-controlled), Matching, Synchronverter, and VOC-based controls. Future research should prioritize adaptive coordination between GFL and GFM units to enhance dynamic grid stability in high-renewable penetration scenarios.

- **Future Directions and Strategic Transition Pathways:** Advancing inverter technologies for REZs requires coordinated regulatory frameworks, adaptive control innovations, and large-scale GFM-GFL demonstrations. While hybrid integration and grid modernization efforts are accelerating, significant gaps remain in standards, economic viability, and technical coordination. Future work should focus on quantifying inverter contributions to system strength and developing scalable, interoperable solutions for long-duration support in weak and low-inertia networks.

In conclusion, this study highlights inverter technologies, particularly GFM and GFL inverters, as critical enablers for enhancing RE utilization and addressing the challenges of weak grid environments in Australian REZs. Real-world deployments such as the 150 MW/194 MWh Hornsdale Power Reserve in SA and the 500 MW/1000 MWh Liddell Project in NSW demonstrate the effectiveness of GFM-based BESS in improving grid stability and minimizing curtailment. By examining IBR modelling approaches, simulation environments, benchmark networks, performance metrics, and real-world project applications, this review outlines a comprehensive road map for advancing coordinated GFM-GFL deployment in REZs. These insights support the broader transition toward clean, affordable, and sustainable energy systems aligned with a zero-carbon future.

2.20 Chapter summary

This chapter reviewed the technical challenges and existing methodologies relevant to renewable integration in weak transmission networks and REZ environments. The first part synthesised current research on BESS applications for weak-grid stability and revealed key gaps, including the absence of coordinated multi-layer controller optimisation, limited system-level approaches to voltage stability and FRT enhancement, and the lack of quantitative resilience metrics suitable for weak-grid evaluation. These gaps directly motivate the cascaded control optimisation framework developed in Chapter 3. The second part examined inverter-based control strategies, highlighting critical limitations in existing studies such as insufficient coordination between GFM and GFL inverters, incomplete understanding of multi-inverter interactions under low system strength, and the scarcity of REZ-specific modelling insights for evaluating GFM strategies. These shortcomings form the basis for the severity-aware coordinated BESS control framework presented in Chapter 4.

CHAPTER 3

WEAK-RENEWABLE-GRID STABILITY ENHANCEMENT

Chapter Composition

This chapter addresses Research Question 1 by developing a cascaded control parameter optimisation framework to enhance voltage stability and fault-ride-through performance in renewable-rich weak transmission networks. Building on the gaps identified in Part 1 of the literature review, including insufficient multi-layer controller coordination, the absence of a unified resilience metric, and limited weak-grid optimisation methods, the chapter introduces a DRM that captures transient voltage deviations, permissible fault-clearing durations, and post-fault recovery behaviour. An enhanced PSO algorithm is then employed to simultaneously tune plant-level, network-level, and converter-level controls within a hierarchical structure. PSO is adopted due to its suitability for solving non-linear, non-convex optimisation problems without requiring gradient information. It is applied to optimise controller parameters and the GFM:GFL penetration ratio, treated as a bounded decision variable and evaluated using the proposed stability metrics. The framework is implemented on the Simplified 14 Generator Test System (Area 5), representative of Southeast Australia and evaluated against AEMC and IEEE stability requirements. Case studies show significant improvements in overshoot reduction, extended clearing times, and smoother recovery, demonstrating the framework's effectiveness in addressing weak-grid stability challenges under high renewable penetration.

3.1 Introduction

3.1.1 Background

The accelerating global transition toward low-carbon and sustainable energy systems has encouraged large-scale renewable energy deployment, particularly solar photovoltaics (PV) and wind power. The rapid adoption of these technologies has become a cornerstone of global carbon neutrality efforts [13], supporting the reduction of dependence on fossil-based generation [257]. Maintaining a diversified renewable portfolio is also recognized as essential for long-term energy sustainability and system resilience [152]. Despite their environmental and economic benefits, large-scale renewable integrations introduce operational and stability challenges for conventional power systems. The intermittency of renewable generation and the lack of physical inertia complicate voltage and frequency regulation during network disturbances [43]. Inverter-interfaced resources differ fundamentally from synchronous machines because they lack mechanical damping and voltage support mechanisms that have historically ensured stable system operation [12]. This reduced inertial response makes grid dynamics highly sensitive to faults and disturbances, especially in weak transmission networks [258]. Such weak grids are characterized by high line impedance, low short-circuit capacity, and limited reactive power reserves, conditions commonly found in remote REZs where transmission development has not kept pace with renewable expansion [13]. Reports from the Australian Energy Market Operator indicate that these regions frequently experience reduced voltage stability margins under high renewable penetration [12]. Similar assessments highlight that inadequate grid reinforcement amplifies transient instability risks [43]. Consequently, maintaining stable voltage profiles and ensuring robust fault-ride-through (FRT) capability have become critical priorities for modern power systems, as emphasized by current regulatory frameworks [155] and verified in recent analytical investigations [259].

3.1.2 Motivation

The stability challenges deepen due to the absence of self-synchronizing properties in inverter-based resources. During network faults, poorly tuned inverters may disconnect abruptly, leading to voltage dips, oscillations, and, in severe cases, cascading system failures. Hardware-based protection schemes such as voltage booster circuits [260] and fuzzy logic-controlled fault current limiters (FCLs) [261] have demonstrated effectiveness in suppressing fault currents. However, these methods often offer limited reactive power

support, delaying voltage recovery during post-fault transients. Optimization-driven approaches, including multi-objective PSO techniques for reactive power coordination [262], have partially mitigated this limitation but remain sensitive to system operating conditions. At the same time, control-oriented improvements, such as real-time current limiting for grid-feeding inverters [263], modified converter control for DFIG-based wind systems [264], and low-voltage ride-through (LVRT) strategies employing current relaxation zones [265] have enhanced individual inverter performance but lack scalability across diverse renewable assets. Furthermore, weak networks with limited inertia continue to experience frequency instability even under improved control settings [266]. These challenges collectively underscore the need for an adaptive, system-level control framework capable of ensuring both voltage stability and fault tolerance in renewable-rich grids.

3.1.3 Problem Statement

Although a wide range of control and protection schemes has been developed to enhance grid performance during faults, most existing approaches address only isolated aspects of system stability. Recent advances in grid-forming converter technology have introduced adaptive FRT and current-limiting mechanisms [267], while complementary designs aim to achieve rapid grid-code compliance through dynamic current restriction [24]. Cooperative fault management strategies that coordinate photovoltaic and wind assets [268] and emergency current-limiting controls for virtual synchronous generators [269] have improved localized resilience, yet their applicability across heterogeneous assets remains limited.

Cascaded or hierarchical control loops implemented in hybrid renewable systems have also demonstrated promising fault responses. Studies examining the impact of photovoltaic penetration under symmetrical and asymmetrical faults [270] and subsequent improvements in transient stability using virtual synchronous generator control [271] highlight progress in this direction. Similarly, coordinated offshore wind-wave energy systems have exhibited improved voltage recovery during disturbances [272]. Nonetheless, these configurations are typically restricted to specific system architectures.

Adaptive LVRT schemes continue to evolve through flexible current injection regions [265] and optimized current-limiting logic [24], offering improved transient support but limited coordination across plant, electrical, and converter-level controllers. Predictive and optimization-based approaches have also been introduced, such as cascaded model predictive control with arc suppression under grounding faults [273] and model-free

inverter algorithms for loss minimization and LVRT enhancement [274]. In parallel, intelligent and hardware-assisted solutions including fuzzy logic-based fault current limiters [261], resonant limiter designs [275], and smart transformer architectures for flexible grid interfacing [11, 276] provide reactive power and stability improvements but often require extensive parameter tuning or additional equipment.

At the device level, several protection-oriented studies on DFIG systems have pursued FRT enhancement through modified protection circuits and control refinements. Enhanced crowbar and fault-current protection schemes [277, 278] and hybrid control strategies combining active and reactive current regulation in grid-tied wind turbines [279] have all improved machine-level LVRT capability. A conceptually related approach [280] proposed a modified demagnetisation control method that introduces an external stator resistance and rotor-side impedance network to accelerate flux damping and suppress transient overcurrents during grid faults. While these studies significantly strengthen equipment-level LVRT performance, they do not translate into coordinated, system-wide resilience across multiple renewable sources.

Moreover, many control strategies continue to rely on simplified test networks rather than realistic weak-grid configurations that capture line impedance, low short-circuit capacity, and reactive power constraints [39, 281]. Hardware-based protection methods such as crowbar circuits and dynamic voltage restorers (DVRs) also increase implementation cost and design complexity [260, 261]. Optimization frameworks built on static parameter settings frequently struggle to adapt under variable renewable conditions, leading to degraded stability margins [275]. Although decentralized control paradigms have achieved centre-piece access in distributed environments [268], questions remain regarding their computational scalability and effectiveness for heterogeneous renewable portfolios [267, 274].

3.1.4 Novelty

To address the identified research gaps, this study introduces a cascaded control parameter optimization framework specifically designed for weak transmission networks with high renewable energy penetration. The core of the framework is an enhanced PSO algorithm that simultaneously fine-tunes control parameters across three hierarchical levels, plant-level, electrical-level, and generator/converter-level controllers. This coordinated tuning enables a unified and resilient system response to dynamic disturbances.

A novel $\mathscr{R}^{\Delta V\downarrow}_{t_{\text{clear}}\uparrow}$ is also formulated to comprehensively assess network performance by combining time-weighted voltage deviations, fault-clearing durations, and post-fault

recovery smoothness into a single quantitative indicator. Unlike conventional indices that focus only on transient stability, the $\mathscr{R}^{\Delta V\downarrow}_{t_{\text{clear}}\uparrow}$ jointly evaluates both short-term and long-term resilience, offering a balanced performance measure under varying renewable penetration scenarios.

Table 3.1: Comparison of this work with existing studies on voltage stability enhancement, FRT improvement, and renewable-rich weak-grid control.

Ref	Voltage Stability & FRT Enhancement	Cascaded Multi-Level Control Optimization	Validation under Weak Transmission Networks	Applicability in Renewable-Dominated Systems
[267]	✓	✗	✓	✓
[24]	✓	✓	✗	✓
[277]	✓	✗	✗	✗
[278]	✓	✗	✗	✓
[279]	✓	✗	✗	✓
[280]	✓	✗	✗	✗
[282]	✓	✗	✓	✓
This Work	✓	✓	✓	✓

The proposed framework is validated using a modified version of Area 5 of the Australian 14-generator test system, configured to emulate weak-grid operating conditions with multiple renewable energy technologies. Simulation outcomes demonstrate substantial improvements in voltage overshoot reduction, extended fault-clearing capability, and faster voltage settling times compared with traditional tuning approaches. Moreover, the optimised control parameters ensure consistent performance across PV, wind, and BESS-based systems, highlighting the versatility and scalability of the proposed method.

The comparative assessment presented in Table 3.1 highlights how this work advances beyond existing studies on voltage stability enhancement, FRT improvement, and weak-grid control. Prior research efforts, such as grid-forming control schemes [24, 267], and DFIG-oriented protection strategies [277–280], primarily addressed isolated aspects of fault resilience or relied on device-level interventions. In contrast, the proposed cascaded framework uniquely integrates multi-level control optimization, system-wide

validation under weak-grid conditions, and broad applicability to renewable-dominated systems, establishing a comprehensive pathway for strengthening renewable-rich weak grids.

A concise depiction of the research flow is shown in Figure 3.1, illustrating the progression from problem identification to cascaded control optimization and performance validation across multiple case studies.

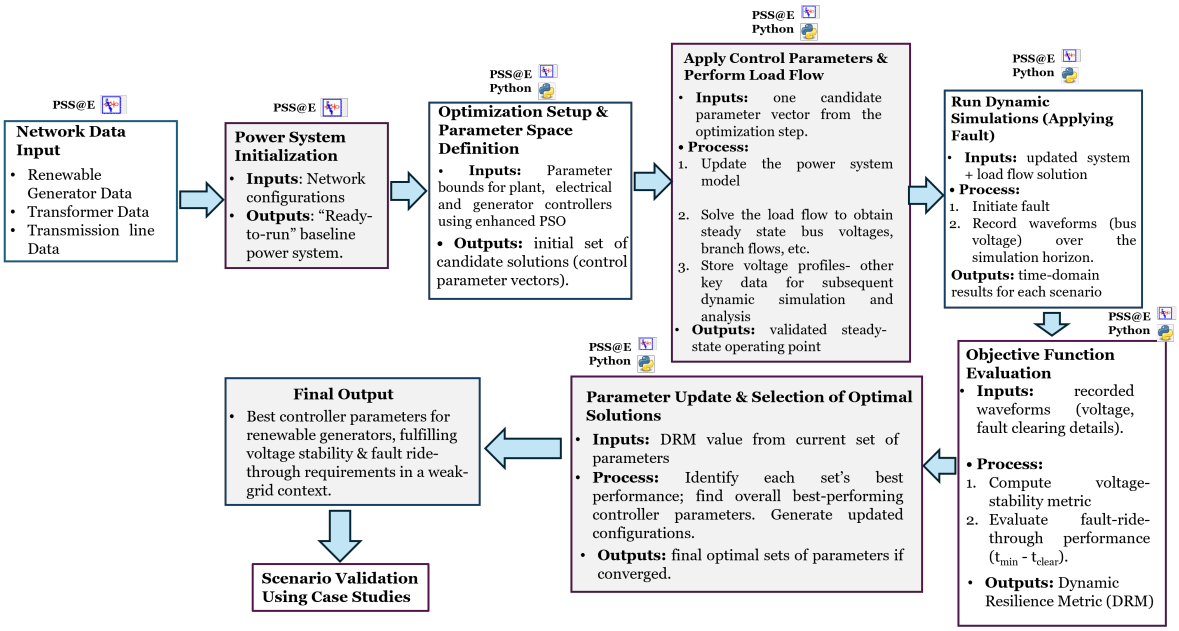


Figure 3.1: Overall methodology for this research

3.1.5 Contributions

The main contributions of this research are summarised as follows:

- **Integrated Optimization Criterion:** A novel multi-objective optimization criterion is developed to simultaneously minimize voltage deviations and enhance fault-clearing capability. This approach effectively bridges the gap between short-term voltage stability and long-term fault ride-through (FRT) performance in renewable power systems.

- **Hierarchical Cascaded Optimization Framework:** A coordinated cascaded optimization strategy is proposed to fine-tune the control parameters of renewable generation units across plant-level, electrical network-level, and generator-level

controls. The unified optimization ensures robust dynamic performance and system stability, with parameter sets validated under diverse operating conditions.

- **Extensive System Validation:** Comprehensive simulation and validation studies confirm that the proposed framework significantly improves voltage stability and extends fault-clearing time (FRTt), ensuring reliable post-fault recovery and enhanced resilience of renewable-integrated power systems under a wide range of disturbances.

3.1.6 Organisation of the Chapter

Collectively, these contributions form a scalable and computationally efficient framework for the control of renewable-rich weak grids. The remainder of this chapter is organized as follows: Section 2 details the cascaded control framework for renewable energy integration in weak transmission networks. Section 3 presents the proposed methodology. Section 4 discusses the network model and case studies. Section 5 provides the results and discussion, and Section 6 concludes with key findings and future research directions.

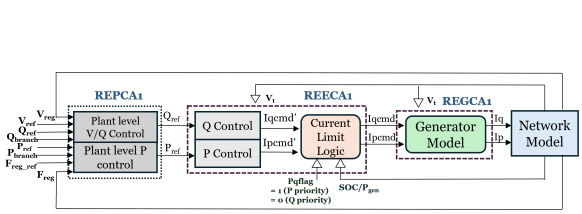
3.2 Cascaded Control Framework for Renewable Energy Integration in Weak Transmission Networks

This research adopts a cascaded control framework comprising plant level, electrical level, and generator/converter level controllers [283], with coordinated parameter optimization to improve voltage stability and FRT performance [284, 285]. Simultaneous tuning of these controllers enhances dynamic response in REZ-integrated weak grids. The next subsection outlines the functional roles of each controller in managing wind and solar integration.

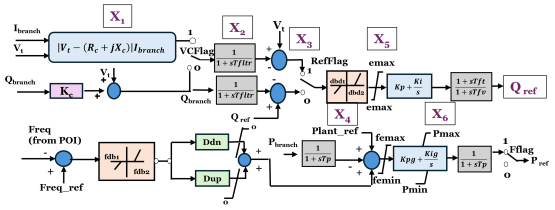
3.2.1 Multilevel Control Framework for Renewable Energy Integration in Weak Transmission Networks

The cascaded control framework for renewable energy systems ensures grid compliance, voltage stability, and effective power injection, particularly in weak transmission networks where high impedance and limited transfer capacity exacerbate the volatility

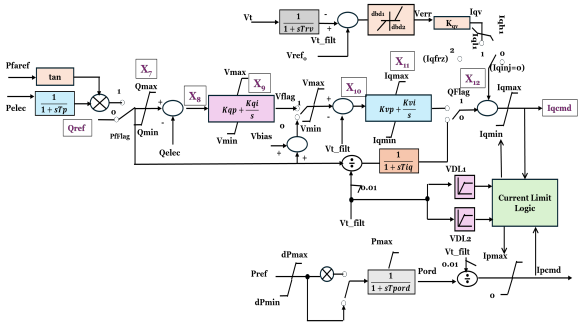
introduced by large-scale wind and solar integration [284, 286]. As shown in the overall block diagram in figure 3.2(a), this framework consists of three interconnected control layers: plant-level, electrical-level, and generator/converter-level. The plant controller in figure 3.2(b) governs voltage and active power regulation, setting reference points for downstream controllers [284]. The electrical controller in figure 3.2(c) manages reactive power dynamics and current limit enforcement, ensuring stability under dynamic conditions. Lastly, the generator/converter controller in figure 3.2(d) oversees inverter response and network interactions, maintaining secure grid operation [286]. The following subsections provide a detailed breakdown of each control level.



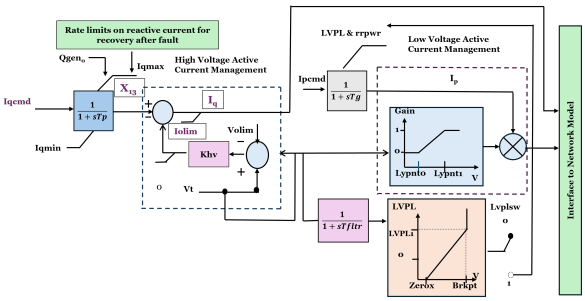
((a)) Cascaded control framework



((b)) Plant Control



((c)) Electrical Control



((d)) Generator Control

Figure 3.2: Block diagrams of the hierarchical control structure: (a) Cascaded framework, (b) Plant-Level Control, (c) Electrical Control, (d) Generator/Converter-Level Control

3.2.1.1 Plant-Level Control

At the plant level, control begins by measuring the terminal voltage and branch current, given by

$$X_1(t) = |V_t - (R_c + jX_c)I_{\text{branch}}(t)| \tag{3.1}$$

This estimate is passed through a first-order low-pass filter, where the VCFlag is chosen as 1 for voltage control, yielding a smoothed signal:

$$\dot{X}_2 = \frac{1}{T_{\text{fltr}}}(X_1(t) - X_2(t)) \tag{3.2}$$

Next, a voltage error is computed by comparing the filtered voltage to a reference:

$$X_3(t) = V_{\text{ref}} - X_2(t) \tag{3.3}$$

To prevent control response to small fluctuations, the error is passed through a deadband block:

$$X_4(t) = \begin{cases} 0, & \text{if } |X_3(t)| \le \epsilon \\ X_3(t) - \text{sign}(X_3(t)) \cdot \epsilon, & \text{otherwise} \end{cases} \tag{3.4}$$

The deadband output is then passed through a limiter to constrain its range:

$$X_5(t) = \min(\max(X_4(t), -e_{\max}), e_{\max}) \tag{3.5}$$

The limited signal is then processed by a Proportional-Integral (PI) controller, generating the control output:

$$X_6(t) = K_p X_5(t) + K_i \int_0^t X_5(\tau)\, d\tau \tag{3.6}$$

Finally, this output is shaped by a lead-lag compensator to improve transient response, resulting in the reactive power reference:

$$T_{\text{fv}} \dot{Q}_{ref} + Q_{\text{ref}}(t) = T_{\text{ft}} \dot{X}_6 + X_6(t) \tag{3.7}$$

This control chain ensures effective voltage tracking and generates $Q_{\text{ref}}(t)$ for downstream control of converter reactive power output.

3.2.1.2 Electrical Control

At the electrical control level, the reactive power reference $Q_{\text{ref}}(t)$, typically provided by the plant-level controller, is first passed through a saturation block to enforce converter physical and regulatory limits, where Pfflag is chosen as 0 for $Q_{\text{ref}}(t)$ control, producing a limited reactive power reference:

$$X_7(t) = \min(\max(Q_{\text{ref}}(t), Q_{\min}), Q_{\max}) \tag{3.8}$$

This limited reference is compared with the actual reactive power output $Q_{\text{elec}}(t)$, and the resulting error drives the reactive current control loop:

$$X_8(t) = X_7(t) - Q_{\text{elec}}(t) \tag{3.9}$$

The error signal $X_8(t)$ is then processed by a PI controller to generate an intermediate control signal, which is then limited to the range $[V_{\min}, V_{\max}]$, where the VFlag is set to 1 for overall power control:

$$X_9(t) = \min\left(\max\left(K_{qp}X_8(t) + K_{qi}\int_0^t X_8(\tau)\,d\tau, V_{\min}\right), V_{\max}\right) \tag{3.10}$$

The measured terminal voltage $V_t(t)$ is passed through a voltage-dependent limiter (VDL) block, which shapes the signal based on dynamic voltage support characteristics:

$$V_{t\_\text{filt}}(t) = \text{VDL}(V_t(t)) \tag{3.11}$$

The difference between the limited controller output $X_9(t)$ and the filtered terminal voltage $V_{t\_\text{filt}}(t)$ forms the voltage deviation signal:

$$X_{10}(t) = \min\left(\max(X_9(t), V_{\min}), V_{\max}\right) - V_{t\_filt}(t) \tag{3.12}$$

This voltage deviation is then passed through a second PI controller, tuned for voltage control, to generate a reactive current reference:

$$X_{11}(t) = \min\left(\max\left(K_{vp}X_{10}(t) + K_{vi}\int_0^t X_{10}(\tau)\,d\tau, I_{q\min}\right), I_{q\max}\right) \tag{3.13}$$

To enhance fault performance or provide grid support, an additional injected current signal $I_{q\text{inj}}(t)$ can be added, where the QFlag is to 1 for voltage control:

$$X_{12}(t) = X_{11}(t) + I_{q\text{inj}}(t) \tag{3.14}$$

Finally, the sum is passed through a current limiter to ensure the output does not exceed the inverter's reactive current capacity:

$$I_{qcmd}(t) = \min\left(\max\left(X_{12}(t), I_{q\min}\right), I_{q\max}\right) \tag{3.15}$$

3.2.1.3 Generator/Converter-Level Control

At the generator level, the reactive current command $I_{q\text{cmd}}(t)$, generated by the electrical controller for voltage regulation, passes through a first-order lag block with time constant T_g and negative gain to model inverter dynamics, then is limited to $I_{q\min}$ and $I_{q\max}$:

$$T_g\dot{X}_{13} + X_{13}(t) = -I_{q\text{cmd}}(t) \tag{3.16}$$

$$X_{13}(t) = \min\left(\max\left(X_{13}(t), I_{q\,\min}\right), I_{q\,\max}\right) \tag{3.17}$$

This output, $X_{13}(t)$, is then passed through the high voltage reactive current management logic. This block ensures that when the terminal voltage $V_t(t)$ exceeds a predefined threshold V_{olim}, the reactive current is reduced proportionally to avoid worsening overvoltage conditions. The reduction is scaled by the high-voltage gain K_{hv}:

$$I_{\text{olim}}(t) = X_{13}(t) - K_{hv} \cdot \max(0, V_t(t) - V_{\text{olim}}) \tag{3.18}$$

The final reactive current sent to the network is the more conservative of the two:

$$I_q(t) = \min(X_{13}(t), I_{\text{olim}}(t)) \tag{3.19}$$

This final output $I_q(t)$ is passed to the network model interface, representing the converter's contribution to reactive current injection. In the implemented converter model, the DC-link voltage (V_{dc}) is continuously regulated by the grid-side converter's inner control loop to remain within its allowable range of $0.9\,\text{p.u.} \leq V_{dc} \leq 1.1\,\text{p.u.}$ (corresponding to $\pm 10\%$ of the nominal value). The relationship between the converter's DC-link voltage and the AC-side RMS voltage can be expressed as [287]:

$$V_{dc} = \frac{2K}{m} \frac{\sqrt{2}}{\sqrt{3}} V_{L\text{–}L} \tag{3.20}$$

where K denotes the voltage compensation factor and m is the modulation index. For an ideal converter ($K = 1$) and unity modulation ($m = 1$), this reduces to $V_{dc} \approx 2V_{L\text{–}N}^{\text{RMS}}$, illustrating the direct proportionality between the DC-link potential and the AC bus voltage. This relation, also verified by [280] and [287], ensures that maintaining V_{dc} within 0.9–1.1 p.u. prevents over-voltage stress and preserves the linear modulation range required for LVRT compliance.

Based on the equations, it is seen that the cascaded control framework enables coordinated regulation across plant-level voltage sensing, electrical-level current commands, and generator-level converter actions as shown in Figure 3.2(a), ensuring stable power injection and compliance with grid codes in REZs, especially under fault conditions in weak networks. Achieving this stability requires simultaneous optimization of key parameters summarized in Table 3.2. Independent tuning can lead to parameter misalignment, delayed responses, and voltage oscillations under high renewable penetration [284, 286]. The following section presents the proposed methodology of this research.

Table 3.2: Key Parameters and Their Roles in the Cascaded Control Framework

Model	Parameter	Description & Role
Plant Control	Proportional Gain (K_p)	Governs the rate of response for voltage.
	Integral Gain (K_i)	Addresses steady-state errors for precise voltage.
	Voltage Compensation (R_c,X_c)	Corrects line losses to maintain accurate voltage.
Electrical Control	Proportional Gain (K_{qp})	Modulates terminal voltage error response.
	Integral Gain (K_{qi})	Ensures steady-state accuracy in voltage.
	Reactive Current Limits (I_{qh1},I_{ql1})	Enforces safety for reactive current injection.
	Time Constant (T_p)	Smooths transient shifts in current injection.
Generator Control	Overvoltage Gain (K_{hv})	Regulates I_q in overvoltage scenarios.
	Converter Time Constant (T_g)	Limits how quickly reactive current responds to voltage deviations.
	Current Limits (I_{qrmax},I_{qrmin})	Caps total current for operational safety.

3.3 Proposed Methodology

This section details the proposed methodology for optimizing cascaded controller parameters in weak transmission networks. The approach consists of several stages, from initial system setup to final controller validation. Figure 3.3 presents an overview of the proposed methodology flow, and Algorithm 1 summarizes the integration of the cascaded control framework described in Section 2 with the enhanced PSO routine, showing how each Control and Operating Parameter (COP) is iteratively applied and evaluated through dynamic simulations for voltage and FRT improvement.

3.3.1 Power System Modeling & Initialization

The methodology begins by constructing a dynamic power system model that includes both the network (transmission lines, transformers, loads) and detailed representations of the cascaded renewable controllers. A load flow is solved to establish baseline operating points, including bus voltages, branch flows, and initial controller states under normal conditions. This initial solution ensures consistency before undertaking time-domain simulations of fault scenarios. The fault scenarios (bus fault) are specified at the outset and applied consistently during the optimization process to assess each candidate parameter set.

3.3.2 Parameter Space Definition & PSO Initialization

Each of the cascaded controllers is associated with a vector of Control and Operating Parameters (COPs), which include parameters as shown in Table 3.2. Bounds for these parameters are set according to engineering constraints (Table 3.3). These bounds are defined based on controller tuning practices, inverter capability limits (current and voltage constraints), and stability requirements to ensure physically feasible and grid-compliant operation. A uniform yet comprehensive search of this multidimensional parameter space is enabled by Latin Hypercube Sampling (LHS). Specifically, each parameter dimension is divided into intervals, and random draws are made within each interval to reduce clustering effects that can occur with naive random sampling. The LHS initialization is described by

$$x_j^{(k)} = \frac{\text{perm}(i) + \text{rand}}{N}, \quad i \in \{1,2,\ldots,N\}, \quad j \in \{1,2,\ldots,D\}, \tag{3.21}$$

where perm(i) is a random permutation of $\{1,2,\ldots,N\}$ and rand $\sim U(0,1)$. These normalized positions are then mapped to actual parameter ranges via

$$z_j^{(k)} = z_{\min,j} + \left(x_j^{(k)} \cdot \frac{(z_{\max,j} - z_{\min,j})}{1 + \delta \cdot e^{-\theta \cdot x_j^{(k)}}} \right), \tag{3.22}$$

where $z_j^{(k)}$ is the position of the k-th particle in the j-th dimension, $z_{\min,j}$ and $z_{\max,j}$ are the lower and upper parameter bounds, and δ, θ introduce a nonlinear scaling for enhanced flexibility. Once each particle's COPs are determined, the PSO routine proceeds to evaluate and refine them iteratively.

3.3.3 Iterative Load Flow & Dynamic Simulation

In each iteration, the COPs generated by PSO are applied to the controllers in the dynamic power system model. A new load flow is computed to ensure valid initial conditions; then, a fault (bus fault) is simulated. Voltage trajectories, generator currents, and other pertinent signals are recorded throughout the fault period and after fault clearing at t_{clear}. Each particle's performance is assessed by examining the resulting transient response and comparing it against the research objectives of voltage stability and fault ride-through compliance.

Table 3.3: Control Variables and Parameter Bounds

Controllers	**Position (Bus)**	**Parameter Bounds**	**PV**		**Wind**	
			Lower Limit	**Upper Limit**	**Lower Limit**	**Upper Limit**
Plant Controller	Zone 1, Zone 2, Zone 3	Proportional Gain (K_p)	0	1	0	1
		Integral Gain (K_i)	0	5	0	3
		Voltage Compensation (R_c)	0	0.2	0	0.1
		Voltage Compensation (X_c)	0	0.2	0	0.1
Electrical Controller	Zone 1, Zone 2, Zone 3	Proportional Gain (K_{qp})	0	2	1	1.5
		Integral Gain (K_{qi})	0	10	0	10
		Reactive Max Current Limits (I_{qh1})	-1.5	-1	1.0	1.1
		Reactive Min Current Limits (I_{ql1})	1	1.5	-1.1	-1.0
		Time Constant (T_p)	0.01	0.03	0.01	0.02
Generator Controller	Zone 1, Zone 2, Zone 3	Converter Time Constant (T_g)	0	0.05	0.01	0.02
		Current Max limits (I_{qrmax})	0	99	0	999
		Current Min limits (I_{qrmin})	-99	0	-999	0
		Overvoltage Gain (K_{hv})	0	1	0.5	1

3.3.4 Objective Function Evaluation

A key performance measure is the $\mathscr{R}^{\Delta V\downarrow}_{t_{\text{clear}}\uparrow}$. The proposed study aims to *minimize* it subject to practical operating constraints for each renewable controller parameter. Specifically, $\mathscr{R}^{\Delta V\downarrow}_{t_{\text{clear}}\uparrow}$ is defined as

$$\begin{aligned} &\text{Minimize} \quad \mathscr{R}^{\Delta V\downarrow}_{t_{\text{clear}}\uparrow} = \alpha \times \int_0^T t\left|V(t)-V_{\text{ref}}\right| \mathrm{d}t + \beta \times \left(t_{\min}-t_{\text{clear}}\right) \\ &\text{Subject to} \quad X_{\text{PV,lower}} \le X_{\text{PV}} \le X_{\text{PV,upper}}, X_{\text{Wind,lower}} \le X_{\text{Wind}} \le X_{\text{Wind,upper}} \end{aligned} \tag{3.23}$$

The weighting factors α and β are selected empirically to balance the relative importance of voltage stability and fault-clearing performance. A sensitivity-based tuning approach is adopted, in which different combinations of α and β are tested to ensure that neither term dominates the optimisation. The final values are chosen to provide a balanced trade-off, ensuring adequate penalisation of prolonged voltage deviations while promoting improved fault ride-through capability. In this expression, $\int_0^T t\,|V(t)-V_{\text{ref}}|\,\mathrm{d}t$ time-weights voltage deviations, penalising prolonged errors, while $t_{\min}-t_{\text{clear}}$ drives the system to withstand longer clearing intervals and thus strengthens fault-ride-through. Controller

parameters are bounded, e.g., $X_{PV,\text{lower}} \leq X_{PV} \leq X_{PV,\text{upper}}$ for PV and $X_{Wind,\text{lower}} \leq X_{Wind} \leq X_{Wind,\text{upper}}$ for wind. Minimising $\mathscr{R}^{\Delta V\downarrow}_{t_{\text{clear}}\uparrow}$ within these limits trims time-weighted voltage error and rewards extended clearing times, ensuring reliable operation in weak grids.

In this study, the term t_{clear} within the $\mathscr{R}^{\Delta V\downarrow}_{t_{\text{clear}}\uparrow}$ represents the FRT duration that the system can withstand before instability occurs. The optimization process, therefore, seeks to maximize this allowable clearing time while minimizing voltage deviations, ensuring compliance with the Australian Energy Market Commission (AEMC) fault-clearing requirements for high-voltage networks.

3.3.5 Optimization & Parameter Update

After each simulation, the PSO algorithm updates each particle's Local Best Operating Point (LBOP) and the Global Best Operating Point (GBOP) if improvements are found. To guide this search process, a **Nonlinear Decreasing Inertia Weight (NDIW)** is employed:

$$\omega = \omega_{\min} + \left(\omega_{\max} - \omega_{\min}\right) \exp\!\left(-\beta \cdot \frac{\text{iter}}{\text{MaxIter}}\right), \tag{3.24}$$

where $\omega_{\max}$ and $\omega_{\min}$ bracket the initial and final inertia weights, β is a decay constant, `iter` is the current iteration index, and `MaxIter` is the maximum allowable iterations. Early in the search, a larger ω encourages broad, global exploration of COPs. As iterations progress, ω declines exponentially, promoting finer, local refinements near promising operating points. Each particle's velocity (or Tuning increment, TI) and position (COP) are then recalculated:

$$\text{TI}_d^{(k+1)} = \omega\,\text{TI}_d^{(k)} + c_1 r_1\left(\text{LBOP}_d - \text{COP}_d^{(k)}\right) + c_2 r_2\left(\text{GBOP}_d - \text{COP}_d^{(k)}\right), \tag{3.25}$$

$$\text{COP}_d^{(k+1)} = \text{COP}_d^{(k)} + \text{TI}_d^{(k+1)}, \tag{3.26}$$

where c_1 and c_2 are the cognitive and social coefficients, r_1 and r_2 are uniform random numbers in $[0,1]$, and LBOP_d, GBOP_d are the local and global best positions in the d-th dimension. This iterative cycle is repeated until convergence criteria such as a maximum iteration count or negligible improvement in $\mathscr{R}^{\Delta V\downarrow}_{t_{\text{clear}}\uparrow}$ are satisfied.

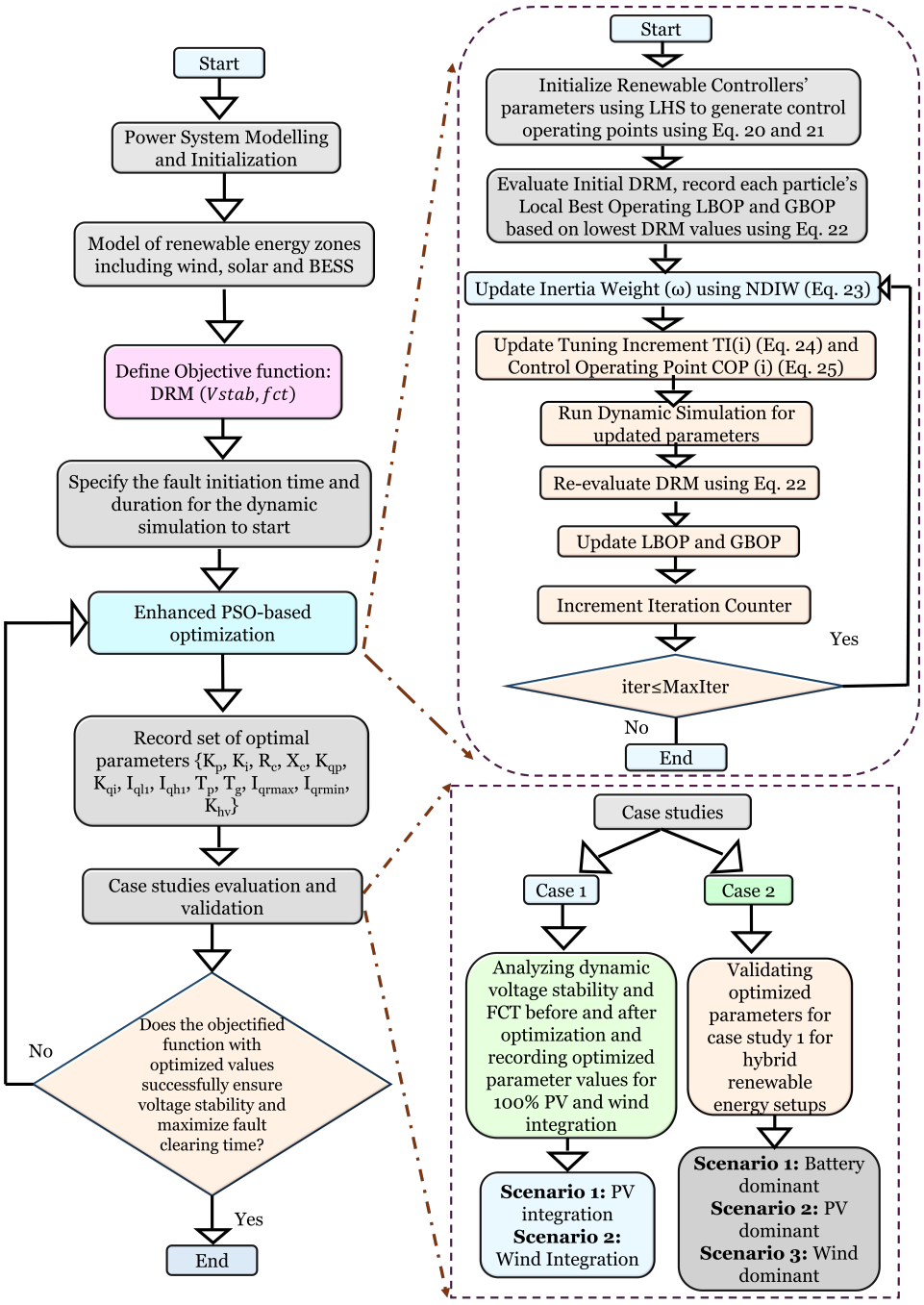


Figure 3.3: Flowchart of proposed methodology

3.3.6 Final Controller Selection & Validation

Upon convergence, the final GBOP is taken to be the parameter set that yields the lowest $\mathscr{R}^{\Delta V\downarrow}_{t_{\text{clear}}\uparrow}$. These optimised COPs are then revalidated through additional simulations to confirm their robustness under various fault locations, load levels, and operating

conditions. The proposed methodology ensures that renewable generators meet strict grid code requirements, even in weak networks with high renewable penetration by minimising extended voltage deviations and maximising permissible fault duration. Ultimately, this approach provides a structured pathway for identifying reliable and high-performance controller settings across various operating scenarios.

The step-by-step procedure of the proposed control and optimisation framework is outlined in Algorithm 1. This algorithm explicitly defines the iterative learning process of the enhanced PSO, where control parameters are continuously refined through dynamic simulations to achieve optimal fault-ride-through and voltage recovery performance.

The following section presents the network model and the test cases considered to validate the proposed methodology.

Algorithm 1 Comprehensive NDIW-Enhanced PSO Algorithm for Renewable Energy Controller Optimization Using LHS and Dynamic Simulations

Input: MaxIter, numParticles, parameter bounds, grid data
Output: GBOP, minimized $\mathscr{R}^{\Delta V\downarrow}_{t_{\text{clear}}\uparrow}$, stable FRT
Begin
Initialize the software environment and load case and dynamic data files.
Generate the initial swarm of COPs using LHS (Eq. (20)–(21)).
Evaluate the initial $\mathscr{R}^{\Delta V\downarrow}_{t_{\text{clear}}\uparrow}$ for each particle, record each LBOP, and determine the GBOP.
while $iter \leq MaxIter$ **do**
  for *each particle* $i = 1, 2, \ldots, N$ **do**
    Update inertia weight ω using the NDIW strategy (Eq. (23)).
    Update TI_i and COP_i using PSO relations (Eq. (24)–(25)), ensuring updated COPs remain within valid parameter bounds.
    Apply the updated COP to the power system model.
    Run dynamic simulations (fault application and clearing).
    Compute the new $\mathscr{R}^{\Delta V\downarrow}_{t_{\text{clear}}\uparrow}(\text{COP}_i)$ using Eq. (22).
    if $\mathscr{R}^{\Delta V\downarrow}_{t_{\text{clear}}\uparrow}(\text{COP}_i) < \mathscr{R}^{\Delta V\downarrow}_{t_{\text{clear}}\uparrow}(\text{LBOP}_i)$ **then**
      Update $\text{LBOP}_i \leftarrow \text{COP}_i$ and $\mathscr{R}^{\Delta V\downarrow}_{t_{\text{clear}}\uparrow}(\text{LBOP}_i) \leftarrow \mathscr{R}^{\Delta V\downarrow}_{t_{\text{clear}}\uparrow}(\text{COP}_i)$.
    if $\mathscr{R}^{\Delta V\downarrow}_{t_{\text{clear}}\uparrow}(\text{COP}_i) < \mathscr{R}^{\Delta V\downarrow}_{t_{\text{clear}}\uparrow}(\text{GBOP})$ **then**
      Update $\text{GBOP} \leftarrow \text{COP}_i$ and $\mathscr{R}^{\Delta V\downarrow}_{t_{\text{clear}}\uparrow}(\text{GBOP}) \leftarrow \mathscr{R}^{\Delta V\downarrow}_{t_{\text{clear}}\uparrow}(\text{COP}_i)$.
  Increment iteration counter: $iter \leftarrow iter + 1$.
Return final GBOP and associated $\mathscr{R}^{\Delta V\downarrow}_{t_{\text{clear}}\uparrow}$ including fault clearing time.
End

3.4 Network and Cases Considered

This section presents the network configuration and corresponding case studies employed to validate the proposed methodology. The considered system is the Simplified 14-Generator Model of the South East Australian Power System. Two case studies, highlighted in Figure 3.3, are implemented to investigate the effects of high renewable penetration under the proposed cascaded control parameter optimization. The following subsections detail the network model and the specific cases analyzed.

3.4.1 Simplified 14-Generator Model of the South East Australian Power System

Figure 3.4 illustrates the Simplified Australian 14-Generator Model, consisting of 10 buses, 3 synchronous generators (totalling 2325 MW), 2 static VAR compensators, 5 loads, and 3 transformers. Plant, electrical, and generator-level controllers are incrementally introduced to enable large-scale renewable integration in a weak transmission network. Buses 501, 502, 503, and 507 are designated as REZs 1-4, each hosting PV, wind, or battery systems operating at a power factor of $\cos(\theta) = 0.95$. Table 3.3 summarizes the controller parameter bounds for PV and wind technologies in Case 1, standardized in per-unit (p.u.) for consistent tuning and simulation. These REZs form the foundation for the case studies, which assess system behavior under varying renewable penetration levels. Further modeling details of this network are available in [288].

3.4.2 Cases Considered

Building on the previous subsection, the proposed methodology is evaluated using the Simplified Model of the South East Australian Power System. This section outlines the two case studies designed to assess the impact of high renewable penetration and cascaded control optimization on voltage stability and FRT performance.

In Case 1, the entire 2325 MW of synchronous generation is replaced with renewable sources, either PV (Scenario 1) or wind (Scenario 2), to simulate fully renewable conditions. Cascaded controller parameters are tested under varying fault-clearing times, comparing fixed values recommended by the PJM Model Guidelines (Table 3.4) with optimized values derived from bounded ranges (Table 3.3). These scenarios aim to identify the most effective parameter configurations across plant, electrical, and generator-level controllers.

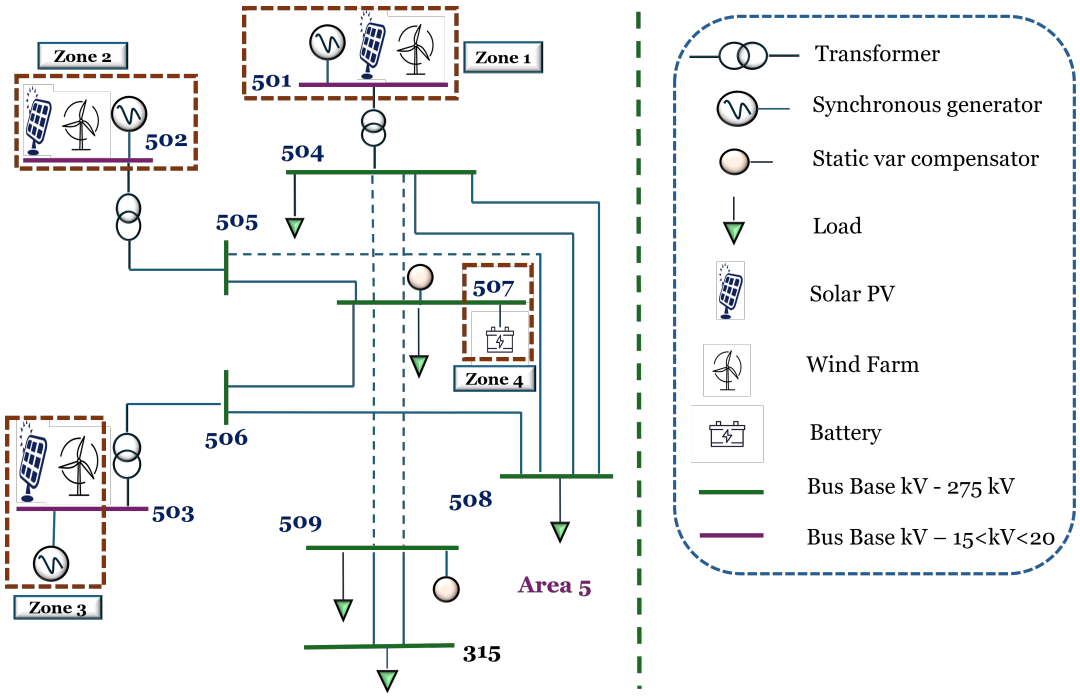


Figure 3.4: Simplified Australian Power System.

Case 2 validates the robustness of the optimized parameters obtained from case 1 under mixed-generation conditions by implementing three hybrid scenarios. Each setup features one dominant technology (60%) and two supporting technologies (20%), as outlined in Table 3.5.

All simulations are conducted in Power System Simulator for Engineering (PSSE) 35.6 with Python 3.9 on a 12th Gen Intel(R) Core i7-1265U CPU (1.80 GHz, 32 GB RAM). The results focusing on voltage stability, fault-clearing time (FCT), and the proposed $\mathscr{R}^{\Delta V\downarrow}_{t_{\text{clear}}\uparrow}$ are presented in the next section to demonstrate the effectiveness of the proposed methodology across different renewable penetration levels.

3.5 Results and Discussion

The following section presents the findings of the study, which aimed to investigate the effects of large-scale renewable sources in the network as shown in Figure 3.4. It presents the results from two case studies as mentioned in previous sections, detailing the specific scenarios analyzed to evaluate cascaded renewable control parameter optimization on system stability and FRT.

Table 3.4: Controller parameters values used for PV and Wind for before optimization cases.

Controllers	**Parameters**	**PV Values**	**Wind Values**
Plant Controller	Proportional Gain (K_p)	0.5	2
	Integral Gain (K_i)	3	1
	Voltage Compensation (R_c)	0	0
	Voltage Compensation (X_c)	0	0
Electrical Controller	Proportional Gain (K_{qp})	1	0
	Integral Gain (K_{qi})	5	0.41
	Reactive Max Current Limits (I_{qh1})	1	1.0025
	Reactive Min Current Limits (I_{ql1})	-1	-1.0025
	Time constant (T_p)	0.01	0.05
Generator Controller	Converter time constant (T_g)	0.01	0.02
	Current Max limits (I_{qrmax})	99	999
	Current Min limits (I_{qrmin})	-99	-999
	Overvoltage Gain (K_{hv})	0.00	0.2

Table 3.5: Hybrid renewable energy configuration scenarios with power allocations.

Scenario	**Dominant Technology (60%) - 1395 MW**	**Supporting Technologies (20% Each) - 465 MW**
Scenario 1	BESS	PV, Wind
Scenario 2	PV	Wind, BESS
Scenario 3	Wind	PV, BESS

3.5.1 Case Study 1: Dynamic Voltage Stability and Fault-Clearing Time Analysis for PV and Wind Integration

Case Study 1 examines two scenarios: **Scenario 1**, where the entire generation is replaced with PV, and **Scenario 2**, where only wind generation is used. The study evaluates voltage stability and FCT, comparing system performance before (Table 3.4) and after (Table 3.3) controller parameter optimization using the modified PSO algorithm. Improvements are validated using the $\mathscr{R}^{\Delta V\downarrow}_{t_{\text{clear}}\uparrow}$, highlighting the effectiveness of the proposed framework in enhancing FRT and reducing voltage deviations. These scenarios demonstrate the framework's ability to address challenges in weak grids with high renewable penetration. The next subsection will present detailed analyses of voltage and FCT improvements.

3.5.1.1 Scenario 1: Voltage Stability and Fault-Clearing Analysis for PV-Based Solar Integration

This section will focus on assessing improvements in dynamic voltage stability through time domain indices and FCT, alongside the overall $\mathscr{R}^{\Delta V\downarrow}_{t_{\text{clear}}\uparrow}$ in PV scenario. Figure 3.5 illustrate representative simulation results for key buses 501 (Zone 1), 502 (Zone 2), 503 (Zone 3), 504, 505, 506, and 507 (Zone 4), while Table 3.6 and Table 3.7 provide a numerical comparison of voltage stability metrics before and after parameter optimization.

3.5.1.2 Voltage Stability Improvements

Tables 3.6 and 3.7 summarize critical voltage stability indicators minimum and maximum post-fault voltages, final steady-state voltage, rise time, settling time, steady-state error, and overshoot for Buses 501 through 507. Before optimization, the system exhibits substantial overshoot (e.g., 26.96 % at Bus 501, 45.45% at Bus 504) and prolonged settling times (around 9.99 s). By contrast, after optimization, the overshoot decreases markedly at each bus (e.g., from 26.96% to 10.10 % at Bus 501), and settling times drop to approximately 3.3-3.8 s. Notably, the minimum voltage during the fault also improves: for instance, Bus 501's voltage dip changes from 0.11 p.u. (pre-optimization) to 0.21 p.u. (post-optimization), reflecting a more stable voltage profile in the face of severe disturbances.

Table 3.6: Voltage stability metrics using before optimized PV values

Bus	Pre-Fault (V)	Min (V) After Fault	Max (V) After Fault	Final (V) at 10 s	Rise Time (s)	Settling Time (s)	Steady State Error	Over-shoot (%)
501	0.99	0.11	1.46	1.15	1.11	9.45	0.16	26.96
502	0.99	0.23	1.40	1.12	1.13	9.75	0.13	25.00
503	0.99	0.20	1.37	1.11	1.09	9.45	0.12	23.45
504	1.04	0.07	1.60	1.10	1.14	9.55	0.06	45.45
505	1.02	0.09	1.57	1.12	1.13	9.25	0.10	40.18
506	1.00	0.00	1.56	1.16	1.11	9.99	0.16	34.48
507	1.01	0.05	1.63	1.14	1.12	9.85	0.13	43.86

3.5.1.3 Fault-Clearing Time and Dynamic Resilience Metric

Figure 3.5(d) illustrates a significant improvement in both the $\mathscr{R}^{\Delta V\downarrow}_{t_{\text{clear}}\uparrow}$ and FCT following optimization. At Bus 501, $\mathscr{R}^{\Delta V\downarrow}_{t_{\text{clear}}\uparrow}$ drops from 3.03 to 0.40, with similar reductions at

Table 3.7: Voltage stability metrics using after optimized PV values

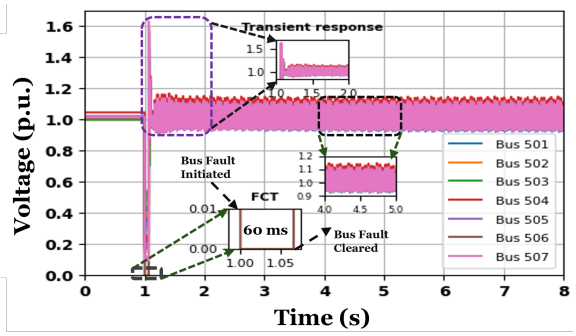
Bus	Pre-Fault (V)	Min (V) After Fault	Max (V) After Fault	Final (V) at 10 s	Rise Time (s)	Settling Time (s)	Steady State Error	Over-shoot (%)
501	0.99	0.21	1.09	0.99	1.10	3.30	0.007	10.10
502	0.99	0.33	1.09	0.99	1.1	3.74	0.008	10.10
503	0.99	0.36	1.05	0.99	1.08	3.74	0.004	6.06
504	1.03	0.13	1.12	1.02	1.11	3.31	0.004	9.80
505	1.00	0.15	1.10	1.00	1.12	3.32	0.005	9.09
506	0.99	0.01	1.10	0.99	1.08	3.18	0.001	10.00
507	0.99	0.07	1.08	0.99	1.07	3.32	0.003	9.09

Buses 503, 505, and 506, indicating enhanced voltage stability. Meanwhile, the FCT increases substantially, from 55 ms to 220 ms at Bus 501 and from 65 ms to 280 ms at Bus 506, demonstrating improved FRT capability across the system.

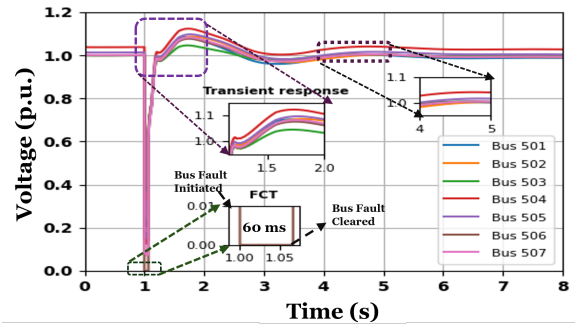
The optimised controllers significantly extend the system's FRT capability, with fault-clearing times reaching up to 270 ms at key buses, an improvement of more than 200 ms compared to the pre-optimised configuration. This performance aligns with the AEMC benchmark of 250 ms for 250-400 kV networks, confirming that the proposed framework ensures stable operation within the prescribed FRT compliance range.

3.5.1.4 Time-Domain Voltage Waveforms

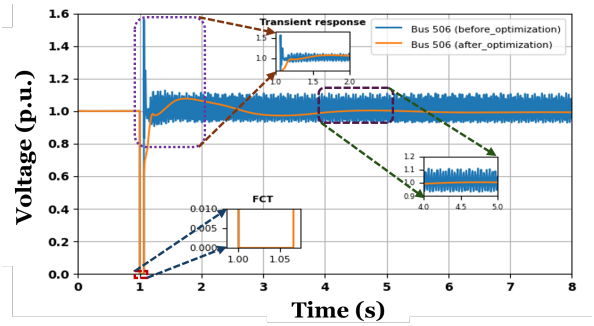
Figures 3.5(a) and 3.5(b) show the voltage waveforms during a bus fault and its clearance at 60 ms. The results demonstrate notable improvements after optimization. Firstly, the overshoot is significantly reduced. At Bus 506 (Figure 3.5(c)), the voltage peak that previously exceeded 1.5 p.u. is markedly lower, resulting in quicker voltage recovery. Secondly, the system stabilizes more rapidly, with voltages returning to nominal levels within 3 to 4 seconds compared to nearly 10 seconds before optimization. This aligns with the improved settling times shown in Table 3.7. Finally, the extended fault clearing times exceeding 200 ms at multiple buses highlight enhanced fault tolerance and system resilience, as further reflected by the substantial reductions in the $\mathscr{R}^{\Delta V\downarrow}_{t_{\text{clear}}\uparrow}$ (Figure 3.5(d)).



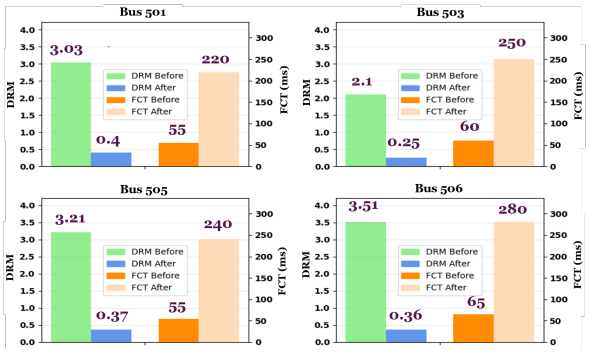
((a)) Voltage profile before using PV values



((b)) Voltage profile after using PV values



((c)) Voltage profile at Bus 506 (before vs. after)



((d)) DRM and FCT comparison across buses

Figure 3.5: Voltage performance comparison under different conditions in PV scenario

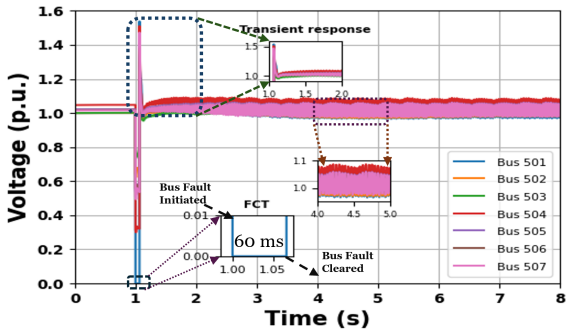
3.5.1.5 Scenario 2: Voltage Stability and Fault-Clearing Analysis for Wind Integration

This section will focus on assessing improvements in dynamic voltage stability through time domain indices and FCT, alongside the overall $\mathscr{R}^{\Delta V\downarrow}_{t_{\text{clear}}\uparrow}$ in wind scenario. Figure 3.6 illustrate representative simulation results for key buses 501 (Zone 1), 502 (Zone 2), 503 (Zone 3), 504, 505, 506, and 507 (Zone 4), while Table 3.8 and Table 3.9 provide a numerical comparison of voltage stability metrics before and after parameter optimization in wind scenario.

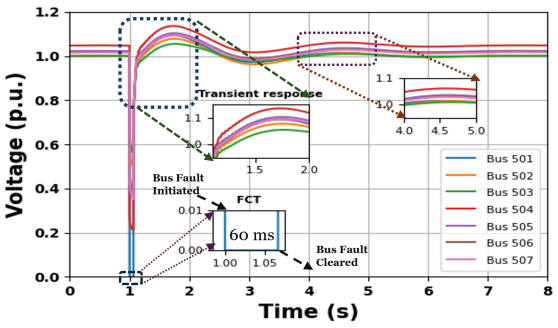
3.5.1.6 Volage Stability Improvements

Tables 3.8 and 3.9 present key voltage stability indicators, including post-fault voltage extremes, final voltage, rise time, settling time, steady state error, and overshoot. Significant improvements are observed after optimization. Overshoot is substantially reduced, for example, from 40.00% to 11.11% at Bus 501 and from 34.82% to 9.62% at Bus 504, demonstrating milder transients during voltage recovery. Settling times also improve

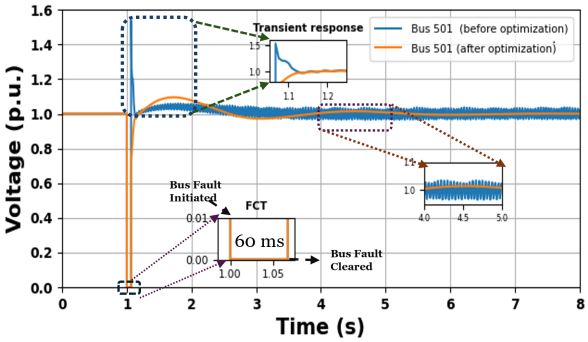
dramatically, decreasing from nearly 9.99 s to around 3.72 to 4.01 s, while steady state errors fall from as high as 0.16 to below 0.01 at all buses, indicating better voltage regulation. Additionally, minimum voltage values during the fault increase slightly, such as Bus 501, improving from 0.00 to 0.01 p.u., suggesting reduced voltage dips.



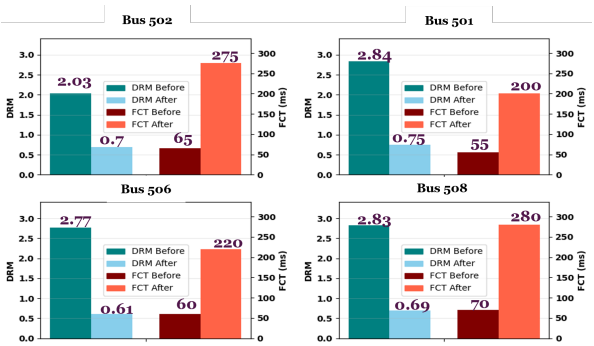
((a)) Voltage profile before in wind scenario



((b)) Voltage profile after in wind scenario



((c)) Voltage profile at Bus 501 (before vs. after)



((d)) DRM and FCT comparison across buses

Figure 3.6: Voltage performance comparison under different conditions in wind scenario.

3.5.1.7 Fault Clearing Time and Dynamic Resilience Metric

Figure 3.6(d) illustrates improvements in the $\mathscr{R}^{\Delta V\downarrow}_{t_{\text{clear}}\uparrow}$ and FCT across key buses. At Bus 501, $\mathscr{R}^{\Delta V\downarrow}_{t_{\text{clear}}\uparrow}$ drops significantly from 2.84 to 0.75, while Bus 502 shows a similar reduction from 2.03 to 0.70, confirming improved FRT capability and reduced time-weighted voltage deviations. Additionally, critical FCT improve markedly. Bus 502's FCT extends from 65 ms to 275 ms, and Bus 501's from 55 ms to 200 ms, indicating enhanced system tolerance to prolonged faults and improved post-fault recovery.

Table 3.8: Voltage stability metrics using before optimized wind values

Bus	Pre-Fault (V)	Min (V) After Fault	Max (V) After Fault	Final (V) at 10 s	Rise Time (s)	Settling Time (s)	Steady State Error	Over-shoot (%)
501	0.99	0.00	1.54	1.10	1.15	9.99	0.11	40.00
502	0.99	0.40	1.29	1.15	1.14	9.80	0.16	12.20
503	0.99	0.50	1.30	1.13	1.13	9.75	0.14	15.04
504	1.04	0.15	1.51	1.12	1.15	9.85	0.09	34.82
505	1.02	0.25	1.43	1.10	1.17	9.95	0.10	30.00
506	1.01	0.30	1.38	1.08	1.17	9.45	0.09	27.78
507	1.01	0.30	1.47	1.10	1.18	9.35	0.11	33.64

Table 3.9: Voltage stability metrics using after optimized wind values

Bus	Pre-Fault (V)	Min (V) After Fault	Max (V) After Fault	Final (V) at 10 s	Rise Time (s)	Settling Time (s)	Steady State Error	Over-shoot (%)
501	0.99	0.01	1.10	0.99	1.10	3.92	0.007	11.11
502	0.99	0.50	1.08	0.99	1.09	4.01	0.003	9.09
503	0.99	0.55	1.05	1.00	1.09	2.72	0.002	5.00
504	1.04	0.21	1.14	1.04	1.10	3.94	0.006	9.62
505	1.02	0.39	1.10	1.02	1.08	3.97	0.004	7.84
506	1.01	0.38	1.10	1.01	1.10	3.92	0.004	8.91
507	1.01	0.35	1.09	1.01	1.10	3.95	0.004	7.92

3.5.1.8 Time-Domain Waveforms

Figures 3.6(a), 3.6(b), and 3.6(c) show that the optimized controller significantly reduces peak voltages and accelerates recovery. For instance, voltage spikes at Bus 501, which previously reached around 1.5 p.u., are now limited to 1.1-1.2 p.u., with recovery to nominal levels in under 4 seconds. Post-fault stabilization is also faster and more uniform, with voltage convergence across the network achieved within 4 seconds, compared to nearly 10 seconds in the non-optimized case, which also exhibited higher overshoot.

The results from case 1, encompassing both PV-only and wind-only scenarios, validate contribution 1 by confirming that the proposed optimization approach effectively minimizes voltage deviations and improves fault-clearing performance. These outcomes also support contribution 2, demonstrating that a single optimized parameter set enables robust post-fault recovery in weak transmission networks under high renewable penetration. The optimized values (Table 3.11) will be used in case 2 to assess the cascaded

framework's performance under hybrid configurations, further validating its system-wide robustness.

Table 3.10: Parameter settings for optimization algorithms.

Algorithms	**Settings**
Generalized PSO	Population size = 50, iterations = 300, inertia weight: constant, initialization method: random initialization within parameter bounds.
Modified PSO (LHS-NDIW Enhanced)	Population size = 50, iterations = 300, inertia weight: calculated using the NDIW function Eq. 24 with $\beta = 0.1$, $\omega_{\max} = 0.9$, and $\omega_{\min} = 0.4$, initialization method: using Latin Hypercube Sampling (LHS).

3.5.1.9 Convergence Behavior of the Optimization Framework

Table 3.10 summarizes the parameter configurations adopted for the two optimization algorithms investigated in this study. To ensure a fair and unbiased comparison, both the generalized PSO and the proposed Modified PSO were implemented using identical population size, maximum iteration count, parameter bounds, and objective function. The generalized PSO employs a constant inertia weight with random initialization, whereas the Modified PSO incorporates a NDIW strategy and LHS to enhance population diversity and balance global exploration with local exploitation.

Figure 3.7 presents the convergence characteristics of the two algorithms in terms of the $\mathscr{R}^{\Delta V\downarrow}_{t_{\text{clear}}\uparrow}$, defined in Eq. (23), where lower values correspond to improved voltage stability and fault ride-through performance. Specifically, Fig. 3.7(a) illustrates the evolution of $\mathscr{R}^{\Delta V\downarrow}_{t_{\text{clear}}\uparrow}$ with respect to iteration count, while Fig. 3.7(b) shows the normalized cumulative improvement, expressed as the relative reduction in $\mathscr{R}^{\Delta V\downarrow}_{t_{\text{clear}}\uparrow}$ with respect to the initial best objective This form of normalized convergence assessment has been widely adopted in recent PSO-based optimization studies to facilitate transparent comparison between algorithms operating under identical constraints and iteration budgets [289].

As observed in Fig. 3.7(a), the generalized PSO exhibits early stagnation and converges to a $\mathscr{R}^{\Delta V\downarrow}_{t_{\text{clear}}\uparrow}$ value slightly above 2.7. In contrast, the Modified PSO continues to improve throughout the optimization process and converges to a lower $\mathscr{R}^{\Delta V\downarrow}_{t_{\text{clear}}\uparrow}$ value of ap-

proximately 2.1 within the same iteration budget. This behaviour is further corroborated by Fig. 3.7(b), where the Modified PSO achieves an overall cumulative improvement of approximately 25%, compared to about 5% for the generalized PSO.

The improved convergence performance of the Modified PSO can be attributed to the enhanced initial population diversity provided by LHS and the adaptive exploration–exploitation balance introduced by the NDIW mechanism. The consistent reduction in $\mathscr{R}^{\Delta V\downarrow}_{t_{\text{clear}}\uparrow}$ across iterations confirms the robustness and efficiency of the proposed optimization framework in minimizing time-weighted voltage deviations and strengthening fault ride-through capability under weak-grid conditions.

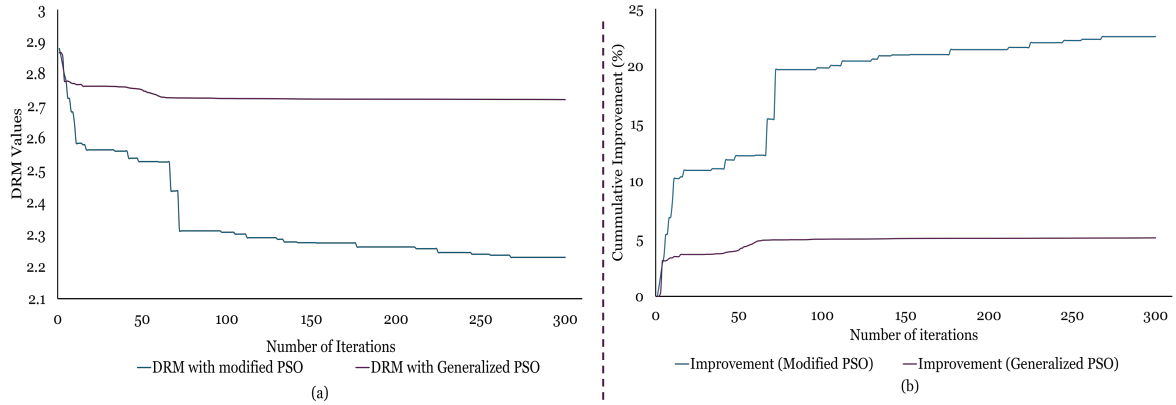


Figure 3.7: Convergence comparison of generalized and Modified PSO using $\mathscr{R}^{\Delta V\downarrow}_{t_{\text{clear}}\uparrow}$.

3.5.1.10 Dynamic Voltage Stability Assessment

In this study, system stability is evaluated from a large-disturbance dynamic voltage stability perspective, with emphasis on post-fault voltage recovery in renewable-rich weak transmission networks. Stability performance is quantified using time-domain metrics, including minimum voltage during fault, voltage overshoot, settling time, steady-state voltage deviation, and maximum allowable fault-clearing time. These indicators collectively reflect the system's ability to withstand and recover from severe disturbances while maintaining FRT compliance.

Unlike small-signal stability approaches based on linearized system models and eigenvalue analysis, such as those reported in recent control-oriented studies [290], this work focuses on nonlinear voltage stability under symmetrical and unsymmetrical fault conditions. The adopted large-disturbance, time-domain assessment is consistent with grid-code-oriented FRT requirements and is particularly suitable for weak transmission

networks dominated by inverter-based renewable resources, where severe disturbances and voltage recovery characteristics play a critical role in overall system stability.

Table 3.11: Control Variables and Optimized Parameters

Control Variable	Position (Bus)	Parameter	Optimized Value PV	Optimized Value Wind
Plant Controller	Zone 1, Zone 2, Zone 3	Proportional Gain (K_p)	0.5075, 0.5, 0.5	0.5125, 0.45, 0.4317
		Integral Gain (K_i)	3.0657, 3.0, 3.1	0.6121, 0.72, 0.75
		Voltage Compensation (R_c)	0.1, 0.08, 0.1	0.05, 0.1, 0.15
		Voltage Compensation (X_c)	0.0472, 0.1, 0.1	0.01, 0.03, 0.05
Electrical Controller	Zone 1, Zone 2, Zone 3	Proportional Gain (K_{qp})	1, 1, 1.3882	1, 1, 1.3035
		Integral Gain ($K_q i$)	5.4482, 5.5, 5.4017	5.2215, 5.25, 5.152
		Time Constant (T_p)	0.025, 0.02, 0.025	0.015, 0.02, 0.115
		Reactive Max Current Limits ($I_{q\mathrm{h1}}$)	1.2, 1.1, 1.1	1.1, 1, 0.9875
		Reactive Min Current Limits ($I_{q\mathrm{l1}}$)	-1.2, -1.2, -1.2	-1.15, -1, -0.9875
Generator Controller	Zone 1, Zone 2, Zone 3	Overvoltage Gain (K_{hv})	0.65, 0.65, 0.7	0.65, 0.65, 0.7
		Converter time constant Constant (T_{g})	0.02, 0.02, 0.02	0.015, 0.02, 0.0172
		Current Max Limits ($I_{q\mathrm{rmax}}$)	0.9, 0.7786, 1.0	1.15, 1.2, 0.9574
		Current Min Limits ($I_{q\mathrm{rmin}}$)	-0.8, -0.8012, -1	-1.1, -1.2, -0.9987

3.5.2 Case Study 2: Hybrid Renewable Energy Configurations

This case study assesses the proposed optimization framework under hybrid conditions using the Simplified Australian 14-Generator Model. The total capacity remains 2325 MW, distributed as 60% from one technology (battery, PV, or wind) and 20% from each of the other two, forming three scenarios (Table 3.5). Using the optimized controller values from Case 1 (Table 3.11), the study evaluates post-fault voltage recovery and whether fault-clearing times exceed AEMC's 250 ms guideline (Table 3.12), confirming the framework's robustness in diverse renewable mixes.

3.5.2.1 Spatial and Technological Coordination of Renewable Resources

To investigate coordinated operation of heterogeneous renewable technologies, PV, wind, and BESS units are strategically distributed across multiple buses and zones of the

transmission network, as illustrated in Figure 3.4. This spatial deployment reflects practical REZs integration, where different technologies contribute to system support from geographically distinct locations.

In addition, hybrid renewable configurations with predefined power-sharing ratios are explicitly considered, as summarized in Table 3.5. For each scenario, a dominant technology supplies 60% of the total renewable capacity, while the remaining 40% is shared equally between supporting technologies. This configuration enables systematic assessment of coordinated voltage regulation and fault ride-through performance under varying technology dominance.

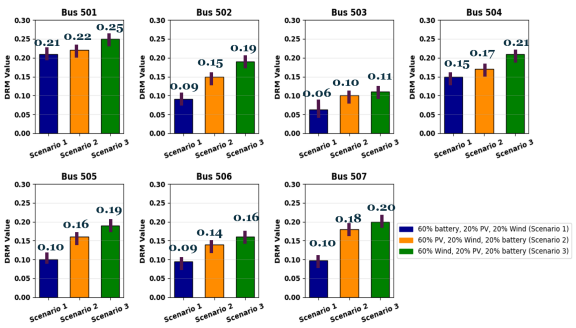
All renewable units operate under a common cascaded control structure and are tuned simultaneously using a unified system-level objective function. This approach ensures implicit coordination among PV, wind, and BESS resources, resulting in coherent dynamic behaviour across the network without relying on explicit communication-based coordination mechanisms. Unlike explicit coordination strategies that employ supervisory or communication-based control for PV-wind interaction, as reported in [291], the proposed framework emphasizes scalable, grid-code-oriented coordination suitable for renewable-rich weak transmission networks.

Table 3.12: Breakdown of Fault Clearing Times by Voltage Levels

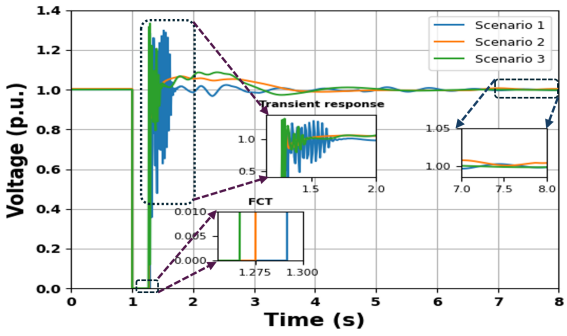
Voltage Level at Fault Location (kV)	**Fastest t_{clear}(ms)**	**Backup Protection (ms)**	**Maximum Allowable t_{clear}(ms)**
400kV and above	80	100	175
250kV to less than 400kV	100	120	250
More than 100kV but less than 250kV	120	220	430
100kV and below	As necessary	As necessary	As necessary

3.5.2.2 DRM ($\mathscr{R}^{\Delta V\downarrow}_{t_{\text{clear}}\uparrow}$) Analysis

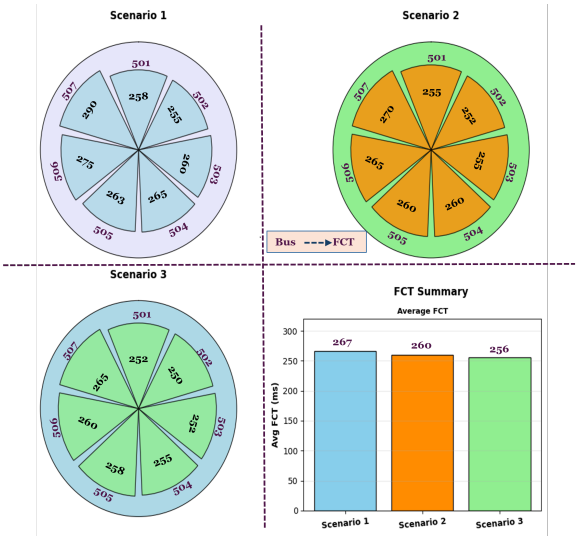
Figure 3.8(a) illustrates the $\mathscr{R}^{\Delta V\downarrow}_{t_{\text{clear}}\uparrow}$ across Buses 501-507 for all three hybrid scenarios. In Scenario 1 (60% BESS), the system shows the lowest $\mathscr{R}^{\Delta V\downarrow}_{t_{\text{clear}}\uparrow}$ values, particularly at Buses 505 and 506 (around 0.09-0.10), indicating strong voltage stability. Scenario 2 (60% PV) exhibits slightly higher $\mathscr{R}^{\Delta V\downarrow}_{t_{\text{clear}}\uparrow}$ at a few buses, such as 501 and 507, though all values remain under 0.25, confirming reliable FRT. In Scenario 3 (60% Wind), most $\mathscr{R}^{\Delta V\downarrow}_{t_{\text{clear}}\uparrow}$ values stay below 0.20, with slight increases at Bus 501 and 504 (up to 0.25), reflecting good resilience. Overall, all buses maintain $\mathscr{R}^{\Delta V\downarrow}_{t_{\text{clear}}\uparrow}$ below 0.26, validating the controller's effectiveness in limiting prolonged voltage deviations in diverse hybrid configurations.



((a)) DRM values comparison across scenarios ios



((b)) Voltage profile comparison across scenar-



((c)) Comparative radial visualization of FCT

Figure 3.8: Performance comparison under different conditions in hybrid scenario.

3.5.2.3 Voltage Stability and FCT Analysis

Figure 3.8(c) presents the FCT across buses for the three hybrid scenarios. Scenario 1 (60% BESS) shows the highest average FCT at 267 ms, followed by Scenario 2 at 260 ms and Scenario 3 at 256 ms. In all cases, the average bus-level FCT exceeds 250 ms, aligning with AEMC standards [155]. Additionally, voltage waveforms in Figure 3.8(b) reveal consistent post-fault recovery across scenarios, with voltages stabilizing within 3-4 seconds. Although Scenario 3 (wind-dominant) experiences slightly greater voltage overshoot and oscillation, all scenarios successfully maintain stability, even under extended fault durations exceeding 250 ms. These findings verify that the optimized controller parameters from Case 1 remain effective and robust under hybrid configurations.

Across all hybrid scenarios, the optimized cascaded control framework sustains stable

post-fault recovery even under extended fault-clearing durations exceeding 250 ms, demonstrating full FRT compliance and reinforcing the framework's robustness for renewable-rich weak grids.

3.5.2.4 Extended Fault Duration Comparison in Scenario 2

To further illustrate the robustness of the proposed cascaded control framework, this subsection compares the system's performance in Scenario 2 (60% PV, 20% Wind, 20% BESS) under two distinct FCT: a shorter 60 ms FCT before optimization and an extended 270 ms FCT after optimization. Figures 3.10(a)-3.10(b) show representative voltage waveforms at key buses, while Tables 3.13 and 3.14 detail the corresponding voltage stability metrics. The optimized cascaded control framework achieves fault-clearing durations up to 270 ms for 250-400 kV networks, aligning the 250 ms maximum allowable limit defined by the AEMC grid-code standards. This confirms compliance with national FRT performance requirements.

3.5.2.5 Unsymmetrical Fault Response and DC-Link Dynamics

Unsymmetrical fault scenarios, including single line-to-ground (LG), line-to-line (LL), and double line-to-ground (LLG) faults, are simulated in PSSE to evaluate system-level voltage recovery and fault ride-through (FRT) performance under unbalanced conditions. The analysis focuses on nonlinear time-domain voltage behaviour rather than detailed sequence-domain current control.

The observed DC-link voltage dynamics are consistent with the established relationship between AC-side voltage magnitude and DC-link voltage in VSI-based systems [287]. During unsymmetrical faults, voltage unbalance and reduced effective AC RMS voltage lead to transient DC-link deviations, which are captured in the simulations. Although sequence components are not explicitly modelled, this approach provides relevant insight into large-disturbance voltage stability and post-fault recovery characteristics in renewable-dominated weak transmission networks.

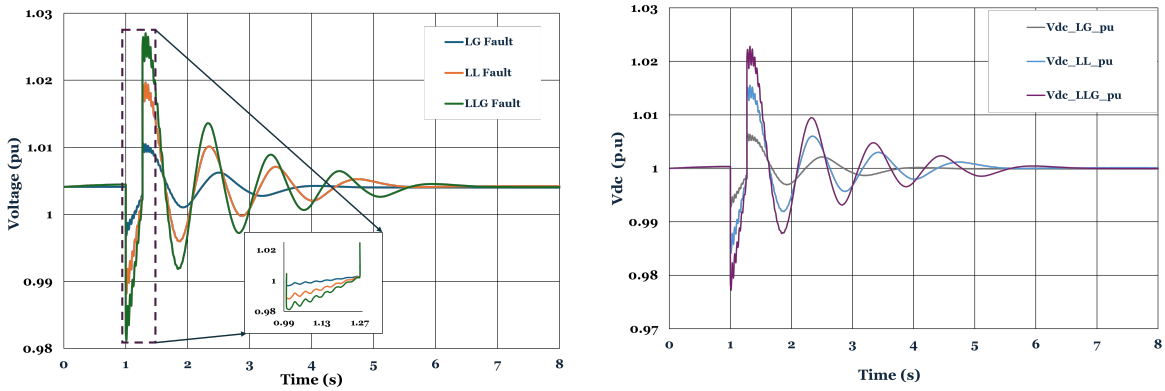
3.5.2.6 Analysis Under Unsymmetrical Fault Conditions

To further validate the effectiveness of the proposed cascaded control and optimization framework, additional dynamic simulations were conducted under three unsymmetrical fault conditions: single line-to-ground (LG), line-to-line (LL), and double line-to-ground (LLG). The corresponding AC voltage responses, shown in Figure 3.9(a), demonstrate

that the proposed control system effectively maintains voltage stability and ensures smooth post-fault recovery across all cases. Although the LLG fault presents the most severe disturbance, voltage deviations remain within acceptable limits, and the system returns to steady-state within approximately 3–4 seconds after fault clearance.

In addition to the AC responses, the corresponding DC-link voltage (V_{dc}) was analyzed to verify the converter's internal voltage stability during these unsymmetrical fault events. Using the analytical relation expressed in equation 3.20, V_{dc} was derived from the measured AC line-to-line voltage, and its transient behavior is illustrated in Figure 3.9(b). The computed V_{dc} values for LG, LL, and LLG faults remained confined within the permissible 0.9–1.1 p.u. range, confirming effective DC-link regulation and validating that the converter sustained stable energy exchange and modulation control even under transient voltage unbalance.

These results confirm that the proposed framework provides robust FRT capability and reliable performance under diverse fault scenarios in weak transmission networks.



((a)) AC voltage responses under unsymmetrical fault conditions.

((b)) DC-link voltage responses under unsymmetrical fault conditions.

Figure 3.9: Voltage and DC-link responses under unsymmetrical fault conditions. (a) AC bus voltage profiles; (b) corresponding DC-link voltage variations.

3.5.2.7 Voltage Stability and Time-Domain Observations

As shown in Table 3.13, the pre-optimized system experiences substantial voltage overshoots (over 50% at Bus 501 and Bus 504) and severe voltage dips during a 60 ms fault. In contrast, the optimized system (Table 3.14), despite a longer 270 ms fault, limits overshoot to 48.48% (Bus 501), significantly improves settling time (3.5-3.8 s compared to 9.99 s), and notably reduces steady-state errors at all buses.

Table 3.13: Voltage stability metrics using before optimized values in hybrid scenario

Bus	Pre-Fault (V)	Min (V) After Fault	Max (V) After Fault	Final (V) at 10 s	Rise Time (s)	Settling Time (s)	Steady State Error	Over-shoot (%)
501	0.99	0.40	1.69	1.11	1.10	9.95	0.12	52.25
502	0.99	0.57	1.45	1.12	1.09	9.75	0.13	29.46
503	0.99	0.63	1.37	1.11	1.07	9.45	0.16	23.42
504	1.03	0.24	1.72	1.10	1.06	9.85	0.07	56.36
505	1.02	0.45	1.66	1.11	1.08	9.65	0.09	49.55
506	1.01	0.42	1.64	1.13	1.09	9.55	0.12	45.13
507	1.01	0.00	1.72	1.15	1.10	9.99	0.14	49.57

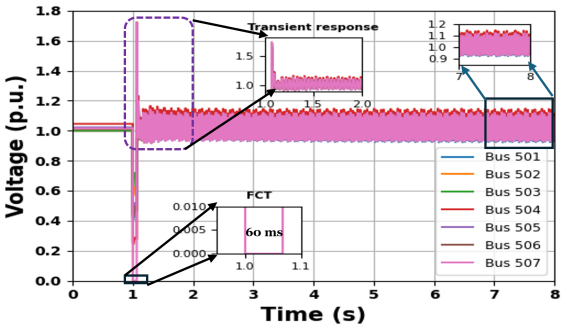
Figures 3.10(a) and 3.10(b) illustrate these improvements. Before optimization, transient peaks exceeded 1.65 p.u. at buses 501 (Zone 1), 504, 505 and 507 (Zone 4). After optimisation, voltages remain slightly above 0 p.u. during faults and recover to nominal within 3-4 seconds, exemplified by Bus 507 peaking below 1.5 p.u. with a smoother recovery. These results validate the effectiveness of the optimised controller in ensuring dynamic voltage stability under extended fault conditions.

Table 3.14: Voltage stability metrics using after optimized values in hybrid scenario

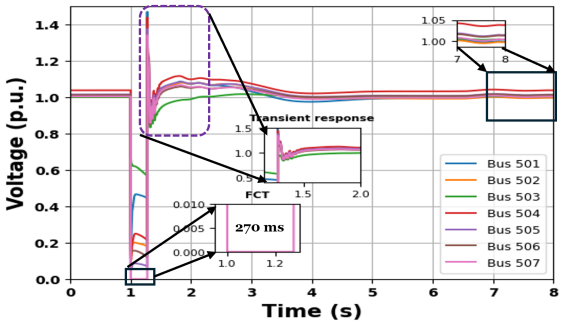
Bus	Pre-Fault (V)	Min (V) After Fault	Max (V) After Fault	Final (V) at 10 s	Rise Time (s)	Settling Time (s)	Steady State Error	Over-shoot (%)
501	0.99	0.21	1.47	0.99	1.271	3.83	0.005	48.48
502	0.99	0.13	1.36	0.99	1.271	3.58	0.005	37.37
503	0.99	0.57	1.20	1.00	1.272	2.36	0.003	20.00
504	1.03	0.11	1.44	1.04	1.275	3.73	0.008	38.46
505	1.02	0.05	1.38	1.02	1.272	3.51	0.008	35.29
506	1.01	0.12	1.27	1.01	1.270	3.45	0.007	25.74
507	1.01	0.01	1.34	1.00	1.272	3.67	0.008	34.00

The hybrid scenario further demonstrates that the cascaded control framework, with optimized parameters, consistently achieves $\mathscr{R}^{\Delta V\downarrow}_{t_{\text{clear}}\uparrow} < 0.25$ and fault-clearing times above 250 ms across all renewable cases, despite fault durations 4.5 times longer (270 ms) than in the pre-optimized system (60 ms), underscoring its robustness in renewable scenario as shown in Figure 3.10(c).

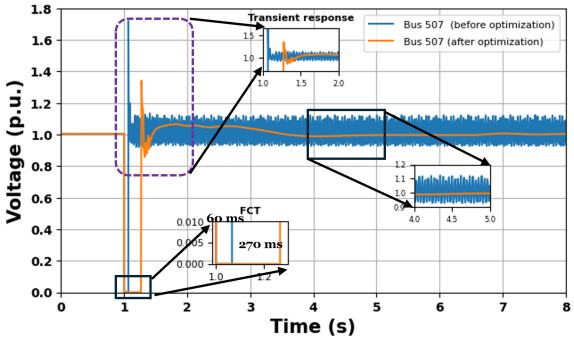
In addition to transient and steady-state voltage performance, the harmonic content of the system voltage was evaluated to quantify the overall improvement in power



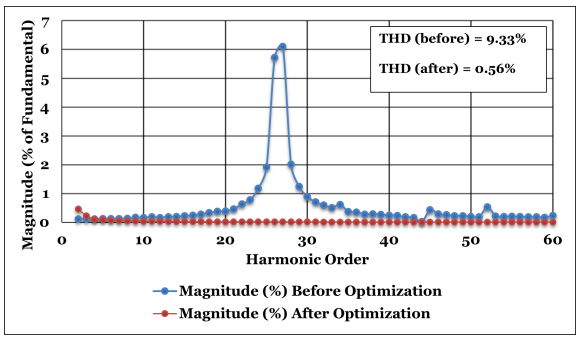
((a)) Voltage profile before optimization



((b)) Voltage profile after optimization



((c)) Voltage profile at Bus 507 (before vs. after)



((d)) Harmonic spectrum comparison

Figure 3.10: Voltage and harmonic performance comparison under different conditions in Case Study 2, Scenario 2. (a) Voltage profile before optimization; (b) Voltage profile after optimization; (c) Voltage profile at Bus 507 (before vs. after); (d) Harmonic spectrum comparison.

quality achieved through the proposed optimisation strategy. Figure 3.10(d) presents the harmonic spectra of the voltage waveform at Bus 507 before and after optimisation, corresponding to the three-phase bus fault applied in the hybrid scenario. Prior to optimisation, the system exhibited a Total Harmonic Distortion (THD) of 9.33%, with dominant harmonic components concentrated around the 25^{th}-30^{th} orders, primarily attributed to switching dynamics and control interactions between inverter modules. After applying the optimised cascaded control framework, the THD decreased drastically to 0.56%, indicating a 94% reduction in overall distortion. This substantial improvement reflects the enhanced harmonic suppression capability of the optimised controller, ensuring smoother inverter operation and reduced spectral pollution in the grid voltage. Consequently, the optimised configuration not only enhances dynamic voltage stability under extended fault conditions but also significantly improves power quality compliance, as the obtained THD level (<5%) satisfies the harmonic distortion limits prescribed in

the IEEE 519 standard [280].

The results obtained from case 2 validate contribution 3, confirming the framework's capability to maintain voltage stability and notably extend FRTt, thereby ensuring robust recovery from severe disturbances.

3.6 Conclusion and future work

This chapter presented a novel cascaded control and optimization framework designed to enhance voltage stability and FRT capability in weak transmission networks with high renewable energy penetration. Unlike conventional techniques that primarily emphasize reactive power compensation, the proposed methodology integrates an enhanced PSO routine with a $\mathscr{R}^{\Delta V\downarrow}_{t_{\text{clear}}\uparrow}$ to simultaneously minimize voltage deviations and extend permissible fault-clearing durations. Through coordinated tuning of plant-level, electrical-level, and generator/converter-level controllers, the framework ensures coherent system behavior and maintains voltage profiles within acceptable limits under both symmetrical and unsymmetrical fault conditions.

Extensive time-domain simulations conducted on a simplified Australian 14-Generator Test System demonstrated the robustness of the proposed approach. Across single-technology scenarios (fully PV or wind) and hybrid configurations (PV-wind-BESS), the cascaded controllers effectively restored bus voltages within 3-4 s and supported fault-clearing intervals up to 270 ms without compromising system stability. These improvements confirm that the proposed optimisation-driven control design substantially strengthens the resilience, damping response, and fault tolerance of renewable-rich weak grids.

Despite these promising outcomes, one key limitation of this study is the absence of load variability modeling across buses. Future work will incorporate diverse and time-varying load profiles to further validate and refine the framework's performance under realistic operating conditions. Additionally, the next phase of research will extend the current analysis to include a detailed THD evaluation across several scenarios, enabling a more comprehensive assessment of the power-quality improvements achieved through the cascaded control architecture. Future research will also extend the present time-domain analysis to include eigenvalue-based small-signal stability assessment and detailed sequence-domain investigations under unsymmetrical faults, providing complementary insight into oscillatory stability characteristics and control interactions.

Overall, the proposed framework provides a scalable and reliable pathway for re-

inforcing renewable-dominated weak transmission networks. By ensuring compliance with AEMC grid-code standards and the IEEE 519 standard, while delivering enhanced voltage stability and FRT resilience, the approach offers a technically robust solution for the next generation of sustainable and resilient power systems.

3.7 Chapter summary

This chapter developed and validated a cascaded control parameter optimisation framework designed to improve voltage stability and fault-ride-through performance in renewable-dominated weak transmission networks. By introducing the Dynamic Resilience Metric and applying an enhanced PSO-based hierarchical optimisation across plant-level, network-level, and converter-level controllers, the proposed approach demonstrated significant improvements in transient behaviour, permissible fault-clearing times, and post-fault recovery on the Simplified 14 Generator Test System. These results confirm the effectiveness of coordinated, system-level optimisation in addressing the weak-grid challenges identified in the literature review. While this chapter focused on voltage stability and FRT enhancement, the broader resilience of weak-grid REZs also depends on robust frequency support and inverter coordination, a challenge explored in detail in Chapter 4 through the development of a severity-aware GFM-GFL BESS control framework.

CHAPTER 4

SEVERITY-AWARE GFM-GFL BESS COORDINATION

Chapter Composition

This chapter addresses Research Question 2 by developing a severity-aware coordinated BESS control framework to improve frequency stability, voltage resilience, and overall robustness in renewable-rich weak grids. Building on the gaps identified in Part 2 of the literature review, it introduces a severity index that dynamically switches BESS operation between GFL and GFM modes. Detailed inverter models are presented, followed by a parametric analysis of GFM:GFL penetration ratios to assess their effects on frequency nadir, RoCoF suppression, and voltage recovery. The chapter also compares droop and VSM strategies at representative GFM shares. Dynamic simulations demonstrate that severity-aware GFM-GFL coordination offers a scalable pathway for strengthening REZ-based weak-grid operation, complementing the optimisation framework established in Chapter 3.

4.1 Introduction

The rapid transition toward renewable-dominated power systems is transforming conventional grid dynamics [292]. The displacement of SGs with inverter-based RESs, such as solar photovoltaics and wind turbines, has resulted in declining system inertia and increased vulnerability to frequency and voltage instability, especially in weak transmission networks characterized by low short-circuit ratios (SCR), poor damping, and high

rates of change of frequency (RoCoF) [293, 294]. In this context, Battery Energy Storage Systems (BESS) have emerged as key stabilizing assets due to their rapid response capabilities and controllability [294, 295]. However, the effectiveness of BESS depends heavily on the control strategy employed at the inverter interface, particularly under low-inertia, fault-prone grid conditions [292, 293].

Two dominant control approaches are employed for grid-interfaced inverters: Grid-Following (GFL) and Grid-Forming (GFM). GFL inverters synchronize to the grid using a phase-locked loop (PLL) and inject current based on a reference, making them susceptible to instability in weak grid environments and incapable of black start operations [1, 18, 296]. GFM inverters, in contrast, regulate voltage and frequency independently, emulating synchronous machine behavior and offering advantages such as inertia provision, frequency support, and fault ride-through (FRT) [5, 149, 178]. Various GFM control strategies have been developed, including droop control [178], virtual synchronous generator (VSG), compensated generalized VSG (CGVSG), adaptive VSG (AVSG) [19], virtual oscillator control (VOC) [171], and most recently, frequency-following voltage-forming (FFL-VFM) schemes [169].

While these strategies have shown promise individually, the literature still lacks a cohesive framework for integrating and coordinating GFM and GFL inverters within a unified BESS control architecture. Previous studies have shown that significant performance gaps exist between GFM and GFL modes, particularly under fault and islanding scenarios [178, 297]. Advanced control techniques, such as fictive dq control, have been proposed to manage unbalanced load conditions in mini-grid environments using GFM-based BESS, but these approaches remain limited in scope [18]. Dynamic modelling efforts have successfully integrated GFM inverter behaviour into industry-standard tools like Power System Simulation for Engineering (PSSE) and MODES, yet coordination with GFL counterparts has not been systematically addressed [149]. Several works have carried out comparative analyses of GFM strategies, such as droop control, VSG, CGVSG, and AVSG based on time-domain and impedance-domain metrics; however, these studies typically examine each strategy in isolation rather than within mixed GFM-GFL deployments [19]. Moreover, while the influence of inverter penetration levels on frequency response and damping has been analytically explored [178], and the impact of BESS control on frequency containment under high renewable penetration has been evaluated using large-scale simulation frameworks [5], coordinated control between inverter types and the effect of varying GFM:GFL ratios have remained largely unexamined. Additional work has replicated real-world blackout events to validate the FRT benefits of GFM

inverters, yet still did not consider multi-inverter coordination strategies [174].

Recent research has increasingly focused on addressing the remaining gaps in coordinated inverter control. Comparative benchmarks of GFM and GFL BESS under real-world load-shedding events have revealed notable differences in RoCoF and frequency nadir across multiple operational modes [8, 298]. Comprehensive taxonomies have also been developed to classify existing GFM control strategies while outlining future research directions, including hybrid angle-control schemes and Multiple-Input Multiple-Output (MIMO)-based architectures [171]. To improve frequency stability assessments under realistic system conditions, new stability indices have been proposed that incorporate stochastic variations in renewable generation and load demand [188]. Advances in short-circuit modeling of inverter-interfaced generation stations (IIGS) under low short-circuit ratio (SCR) conditions have further introduced decoupled sequence-control approaches, improving both convergence and modeling accuracy [203]. Control-design developments have explored the decoupling of frequency-following and voltage-forming behaviors in inverters, leading to hybrid architectures particularly well suited for constant-power renewable sources [169, 299]. Moreover, coordinated control frameworks based on leader-follower consensus mechanisms have demonstrated enhanced multi-inverter operation, enabling improved frequency regulation, reactive-power sharing, and resilience to communication disturbances in microgrids [172].

Despite these advances, several important research challenges remain unaddressed. A key limitation is the absence of a unified control framework that dynamically coordinates GFM and GFL inverter modes within BESS, particularly during fault and disturbance scenarios in weak grids, where most existing studies continue to treat these control strategies in isolation [1, 19, 172, 190]. Additionally, there is a noticeable lack of systematic investigations into how varying the sharing of GFM and GFL inverters, affects critical stability indicators like RoCoF, frequency nadir, and FRT performance in low-inertia systems [8, 174, 300, 301]. Furthermore, although a range of GFM strategies have been proposed in the literature, comparative evaluations under consistent test conditions remain scarce. In particular, the relative strengths and weaknesses of droop control and VSG approaches are rarely assessed side by side within standardised weak grid environments, making it difficult to draw meaningful conclusions about their suitability for next-generation inverter-based systems [19].

Building on these observations, this work addresses three major gaps. First, existing studies lack a coordinated GFM-GFL architecture capable of adapting contributions based on real-time disturbance severity. Second, no prior work offers an optimisation-

based analysis of GFM:GFL penetration using unified frequency and voltage metrics. Third, fair comparisons of GFM controls, such as droop and VSM, under identical weak-grid conditions remain absent. This study fills these gaps by proposing a severity-aware blended GFM-GFL coordination scheme, an optimisation-driven penetration analysis, and a unified evaluation of droop and VSM controls, including black-start capability.

Table 4.1 further highlights these gaps, indicating that prior studies rarely integrate GFM-GFL coordination, penetration-level assessment, and weak-grid validation within a unified analytical framework. The present work is the first to provide such a comprehensive integration.

Table 4.1: Comparison of studies on GFM-GFL coordination and weak-grid, renewable-dominated system performance.

Ref	Severity-Aware GFM–GFL Coordination	Comparative Evaluation of GFM Control Strategies	Parametric Analysis of GFM:GFL Ratios	Assessment under Weak Grid Conditions	Renewable-Dominated System Context
[1]	✗	✗	✗	✓	✓
[18]	✗	✗	✗	✓	✓
[5]	✗	✗	✓	✓	✓
[19]	✗	✓	✗	✓	✓
[169]	✗	✗	✓	✓	✓
[8]	✗	✗	✗	✓	✓
[172]	✗	✗	✗	✓	✓
This Work	✓	✓	✓	✓	✓

The workflow is summarized in the overall methodology framework shown in Figure 4.1. The main contributions of this work are as follows:

- **Severity-Aware BESS Control Framework:** A novel severity-aware BESS coordination framework is proposed in which GFL and GFM modes operate cooperatively, guided by a severity index and validated against grid-code fault-clearing times. Unlike conventional approaches that treat the two modes as independent or mutually exclusive, the framework enables GFL to deliver efficient current-following during mild disturbances while GFM progressively assumes voltage-forming dominance under prolonged or severe faults. This adaptive interaction

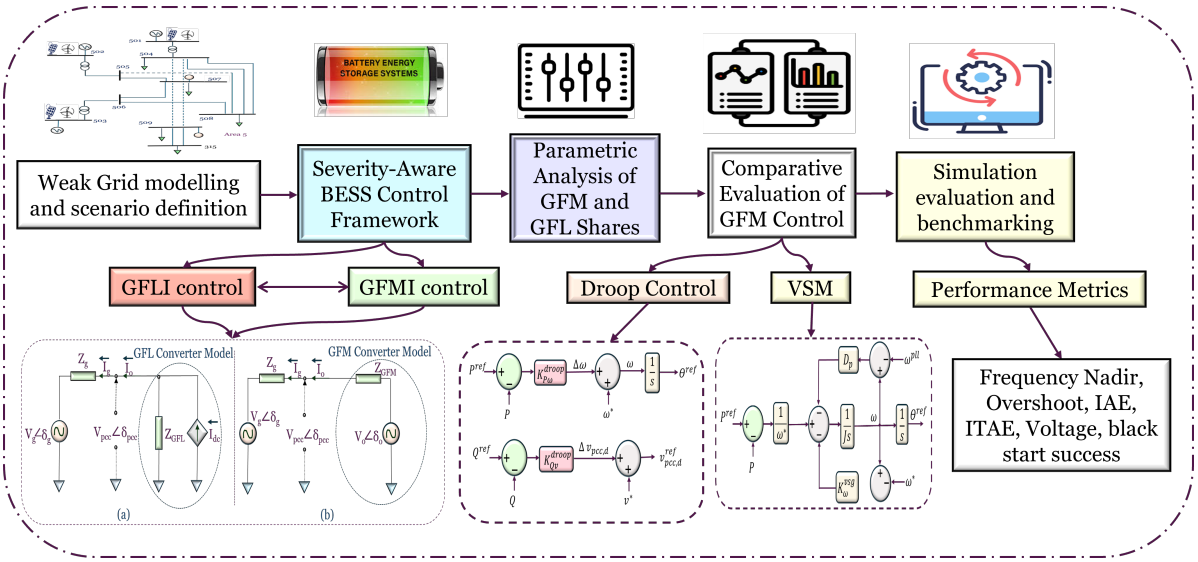


Figure 4.1: Overall proposed methodology framework

improves resilience in weak grids while preserving efficient operation under normal conditions.

- **Parametric Analysis of GFM and GFL Shares:** Building on the coordination framework in Contribution 1, a systematic parametric analysis of GFM-GFL shares is conducted using normalised frequency metrics and voltage stability margins within a unified composite stability measure. Unlike prior studies that assess inverter penetration only qualitatively or under isolated scenarios, this analysis provides a structured, quantitative evaluation of how varying GFM:GFL ratios affect weak-grid dynamics. Results show consistent monotonic gains in frequency and voltage resilience as GFM share increases, offering evidence-based insight into the stabilising role of GFM in weak transmission networks.

- **Comparative Evaluation of droop and VSM Control:** Extending the previous parametric analysis, a unified comparison of two GFM control strategies, droop and VSM, is performed at representative GFM penetration levels of 50% and 75%. Unlike earlier studies conducted under inconsistent network assumptions, this evaluation is carried out within a coordinated GFM-GFL framework, ensuring fair and meaningful benchmarking. The results highlight clear behavioural differences: droop provides faster primary response, while VSM offers stronger damping and black-start capability, giving practical guidance on their suitability for future high-IBR grids.

Collectively, these contributions advance robust BESS control strategies for inverter-dominated renewable-rich systems, providing a foundation for resilient operation in weak grids. The chapter is organised as follows: Section 4.2 outlines the proposed methodology, Section 4.3 describes the network and cases, Section 4.4 discusses results, and Section 4.5 concludes with key findings and future work.

4.2 Proposed Methodology

This section outlines the proposed BESS control methodology, comprising: (i) a severity-aware GFL-GFM blending scheme, (ii) multi-objective optimisation of GFM:GFL penetration, and (iii) comparative assessment of droop and VSM at mid-level penetration. The overall framework appears in Figure 4.1.

4.2.1 Severity-Aware Coordination Framework

The first contribution introduces a severity-aware BESS control framework in which GFM and GFL operate in *coordination* during grid disturbances, rather than in an exclusive switching manner. The aim is to exploit the current-following efficiency of GFL under mild conditions while simultaneously enabling voltage-forming robustness of GFM during severe faults.

4.2.1.1 Severity Index

A dimensionless severity index $S(t)$ is defined to quantify the disturbance level, normalised against grid code thresholds for frequency deviation, RoCoF, and voltage deviation:

$$S(t) = \alpha \frac{|f(t) - f_{\text{ref}}|}{\Delta f_{\max}} + \beta \frac{\left|\frac{df}{dt}\right|}{\text{RoCoF}_{\max}} + \gamma \frac{|V_{\text{ref}} - V(t)|}{\Delta V_{\max}} \tag{4.1}$$

where $\Delta f_{\max}$, $\text{RoCoF}_{\max}$, and $\Delta V_{\max}$ denote the allowable limits for frequency deviation, RoCoF, and voltage deviation. The severity index applies grid-code normalisation to keep all metrics dimensionless and comparable, enabling equal weights ($\alpha = \beta = \gamma = 1$) as a neutral baseline. Sensitivity tests ($\neg \pm 50\%$) show only minor variation (≈3.4–3.6; Figure 4.2), indicating that the GFM–GFL coordination remains robust to weighting choices. Equal weighting is selected as a neutral, unbiased baseline, as all three indicators are normalised with respect to their grid-code limits, ensuring comparable scales. This avoids preferential emphasis on any single metric and provides a generalised formulation

that remains applicable across different power system conditions, where the relative importance of frequency, RoCoF, and voltage may vary.

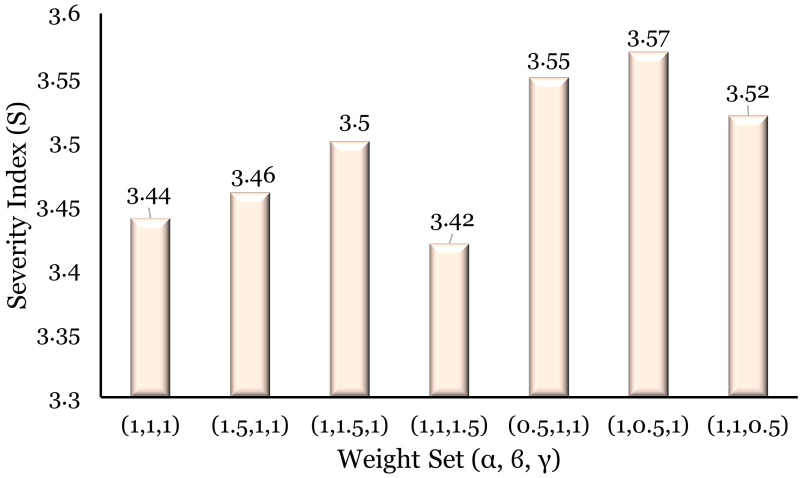


Figure 4.2: Sensitivity of S to variations in the weighting coefficients α, β, and γ

4.2.1.2 Fault Duration and Grid-Code Validation

To validate the coordination mechanism, disturbances are modelled at distribution-level buses (20 kV). According to the National Electricity Rules (NER) [302], systems at 100 kV and below follow "as necessary" clearing guidelines. In this study, two representative cases are applied, namely a fault duration of $t_{\text{fault}}^{(501)} = 60$ ms at bus 501 (20 kV) and $t_{\text{fault}}^{(502)} = 100$ ms at bus 502 (20 kV). The first represents a disturbance cleared within the fast-protection time frame, while the second represents an extended disturbance within the backup protection range. This setup aligns with NER practices while enabling validation of the proposed control.

4.2.1.3 Coordinated Mode Transition Logic

Instead of exclusive mode switching, a *blended control law* governs inverter operation during disturbances. The coordinated reference is expressed as:

$$u^*(t) = (1-\lambda)\,u^*_{\text{GFL}}(t) + \lambda\,u^*_{\text{GFM}}(t); \lambda(t) = \min\left(1, \frac{S(t)}{S_{\text{th,high}}} \cdot \frac{t_{\text{fault}}}{t_{\text{clear,max}}}\right) \tag{4.2}$$

where $x(t)$ is the hybrid blending factor in $[0,1]$ that sets the relative GFL-GFM contribution. It increases with the severity index $S(t)$ and the ratio $t_{\text{fault}}/t_{\text{clear,max}}$. Thus, $x = 0$ gives pure GFL, $x = 1$ gives pure GFM, and intermediate values yield a smooth

hybrid response. For short disturbances (≈60 ms), $x \approx 0.5$ indicates balanced coordination, while more severe faults (≈100 ms) drive $x \to 1$, shifting toward dominant GFM support.

4.2.1.4 Control Laws

The coordinated framework employs complementary GFL and GFM control laws that operate simultaneously and transition smoothly based on disturbance severity. In GFL mode, the inverter behaves as a current-controlled device, tracking dq-axis current references derived from the active and reactive power setpoints:

$$i^*_{dq}(t) = \frac{P^*}{V_{dq}(t)} + j\,\frac{Q^*}{V_{dq}(t)}, \tag{4.3}$$

where P^*, Q^* are the commanded active and reactive powers and $V_{dq}(t)$ is the measured dq-frame voltage. This mode provides fast current-limited response and effective damping during mild disturbances where PLL synchronisation remains reliable.

In contrast, the GFM mode regulates voltage and frequency directly through droop control:

$$\begin{aligned} \dot{\delta}(t) &= \omega(t) = \omega_{\text{ref}} - K_f\big(P(t) - P^*\big), \\ V^*_{dq}(t) &= V_{\text{ref}} - K_v\big(Q(t) - Q^*\big), \end{aligned} \tag{4.4}$$

where $P(t)$ and $Q(t)$ are instantaneous powers, $\delta(t)$ is the phase angle with angular frequency $\omega(t)$, ω_{ref} and V_{ref} are nominal settings, and K_f, K_v are the active- and reactive-power droop gains. This mode provides voltage formation, inertia-like support, and improved robustness under severe faults.

Blending this behaviour through the severity-dependent factor $\lambda(t)$ allows fast GFL response during mild events and a smooth shift to GFM dominance as severity increases, ensuring stable and adaptive performance across varying disturbances.

4.2.2 Multi-Objective Optimization of GFM:GFL Penetration Ratios

Building upon the coordination framework, the second contribution evaluates the dynamic impact of varying GFM:GFL shares. A total generation of 330 MW is maintained, with penetration ratios ranging from fully GFL ($x = 0$) to fully GFM ($x = 1$) across bus 502, as shown in Table 4.2.

Table 4.2: Allocation of GFM and GFL Power Across Scenarios

GFM Share (x)	**GFM (MW)**	**GFL (MW)**
0.00	0	330
0.25	82.5	247.5
0.50	165	165
0.75	247.5	82.5
1.00	330	0

4.2.2.1 Stability Metrics

To assess dynamic performance under different GFM:GFL ratios, both frequency- and voltage-domain indicators are used. Frequency deviations are measured using the integral of absolute error (IAE) and the integral of time-weighted absolute error (ITAE), defined as:

$$\text{IAE} = \int_0^T \left| f(t) - f_{\text{ref}} \right| dt, \text{ITAE} = \int_0^T t \cdot \left| f(t) - f_{\text{ref}} \right| dt; \tag{4.5}$$

In the voltage domain, performance is assessed through the minimum and maximum values of the voltage trajectory, together with their deviation, expressed as:

$$V_{\min} = \min_{t \in [0,T]} V(t), \quad V_{\text{over}} = \max_{t \in [0,T]} V(t), \quad \Delta V = V_{\text{over}} - V_{\min}. \tag{4.6}$$

where $V_{\min}$ and V_{over} are the minimum and maximum voltages, with ΔV their deviation, capturing dips, overshoot, and recovery for the composite stability index.

4.2.2.2 Composite Stability Index

The optimization problem is formulated to determine the optimal GFM share $x \in [0,1]$ that maximises overall stability performance. The composite stability index consolidates frequency and voltage domain metrics as follows:

$$\begin{aligned} \text{Maximise} \quad J(x) = w_f \cdot \Big(& \alpha_1 m_{f_{\text{nadir}}} + \alpha_2 m_{f_{\text{peak}}} + \alpha_3 m_{\text{IAE}} + \alpha_4 m_{\text{ITAE}} + \alpha_5 m_{T_s} \Big) \\ & + w_v \cdot \Big(\beta_1 m_{V_{\min}} + \beta_2 m_{V_{\text{over}}} + \beta_3 m_{\Delta V} \Big), \end{aligned} \tag{4.7}$$

$$m_\cdot = \frac{\text{Margin Value}}{\text{Threshold}}, \qquad m_\cdot \in [0,1]. \tag{4.8}$$

where m is the normalised stability margin for each metric relative to its limit. The weights w_f and w_v set the relative importance of frequency and voltage objectives in the optimisation.

Subject to:

$$f_{\min} \le f(t) \le f_{\max}, \quad \left|\frac{df}{dt}\right| \le \mathrm{RoCoF}_{\max}, V_{\min} \le V(t) \le V_{\max}, \quad 0 \le x \le 1, \tag{4.9}$$

where $f_{\min}$ and $f_{\max}$ denote allowable frequency bounds, $\mathrm{RoCoF}_{\max}$ is the maximum permissible rate-of-change of frequency, and $V_{\min}, V_{\max}$ are the voltage limits as per grid code requirements.

4.2.2.3 Optimization Algorithm

The GFM:GFL penetration ratio is optimised using Particle Swarm Optimisation (PSO), where each particle represents a candidate share $x \in [0,1]$ and the objective is to maximise the composite stability index $J(x)$. The particle update rule is:

$$\Delta x_i^{k+1} = \omega \Delta x_i^k + c_1 r_1 \left(x_{i,\text{best}} - x_i^k\right) + c_2 r_2 \left(x_{\text{global}} - x_i^k\right); \quad x_i^{k+1} = x_i^k + \Delta x_i^{k+1} \tag{4.10}$$

where Δx_i is the GFM-share update, ω the inertia weight, c_1, c_2 the acceleration gains, and r_1, r_2 random terms. Here, $x_{i,\text{best}}$ and x_{global} are the particle and global best values. Iterations continue until the GFM share that maximises $J(x)$ is found.

4.2.3 Comparative Evaluation of Droop and VSM Control

Following the parametric analysis in contribution 2, this contribution compares *Droop* and *VSM* controls at 50% and 75% GFM shares, evaluating frequency-voltage performance and black-start capability. Droop and VSM serve as alternative GFM outer loops: for each GFM share x, BESS units operate either Droop or VSM, with the remainder in GFL mode; no inverter uses both controls simultaneously.

4.2.3.1 Droop Control

Droop control applies proportional P–f and Q–V laws:

$$\Delta f = -k_p \left(P - P^*\right), \qquad \Delta V = -k_q \left(Q - Q^*\right), \tag{4.11}$$

where k_p and k_q are droop coefficients. It enables simple power sharing but lacks inertia emulation, making weak grids more sensitive to frequency disturbances. This algebraic

structure enables a rapid response to disturbances, a behaviour also reported in prior studies, such as [171] and the experimental results of [174], where droop-based GFM inverters consistently exhibited the quickest frequency arrest.

4.2.3.2 VSM Control

VSM incorporates swing dynamics to emulate synchronous machine behaviour:

$$M\frac{d\omega}{dt} + D\left(\omega - \omega^*\right) = P^* - P, \tag{4.12}$$

where M is virtual inertia and D is damping. This provides an inertia-like response and enhanced damping, improving transient stability. These additional dynamic elements slow the initial response but significantly enhance oscillation attenuation and settling behaviour. This inertia damping effect is discussed in the VSM literature [171], where VSM implementations demonstrate smoother trajectories and superior transient damping compared with droop control.

4.2.3.3 Black Start Capability

In weak-grid conditions, droop control can cause frequency drift while VSM offers smoother recovery, though their effectiveness depends on system conditions [17]. Here, P and Q denote active and reactive power, respectively, and $\sigma_G(t)$ represents the generator state. This can be expressed by droop-style balance:

$$\sum_j (P_{ij} + jQ_{ij}) = (P_L + jQ_L) - (P_G + jQ_G), \tag{4.13}$$

and VSM-like cranking dynamics:

$$P_G(t) = \sigma_G(t)P_{\text{avail}} - \left(1 - \sigma_G(t)\right)P_{\text{crank}}, \qquad Q_G(t) = \sigma_G(t)Q_{\text{avail}} - \left(1 - \sigma_G(t)\right)Q_{\text{crank}}, \tag{4.14}$$

which capture system balancing and generator startup in restoration. The next section introduces the network and cases for evaluating the proposed methodology.

4.3 Network and Cases Considered

This section outlines the network setup and case studies used to demonstrate the validity of the proposed methodology.

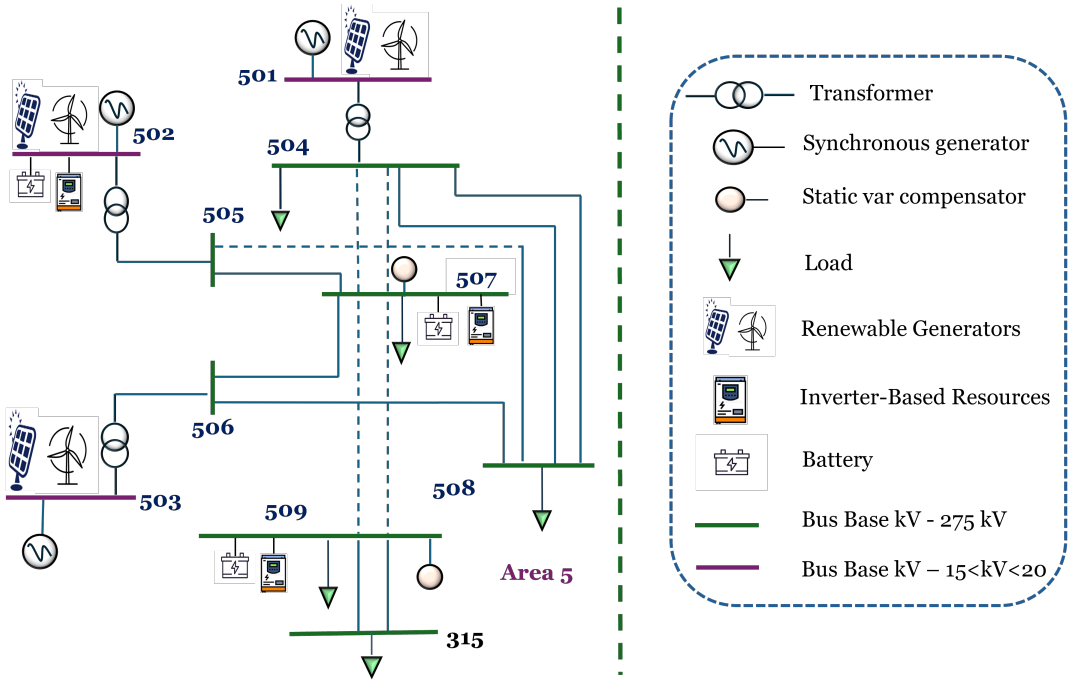


Figure 4.3: Simplified Australian power system test network (Area 5).

4.3.1 Network Considered

The test system is based on Area 5 of the simplified Australian 14-bus generator network (Figure 4.3), which has been widely used in stability studies of inverter-dominated grids. Detailed specifications are provided in [303, 304]. Area 5 represents a weak-grid environment with synchronous machines, inverter-based renewables, and interconnected loads, making it well-suited for evaluating the proposed coordinated BESS control framework. In this work, the bus hosting both GFM and GFL units represents the medium-voltage collector bus of a multi-inverter BESS plant, where several inverter blocks operate in parallel [305, 306]. In line with modern practice, some blocks are configured in GFM mode to establish local voltage and frequency, while others remain GFL for power dispatch and charging control [8, 172].

4.3.2 Cases Considered

The simulation cases correspond directly to the three methodological contributions. Contribution 1 considers four benchmarks: a baseline without IBRs, GFL-only, GFM-only, and coordinated GFM–GFL control governed by the severity index, thereby illustrating the incremental benefits of adaptive coordination. Contribution 2 extends this through a systematic parametric sweep of GFM shares $x \in \{0, 0.25, 0.5, 0.75, 1.0\}$, assessed using a

composite frequency–voltage stability index that consolidates nadir, overshoot, settling behavior, and voltage margins into a unified measure of dynamic resilience. Contribution 3 compares Droop and VSM control at representative shares of 50% and 75%, focusing not only on transient stability but also on black start capability, which provides insight into post-disturbance recovery. All simulations are conducted in Power System Simulation for Engineering (PSSE 36.2) with Python 3.12 on a 12th Generation Intel® Core™ i7-1265U Central Processing Unit (CPU) with a base clock speed of 1.80 gigahertz (GHz) and 32 gigabytes (GB) of Random Access Memory (RAM); which is appropriate for system-level assessment of transmission networks; experimental and HIL validation are left for future work. The next section discusses the corresponding results in detail.

4.4 Results and Discussion

This section validates the methodology through dynamic simulations, presenting results from coordination analysis to parametric evaluation and strategy comparison.

4.4.1 Severity-Aware GFM–GFL Coordination

The proposed severity-aware GFM–GFL coordination strategy is benchmarked against three baselines: (i) no IBRs, (ii) GFL-only operation, and (iii) GFM-only operation. Quantitative results are summarised in Table 4.3, with the corresponding dynamic responses shown in Figures 4.4-4.5.

Table 4.3: Voltage and frequency performance across four cases.

Case	Peak voltage (p.u.)	Peak voltage time (s)	Overshoot (%)	Lowest voltage (p.u.)	Lowest voltage time (s)	Average RoCoF (Hz/s)	Frequency Nadir (Hz)	Severity Index (S)
Without IBRs	1.159	5.75	14.2	0.166	5.10	2.9544	47.5071	4.77
With GFL	1.177	5.23	16.0	0.183	5.09	1.2470	48.1359	4.10
With GFM	1.061	1.46	4.4	0.197	5.10	1.0950	48.9474	3.50
Coordinated GFM & GFL	1.051	1.15	3.4	0.200	5.10	0.8081	48.9768	3.44

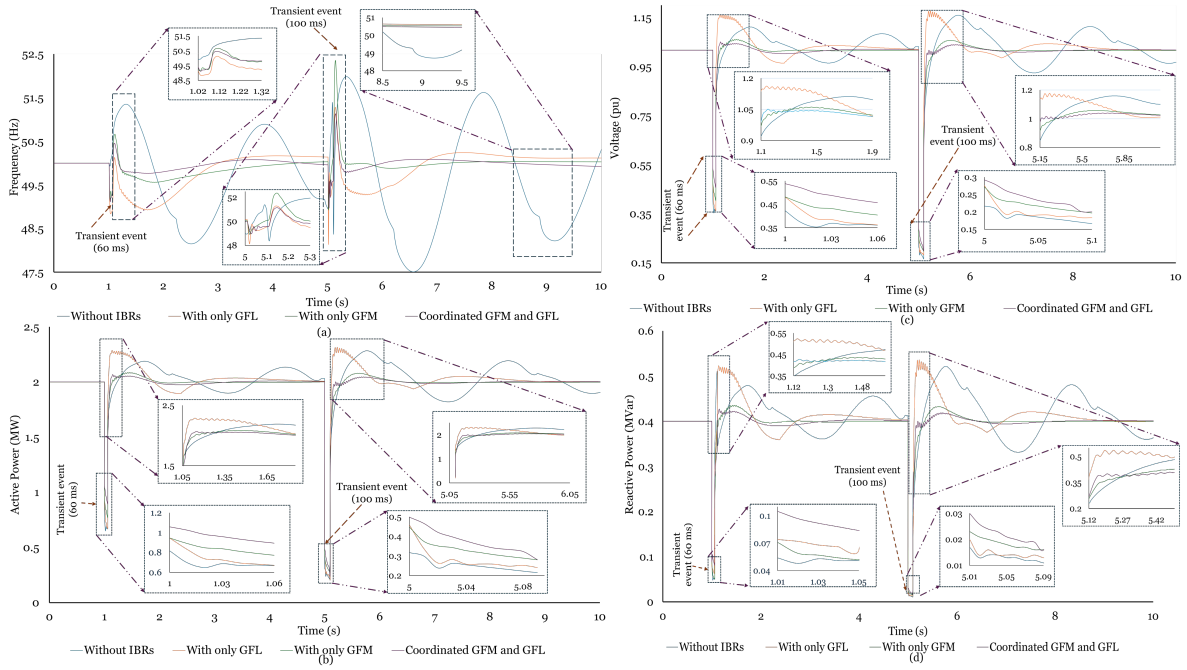


Figure 4.4: Dynamic response at Bus 509 across four cases: (a) frequency, (b) active power, (c) voltage, and (d) reactive power

Without IBRs, the system exhibits the most critical instability, with a frequency nadir of 47.5 Hz, 14.2% overshoot, RoCoF of 2.95 Hz/s, and the highest severity index ($S = 4.77$). Under GFL-only operation, the nadir improves to 48.1 Hz and RoCoF falls to 1.25 Hz/s, but overshoot increases to 16%, highlighting the limited ability of PLL-driven current control to stabilise post-fault voltage. In contrast, GFM-only operation reduces overshoot to 4.4% and raises the nadir to 48.95 Hz, yet voltage recovery is slower (minimum 0.197 p.u. at 5.1 s), indicating degraded performance under prolonged low-voltage conditions.

The coordinated GFM–GFL strategy delivers the most balanced response: overshoot is limited to 3.4%, RoCoF is reduced to 0.81 Hz/s (a 73% improvement relative to the no-IBR case), and the nadir increases to 48.98 Hz, yielding the lowest severity index ($S = 3.44$). These gains arise from the complementary roles of GFL and GFM modes: GFL control provides fast, current-limited active–reactive support, while GFM control supplies robust voltage formation and inertia-like frequency support as severity increases. Through the severity-dependent blending factor $\lambda(t)$, the controller smoothly shifts from GFL-dominant behaviour during mild events to greater GFM contribution during deeper faults. This improved performance compared to pure GFM arises because, while GFM provides robust voltage and frequency support, it can exhibit slower transient response and

increased control effort under certain conditions. In contrast, the coordinated approach combines the fast current-limited response of GFL during initial disturbances with the sustained voltage-forming capability of GFM, resulting in a more balanced and effective dynamic response.

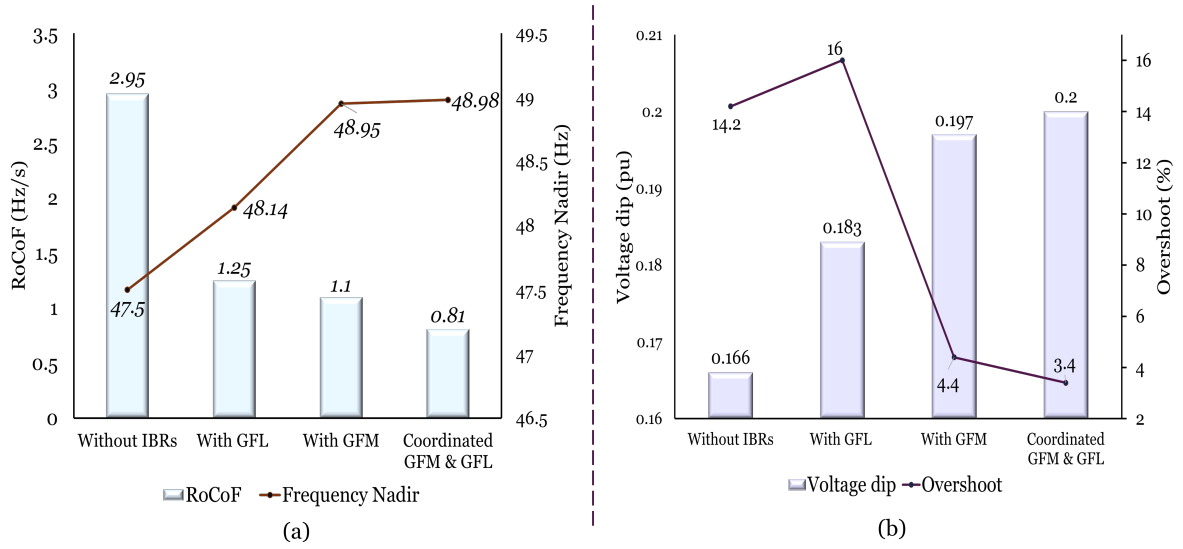


Figure 4.5: Comparative performance across four control schemes: (a) RoCoF and frequency nadir, and (b) voltage dip and overshoot.

From a control viewpoint, the shared bus functions as a multi-inverter BESS plant where GFM units act as stiff voltage sources and GFL units operate as PLL-synchronised current sources. Guided by the severity index, GFM provides a strong local voltage-frequency reference while GFL delivers rapid current support, and shifting part of the plant from pure GFL to blended GFM-GFL operation improves frequency nadir, reduces overshoot, and accelerates voltage recovery (Table 4.3).

Overall, the results show that the severity-aware coordinated strategy consistently outperforms either single-mode configuration, combining their strengths to enhance stability, damping, and resilience under grid-code fault conditions, thereby substantiating the claims of Contribution 1.

4.4.2 Optimisation of GFM:GFL Penetration Ratios

The second contribution examines the impact of varying GFM:GFL penetration ratios ($x \in \{0, 0.25, 0.5, 0.75, 1.0\}$) while maintaining a fixed total generation of 330 MW. Frequency and voltage dynamics are evaluated at bus 502, with results summarised in Tables 4.4-

4.5 and illustrated in Figures 4.6-4.7. The analysis demonstrates a consistent trend: higher GFM penetration yields progressively enhanced stability across both domains.

At full GFL operation ($x = 0$), frequency resilience is weakest, with a nadir of 48.71 Hz, overshoot of 3.50 Hz, settling time of 5.05 s, and the lowest $V_{\min}$ of 0.525 p.u. Introducing partial GFM support ($x = 0.25$) raises the nadir and shortens settling time, but error indices remain high (IAE = 0.940, ITAE = 1.750). A more balanced response appears at $x = 0.5$, where overshoot falls to 2.89 Hz, settling time reduces to 4.65 s, and both IAE and ITAE drop markedly. The strongest performance occurs at full GFM ($x = 1.0$), with the highest nadir (49.19 Hz), lowest overshoot (2.50 Hz), fastest settling (4.21 s), and minimum error values (IAE = 0.568, ITAE = 0.937). Voltage stability also improves monotonically, as $V_{\min}$ increases from 0.525 to 0.621 p.u. and ΔV contracts from 0.525 to 0.419 p.u.

Table 4.4: Frequency stability metrics under different GFM:GFL ratios.

x	Nadir (Hz)	Peak (Hz)	Δf (Hz)	Settling Time (s)	IAE	ITAE
0.00	48.71	52.21	3.50	5.05	1.361	2.364
0.25	49.22	52.61	3.39	4.90	0.940	1.750
0.50	49.09	51.98	2.89	4.65	0.815	1.509
0.75	49.15	51.84	2.69	4.50	0.661	1.124
1.00	49.19	51.69	2.50	4.21	0.568	0.937

Table 4.5: Voltage stability metrics under different GFM:GFL ratios.

x	$V_{\min}$ (p.u.)	V_{over} (p.u.)	ΔV (p.u.)	Objective Function J
0.00	0.525	1.10	0.525	0.175
0.25	0.572	1.02	0.448	0.456
0.50	0.588	1.03	0.442	0.497
0.75	0.614	1.04	0.426	0.569
1.00	0.621	1.04	0.419	0.619

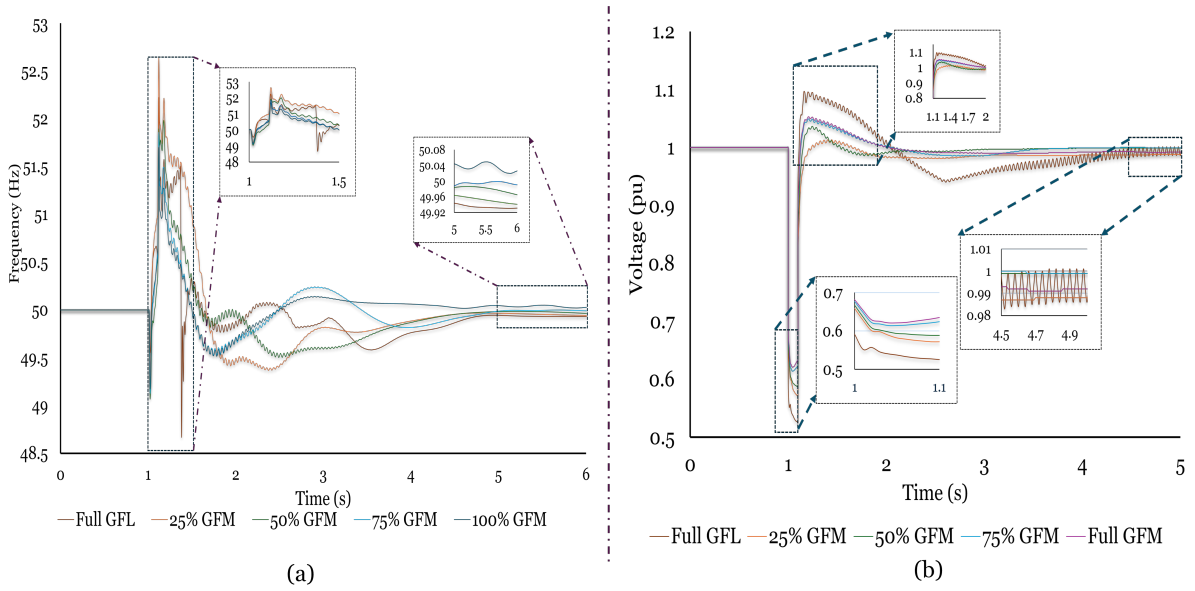


Figure 4.6: Frequency (a) and voltage (b) responses at Bus 502 under varying GFM/GFL penetration levels

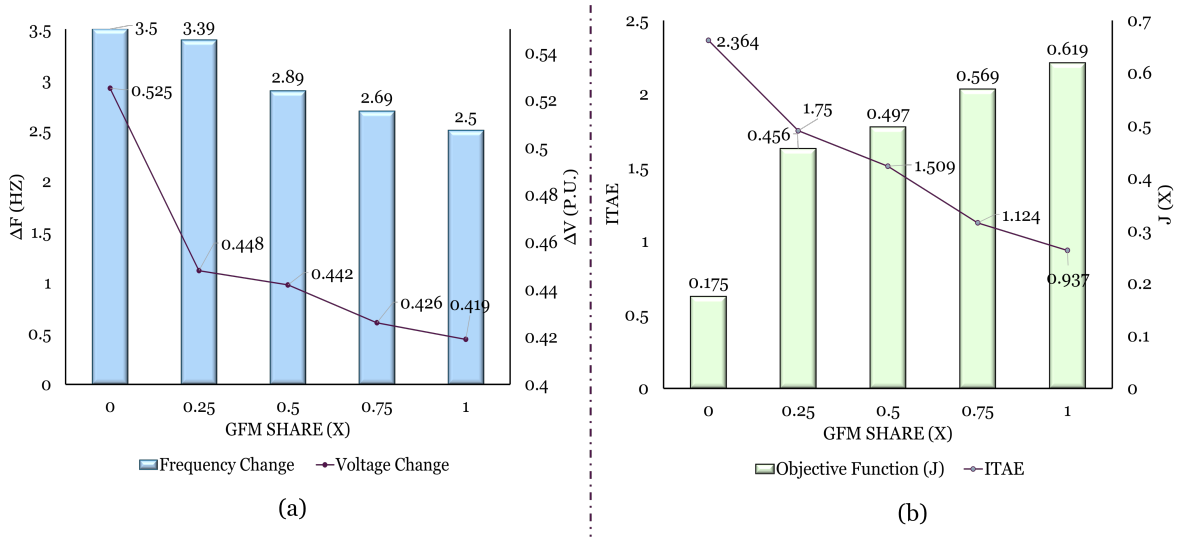


Figure 4.7: Variation of (a) frequency and voltage indicators, and (b) objective function (J) and ITAE across different GFM penetration levels.

This monotonic trend reflects the complementary control roles of GFM and GFL inverters. For a fixed 330 MW BESS, increasing the GFM share x shifts more capacity from current-following to voltage-forming, enhancing virtual inertia and voltage stiffness at bus 502 and thus improving nadir, reducing overshoot, and accelerating damping. The remaining GFL units exploit this strengthened reference to deliver rapid active

and reactive current injection. Together, this coordination yields an $\approx 60\%$ reduction in ITAE, an $\approx 20\%$ narrowing of ΔV, and a 3.5 fold increase in $J(x)$ between $x = 0$ and $x = 1$. $J(x)$ rises steadily with GFM share, peaking at 0.619 when $x = 1$. Higher GFM fractions deliver stability levels close to full GFM, improving frequency nadir, damping, recovery, and voltage support. This confirms Contribution 2 and validates the optimisation framework in weak-grid conditions.

4.5 Comparative Evaluation of Droop and VSM Control

The final contribution compares droop and VSM performance at 50% and 75% GFM (Table 4.6, Fig. 4.8), highlighting trade-offs in transient response and robustness. Four cases are evaluated: droop–50%, droop–75%, VSM–50%, VSM–75% with each scenario using a single control law.

Droop control provides faster and more bounded transients, with nadirs of 49.09 Hz (50% GFM) and 49.15 Hz (75% GFM) and overshoots of 51.91–51.84 Hz. However, its proportional P–f and Q–V response lacks inertia emulation, leading to reduced long-term frequency restoration, as reflected in the lower settling frequency at 75% GFM (48.96 Hz). VSM control, by contrast, delivers superior inertial buffering and damping, improving nadir recovery and raising settling frequency to 49.98 Hz (50% GFM) and 49.62 Hz (75% GFM), albeit with slightly higher voltage overshoot (1.05 p.u. versus 1.02 p.u. for droop).

Table 4.6: Comparison of droop and VSM control at 50% and 75% GFM share.

Metric	Droop (50%)	Droop (75%)	VSM (50%)	VSM (75%)
Frequency nadir (Hz)	49.09	49.15	47.9	49.07
Peak overshoot (Hz)	51.91	51.84	50.95	51.77
Settling frequency (Hz)	49.91	48.96	49.98	49.62
Voltage dip (p.u.)	0.57	0.61	0.63	0.62
Voltage overshoot (p.u.)	1.02	1.04	1.05	1.04

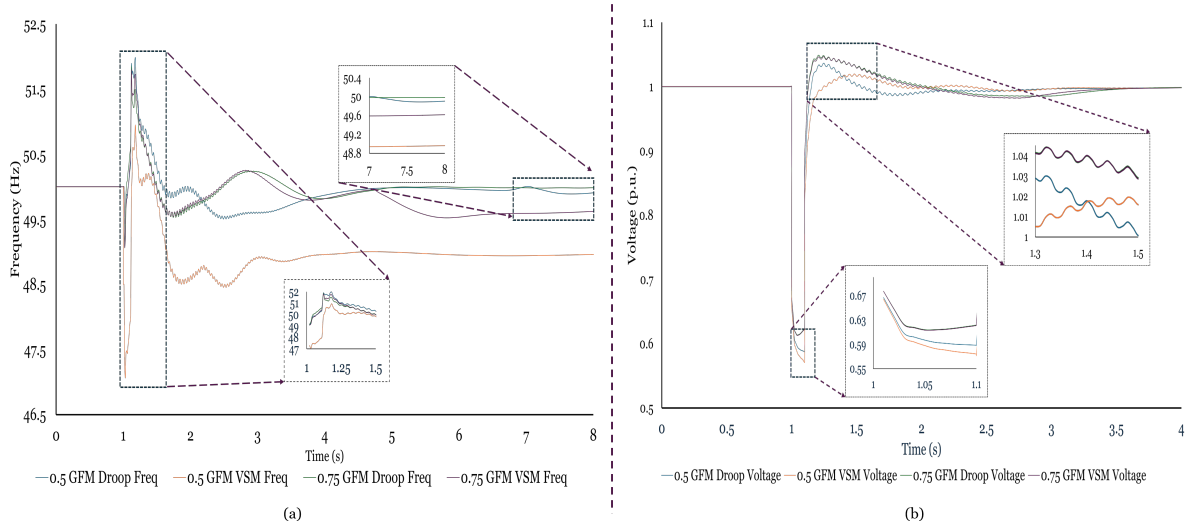


Figure 4.8: Frequency (a) and voltage (b) responses of droop and VSM controls at 50% and 75% GFM penetration levels.

Sensitivity analysis (Figure 4.9) shows that varying the droop gain k_p (0.1–0.5) or the VSM inertia constant M (1–5) produces only marginal changes in voltage dip (≈0.565–0.570 p.u.) and overshoot (≈1.01–1.05%). This narrow response band confirms that both control methods are highly robust to parameter tuning.

Overall, droop is favourable when rapid transient response and bounded overshoot are prioritised, whereas VSM offers improved frequency recovery and resilience in low-inertia weak grids. The complementary strengths identified here reinforce the need for coordinated GFM–GFL deployment in high-renewable networks.

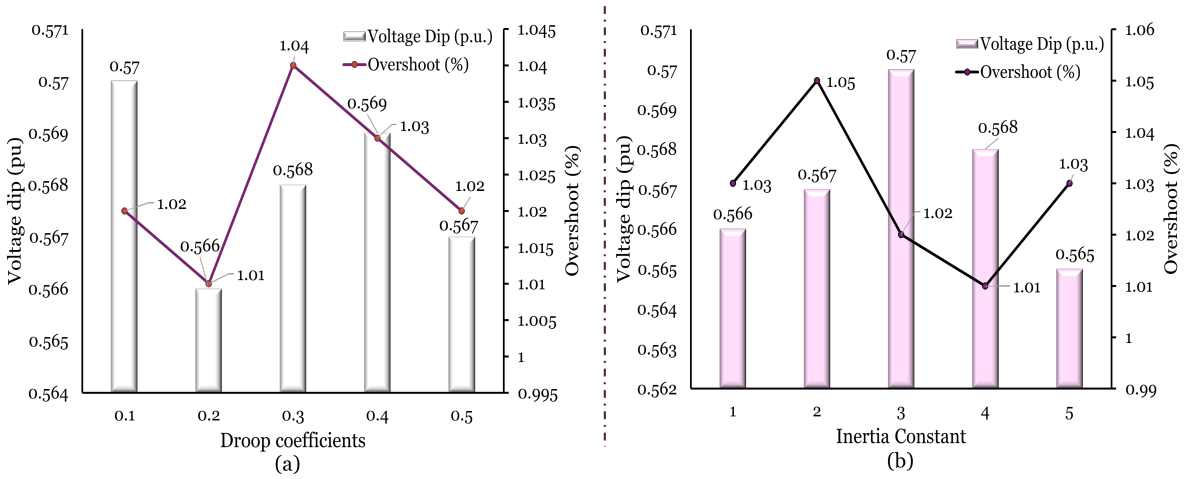


Figure 4.9: Variation of (a) droop coefficients and (b) inertia constants.

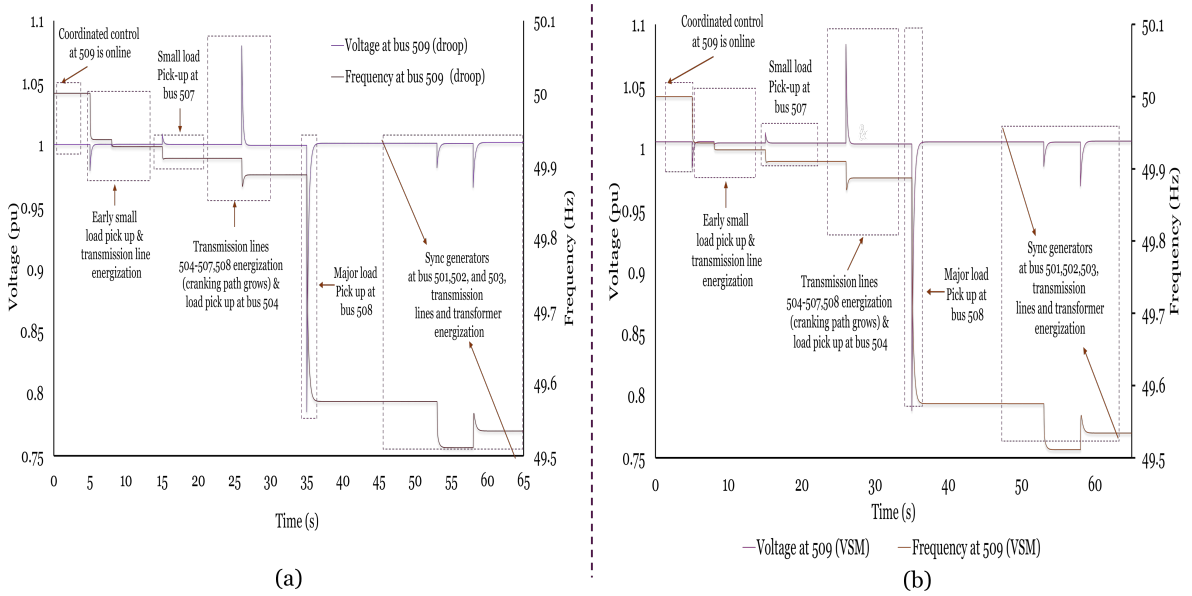


Figure 4.10: Black start restoration at Bus 509 using GFM-BESS showing voltage and frequency performance with (a) droop control and (b) VSM control.

4.5.1 Black Start Capability

The black-start analysis was conducted with a 75% GFM share for both the droop and VSM strategies to verify whether coordinated GFM-GFL control can reliably achieve restoration, rather than emphasising differences between the two modes. Results (Table 4.7, Figure 4.10) confirm that both strategies enable successful staged re-energisation of the system through GFM-BESS resources, including load pickup, generator cranking, and island synchronisation.

Droop and VSM show broadly similar restoration performance, with droop offering faster initial transients and VSM providing smoother trajectories with reduced oscillations. This close alignment demonstrates that the coordinated framework itself is capable of facilitating black start restoration in weak grids when sufficient GFM share is present. These findings highlight the viability of the proposed control architecture, which not only enhances dynamic stability under disturbances but also enables full grid restoration. This concludes the evaluation of the three contributions and leads to the final discussion on conclusions and future work.

Table 4.7: Black start restoration sequence enabled by GFM-BESS.

Time (s)	Action
0	Energise Bus 509 in GFM mode (black start resource)
5	Staged load pickup at Bus 509
8	Staged load pickup at Bus 315
12	Close line 507–509: energise cranking path
15	Load pickup at Bus 507
20	Generator cranking at Bus 507
22	Continue energisation toward backbone
26	Additional load pickup at Bus 507
30	Close line 504–508: transmission strengthening
35	Load pickup at Bus 508
40	Transformer energisation (Bus 501–504)
45	Generator cranking at Bus 501
50	Backbone energisation (504–508 and 505–507)
50–60	Synchronisation of islands/generators at Buses 501, 502, 503

4.6 Conclusion and Future Work

This chapter has addressed the stability challenges of renewable-dominated weak grids by proposing a severity-aware BESS control framework where GFL and GFM inverters operate in a blended manner governed by a severity index. The framework ensures efficient current-following during mild disturbances while adaptively transitioning to voltage-forming dominance under severe faults, thus combining operational efficiency with resilience. Validation through parametric analysis confirmed monotonic improvements in frequency nadir, RoCoF suppression, and voltage stability with increasing GFM share, while comparative evaluation of droop and VSM strategies highlighted the trade-off between droop's faster transients and VSM's superior damping and black start capability.

The findings highlight severity-aware GFM-GFL coordination as a practical pathway to resilient inverter-dominated grids, directly supporting SDG 7. Nonetheless, the study is limited to simulation-based validation on simplified test systems. The detailed RMS-domain simulations presented are suitable for system-level evaluation under weak

grid conditions. By contrast, hardware or hardware-in-the-loop (HIL) implementation would require extensive laboratory infrastructure and is therefore identified as an important direction for future work. Future research should extend the framework to larger networks with renewable variability, demand fluctuations, and real-world contingencies, while exploring real-time optimisation of GFM:GFL allocation, hybrid droop-VSM schemes, advanced black start protocols, and experimental or HIL implementations (e.g., on RTDS/OPAL-RT platforms with physical inverters) to bridge the gap between simulations and field deployment.

4.7 Chapter summary

This chapter developed a severity-aware coordinated GFM-GFL BESS control framework to enhance frequency stability, voltage resilience, and overall dynamic robustness in weak transmission networks dominated by inverter-based renewables. By introducing a severity index to regulate real-time transitions between current-following and voltage-forming behaviour, the framework demonstrated clear improvements in frequency nadir, RoCoF suppression, and post-fault voltage recovery across varying GFM:GFL penetration levels. A comparative analysis of droop and VSM strategies further highlighted distinct advantages in transient response, damping, and black-start capability, providing practical insights for future REZ deployment. Together, these findings confirm that coordinated inverter behaviour is essential for maintaining system resilience under high renewable penetration and complement the cascaded optimisation results established in Chapter 3. Notably, increasing the GFM contribution from $x = 0.00$ to $x = 1.00$ improves the frequency nadir from 48.71 Hz to 49.19 Hz while raising the minimum voltage from 0.525 p.u. to 0.621 p.u., demonstrating enhanced frequency and voltage stability. The next chapter synthesises the key outcomes of this research, discusses its broader implications for REZ stability, and outlines potential directions for future work, including full-scale REZ modelling, hybrid storage integration, and advanced adaptive control strategies.

CHAPTER 5

CONCLUSION AND FUTURE WORK

Chapter Composition

This chapter summarises the thesis by revisiting its research aims, synthesising the key findings from the literature review and the two methodological chapters, and highlighting the original contributions made to weak-grid renewable integration. It discusses the limitations of the proposed frameworks, outlines opportunities for extending the research through improved modelling, advanced control design, and experimental validation, and concludes with final reflections on the significance of the work for future Renewable Energy Zone development and inverter-dominated power systems.

5.1 Overview

The increasing reliance on inverter-based renewable energy resources has imposed significant operational challenges on weak transmission networks, particularly within Australia's Renewable Energy Zones (REZs). These networks, characterised by low short-circuit strength, high impedance, and reduced inertia, exhibit heightened vulnerability to voltage instability, fault-induced disturbances, and frequency degradation. This thesis addressed these vulnerabilities through two complementary research objectives: the development of a cascaded control optimisation framework to enhance voltage stability and fault-ride-through (FRT) capability, and the formulation of a severity-aware coordi-

nated BESS control strategy to improve frequency support and inverter interoperability. Together, these contributions provide a systematic pathway for reinforcing the dynamic stability of renewable-dominated weak grids and directly support the broader transition toward sustainable and resilient energy systems.

5.2 Summary of Research Outcomes

5.2.1 Insights from Literature Review Part 1

The first part of the literature review examined the role of Battery Energy Storage Systems (BESS) in mitigating the technical challenges inherent to weak-grid REZ environments. This analysis showed that weak grids consistently suffer from limited inertia, high voltage volatility, frequency instability, and poor power quality, all of which hinder large-scale renewable integration. Although a wide range of energy storage and control solutions has been proposed, the review revealed that existing approaches remain fragmented, frequently focusing on isolated device-level improvements rather than system-level coordination. In particular, there is a lack of unified optimisation strategies that simultaneously address plant-level, network-level, and converter-level dynamics, and existing performance metrics do not adequately capture resilience under faulted conditions. These insights underscored the need for an optimisation-driven, resilience-oriented framework, which ultimately shaped the development of the cascaded control methodology presented in Chapter 3.

5.2.2 Insights from Literature Review Part 2

The second part of the literature review evaluated the capabilities and limitations of grid-following (GFL) and grid-forming (GFM) inverters, emphasising their foundational role in enabling renewable-dominated networks. While GFM inverters provide essential grid-supportive functions such as virtual inertia, frequency regulation, and enhanced FRT stability, the review highlighted several persistent gaps, including insufficient coordination between GFM and GFL modes, inadequate modelling tools for low-inertia networks, and a lack of standardised test frameworks for evaluating inverter behaviour under REZ-specific conditions. Simulation studies and real-world deployments demonstrate promising results, but the absence of adaptive, disturbance-aware coordination strategies limits the effectiveness of existing inverter technologies. These findings moti-

vated the need for an intelligent GFM-GFL coordination mechanism, ultimately forming the conceptual basis of the severity-aware control framework introduced in Chapter 4.

5.2.3 Key Findings from Chapter 3

Chapter 3 presented a novel cascaded control optimisation framework that integrates an enhanced Particle Swarm Optimisation routine with a Dynamic Resilience Metric (DRM). This approach enabled simultaneous tuning of plant-level, network-level, and converter-level controllers, resulting in a coherent, system-wide enhancement of stability across a variety of renewable penetration scenarios. Simulation results on the simplified Australian 14-Generator Test System demonstrated substantial improvements in both voltage stability and FRT capability. The optimised controller designs consistently restored voltage profiles within three to four seconds following disturbances and supported fault-clearing durations of up to 270 ms, significantly exceeding the performance achieved with conventional reactive-power-based approaches. These outcomes confirm that coordinated multi-layer optimisation is not only feasible but essential for reinforcing renewable-rich weak transmission networks.

5.2.4 Key Findings from Chapter 4

Building upon the need for improved frequency resilience and inverter coordination, Chapter 4 introduced a severity-aware GFM-GFL BESS control framework. This approach employed a severity index to dynamically adjust the contribution of GFM and GFL inverters based on disturbance intensity. Parametric studies revealed monotonic improvements in frequency nadir, rate-of-change-of-frequency (RoCoF), and voltage recovery as the proportion of GFM increased. In addition, a comparative evaluation of Droop and Virtual Synchronous Machine (VSM) controls demonstrated that Droop-based strategies offer faster transient response, whereas VSM-based controls provide superior damping and black-start capability. These findings demonstrate that adaptive inverter coordination offers significant benefits for weak grids and complements the voltage-oriented optimisation framework developed in Chapter 3.

5.3 Research Contributions

This thesis provides a number of original contributions to the field of weak-grid renewable integration. First, it develops a unified cascaded control optimisation framework that si-

multaneously tunes multiple control layers using an enhanced PSO algorithm guided by a novel Dynamic Resilience Metric. This represents a substantial advance over existing single-layer or device-focused approaches. Second, it introduces a severity-aware coordinated GFM-GFL BESS control strategy that adaptively allocates inverter roles according to real-time system conditions, significantly improving frequency stability, fault recovery, and inverter interoperability. Third, the thesis offers a comprehensive evaluation methodology that integrates weak-grid modelling, parametric inverter studies, and comparative assessments of advanced GFM strategies. Collectively, these contributions establish a robust foundation for enhancing the stability and resilience of renewable-dominated weak transmission networks.

5.4 Limitations

Although the results achieved in this thesis are promising, several limitations should be acknowledged. The cascaded optimisation framework presented in Chapter 3 does not incorporate the effects of time-varying load profiles, which may influence optimal controller behaviour under real-world conditions. Similarly, the study did not include harmonic distortion analysis, limiting the extent to which power quality improvements could be assessed. The severity-aware coordination framework developed in Chapter 4 was validated exclusively through RMS-domain simulations. While this approach is suitable for system-level analysis, it does not capture fast electromagnetic transients and detailed inverter switching dynamics, which may influence system behaviour under very weak grid conditions. Furthermore, the thesis did not include hardware or hardware-in-the-loop validation due to infrastructure constraints, leaving experimental verification as an important avenue for future work.

5.5 Future Research Directions

There are several promising directions for extending the work presented in this thesis. Future research should incorporate realistic and time-varying load models to improve the fidelity of optimisation outcomes and expand weak-grid simulations to full-scale REZ networks featuring diverse renewable and storage technologies. Additional emphasis should be placed on assessing power quality through harmonic distortion and interharmonic analysis, especially under high GFM penetration. Further development of real-time optimisation algorithms for GFM-GFL coordination would enable adaptive

resource allocation in response to evolving operating conditions. Hybrid Droop-VSM strategies also warrant investigation as they may offer a desirable balance between transient speed and damping strength. Finally, hardware testing through HIL platforms such as RTDS or OPAL-RT will be essential for bridging the gap between simulation and deployment and for establishing standardised validation procedures aligned with emerging international grid codes.

5.6 Final Remarks

In summary, this thesis advances the technical foundations required to support large-scale renewable integration into weak transmission networks. By combining a cascaded control optimisation framework with a severity-aware GFM-GFL coordination strategy, the research provides a cohesive suite of tools capable of enhancing voltage stability, fault resilience, frequency support, and overall system robustness. These contributions not only address critical gaps in existing literature but also support Australia's broader REZ development strategy and global efforts toward clean, reliable, and sustainable energy systems. The outcomes of this work lay the groundwork for continued innovation through experimental validation, standardisation, and large-scale deployment of advanced inverter and storage technologies in weak-grid environments.

BIBLIOGRAPHY

[1] V. V. Babu, J. P. Roselyn, C. Nithya, P. Sundaravadivel, Development of grid-forming and grid-following inverter control in microgrid network ensuring grid stability and frequency response, Electronics 13 (10) (2024) 1958.

[2] Solar Emporium, What is the level of support for renewables in australia?, accessed: 2025-06-12 (2024).
URL https://solaremporium.com.au/what-is-the-level-of-support-for-renewables-i

[3] A. E. M. Operator, 2024 integrated system plan for the national electricity market: a roadmap for the energy transition (2024).

[4] Energy.gov.au, Australian electricity generation renewable sources, available at: https://www.energy.gov.au/energy-data/australian-energy-statistics/data-charts/australian-electricity-generation-renewable-sources (Accessed: 25 February 2025) (n.d.).

[5] Y. Zuo, Z. Yuan, F. Sossan, A. Zecchino, R. Cherkaoui, M. Paolone, Performance assessment of grid-forming and grid-following converter-interfaced battery energy storage systems on frequency regulation in low-inertia power grids, Sustainable Energy, Grids and Networks 27 (2021) 100496.

[6] K. Yin, Y. Xiao, X. Shen, Y. Zhu, Y. Yang, Review of photovoltaic–battery energy storage systems for grid-forming operation, Batteries 10 (8) (2024) 288.

[7] N. Baeckeland, D. Chatterjee, M. Lu, B. Johnson, G.-S. Seo, Overcurrent limiting in grid-forming inverters: A comprehensive review and discussion, IEEE Transactions on Power Electronics (2024).

[8] O. D. Garzon, A. B. Nassif, M. Rahmatian, Grid forming technologies to improve rate of change in frequency and frequency nadir: Analysis-based replicated load shedding events, Electronics 13 (6) (2024) 1120.

[9] P. Osman, J. Hayward, J. Foster, Dispatchability and energy storage costs for complementary wave, wind, and solar pv systems, Tech. rep., Technical Report (2022).

[10] M. Sarkar, L. Meegahapola, M. Datta, Reactive power management in renewable rich power grids: A review of grid-codes, renewable generators, support devices, control strategies and optimization algorithms, IEEE Access 6 (2018) 41458–41489.
doi:10.1109/ACCESS.2018.2838563.

[11] J. Rodrigues, C. Moreira, J. P. Lopes, Fault-ride-through strategies for grid-tied and grid-forming smart-transformers suited for islanding and interconnected operation, Electric Power Systems Research 189 (2020) 106616.

[12] AEMO, Renewable Integration Study, Stage 1, Tech. rep., Australian Energy Market Operator (AEMO) (2020).

[13] F. Shahnazian, K. Das, R. Yan, P. Sørensen, Challenges of renewable energy integration to weak grids, in: IET Conference Proceedings CP847, Vol. 2023, IET, 2023, pp. 529–536.

[14] Z. Liu, Y. Sun, C. Ma, An overview of grid-forming technology and its application in new-type power system, Global Energy Interconnection 7 (5) (2024) 541–552.

[15] T. Vo, C. Samarasinghe, Comparison of dc/ac grid-following and grid-forming converters in weak power systems, in: 2024 IEEE 9th Southern Power Electronics Conference (SPEC), IEEE, 2024, pp. 1–6.

[16] M. Faisal, M. Hannan, P. Ker, A. Hussain, M. Mansor, F. Blaabjerg, Review of energy storage system technologies in microgrid applications: Issues and challenges, IEEE Access 6 (2018) 35143–35164.
doi:10.1109/ACCESS.2018.2841407.

[17] A. B. Birchfield, Graph decomposition for constructing blackstart restoration strategies in benchmark cases, Electric Power Systems Research 212 (2022) 108402.
doi:10.1016/j.epsr.2022.108402.

[18] M. Singh, L. A. Lopes, N. A. Ninad, Grid forming battery energy storage system (bess) for a highly unbalanced hybrid mini-grid, Electric Power Systems Research 127 (2015) 126–133.

[19] N. Mohammed, H. Udawatte, W. Zhou, D. J. Hill, B. Bahrani, Grid-forming inverters: A comparative study of different control strategies in frequency and time domains, IEEE Open Journal of the Industrial Electronics Society 5 (2024) 185–214.

[20] Australian Renewable Energy Agency, Transgrid wallgrove battery, accessed: 2025-06-29 (2020).
URL https://arena.gov.au/projects/transgrid-wallgrove-battery/

[21] L. Yu, K. Meng, W. Zhang, Y. Zhang, An overview of system strength challenges in australia's national electricity market grid, Electronics 11 (2) (2022) 224.

[22] M. N. H. Shazon, H. M. Ahmed, Z. Tasnim, M. A. Rahman, Nahid-Al-Masood, Frequency response and its improvement using bess in a low inertia power system, in: 2019 IEEE Region 10 Conference (TENCON), IEEE, 2019, pp. 1032–1036.
doi:10.1109/TENCON.2019.8929304.

[23] Energy Corporation of New South Wales, Renewable energy zones, accessed: 2025-06-29 (2025).
URL http://energyco.nsw.gov.au/renewable-energy-zones

[24] A. Pal, P. D. Achlerkar, B. K. Panigrahi, Fault-induced current limitation control for grid-forming inverters: A framework for rapid grid code compliance, Electric Power Systems Research 242 (2025) 111471.

[25] P. G. Bueno, J. C. Hernandez, F. J. Ruiz-Rodriguez, Stability assessment for transmission systems with large utility-scale photovoltaic units, IET Renewable Power Generation 10 (5) (2016) 584–597.
doi:10.1049/iet-rpg.2015.0331.

[26] N. Modi, M. V. Escudero, K. Aramaki, X. Zhou, P. Partinen, High inverter-based resource integration: The experience of five system operators, IEEE Power and Energy Magazine 22 (2) (2024) 78–88.

[27] D. B. Rathnayake, M. Akrami, C. Phurailatpam, S. P. Me, S. Hadavi, G. Jayasinghe, B. Bahrani, Grid forming inverter modeling, control, and applications, IEEE Access 9 (2021) 114781–114807.

[28] S. D. Ahmed, F. S. Al-Ismail, M. Shafiullah, F. A. Al-Sulaiman, I. M. El-Amin, Grid integration challenges of wind energy: A review, Ieee Access 8 (2020) 10857–10878.

[29] A. Murdan, I. Jahmeerbacus, S. S. Hassen, Challenges of existing grid codes and the call for enhanced standards, Clean Technologies and Recycling 3 (4) (2023) 241–256.

[30] S. Khadem, M. Basu, M. Conlon, Power quality in grid connected renewable energy systems: Role of custom power devices, IEEE Transactions on Power Delivery 26 (1) (2010) 372–380.
doi:10.1109/TPWRD.2010.2070848.

[31] H. Erofülu, E. Cuce, P. Cuce, F. Gul, A. Iskenderofülu, Harmonic problems in renewable and sustainable energy systems: A comprehensive review, Sustainable Energy Technologies and Assessments 48 (2021) 101566.
doi:10.1016/j.seta.2021.101566.

[32] J. Engels, B. Claessens, G. Deconinck, Optimal combination of frequency control and peak shaving with battery storage systems, IEEE Transactions on Smart Grid 11 (4) (2019) 3270–3279.
doi:10.1109/TSG.2019.2963098.

[33] M. S. Alam, T. A. Chowdhury, A. Dhar, F. S. Al-Ismail, M. Choudhury, M. Shafiullah, M. I. Hossain, M. A. Hossain, A. Ullah, S. M. Rahman, Solar and wind energy integrated system frequency control: A critical review on recent developments, Energies 16 (2) (2023) 812.

[34] K. C. Divya, J. Østergaard, Battery energy storage technology for power systems-an overview, Electric power systems research 79 (4) (2009) 511–520.

[35] M. Lawder, B. Suthar, P. Northrop, S. De, C. Hoff, O. Leitermann, M. Crow, S. Santhanagopalan, V. Subramanian, Battery energy storage system (bess) and battery management system (bms) for grid-scale applications, Proceedings of the IEEE 102 (6) (2014) 1014–1030.
doi:10.1109/JPROC.2014.2317451.

[36] M. Hannan, S. Wali, P. Ker, M. Abd Rahman, M. Mansor, V. Ramachandaramurthy, K. Muttaqi, T. Mahlia, Z. Dong, Battery energy-storage system: A review of technologies, optimization objectives, constraints, approaches, and outstanding issues, Journal of Energy Storage 42 (2021) 103023.
doi:10.1016/j.est.2021.103023.

[37] J. Park, S. Jeong, M. Yoon, Grid forming inverter power control stability analysis, IEEE Access 12 (2024) 112626–112636.
doi:10.1109/ACCESS.2024.3443611.

[38] K. Gholami, B. Behi, A. Arefi, P. Jennings, Grid-forming virtual power plants: concepts, technologies and advantages, Energies 15 (23) (2022) 9049.

[39] J. S. Döhler, R. Eriksson, J. G. Oliveira, C. Boström, Voltage regulation during short-circuit faults in low voltage distributed generation systems, Electric Power Systems Research 234 (2024) 110596.

[40] K. Vidyanandan, B. Kamath, Grid integration of renewables: challenges and solutions, Indian Journal of Power and River Valley Development (2021) 150–158.

[41] F. Arraño-Vargas, Z. Shen, S. Jiang, J. Fletcher, G. Konstantinou, Challenges and mitigation measures in power systems with high share of renewables-the australian experience, Energies 15 (2) (2022) 429.

[42] M. I. Saleem, S. Saha, U. Izhar, L. M. Ang, Integration challenges of inverter based renewable energy sources in weak grids, in: Conference Record - IAS Annual Meeting (IEEE Industry Applications Society), Institute of Electrical and Electronics Engineers Inc., 2022.
doi:10.1109/IAS54023.2022.9939753.

[43] X. Liu, Y. Yue, X. Huang, W. Xu, X. Lu, A review of wind energy output simulation for new power system planning, Frontiers in Energy Research 10 (2022) 942450.

[44] S. Shahzad, E. Jasińska, Renewable revolution: A review of strategic flexibility in future power systems, Sustainability 16 (13) (2024) 5454.

[45] P. Simshauser, F. Billimoria, C. Rogers, Optimising vre capacity in renewable energy zones, Energy Economics 113 (2022) 106239.
doi:10.1016/j.eneco.2022.106239.

[46] W. Jackson, R. Argen, N. Bax, G. Clark, S. Coleman, I. Cresswell, K. Emmerson, K. Evans, M. Hibberd, E. Johnston, M. Keywood, Australia state of the environment 2016: overview, Department of the Environment and Energy (Australia), 2017.

[47] P. Adey, S. Pink, R. Raven, P. Hadfield, A. Badger, Y. Strengers, D. Sharp, O. Bock-Brown, B. Lyall, R. Martin, S. Wright, Just transitions in Australia: moving towards low carbon lives across policy, industry and practice, 2022.

[48] J. Black, H. Nakanishi, Towards net-zero emissions from urban transport: Ex post policy evaluation in canberra, the australian capital territory, Sustainability 16 (19) (2024) 8656.
doi:10.3390/su16198656.

[49] D. Roche, E. Langham, M. Mouritz, J. Breadsell, D. Sharp, K. Nagrath, S. White, D. McCartney, J. Prendergast, S. Parida, R. Bona, The Green Wave: Adding value through net zero energy strategy, 2022.

[50] J. Murray, C. Dey, The carbon neutral free for all, International Journal of Greenhouse Gas Control 3 (2) (2009) 237–248.
doi:10.1016/j.ijggc.2008.07.004.

[51] D. Beriro, J. Nathanail, J. Salazar, A. Kingdon, A. Marchant, S. Richardson, A. Gillet, S. Rautenberg, E. Hammond, J. Beardmore, T. Moore, A decision support system to assess the feasibility of onshore renewable energy infrastructure, Renewable and Sustainable Energy Reviews 168 (2022) 112771.
doi:10.1016/j.rser.2022.112771.

[52] S. Khaparde, Infrastructure for sustainable development using renewable energy technologies in india, in: 2007 IEEE Power Engineering Society General Meeting, IEEE, 2007, pp. 1–6.

[53] M. Piechowski, A. Weerakkody, Integrated renewable energy infrastructure- challenges and opportunities, Energy (2011) 52–57.

[54] V. Kouloumpis, X. Yan, Sustainable energy planning for remote islands and the waste legacy from renewable energy infrastructure deployment, Journal of Cleaner Production 307 (2021) 127198.
doi:10.1016/j.jclepro.2021.127198.

[55] H. Li, D. Edwards, M. Hosseini, G. Costin, A review on renewable energy transition in australia: An updated depiction, Journal of Cleaner Production 242 (2020) 118475.
doi:10.1016/j.jclepro.2019.118475.

[56] M. Bagheri, N. Shirzadi, E. Bazdar, C. Kennedy, Optimal planning of hybrid renewable energy infrastructure for urban sustainability: Green vancouver, Renewable and Sustainable Energy Reviews 95 (2018) 254–264.
doi:10.1016/j.rser.2018.07.037.

[57] V. Kumar, A. Pandey, S. Sinha, Grid integration and power quality issues of wind and solar energy system: A review, in: 2016 International Conference on Emerging Trends in Electrical Electronics Sustainable Energy Systems (ICETEESES), IEEE, 2016, pp. 71–80.
doi:10.1109/ICETEESES.2016.7581341.

[58] M. Khalid, Smart grids and renewable energy systems: Perspectives and grid integration challenges, Energy Strategy Reviews 51 (2024) 101299.
doi:10.1016/j.esr.2024.101299.

[59] X. Shen, H. Tang, W. He, H. Wang, Y. Li, D. Li, X. Yu, F. He, Q. Yuan, Study on the impact of renewable energy power generation transient characteristics on system stability in weak grid, in: Journal of Physics: Conference Series, Vol. 2166, IOP Publishing, 2022, p. 012054.
doi:10.1088/1742-6596/2166/1/012054.

[60] A. Etxegarai, P. Eguia, E. Torres, A. Iturregi, V. Valverde, Review of grid connection requirements for generation assets in weak power grids, Renewable and Sustainable Energy Reviews 41 (2015) 1501–1514.
doi:10.1016/j.rser.2014.09.030.

[61] G. Hollweg, S. Khan, S. Chaturvedi, Y. Fan, M. Wang, W. Su, Grid-connected converters: A brief survey of topologies, output filters, current control, and weak grids operation, Energies 16 (9) (2023) 3611.
doi:10.3390/en16093611.

[62] A. Zahedi, A review of drivers, benefits, and challenges in integrating renewable energy sources into electricity grid, Renewable and Sustainable Energy Reviews 15 (9) (2011) 4775–4779.

doi:10.1016/j.rser.2011.07.074.

[63] M. Bakht, Z. Salam, M. Gul, W. Anjum, M. Kamaruddin, N. Khan, A. Bukar, The potential role of hybrid renewable energy system for grid intermittency problem: a techno-economic optimisation and comparative analysis, Sustainability 14 (21) (2022) 14045.
doi:10.3390/su142114045.

[64] A. Boretti, Green hydrogen is a necessary component of a grid with an increasing non-dispatchable renewable energy supply, International Journal of Hydrogen Energy 48 (84) (2023) 32589–32597.
doi:10.1016/j.ijhydene.2023.05.057.

[65] D. Eltigani, S. Masri, Challenges of integrating renewable energy sources to smart grids: A review, Renewable and Sustainable Energy Reviews 52 (2015) 770–780.
doi:10.1016/j.rser.2015.07.140.

[66] M. Rana, M. Uddin, M. Sarkar, S. Meraj, G. Shafiullah, S. Muyeen, M. Islam, T. Jamal, Applications of energy storage systems in power grids with and without renewable energy integration,Äîa comprehensive review, Journal of Energy Storage 68 (2023) 107811.
doi:10.1016/j.est.2023.107811.

[67] S. Koohi-Fayegh, M. Rosen, A review of energy storage types, applications and recent developments, Journal of Energy Storage 27 (2020) 101047.
doi:10.1016/j.est.2019.101047.

[68] J. Kim, J. Song, C. Kim, J. Mahseredjian, S. Kim, Consideration on present and future of battery energy storage system to unlock battery value, Journal of Modern Power Systems and Clean Energy (2024).

[69] E. Kalaiyarasan, S. Singaravelu, Efficient power management system of pv, fuel cell and bess-based dc microgrid system, International Journal of Renewable Energy Research (2024).

[70] A. Olabi, C. Onumaegbu, T. Wilberforce, M. Ramadan, M. Abdelkareem, A. Al-Alami, Critical review of energy storage systems, Energy 214 (2021) 118987.
doi:10.1016/j.energy.2020.118987.

[71] R. Kumar, D. Lee, Ü. Ağbulut, S. Kumar, S. Thapa, A. Thakur, R. Jilte, C. A. Saleel, S. Shaik, Different energy storage techniques: recent advancements, applications, limitations, and efficient utilization of sustainable energy, Journal of Thermal Analysis and Calorimetry 149 (5) (2024) 1895–1933.

[72] M. Müller, L. Viernstein, C. N. Truong, A. Eiting, H. C. Hesse, R. Witzmann, A. Jossen, Evaluation of grid-level adaptability for stationary battery energy storage system applications in europe, Journal of Energy Storage 9 (2017) 1–11.

[73] L. Deguenon, D. Yamegueu, A. Gomna, Overcoming the challenges of integrating variable renewable energy to the grid: A comprehensive review of electrochemical battery storage systems, Journal of Power Sources 580 (2023) 233343. doi:10.1016/j.jpowsour.2023.233343.

[74] R. Aljarrah, B. Fawaz, Q. Salem, M. Karimi, H. Marzooghi, R. Azizipanah-Abarghooee, Issues and challenges of grid-following converters interfacing renewable energy sources in low inertia systems: A review, IEEE Access 12 (2024) 5534–5561. doi:10.1109/ACCESS.2024.3349630.

[75] M. Basit, S. Dilshad, R. Badar, S. Sami ur Rehman, Limitations, challenges, and solution approaches in grid-connected renewable energy systems, International Journal of Energy Research 44 (6) (2020) 4132–4162.

[76] M. Qays, I. Ahmad, D. Habibi, A. Aziz, T. Mahmoud, System strength shortfall challenges for renewable energy-based power systems: A review, Renewable and Sustainable Energy Reviews 183 (2023) 113447. doi:10.1016/j.rser.2023.113447.

[77] G. Shafiullah, A. Oo, D. Jarvis, A. Ali, P. Wolfs, Potential challenges: Integrating renewable energy with the smart grid, in: 2010 20th Australasian Universities Power Engineering Conference, IEEE, 2010, pp. 1–6.

[78] M. Worku, Recent advances in energy storage systems for renewable source grid integration: A comprehensive review, Sustainability 14 (10) (2022) 5985. doi:10.3390/su14105985.

[79] M. Rana, M. Uddin, M. Sarkar, S. Meraj, G. Shafiullah, S. Muyeen, M. Islam, T. Jamal, Applications of energy storage systems in power grids with and

without renewable energy integration-a comprehensive review, Journal of Energy Storage 68 (2023) 107811.
doi:10.1016/j.est.2023.107811.

[80] O. Krishan, S. Suhag, An updated review of energy storage systems: Classification and applications in distributed generation power systems incorporating renewable energy resources, International Journal of Energy Research 43 (12) (2019) 6171–6210.
doi:10.1002/er.4285.

[81] M. Mahmoud, M. Ramadan, A. Olabi, K. Pullen, S. Naher, A review of mechanical energy storage systems combined with wind and solar applications, Energy Conversion and Management 210 (2020) 112670.
doi:10.1016/j.enconman.2020.112670.

[82] A. Shaqsi, K. Sopian, A. Al-Hinai, Review of energy storage services, applications, limitations, and benefits, Energy Reports 6 (2020) 288–306.
doi:10.1016/j.egyr.2020.07.028.

[83] A. Olabi, T. Wilberforce, E. Sayed, A. Abo-Khalil, H. Maghrabie, K. Elsaid, M. Abdelkareem, Battery energy storage systems and swot (strengths, weakness, opportunities, and threats) analysis of batteries in power transmission, Energy 254 (2022) 123987.
doi:10.1016/j.energy.2022.123987.

[84] S. Choudhury, Review of energy storage system technologies integration to microgrid: Types, control strategies, issues, and future prospects, Journal of Energy Storage 48 (2022) 103966.
doi:10.1016/j.est.2022.103966.

[85] Z. Zhang, T. Ding, Q. Zhou, Y. Sun, M. Qu, Z. Zeng, Y. Ju, L. Li, K. Wang, F. Chi, A review of technologies and applications on versatile energy storage systems, Renewable and Sustainable Energy Reviews 148 (2021) 111263.
doi:10.1016/j.rser.2021.111263.

[86] K. Tan, T. Babu, V. Ramachandaramurthy, P. Kasinathan, S. Solanki, S. Raveendran, Empowering smart grid: A comprehensive review of energy storage technology and application with renewable energy integration, Journal of Energy Storage 39 (2021) 102591.

doi:10.1016/j.est.2021.102591.

[87] F. Erdiwansyah, F. Mahidin, H. Husin, F. Nasaruddin, M. Zaki, F. Muhibbuddin, A critical review of the integration of renewable energy sources with various technologies, Protection and Control of Modern Power Systems 6 (2021) 1–18.
doi:10.1186/s41601-021-00181-3.

[88] A. Sharma, V. Tyagi, C. Chen, D. Buddhi, Review on thermal energy storage with phase change materials and applications, Renewable and Sustainable Energy Reviews 13 (2) (2009) 318–345.
doi:10.1016/j.rser.2007.10.005.

[89] M. Katsanevakis, R. Stewart, J. Lu, Aggregated applications and benefits of energy storage systems with application-specific control methods: A review, Renewable and Sustainable Energy Reviews 75 (2017) 719–741.
doi:10.1016/j.rser.2016.11.050.

[90] S. Choudhury, Review of energy storage system technologies integration to microgrid: Types, control strategies, issues, and future prospects, Journal of Energy Storage 48 (2022) 103966.
doi:10.1016/j.est.2022.103966.

[91] A. Kebede, T. Kalogiannis, J. Van Mierlo, M. Berecibar, A comprehensive review of stationary energy storage devices for large scale renewable energy sources grid integration, Renewable and Sustainable Energy Reviews 159 (2022) 112213.
doi:10.1016/j.rser.2022.112213.

[92] R. de Fazio, D. Cafagna, G. Marcuccio, P. Visconti, Limitations and characterization of energy storage devices for harvesting applications, Energies 13 (4) (2020) 783.
doi:10.3390/en13040783.

[93] S. Nomura, H. Tsutsui, Structural limitations of energy storage systems based on the virial theorem, IEEE Transactions on Applied Superconductivity 27 (4) (2017) 1–6.
doi:10.1109/TASC.2017.2652858.

[94] C. Bucur, T. Gregory, A. Oliver, J. Muldoon, Confession of a magnesium battery, The Journal of Physical Chemistry Letters 6 (18) (2015) 3578–3591.
doi:10.1021/acs.jpclett.5b01219.

[95] M. Faisal, M. Hannan, P. Ker, A. Hussain, M. Mansor, F. Blaabjerg, Review of energy storage system technologies in microgrid applications: Issues and challenges, IEEE Access 6 (2018) 35143–35164.
doi:10.1109/ACCESS.2018.2841407.

[96] U. Pelay, L. Luo, Y. Fan, D. Stitou, M. Rood, Thermal energy storage systems for concentrated solar power plants, Renewable and Sustainable Energy Reviews 79 (2017) 82–100.
doi:10.1016/j.rser.2017.03.139.

[97] R. Gupta, N. Nigam, A. Gupta, Application of energy storage devices in power systems, International Journal of Engineering, Science and Technology 3 (1) (2011).

[98] T. Faunce, J. Prest, D. Su, S. Hearne, F. Iacopi, On-grid batteries for large-scale energy storage: Challenges and opportunities for policy and technology, MRS Energy Sustainability 5 (2018) E11.
doi:10.1557/mre.2018.11.

[99] O. Olajiga, E. Ani, T. Olatunde, Z. Sikhakane, Assessing the potential of energy storage solutions for grid efficiency: a review, Engineering Science Technology Journal 5 (3) (2024) 1112–1124.

[100] L. Wang, Y. Bu, Y. Wu, Multi-scale risk-informed comprehensive assessment methodology for lithium-ion battery energy storage system, Sustainability 16 (20) (2024) 9046.
doi:10.3390/su16209046.

[101] M. Rafaq, B. Basit, S. Mohammed, J. Jung, A comprehensive state-of-the-art review of power conditioning systems for energy storage systems: Topology and control applications in power systems, IET Renewable Power Generation 16 (10) (2022) 1971–1991.
doi:10.1049/rpg2.12498.

[102] Z. Zhongming, L. Linong, Z. Wangqiang, L. Wei, Handbook on Battery Energy Storage System, Asian Development Bank: Metro Manila, Philippines, 2018.

[103] K. Darcovich, B. Kenney, D. MacNeil, M. Armstrong, Control strategies and cycling demands for li-ion storage batteries in residential micro-cogeneration systems, Applied Energy 141 (2015) 32–41.

doi:10.1016/j.apenergy.2014.11.079.

[104] X. Li, S. Wang, Energy management and operational control methods for grid battery energy storage systems, CSEE Journal of Power and Energy Systems 7 (5) (2019) 1026–1040.
doi:10.17775/CSEEJPES.2019.00160.

[105] M. Kurucan, M. Özbaltan, Z. Yetgin, A. Alkaya, Applications of artificial neural network based battery management systems: A literature review, Renewable and Sustainable Energy Reviews 192 (2024) 114262.

[106] M. Roslan, M. Hannan, P. Ker, M. Uddin, Microgrid control methods toward achieving sustainable energy management, Applied Energy 240 (2019) 583–607.
doi:10.1016/j.apenergy.2019.02.070.

[107] R. Bakhshi-Jafarabadi, J. Sadeh, A. Serrano-Fontova, E. Rakhshani, Review on islanding detection methods for grid-connected photovoltaic systems, existing limitations and future insights, IET Renewable Power Generation 16 (15) (2022) 3406–3421.
doi:10.1049/rpg2.12554.

[108] E. Rokrok, M. Shafie-Khah, J. P. Catalão, Review of primary voltage and frequency control methods for inverter-based islanded microgrids with distributed generation, Renewable and Sustainable Energy Reviews 82 (2018) 3225–3235.

[109] X. Lin, Y. Liu, J. Yu, R. Yu, J. Zhang, H. Wen, Stability analysis of three-phase grid-connected inverter under the weak grids with asymmetrical grid impedance by ltp theory in time domain, International Journal of Electrical Power Energy Systems 142 (2022) 108244.
doi:10.1016/j.ijepes.2022.108244.

[110] K. Wichitkrailat, S. Premrudeepreechacharn, A. Siritaratiwat, S. Khunkitti, Optimal sizing and locations of multiple besss in distribution systems using crayfish optimization algorithm, IEEE Access 12 (2024) 94733–94752.
doi:10.1109/ACCESS.2024.3425963.

[111] O. Akinsooto, O. Ogundipe, S. Ikemba, Regulatory policies for enhancing grid stability through the integration of renewable energy and battery energy storage

systems (bess), International Journal of Frontline Research and Reviews 2 (2024) 022–044.

[112] T. Nguyen, H. Yoo, H. Kim, Application of model predictive control to bess for microgrid control, Energies 8 (8) (2015) 8798–8813.
doi:10.3390/en8088798.

[113] B. Bahmani-Firouzi, R. Azizipanah-Abarghooee, Optimal sizing of battery energy storage for micro-grid operation management using a new improved bat algorithm, International Journal of Electrical Power Energy Systems 56 (2014) 42–54.
doi:10.1016/j.ijepes.2013.10.019.

[114] H. Assem, T. Azib, F. Bouchafaa, C. Laarouci, N. Belhaouas, A. Hadj Arab, Adaptive fuzzy logic-based control and management of photovoltaic systems with battery storage, International Transactions on Electrical Energy Systems 2023 (1) (2023) 9065061.
doi:10.1155/2023/9065061.

[115] G. Liang, P. Liyuan, L. Ruihuan, Z. Fen, L. Jinhui, W. Xin, Study on economic operation for micro-grid based on scenario and pso, in: 2014 International Conference on Power System Technology, IEEE, 2014, pp. 3152–3156.
doi:10.1109/POWERCON.2014.6993966.

[116] P. Ray, S. Mohanty, N. Kishor, Proportional-integral controller based small-signal analysis of hybrid distributed generation systems, Energy Conversion and Management 52 (4) (2011) 1943–1954.
doi:10.1016/j.enconman.2010.11.011.

[117] S. Prabhakar, B. Panigrahi, Fuzzy logic controller for optimal power sharing in multi bess-pv based islanded ac microgrid, in: 2024 IEEE 4th International Conference on Sustainable Energy and Future Electric Transportation (SEFET), IEEE, 2024, pp. 1–6.

[118] M. Islam, I. Bushra, T. Roy, S. Ghosh, A. Oo, Enhanced composite controller for pv/pmsg/pemfc and bess-based dc microgrids voltage regulation: Integrating integral terminal sliding mode controller and recursive backstepping controller, IET Generation, Transmission Distribution 18 (22) (2024) 3608–3632.
doi:10.1049/gtd2.13305.

[119] A. Dinesh, K. Chakravarthi, P. Bhui, A. Mulla, Robust h-infinity control for line power flow tracking in power systems, International Journal of Electrical Power and Energy Systems 156 (2024) 109704.
doi:10.1016/j.ijepes.2023.109704.

[120] Z. Gong, Y. Su, R. Cai, B. Rao, J. Zhou, An adaptive control strategy for vsg based on energy storage capacity optimization of mmc-bess, Electrical Engineering (2024) 1–14doi:10.1007/s00202-024-02867-x.

[121] R. Hemmati, N. Azizi, Advanced control strategy on battery storage system for energy management and bidirectional power control in electrical networks, Energy 138 (2017) 520–528.
doi:10.1016/j.energy.2017.07.071.

[122] D. Li, Z. Wu, B. Zhao, L. Zhang, An improved droop control for balancing state of charge of battery energy storage systems in ac microgrid, IEEE Access 8 (2020) 71917–71929.
doi:10.1109/ACCESS.2020.2987098.

[123] S. Ghosh, T. Roy, M. Pramanik, A. Sarkar, M. Mahmud, An energy management system-based control strategy for dc microgrids with dual energy storage systems, Energies 13 (11) (2020) 2992.
doi:10.3390/en13112992.

[124] R. Hemmati, N. Azizi, Optimal control strategy on battery storage systems for decoupled active-reactive power control and damping oscillations, Journal of Energy Storage 13 (2017) 24–34.
doi:10.1016/j.est.2017.06.003.

[125] L. Silvestri, M. De Santis, Renewable-based load shifting system for demand response to enhance energy-economic-environmental performance of industrial enterprises, Applied Energy 358 (2024) 122562.
doi:10.1016/j.apenergy.2023.122562.

[126] A. Elsanabary, K. Khairullah, N. Ab Aziz, S. Mekhilef, Power management and optimized control of hybrid pv-bess-grid integrated fast ev charging stations, Journal of Energy Storage 90 (2024) 111802.
doi:10.1016/j.est.2024.111802.

[127] G. Farivar, W. Manalastas, H. Tafti, S. Ceballos, A. Sanchez-Ruiz, E. Lovell, G. Konstantinou, C. Townsend, M. Srinivasan, J. Pou, Grid-connected energy storage systems: State-of-the-art and emerging technologies, Proceedings of the IEEE 111 (4) (2022) 397–420.
doi:10.1109/JPROC.2022.3183289.

[128] D. Pattabiraman, R. Lasseter, T. Jahns, 2018 ieee power energy society general meeting (pesgm), in: 2018 IEEE Power Energy Society General Meeting (PESGM), IEEE, 2018.

[129] Y. Yang, W. Zhang, J. Jiang, M. Huang, L. Niu, Optimal scheduling of a battery energy storage system with electric vehicles' auxiliary for a distribution network with renewable energy integration, Energies 8 (10) (2015) 10718–10735.
doi:10.3390/en81010718.

[130] T. Terlouw, T. AlSkaif, C. Bauer, W. Van Sark, Multi-objective optimization of energy arbitrage in community energy storage systems using different battery technologies, Applied Energy 239 (2019) 356–372.
doi:10.1016/j.apenergy.2019.01.227.

[131] Y. Yang, S. Bremner, C. Menictas, M. Kay, Modelling and optimal energy management for battery energy storage systems in renewable energy systems: A review, Renewable and Sustainable Energy Reviews 167 (2022) 112671.
doi:10.1016/j.rser.2022.112671.

[132] G. He, Q. Chen, C. Kang, Q. Xia, K. Poolla, Cooperation of wind power and battery storage to provide frequency regulation in power markets, IEEE Transactions on Power Systems 32 (5) (2016) 3559–3568.
doi:10.1109/TPWRS.2016.2644642.

[133] S. Lee, J. Kim, C. Kim, S. Kim, E. Kim, D. Kim, K. Mehmood, S. Khan, Coordinated control algorithm for distributed battery energy storage systems for mitigating voltage and frequency deviations, IEEE Transactions on Smart Grid 7 (3) (2015) 1713–1722.
doi:10.1109/TSG.2015.2429919.

[134] S. Izadkhast, R. Cossent, P. Frías, P. García-González, A. Rodríguez-Calvo, Performance evaluation of a bess unit for black start and seamless islanding operation, Energies 15 (5) (2022) 1736.

[135] S. Nguyen, W. Peng, P. Sokolowski, D. Alahakoon, X. Yu, Optimizing rooftop photovoltaic distributed generation with battery storage for peer-to-peer energy trading, Applied Energy 228 (2018) 2567–2580.
doi:10.1016/j.apenergy.2018.07.042.

[136] M. Sarkar, L. Meegahapola, M. Datta, Reactive power management in renewable rich power grids: A review of grid-codes, renewable generators, support devices, control strategies and optimization algorithms, IEEE Access 6 (2018) 41458–41489.
doi:10.1109/ACCESS.2018.2838563.

[137] E. Villa-Ávila, P. Arévalo, D. Ochoa-Correa, J. L. Espinoza, E. Albornoz-Vintimilla, F. Jurado, Improving v2g systems performance with low-pass filter and fuzzy logic for pv power smoothing in weak low-voltage networks, Applied Sciences 15 (4) (2025) 1952.

[138] H. Tariq, S. Czapp, S. Tariq, K. Cheema, A. Hussain, A. Milyani, S. Alghamdi, Z. Elbarbary, Comparative analysis of reactive power compensation devices in a real electric substation, Energies 15 (12) (2022) 4453.
doi:10.3390/en15124453.

[139] S. Rusek, R. Goňo, Proceedings of the 2015 16th International Scientific Conference on Electric Power Engineering (EPE): May 20-22, 2015, Hotel Dlouhé Stráně, Kouty Nad Desnou, Czech Republic, VŠB-Technical University of Ostrava, Faculty of Electrical Engineering, 2015.

[140] Z. Yan, L. Xiong, L. You, G. Han, X. Li, Enhancing power quality in distribution networks with self-adaptive vpi-controlled grid-forming battery energy storage system, in: Journal of Physics: Conference Series, Vol. 2932, IOP Publishing, 2025, p. 012014.

[141] F. Lin, J. Liao, C. Chen, P. Chen, Y. Zhang, Voltage restoration control for microgrid with recurrent wavelet petri fuzzy neural network, IEEE Access 10 (2022) 12510–12529.
doi:10.1109/ACCESS.2022.3147357.

[142] B. Yildiz, N. Stringer, T. Klymenko, M. Samhan, G. Abramowitz, A. Bruce, I. MacGill, R. Egan, A. Sproul, Real-world data analysis of distributed pv and

battery energy storage system curtailment in low voltage networks, Renewable and Sustainable Energy Reviews 186 (2023) 113696.
doi:10.1016/j.rser.2023.113696.

[143] F. Arraño-Vargas, S. Jiang, B. Bennett, G. Konstantinou, Mitigation of power system oscillations in weak grids with battery energy storage systems: A real-world case study, Energy 283 (2023) 128648.

[144] EnergyCo, Waratah super battery, available at: https://www.energyco.nsw.gov.au/projects/waratah-super-battery (Accessed: 25 February 2025) (n.d.).

[145] B. Lu, A. Blakers, M. Stocks, C. Cheng, A. Nadolny, A zero-carbon, reliable and affordable energy future in australia, arXiv preprint (2020).
arXiv:arXiv:2007.09586.

[146] H. Kang, S. Jung, M. Lee, T. Hong, How to better share energy towards a carbon-neutral city? a review on application strategies of battery energy storage system in city, Renewable and Sustainable Energy Reviews 157 (2022) 112113.
doi:10.1016/j.rser.2022.112113.

[147] M. Mirmohammad, S. P. Azad, Control and stability of grid-forming inverters: A comprehensive review, Energies 17 (13) (2024) 3186.

[148] S. S. Rangarajan, E. R. Collins, T. Senjyu, Grid forming inverter as an advanced smart inverter for augmented ancillary services in a low inertia and a weak grid system towards grid modernization, Clean Technologies 6 (3) (2024) 1011.

[149] K. Maslo, S. Macejko, T. Haba, Grid forming inverter models for stability studies, in: 2024 24th International Scientific Conference on Electric Power Engineering (EPE), IEEE, 2024, pp. 1–6.

[150] E. Pack, B. Christison, D. Winch, L. Narushevich, Renewable energy zones in australia: Integrated system planning, IEEE Power and Energy Magazine 19 (5) (2021) 56–66.

[151] Australian Renewable Energy Agency (ARENA), What is renewable energy?, accessed: 2025-06-12 (2024).
URL https://arena.gov.au/what-is-renewable-energy/

[152] S. Sakib, M. B. Hossain, M. A. Zamee, M. Hossain, M. A. Habib, Role of battery energy storage systems: A comprehensive review on renewable energy zones integration in weak transmission networks, Journal of Energy Storage 128 (2025) 117223.

[153] NSW Department of Planning, Industry and Environment, Renewable Energy Zones -Access Scheme: Issues Paper on Central-West Orana Renewable Energy Zone Access Scheme, https://energy.nsw.gov.au/media/2001/download, iSBN: 978-1-922558-19-0 (Mar. 2021).
URL https://energy.nsw.gov.au/media/2001/download

[154] M. A. Hossain, M. R. Islam, M. A. Hossain, M. Hossain, Control strategy review for hydrogen-renewable energy power system, Journal of Energy Storage 72 (2023) 108170.

[155] Australian Energy Market Commission, National Electricity Rules - Version 177, https://energy-rules.aemc.gov.au/ner/177/29929, https://energy-rules.aemc.gov.au/ner/177/29929 (2025).

[156] Australian Energy Market Operator (AEMO), Renewable Integration Study: Stage 1 report, https://aemo.com.au/energy-systems/major-publications/renewable-integration-study-ris, accessed: 2025-02-17 (2020).

[157] M. Khan, W. Wu, L. Li, Grid-forming control for inverter-based resources in power systems: A review on its operation, system stability, and prospective, IET Renewable Power Generation 18 (6) (2024) 887–907.

[158] N. Mohammed, H. Udawatte, W. Zhou, D. J. Hill, B. Bahrani, Grid-forming inverters: A comparative study of different control strategies in frequency and time domains, IEEE Open Journal of the Industrial Electronics Society 5 (2024) 185–214.

[159] Australian Energy Market Operator (AEMO), Voluntary Specification for Grid-Forming Inverters: Webinar Presentation, Public webinar presentation, 29 June 2023, accessed from internal distribution or event archive (2023).

[160] R. Aljarrah, B. B. Fawaz, Q. Salem, M. Karimi, H. Marzooghi, R. Azizipanah-Abarghooee, Issues and challenges of grid-following converters interfacing renewable energy sources in low inertia systems: A review, IEEE Access 12 (2024) 5534–5561.

[161] M. Tozak, S. Taskin, I. Sengor, B. P. Hayes, Modelling and control of grid forming converters: A systematic review, IEEE Access (2024).

[162] P. Hu, Y. Li, Y. Yu, F. Blaabjerg, Inertia estimation of renewable-energy-dominated power system, Renewable and Sustainable Energy Reviews 183 (2023) 113481.

[163] L. Deguenon, D. Yamegueu, A. Gomna, et al., Overcoming the challenges of integrating variable renewable energy to the grid: A comprehensive review of electrochemical battery storage systems, Journal of Power Sources 580 (2023) 233343.

[164] A. Prakash, A. Bruce, I. MacGill, Insights on designing effective and efficient frequency control arrangements from the australian national electricity market, Renewable and Sustainable Energy Reviews 161 (2022) 112303.

[165] K. Mahmoud, P. Astero, P. Peltoniemi, M. Lehtonen, Promising grid-forming vsc control schemes toward sustainable power systems: Comprehensive review and perspectives, IEEE Access 10 (2022) 130024–130039.

[166] A. Shrestha, F. Gonzalez-Longatt, Frequency stability issues and research opportunities in converter dominated power system, Energies 14 (14) (2021) 4184.

[167] S. Xu, Y. Xue, L. Chang, Review of power system support functions for inverter-based distributed energy resources-standards, control algorithms, and trends, IEEE open journal of Power electronics 2 (2021) 88–105.

[168] P. Makolo, R. Zamora, T.-T. Lie, The role of inertia for grid flexibility under high penetration of variable renewables-a review of challenges and solutions, Renewable and Sustainable Energy Reviews 147 (2021) 111223.

[169] C. Ai, Y. Li, Z. Zhao, Y. Gu, J. Liu, An extension of grid-forming: A frequency-following voltage-forming inverter, IEEE Transactions on Power Electronics (2024).

[170] Vena Energy Australia, Wandoan south battery energy storage system (bess), accessed: 2025-06-29 (2022).
URL https://www.venaenergy.com.au/all_projects/wandoan-south-bess/

[171] M. Tozak, S. Taskin, I. Sengor, B. P. Hayes, Modelling and control of grid forming converters: A systematic review, IEEE Access (2024).

[172] A. Singhal, T. L. Vu, W. Du, Consensus control for coordinating grid-forming and grid-following inverters in microgrids, IEEE Transactions on Smart Grid 13 (5) (2022) 4123–4133.

[173] X. He, M. A. Desai, L. Huang, F. D¨orfler, Cross-forming control and fault current limiting for grid-forming inverters, IEEE Transactions on Power Electronics (2024).

[174] A. B. Nassif, M. Rahmatian, A. Paaso, H. Othman, V. Gevorgian, X. Fan, M. Elizondo, W. Du, Improving frequency stability and minimizing load shedding events by adopting grid-scale energy storage with grid forming inverters, IEEE, 2023.

[175] Y. Musi, Inclusion in grid codes of the requirements for grid-forming inverters as part of the generational mix, in: 2024 32nd Southern African Universities Power Engineering Conference (SAUPEC), IEEE, 2024, pp. 1–6.

[176] N. Mlilo, J. Brown, T. Ahfock, Impact of intermittent renewable energy generation penetration on the power system networks–a review, Technology and Economics of Smart Grids and Sustainable Energy 6 (1) (2021) 25.

[177] N. O. Imarhiagbe, A. Adebimpe, A. O. Amole, T. A. Kuku, Review of advances in grid-connected inverters and control techniques for power system black start, in: 2024 IEEE 5th International Conference on Electro-Computing Technologies for Humanity (NIGERCON), IEEE, 2024, pp. 1–5.

[178] R. H. Lasseter, Z. Chen, D. Pattabiraman, Grid-forming inverters: A critical asset for the power grid, IEEE Journal of Emerging and Selected Topics in Power Electronics 8 (2) (2019) 925–935.

[179] M. G. Dozein, B. Berry, J. Milanoviæ, P. Mancarella, System strength beyond fault level, IEEE Access (2025).

[180] H. Udawatte, H. Wijayalath, S. Hajtaleb, N. Mohammed, B. Bahrani, N. Rajaei, A. Banaie, Transient stability enhancement of ibr-dominated grids in the presence of grid-forming inverters (2024).

[181] Y. Zahraoui, A. Bouhanik, T. E. K. Zidane, P. E. Campana, S. Mekhilef, Grid-forming technologies for resilient renewable energy integration into power systems: A review, in: 2024 International Conference on Smart Systems and Technologies (SST), IEEE, 2024, pp. 191–196.

[182] L. Benedetti, A. Paspatis, P. N. Papadopoulos, A. Egea-Àlvarez, N. Hatziargyriou, Investigation of grid-forming and grid-following converter multi-machine interactions under different control architectures, Electric Power Systems Research 234 (2024) 110813.

[183] M. O. Qays, I. Ahmad, D. Habibi, A. Aziz, T. Mahmoud, System strength shortfall challenges for renewable energy-based power systems: A review, Renewable and Sustainable Energy Reviews 183 (2023) 113447.

[184] I. Manamperi, I. Ahmad, D. Habibi, A. Aziz, Optimising grid-forming inverters to prevent under-frequency load shedding with minimal energy storage, Journal of Energy Storage 98 (2024) 112842.

[185] Y. Liu, R. Huang, W. Du, A. Singhal, Z. Huang, Highly-scalable transmission and distribution dynamic co-simulation with 10,000+ grid-following and grid-forming inverters, IEEE Transactions on Power Delivery 39 (1) (2023) 578–590.

[186] M. Z. Mansour, M. H. Ravanji, A. Karimi, B. Bahrani, Small-signal synchronization stability enhancement of grid-following inverters via a feedback linearization controller, IEEE Transactions on Power Delivery 37 (5) (2022) 4335–4344.

[187] R. Musca, A. Vasile, G. Zizzo, Grid-forming converters. a critical review of pilot projects and demonstrators, Renewable and Sustainable Energy Reviews 165 (2022) 112551.

[188] M. I. Saleem, S. Saha, T. K. Roy, S. K. Ghosh, Assessment and management of frequency stability in low inertia renewable energy rich power grids, IET Generation, Transmission & Distribution 18 (7) (2024) 1372–1390.

[189] S. Shahzad, T. R. Alsenani, P. Wheeler, H. Kilic, Optimal placement of grid-forming inverters in low inertia power systems using bacterial foraging optimization, in: 2024 Global Energy Conference (GEC), IEEE, 2024, pp. 1–6.

[190] D. Pattabiraman, Ssr performance of droop-controlled grid-forming inverters in series compensated networks, Electric Power Systems Research 241 (2025) 111394.

[191] G. G. Farivar, W. Manalastas, H. D. Tafti, S. Ceballos, A. Sanchez-Ruiz, E. C. Lovell, G. Konstantinou, C. D. Townsend, M. Srinivasan, J. Pou, Grid-connected energy storage systems: State-of-the-art and emerging technologies, Proceedings of the IEEE 111 (4) (2022) 397–420.

[192] A. Hoke, J. C. Boemer, B. Badrzadeh, J. MacDowell, D. Kurthakoti, B. Marszalkowski, M. Meuser, Foundations for the future power system: inverter-based resource interconnection standards, IEEE Power and Energy Magazine 22 (2) (2024) 42–54.

[193] L. R. Goonasekara, L. Meegahapola, S. Yan, Impact of different grid-forming inverter control strategies on system strength and frequency, in: 2024 IEEE 9th Southern Power Electronics Conference (SPEC), IEEE, 2024, pp. 1–6.

[194] M. Ferrari, L. M. Tolbert, E. C. Piesciorovsky, Grid forming inverter with increased short-circuit contribution to address inverter-based microgrid protection challenges, IEEE Open Journal of the Industrial Electronics Society (2024).

[195] E. F. Areed, R. Yan, T. K. Saha, Impact of battery ramp rate limit on virtual synchronous machine stability during frequency events, IEEE Transactions on Sustainable Energy 15 (1) (2023) 567–580.

[196] B. Babak, M. Julia, E. Zia, L. Chao, Guest editorial: Grid-forming converters placement and utilisation to enhance transmission and distribution performances under high penetration of inverter-based resources (2023).

[197] R. A. Khan, F. Akter, S. Khaled, M. P. Akter, K. R. Ullah, Design of grid forming inverter for integration of large-scale wind farm in weak grid, in: 2022 4th International Conference on Sustainable Technologies for Industry 4.0 (STI), IEEE, 2022, pp. 1–6.

[198] A. Halley, A. Groom, M. Davies, Renewable energy on the apple isle: Managing a high penetration of inverter-based energy resources in tasmania, IEEE Electrification Magazine 10 (3) (2022) 71–82.

[199] B. Bahrani, M. H. Ravanji, D. B. Rathnayake, T. Marxsen, Csiro australian research plan for the g-pst.

[200] D. Ramasubramanian, R. Arritt, P. Dattaray, R. Entriken, E. Farantatos, X. Francia, A. Gaikwad, H. Hooshyar, R. Hytowitz, B. Leonardi, et al., Csiro australian research for the gpst.

[201] G. Yuan, Grid-forming technologies enabling a decarbonized power system [technology leaders], IEEE Electrification Magazine 10 (1) (2022) 7–9.

[202] Y. Cheng, L. Fan, J. Rose, S.-H. Huang, J. Schmall, X. Wang, X. Xie, J. Shair, J. R. Ramamurthy, N. Modi, et al., Real-world subsynchronous oscillation events in power grids with high penetrations of inverter-based resources, IEEE Transactions on Power Systems 38 (1) (2022) 316–330.

[203] Y. Tang, G. Luo, Y. Pu, Short-circuit calculation approach of grids with high proportion of inverter-interfaced generator stations, Electric Power Systems Research 241 (2025) 111407.

[204] M. Hishida, T. Redfern, X. Li, D. Hughes, D. Duckwitz, A. Knobloch, Addressing transmission system operability challenges using multi-function large scale grid-forming bess solutions, in: Energy Storage Conference 2023 (ESC 2023), Vol. 2023, IET, 2023, pp. 78–83.

[205] H. Ji, Z. Han, L. Chen, B. Xie, A. Jian, G. Sun, M. Yuan, J. Li, Distribution of power impact among grid-forming devices, in: 2023 IEEE 7th Conference on Energy Internet and Energy System Integration (EI2), IEEE, 2023, pp. 1809–1815.

[206] P. F. Mayer, M. Gordon, W.-C. Huang, C. Hardt, Improving grid strength in a wide-area transmission system with grid forming inverters, IET Generation, Transmission & Distribution 17 (2) (2023) 399–410.

[207] M. J. Li, K. T. Chi, Where should inverter-based resources be located in power networks?, IEEE Transactions on Circuits and Systems I: Regular Papers 71 (3) (2023) 1456–1464.

[208] M. Mirzadeh, R. Strunk, S. Matter, I. Bekker, M. Munderloh, T. Erckrath, L. Hofmann, A. Mertens, A rule-based concept for a bottom-up multi-master black

start of an inverter-dominated low-voltage cell, in: 2022 IEEE 13th International Symposium on Power Electronics for Distributed Generation Systems (PEDG), IEEE, 2022, pp. 1–6.

[209] S. A. Shezan, M. F. Ishraque, S. Muyeen, S. Arifuzzaman, L. C. Paul, S. K. Das, S. K. Sarker, Effective dispatch strategies assortment according to the effect of the operation for an islanded hybrid microgrid, Energy Conversion and Management: X 14 (2022) 100192.

[210] I. Alcaide-Godinez, F. Bai, Frequency support from multiple utility-scale grid-forming battery energy storage systems, in: 2022 IEEE/IAS Industrial and Commercial Power System Asia (I&CPS Asia), IEEE, 2022, pp. 1271–1276.

[211] D. B. Rathnayake, R. Razzaghi, B. Bahrani, Generalized virtual synchronous generator control design for renewable power systems, IEEE Transactions on Sustainable Energy 13 (2) (2022) 1021–1036.

[212] A. Tuckey, S. Round, Grid-forming inverters for grid-connected microgrids: Developing "good citizens" to ensure the continued flow of stable, reliable power, IEEE Electrification Magazine 10 (1) (2022) 39–51.

[213] D. B. Rathnayake, S. P. Me, R. Razzaghi, B. Bahrani, H-infinity based control design for grid-forming inverters with enhanced damping and virtual inertia, IEEE Journal of Emerging and Selected Topics in Power Electronics 11 (2) (2022) 2311–2325.

[214] A. Jain, O. Saborío-Romano, J. N. Sakamuri, N. A. Cutululis, Virtual resistance control for sequential green-start of offshore wind power plants, IEEE Transactions on Sustainable Energy 13 (3) (2022) 1420–1429.

[215] M. R. Amin, M. Negnevitsky, E. Franklin, K. S. Alam, S. B. Naderi, Application of battery energy storage systems for primary frequency control in power systems with high renewable energy penetration, Energies 14 (5) (2021) 1379.

[216] H. D. Tafti, G. Konstantinou, J. E. Fletcher, L. Callegaro, G. G. Farivar, J. Pou, Control of distributed photovoltaic inverters for frequency support and system recovery, IEEE transactions on power electronics 37 (4) (2021) 4742–4750.

[217] W. Su, A. Q. Huang, M. A. Masrur, A. K. Srivastava, T. Bi, D. Shi, Special section on power electronics-enabled smart power distribution grid, IEEE Transactions on Smart Grid 13 (5) (2022) 3851–3856.

[218] J. Matevosyan, J. MacDowell, N. Miller, B. Badrzadeh, D. Ramasubramanian, A. Isaacs, R. Quint, E. Quitmann, R. Pfeiffer, H. Urdal, et al., A future with inverter-based resources: Finding strength from traditional weakness, IEEE Power and Energy Magazine 19 (6) (2021) 18–28.

[219] D. Sharafi, Australia's power systems: Enabling renewable energy integration & resilience [guest editorial], IEEE Power and Energy Magazine 19 (5) (2021) 14–17.

[220] N. A. Cutululis, M. Koivisto, K. Das, Power systems of the future with very large shares of renewable energy sources, in: DTU International Energy Report 2021: Perspectives on Wind Energy, DTU Wind Energy, 2021, pp. 54–62.

[221] N. Lal, T. Price, L. Kwek, C. Wilson, F. Billimoria, T. Morrow, D. Sharafi, Essential system services reform: Australian market design for renewable-dominated grids, IEEE Power and Energy Magazine 19 (5) (2021) 29–45.

[222] Texas A&M University Electric Grids Repository, Simplified 14-generator australian power system, https://electricgrids.engr.tamu.edu/electric-grid-test-cases/simplified-14-generator-australian-power-system/, accessed: 2025-06-24 (Nov. 2016).

[223] S. Geng, I. A. Hiskens, Unified grid-forming/following inverter control, IEEE Open Access Journal of Power and Energy 9 (2022) 489–500.

[224] M. G. Dozein, O. Gomis-Bellmunt, P. Mancarella, Simultaneous provision of dynamic active and reactive power response from utility-scale battery energy storage systems in weak grids, IEEE Transactions on Power Systems 36 (6) (2021) 5548–5557.

[225] M. N. Ambia, K. Meng, W. Xiao, A. Al-Durra, Z. Y. Dong, Interactive grid synchronization-based virtual synchronous generator control scheme on weak grid integration, IEEE Transactions on Smart grid 13 (5) (2021) 4057–4071.

[226] G. M. Tina, G. Maione, D. Stefanelli, The impact of grid-forming vs. grid-following converters on frequency regulation: Comparing centralised or distributed photovoltaic generation, Energies 17 (23) (2024) 5827.

[227] A. Arasteh, L. Zeni, N. A. Cutululis, Fault ride through capability of grid forming wind turbines: A comparison of three control schemes, IET renewable power generation 16 (9) (2022) 1866–1881.

[228] W. Du, Z. Chen, K. P. Schneider, R. H. Lasseter, S. P. Nandanoori, F. K. Tuffner, S. Kundu, A comparative study of two widely used grid-forming droop controls on microgrid small-signal stability, IEEE Journal of Emerging and Selected Topics in Power Electronics 8 (2) (2019) 963–975.

[229] A. Tayyebi, A. Magdaleno, D. Vettoretti, M. Chen, E. Prieto-Araujo, A. Anta, F. Dörfler, System-level performance and robustness of the grid-forming hybrid angle control, Electric Power Systems Research 212 (2022) 108503.

[230] Z. Li, K. W. Chan, J. Hu, J. M. Guerrero, Adaptive droop control using adaptive virtual impedance for microgrids with variable pv outputs and load demands, IEEE Transactions on Industrial Electronics 68 (10) (2020) 9630–9640.

[231] A. A. Hameed, S. Maleki, Investigation of sub-synchronous control interactions with grid forming inverters, in: 2024 IEEE Sustainable Power and Energy Conference (iSPEC), IEEE, 2024, pp. 326–331.

[232] L. A. Lima, E. H. Watanabe, Hybrid control scheme for vsc presenting both grid-forming and grid-following capabilities, IEEE Transactions on Power Delivery 37 (6) (2022) 4570–4581.

[233] V. POWAR, P. PANIYIL, R. SINGH, Photovoltaics and lithium-ion battery-based sustainable energy infrastructure.

[234] G. Zhang, J. Ren, Y. Zeng, F. Liu, S. Wang, H. Jia, Security assessment method for inertia and frequency stability of high proportional renewable energy system, International Journal of Electrical Power & Energy Systems 153 (2023) 109309.

[235] B. Badrzadeh, C. Cardozo, M. Hishida, S. Shah, I. Huq, N. Modi, A. Morton, Grid-forming inverters: Project demonstrations and pilots, IEEE Power and Energy Magazine 22 (2) (2024) 66–77.

[236] Y. Jiang, A. Bernstein, P. Vorobev, E. Mallada, Grid-forming frequency shaping control for low-inertia power systems, in: 2021 American Control Conference (ACC), IEEE, 2021, pp. 4184–4189.

[237] B. Kroposki, A. Hoke, A path to 100 percent renewable energy: Grid-forming inverters will give us the grid we need now, IEEE Spectrum 61 (5) (2024) 50–57.

[238] A. Karisik, W. Ong, T. Bertes, T. Lim, J. Leung, Installation of a synchronous condenser-the kiamal solar farm example, in: 2021 IEEE PES Innovative Smart Grid Technologies-Asia (ISGT Asia), IEEE, 2021, pp. 1–5.

[239] D. Lepour, M. Paolone, G. Denis, C. Cardozo, T. Prevost, E. Guiu, Performance assessment of synchronous condensers vs voltage source converters providing grid-forming functions, in: 2021 IEEE Madrid PowerTech, IEEE, 2021, pp. 1–6.

[240] V. V. Babu, J. P. Roselyn, C. Nithya, P. Sundaravadivel, Development of grid-forming and grid-following inverter control in microgrid network ensuring grid stability and frequency response, Electronics 13 (10) (2024) 1958.

[241] K. Fuller, Illawarra named as nsw's first urban renewable energy zone in push for local power solutions, accessed 9 June 2025 (May 2025).
URL https://www.abc.net.au/news/2025-05-24/illawarra-named-urban-rez-renewable-energy-shift/105330122

[242] J. Li, M. Ali, J. E. Fletcher, H. I. Nurdin, Modeling and analysis of multiple inverters with dual-loop-based virtual oscillator control, IEEE Journal of Emerging and Selected Topics in Power Electronics 10 (4) (2021) 3963–3974.

[243] Neoen Australia, Hornsdale power reserve, accessed: 2025-06-29 (2017).
URL https://hornsdalepowerreserve.com.au/

[244] K. Saxena, S. Vijay, R. Kamalraj, Addressing power grid stability with grid-forming converters in future energy systems, in: 2023 International Conference on Power Energy, Environment & Intelligent Control (PEEIC), IEEE, 2023, pp. 1158–1162.

[245] M. Ismail, R. Shah, N. Amjady, S. Islam, M. S. Miah, Stability of grid-edge distribution system with grid-forming and grid-following resources: an australian

case study, in: 2024 IEEE Power & Energy Society General Meeting (PESGM), IEEE, 2024, pp. 1–5.

[246] J. Fang, W. Si, L. Xing, S. M. Goetz, Analysis and improvement of transient voltage stability for grid-forming converters, IEEE Transactions on Industrial Electronics 71 (7) (2023) 7230–7240.

[247] H. H. Alhelou, B. Bahrani, J. Ma, D. J. Hill, Australia's power system frequency: Current situation, industrial challenges, efforts, and future research directions, IEEE Transactions on Power Systems 39 (3) (2023) 5204–5218.

[248] F. Ahmed, D. Al Kez, S. McLoone, R. J. Best, C. Cameron, A. Foley, Dynamic grid stability in low carbon power systems with minimum inertia, Renewable Energy 210 (2023) 486–506.

[249] Y. Zhou, R. Zhang, D. Kathriarachchi, J. Dennis, S. Goyal, Grid forming inverter and its applications to support system strength–a case study, IET Generation, Transmission & Distribution 17 (2) (2023) 391–398.

[250] S. D. Tavakoli, M. G. Dozein, V. A. Lacerda, M. C. Mañe, E. Prieto-Araujo, P. Mancarella, O. Gomis-Bellmunt, Grid-forming services from hydrogen electrolyzers, IEEE transactions on sustainable energy 14 (4) (2023) 2205–2219.

[251] T. Reimann, B. O. Winter, W. Heckmann, I. Fraunhofer, Need for grid-forming units in the distribution grid and their impact on protection, automation and control, in: Paper TUA07 PAC World Conference, 2023.

[252] D. Charles, Off the grid, Science (New York, NY) 381 (6662) (2023) 1042–1045.

[253] B. Yildiz, N. Stringer, T. Klymenko, M. S. Samhan, G. Abramowitz, A. Bruce, I. MacGill, R. Egan, A. B. Sproul, Real-world data analysis of distributed pv and battery energy storage system curtailment in low voltage networks, Renewable and Sustainable Energy Reviews 186 (2023) 113696.

[254] D. Al Kez, A. M. Foley, F. Ahmed, D. J. Morrow, Overview of frequency control techniques in power systems with high inverter-based resources: Challenges and mitigation measures, IET Smart Grid 6 (5) (2023) 447–469.

[255] B. Babak, M. Julia, E. Zia, L. Chao, Guest editorial: Grid-forming converters placement and utilisation to enhance transmission and distribution performances under high penetration of inverter-based resources (2023).

[256] N. Ma, F. Bai, Comparative study of inertia support for networks with high renewable energy penetration, in: 2022 IEEE PES 14th Asia-Pacific Power and Energy Engineering Conference (APPEEC), IEEE, 2022, pp. 1–6.

[257] K. Dharmapala, A. Rajapakse, Short-term voltage instability prediction using pre-identified voltage templates and machine learning classifiers (2024).

[258] B. Elenga Baningobera, I. Oleinikova, K. Ulhen, B. R. Pokhrel, Challenges and solutions in low-inertia power systems with high wind penetration, IET Generation, Transmission & Distribution 18 (24) (2024) 4221–4244.

[259] R. D. Kordkandi, M. T. Hagh, S. Roozbehani, Real-time low/high-voltage ride-through capability improvement of micro-grid based on coordinated robust grid-following control, IET Generation, Transmission & Distribution 16 (16) (2022) 3318–3332.

[260] F. Jiang, C. Tu, Z. Shuai, F. Xiao, Z. Lan, Combinational voltage booster technique for fault ride-through capability enhancement of squirrel-cage induction generator, Electric Power Systems Research 136 (2016) 163–172.

[261] G. Rashid, M. H. Ali, Fault ride through capability improvement of dfig based wind farm by fuzzy logic controlled parallel resonance fault current limiter, Electric Power Systems Research 146 (2017) 1–8.

[262] K. Honghai, S. Fuqing, C. Yurui, W. Kai, H. Zhiyi, Reactive power optimization for distribution network system with wind power based on improved multi-objective particle swarm optimization algorithm, Electric Power Systems Research 213 (2022) 108731.

[263] F. Benyamina, A. Benrabah, F. Khoucha, M. F. Zia, Y. Achour, M. Benbouzid, Online current limiting-based control to improve fault ride-through capability of grid-feeding inverters, Electric Power Systems Research 201 (2021) 107524.

[264] M. A. S. Ali, K. K. Mehmood, S. Baloch, C.-H. Kim, Modified rotor-side converter control design for improving the lvrt capability of a dfig-based wecs, Electric Power Systems Research 186 (2020) 106403.

[265] Z. Yang, B. Gao, Z. Cao, Low-voltage ride-through strategy for offshore wind turbines based on current relaxation region, Electric Power Systems Research 223 (2023) 109704.

[266] M. I. Saleem, S. Saha, T. K. Roy, S. K. Ghosh, Assessment and management of frequency stability in low inertia renewable energy rich power grids, IET Generation, Transmission & Distribution 18 (7) (2024) 1372–1390.

[267] T. Lin, M. Das, A. Gole, A. Isaacs, Adaptive fault ride through control of vsm grid-forming converters, Electric Power Systems Research 223 (2023) 109606.

[268] W. Wan, P. Zhang, M. A. Bragin, P. B. Luh, Cooperative fault management for resilient integration of renewable energy, Electric Power Systems Research 211 (2022) 108147.

[269] X. Zhao, H. Zhang, H. Zhu, Q. Hu, L. Zhang, An emergency control considering current limitation and transient stability of virtual synchronous generator, IET Generation, Transmission & Distribution 18 (8) (2024) 1641–1652.

[270] R. M. Kamel, S. S. Alanzi, Y. M. Al Hashemi, Effect of photovoltaic penetration level and location on power system transient stability during symmetrical and unsymmetrical faults, Sustainable Energy, Grids and Networks 38 (2024) 101322.

[271] A. Liu, J. Liu, Improved transient stability of virtual synchronous generators for grid voltage cascading faults, Electric Power Systems Research 213 (2022) 108661.

[272] S. Rasool, K. M. Muttaqi, D. Sutanto, A novel fault ride-through capability improvement scheme for the hybrid offshore wind-wave energy conversion systems, Electric Power Systems Research 217 (2023) 109166.

[273] J. Yang, X. Zhao, Cascade model predictive control strategy for medium voltage flexible interconnected systems with arc suppression capability under single phase grounding fault, Electric Power Systems Research 235 (2024) 110511.

[274] I. Murzakhanov, G. M. Vishwanath, K. Vemalaiah, G. Prashal, S. Chatzivasileiadis, N. P. Padhy, A novel decentralized inverter control algorithm for loss minimization and lvrt improvement, Electric Power Systems Research 221 (2023) 109433.

[275] S. Demin, M. Sitbon, I. Aharon, E. Barbi, R. Machlev, J. Belikov, Y. Levron, D. Baimel, A new resonant fault current limiter for improved wind turbine transient stability, Electric Power Systems Research 223 (2023) 109600.

[276] J. Sancho, F. Escobar, G. Valverde, Revisiting the tripping logic of the der_a model for power system stability studies, Electric Power Systems Research 235 (2024) 110764.

[277] R. A. Talani, G. S. Kaloi, A. Ali, G. Abbas, A. Emara, E. Touti, Fault analysis and performance improvement of grid-connected doubly fed induction generator through an enhanced crowbar protection scheme, PLoS One 20 (7) (2025) e0327802.

[278] R. A. Talani, G. S. Kaloi, A. Ali, M. A. Bijarani, G. Abbas, M. Hatatah, P. Mercorelli, E. Touti, Dynamic performance analysis and fault ride-through enhancement by a modified fault current protection scheme of a grid-connected doubly fed induction generator., Machines 13 (2) (2025).

[279] S. A. Dayo, A. Memon, Z. A. Memon, T. A. Jumani, G. Abbas, S. Othmen, A. Yousef, A. A. Wijaya, A new approach for improving dynamic fault ride through capability of gridctied based wind turbines, Scientific Reports 15 (1) (2025) 6144.

[280] M. K. Senapati, C. Pradhan, P. K. Nayak, S. Padmanaban, T. Gjengedal, Modified demagnetisation control strategy for low-voltage ride-through enhancement in dfig-based wind systems, IET Renewable Power Generation 14 (17) (2020) 3487–3499.

[281] M. G. Anany, A. A. ElDesouky, A. A. Salem, Real-time v2g simulator for grid system frequency and voltage regulation with fault ride-through capabilities, Electric Power Systems Research 234 (2024) 110561.

[282] L. Xian, L. Wu, W. Chen, T. Pei, X. Xie, A flexible contact switching method of integrated control mode for enhancing the frt capability of gfm-controlled dfig, Electric Power Systems Research 245 (2025) 111636.

[283] Siemens Industry, Inc., Model Library PSSE 35.6.1, Siemens Power Technologies International, 400 State Street, Schenectady, NY 12301-1058, USA.

[284] North American Electric Reliability Corporation (NERC), Performance, planning, and modeling validation for inverter-based resources.

[285] P. Interconnection, Pjm dynamic model development guidelines for interconnection analysis (September 2024).

[286] Bonneville Power Administration (BPA), Model User Guide for Generic Renewable Energy System Models (2023).

[287] M. S. Rahman, M. Hossain, J. Lu, Coordinated control of three-phase ac and dc type ev–esss for efficient hybrid microgrid operations, Energy conversion and management 122 (2016) 488–503.

[288] M. Gibbard, D. Vowles, Simplified 14-generator model of the south east australian power system, The University of Adelaide, South Australia 18 (2014) 1–38.

[289] H. Jia, C. Zhang, J. Du, N. Kuang, A data-driven approach for reactive power optimization incorporating interval values for renewable power generation, International Transactions on Electrical Energy Systems 2023 (1) (2023) 6678942.

[290] M. K. Senapati, O. Al Zaabi, K. Al Hosani, K. Al Jaafari, C. Pradhan, U. R. Muduli, Advancing electric vehicle charging ecosystems with intelligent control of dc microgrid stability, IEEE Transactions on Industry Applications 60 (5) (2024) 7264–7278.

[291] M. K. Senapati, C. Pradhan, S. R. Samantaray, P. K. Nayak, Improved power management control strategy for renewable energy-based dc micro-grid with energy storage integration, IET generation, transmission & distribution 13 (6) (2019) 838–849.

[292] M. Amir, K. Singh, Frequency regulation strategies in renewable energy-dominated power systems: Issues, challenges, innovations, and future trends, in: Advanced Frequency Regulation Strategies in Renewable-Dominated Power Systems, Elsevier, 2024, pp. 367–381.

[293] R. Aljarrah, B. B. Fawaz, Q. Salem, M. Karimi, H. Marzooghi, R. Azizipanah-Abarghooee, Issues and challenges of grid-following converters interfacing renewable energy sources in low inertia systems: A review, IEEE Access 12 (2024) 5534–5561.

[294] D. Zhang, G. Shafiullah, C. K. Das, K. W. Wong, Optimal allocation of battery energy storage systems to improve system reliability and voltage and frequency stability in weak grids, Applied energy 377 (2025) 124541.

[295] M. Eskandari, A. Rajabi, A. V. Savkin, M. H. Moradi, Z. Y. Dong, Battery energy storage systems (besss) and the economy-dynamics of microgrids: Review,

analysis, and classification for standardization of besss applications, Journal of Energy Storage 55 (2022) 105627.

[296] S. Ghosh, A. Bohra, S. Dutta, S. Verma, Integration strategies for large-scale renewable interconnections with grid forming and grid following inverters, capacitor banks, and harmonic filters, Energies 18 (15) (2025) 3934.

[297] S. Chen, Y. Wang, Z. Tian, X. Xiao, X. Xie, O. Gomis-Bellmunt, Understanding a type of forced oscillation in grid-forming and grid-following inverter connected systems, IEEE Transactions on Power Electronics (2025).

[298] H. Yu, L. Yao, S. Liang, J. Xu, F. Cheng, M. Wu, Coordinated control of grid-following and grid-forming energy storage for virtual inertia response considering frequency modal characteristics, International Journal of Electrical Power & Energy Systems 168 (2025) 110686.

[299] H. Zhao, Q. Zong, H. Zhou, W. Yao, K. Sun, Y. Zhou, J. Wen, Frequency-voltage active support strategy for hybrid wind farms based on grid-following and grid-forming hierarchical subgroup control, CSEE Journal of Power and Energy Systems (2025).

[300] S. Sakib, M. B. Hossain, M. A. Zamee, M. Hossain, M. A. Habib, Role of battery energy storage systems: A comprehensive review on renewable energy zones integration in weak transmission networks, Journal of Energy Storage 128 (2025) 117223.

[301] S. Chen, Y. Wang, M. Yang, X. Xiao, O. Gomis-Bellmunt, Forced oscillation in hybrid system with grid-following and grid-forming inverters, Energy 319 (2025) 134915.

[302] Ner clause s5.1a.8 - fault clearance times (2025).
URL https://energy-rules.aemc.gov.au/ner/177/29929

[303] M. Gibbard, D. Vowles, Simplified 14-generator model of the south east australian power system, Tech. rep., The University of Adelaide, updated 17 May 2014 (February 2014).

[304] N. Al-Masood, Prevention of secondary pv trip in power systems with high penetration of photovoltaics, in: Proceedings of the 2017 IEEE Power & Energy Society General Meeting (PESGM), IEEE, 2017, pp. 1–5.

[305] A. E. M. Operator, Application of advanced grid-scale inverters in the nem, White Paper, August (2021).

[306] Aurecon Australasia Pty Ltd, Hornsdale power reserve expansion project, Tech. rep., Aurecon, revision C, ARENA Knowledge Sharing (2023).